

Essays in Time Series Econometrics

Dissertation **submitted to the** **Faculty of Business, Economics and Informatics** **of the University of Zurich**

to obtain the degree of
Doktor der Wirtschaftswissenschaften, Dr. oec.
(corresponds to Doctor of Philosophy, PhD)

presented by

Stefan Bruder
from Zurich, ZH

approved in July 2018 at the request of

Prof. Michael Wolf, PhD
Prof. Dr. Ashok Kaul

The Faculty of Business, Economics and Informatics of the University of Zurich hereby authorizes the printing of this dissertation, without indicating an opinion of the views expressed in the work.

Zurich, July 18th 2018

Chairman of the Doctoral Board: Prof. Dr. Steven Ongena

Acknowledgments

Undertaking this PhD studies would not have been possible without the substantial support and guidance that I received from many people. I would like to thank a few persons that especially supported me throughout the years at the Department of Economics at the University of Zurich. First and foremost, I would like to express my deepest gratitude to my thesis supervisor Michael Wolf. I am grateful for his profound guidance, his dedicated mentoring, and the support that I experienced from him over the last five years. I also owe special thanks to Ashok Kaul for co-advising this thesis and for his incessant interest in my work.

Further, I would like to express my gratitude to my mentor Johannes Kunz for his continuous support and many inspiring discussions. Moreover, I would like to thank Gianluca De Nard, Adriano Tosi, Cornelia Metzler, Christine Le Grand and Sara Wunderli, who have accompanied me during the process of writing this dissertation, for making the last five years enjoyable and unforgettable.

Finally, I wish to thank my parents for supporting me, encouraging me and giving me the freedom to pursue my academic aspirations.

Stefan Bruder

Zurich, April 2018

Contents

List of Tables	viii
List of Figures	x
1 Dissertation Overview	1
References	3
2 A Comparison of Several Methods to Compute Joint Prediction Regions for Path Forecasts	5
2.1 Introduction	6
2.2 The Model	8
2.2.1 Vector Autoregression	8
2.2.2 Estimation and Finite-Sample Bias	9
2.2.3 Path Forecast and Prediction Error	11
2.3 Joint Prediction Regions	12
2.3.1 Bonferroni-type JPRs	12
2.3.2 Bootstrap JPR	13
2.3.3 Neighbouring Path JPR	15
2.4 Bootstrap Details	16
2.5 Monte Carlo Simulation	17
2.5.1 Data Generating Processes	17
2.5.2 Design	22
2.5.3 Results	23
2.5.4 Summary of Simulation Evidence	30
2.6 Empirical Application	31
2.7 Conclusion	33

References	35
Appendix	38
3 Balanced Bootstrap Joint Confidence Bands for Structural Impulse Responses	96
3.1 Introduction	97
3.2 Structural Impulse Response Functions	98
3.3 New Joint Confidence Bands	101
3.3.1 Motivation and Notation	101
3.3.2 Balanced Bootstrap Joint Confidence Bands	103
3.3.3 Asymptotic Properties	105
3.4 Competing Methods	107
3.4.1 Naïve Confidence Bands	108
3.4.2 Bonferroni Joint Confidence Bands	108
3.4.3 Wald and Adjusted-Wald Joint Confidence Bands	108
3.5 Monte Carlo Simulation	110
3.5.1 Lag Selection and Estimation of Impulse Responses	110
3.5.2 Bootstrap Details	111
3.5.3 Data Generating Processes	113
3.5.4 Simulation Parameters and Performance Evaluation	115
3.5.5 Results	116
3.5.6 Summary of simulation Evidence	120
3.6 Empirical Application	121
3.7 Conclusion	124
References	125
Appendix	128
4 Inference for Structural Impulse Responses in SVAR-GARCH Models	168
4.1 Introduction	169
4.2 The Model	170
4.2.1 Some Preliminaries	170
4.2.2 GO-GARCH Model	172
4.2.3 Identification	173

4.2.4	Estimation	175
4.3	Inference for Structural Impulse Responses	179
4.3.1	Motivation	179
4.3.2	Residual Bootstrap	181
4.4	Competing Methods	183
4.4.1	I.i.d. Bootstrap	183
4.4.2	Moving Block Bootstrap	183
4.5	Monte Carlo Simulation	184
4.5.1	Data Generating Processes	184
4.5.2	Simulation Parameters and Performance Evaluation	185
4.5.3	Results	186
4.6	Conclusion	190
	References	191
	Appendix	194
	Curriculum Vitae	209

List of Tables

2.1	Characteristic Roots of Bivariate VAR(1) Models	18
2.2	Empirical Volumes of Various 90% Joint Prediction Regions	33
3.1	Characteristic Roots	113
3.2	Mean Absolute Deviation of Empirical Marginal Coverage Rates	119
3.3	Empirical Volumes of Various 90% Joint Confidence Bands	122

List of Figures

2.1	Log Real Price of Oil: Path Forecast and 90% JPRs	34
2A.1	Bivariate VAR(1) Models: Empirical Coverages	39
2A.2	Bivariate VAR(1) Models: Overall Performance	40
2A.3	Trivariate VAR(4) Model: Bonferroni vs. Adjusted Bonferroni	41
2A.4	Trivariate VAR(4) Model: Overall Performance	42
2A.5	Six-variate VAR(2) Model: Empirical Coverages with $T = 100$	43
2A.6	Six-variate VAR(2) Model: Empirical Coverages with $T = 400$	44
2A.7	Six-variate VAR(2) Model: Overall Performance	45
2A.8	Change in Global Crude Oil Inventories: Path Forecast and 90% JPRs .	45
2A.9	Change in Global Crude Oil Production: Path Forecast and 90% JPRs .	46
2A.10	Global Real Activity: Path Forecast and 90% JPRs	46
3.1	Estimated Impulse Response of $\Delta prod_t$ to a Shock in $\varepsilon_{t,2}$	123
3A.1	DGP-1: Boxplots of the Empirical Coverages with $T = 100$	131
3A.2	DGP-1: Boxplots of the Empirical Coverages with $T = 400$	132
3A.3	DGP-1: Boxplots of the Volumes with $T = 100$	133
3A.4	DGP-1: Boxplots of the Volumes with $T = 400$	134
3A.5	DGP-2: Boxplots of the Empirical Coverages with $T = 100$	135
3A.6	DGP-2: Boxplots of the Empirical Coverages with $T = 400$	136
3A.7	DGP-2: Boxplots of the Volumes with $T = 100$	137
3A.8	DGP-2: Boxplots of the Volumes with $T = 400$	138
3A.9	DGP-2: Empirical Coverages with $T = 100$	139
3A.10	DGP-2: Empirical Coverages with $T = 400$	140
3A.11	DGP-1: Exogenous Bootstrap vs. Endogenous Bootstrap	141
3A.12	DGP-2: Exogenous Bootstrap vs. Endogenous Bootstrap	142

3A.13	Estimated Impulse Response of $\Delta prod_t$ to a Shock in $\varepsilon_{t,1}$	143
3A.14	Estimated Impulse Response of $real_t$ to a Shock in $\varepsilon_{t,1}$	144
3A.15	Estimated Impulse Response of rpo_t to a Shock in $\varepsilon_{t,1}$	145
3A.16	Estimated Impulse Response of $real_t$ to a Shock in $\varepsilon_{t,2}$	146
3A.17	Estimated Impulse Response of rpo_t to a Shock in $\varepsilon_{t,2}$	147
3A.18	Estimated Impulse Response of $\Delta prod_t$ to a Shock in $\varepsilon_{t,3}$	148
3A.19	Estimated Impulse Response of $real_t$ to a Shock in $\varepsilon_{t,3}$	149
3A.20	Estimated Impulse Response of rpo_t to a Shock in $\varepsilon_{t,3}$	150
4A.1	Root Mean Squared Error of Structural Impulse Response Estimators .	197
4A.2	DGP-1a: Boxplots of Empirical Coverages	198
4A.3	DGP-1a: Boxplots of Empirical Lengths	199
4A.4	DGP-1b: Boxplots of Empirical Coverages	200
4A.5	DGP-1b: Boxplots of Empirical Lengths	201
4A.6	DGP-1c: Boxplots of Empirical Coverages	202
4A.7	DGP-1c: Boxplots of Empirical Lengths	203
4A.8	Residual Bootstrap: Sampling Distribution vs. Bootstrap Sampling Dis- tribution	204
4A.9	Symmetrized Residual Bootstrap: Sampling Distribution vs. Bootstrap Sampling Distribution	205
4A.10	I.i.d. Bootstrap: Sampling Distribution vs. Bootstrap Sampling Distri- bution	206
4A.11	Moving Block Bootstrap: Sampling Distribution vs. Bootstrap Sampling Distribution	207

Chapter 1

Dissertation Overview

The chapters of this thesis contribute to a diverse set of current topics in time series econometrics. The main link between the three chapters is the assumption of a vector autoregression (VAR) model as the data generating process. The VAR is still a workhorse model in applied time series analysis thanks to its simplicity and yet its capability of capturing rich dynamics in linear multivariate time series. Beyond that, the topics of the chapters are quite broad and include prediction regions for paths forecast, joint confidence sets for structural impulse response functions and bootstrap-based inference on structural impulse responses in a conditionally heteroskedastic environment.

Chapter 2 compares several methods to compute joint prediction regions for paths forecasts generated by vector autoregressions. Such a joint prediction region is supposed to contain the entire (random) future path with a prespecified probability, at least asymptotically. The existing literature offers a vast variety of different methods to construct such a joint prediction region; for example, see [Jordà and Marcellino \(2010\)](#), [Staszewska-Bystrova \(2011\)](#) and [Wolf and Wunderli \(2015\)](#). Chapter 2 contributes to the time series literature by investigating the finite-sample performance of a number of joint prediction regions, that have not been investigated yet, through a large-scale Monte Carlo simulation. The focus of the simulation study is on the following issues regarding their effect on the finite-sample performance of the various joint prediction regions: estimation of the lag order of the VAR model, stationarity characteristics of the VAR model, non-normal error distributions, the dimension of the VAR and model misspecification.

Chapter 3, written jointly with Michael Wolf, considers the construction of joint confidence bands for structural impulse response functions based on a VAR model. Such

joint confidence bands are supposed to cover the entire true structural impulse response function with a prespecified probability, at least asymptotically. The literature has already proposed a number of methods to construct such confidence bands; for example, see [Staszewska \(2007\)](#), [Jordà \(2009\)](#), and [Lütkepohl et al. \(2015a,b\)](#). However, these existing methods suffer from deficiencies: they may exhibit empirical coverage rates substantially below the nominal level or they may be excessively large in terms of the aggregate volume. Chapter 3 contributes to the time series literature by proposing new bootstrap-based joint confidence bands for structural impulse response functions that are based on the multiple-testing methodology of [Romano and Wolf \(2010\)](#). Under weak regularity conditions, the new joint confidence bands have asymptotically the desired coverage probability and are asymptotically balanced. The finite-sample properties of the proposed joint confidence bands are compared with those of a set of competing methods by means of an extensive Monte Carlo simulation. The simulation results show that the proposed joint confidence bands improve upon the existing bands in terms of coverage bias and excess volume in most of the scenarios.

Finally, Chapter 4 considers inference on structural impulse responses based on a conditionally heteroskedastic VAR model where the conditional heteroskedasticity is driven by a multivariate generalized autoregressive conditional heteroskedastic (GARCH) process. The presence of conditional heteroskedasticity allows the identification of the structural vector autoregression (SVAR) without imposing additional identifying assumptions; for example, see [Lütkepohl and Netsunajev \(2017\)](#) and the references therein. However, the consequences of identifying the SVAR via conditional heteroskedasticity for inference on structural impulse responses have not yet been investigated in the literature. The main contribution of Chapter 4 is a nonparametric bootstrap procedure to construct marginal confidence intervals for structural impulse responses. The proposed bootstrap procedure is a multivariate generalization of the bootstrap procedure for the univariate ARMA-GARCH model outlined in [Shimizu \(2010\)](#). A Monte Carlo simulation reveals that the confidence intervals based on the proposed bootstrap overall outperform the intervals based on two competing bootstrap procedures. Moreover, Chapter 4 proposes a new estimation procedure of the parameters of the SVAR-GARCH model is proposed that is numerically stable even in demanding scenarios with small sample sizes and/or high dimensions.

References

- Jordà, O. (2009). Simultaneous confidence regions for impulse responses. *Review of Economics and Statistics*, 91(3):629–647.
- Jordà, O. and Marcellino, M. (2010). Path forecast evaluation. *Journal of Applied Econometrics*, 25(4):635–662.
- Lütkepohl, H. and Netšunajev, A. (2017). Structural vector autoregressions with heteroskedasticity: A review of different volatility models. *Econometrics and Statistics*, 1:2–18.
- Lütkepohl, H., Staszewska-Bystrova, A., and Winker, P. (2015a). Comparison of methods for constructing joint confidence bands for impulse response functions. *International Journal of Forecasting*, 31(3):782–798.
- Lütkepohl, H., Staszewska-Bystrova, A., and Winker, P. (2015b). Confidence bands for impulse responses: Bonferroni vs. Wald. *Oxford Bulletin of Economics and Statistics*, 77(6):800–821.
- Romano, J. P. and Wolf, M. (2010). Balanced control of generalized error rates. *Annals of Statistics*, 38(1):pp. 598–633.
- Shimizu, K. (2010). *Bootstrapping stationary ARMA-GARCH models*. Springer, Berlin.
- Staszewska, A. (2007). Representing uncertainty about response paths: The use of heuristic optimisation methods. *Computational Statistics & Data Analysis*, 52(1):121–132.
- Staszewska-Bystrova, A. (2011). Bootstrap prediction bands for forecast paths from vector autoregressive models. *Journal of Forecasting*, 30(8):721–735.
- Wolf, M. and Wunderli, D. (2015). Bootstrap joint prediction regions. *Journal of Time Series Analysis*, 36(3):352–376.

Chapter 2

A Comparison of Several Methods to Compute Joint Prediction Regions for Path Forecasts

Abstract

Path forecasts, defined as sequences of individual forecasts, generated by vector autoregressions are widely used in applied work. It has been recognized that a profound econometric analysis often requires, besides the path forecast, a joint prediction region that contains the entire future path with a prespecified coverage probability, at least asymptotically. The forecasting literature offers several different methods for computing joint prediction regions. The aim of this paper is to investigate the finite-sample performance of five methods for constructing joint prediction regions via extensive Monte Carlo simulations.

JEL classification: C15, C32, C53

Keywords: Path Forecast; Joint Prediction Region; Monte Carlo Simulation.

2.1 Introduction

Prediction is one of the key objectives in wide areas of applied time series analysis. This problem corresponds to the following representative scenario: Given an observed k -dimensional time series $\{y_1, \dots, y_T\}$, one is interested in predicting the future path of one of the variables, that is, $\{\hat{y}_{T,i}(1), \dots, \hat{y}_{T,i}(H)\}$ for some $H \in \mathbb{N}_{>0}$ and $i \in \{1, \dots, k\}$. For example, national banks publish predictions of the monthly core inflation for the next twelve months and commercial banks publish predictions of government bond yields over several time periods.

One of the workhorse models used for the computation of a path forecast $\hat{Y}_{T,i}(H) := (\hat{y}_{T,i}(1), \dots, \hat{y}_{T,i}(H))'$ in applied work is the vector autoregression (VAR) originally proposed by [Sims \(1980\)](#). According to [Stock and Watson \(2001\)](#), the reasons for the widespread use of the VAR model are its simplicity and yet the capability of capturing rich dynamics in multivariate time series. Current research involving path forecasts generated by VAR models includes for example [Baumeister and Kilian \(2015\)](#).

Nevertheless, the amount of information about the future path of the variable of interest that is actually obtained by computing $\hat{Y}_{T,i}(H)$ is almost negligible because the future path will be different from the path forecast generated by a VAR model with probability one, at least for continuous distributions of the involved variables. Thus, a profound econometric analysis often requires, besides $\hat{Y}_{T,i}(H)$, information about the uncertainty about the *entire* future path $Y_{T,H,i} := (y_{T+1,i}, \dots, y_{T+H,i})'$. In other words, there is a need for a *joint prediction region* (JPR) that contains the entire future path with a prespecified nominal coverage probability.

In the context of VAR models, the current literature offers a wide variety of different methods to construct a joint prediction region for $Y_{T,H,i}$ with prespecified coverage probability $(1 - \alpha)$. [Jordà and Marcellino \(2010\)](#) propose an analytic method to construct a rectangular and symmetric joint prediction region. The method is on the one hand based on the assumption that the conditional distribution of the prediction errors is asymptotically normal and on the other hand on the application of results by [Scheffé \(1953, 1959\)](#) and [Bowden \(1970\)](#). [Staszewska-Bystrova \(2011\)](#) proposes a heuristic bootstrap-based method. The rectangular joint prediction region with coverage probability $(1 - \alpha)$ is constructed as the envelope of the remaining $(1 - \alpha)\%$ of generated conditional boot-

strap paths that survived a heuristic iterative elimination procedure. [Staszewska-Bystrova and Winker \(2013\)](#) refine the method of [Staszewska-Bystrova \(2011\)](#) in the sense that a threshold accepting optimization heuristic is applied on the generated conditional bootstrap paths in order to construct a joint prediction region for $Y_{T,H,i}$. [Wolf and Wunderli \(2015\)](#) propose a bootstrap method that produces a rectangular joint prediction region based on the bootstrap predictive distribution of the standardized prediction errors. Finally, [Lütkepohl et al. \(2015\)](#) propose a Bonferroni-type method for the construction of joint confidence bands for orthogonalized impulse response functions of VAR models. However, the proposed method can directly be adapted in the present context of joint prediction regions for paths forecasts generated by VAR's.

The aim of this paper is to compare the finite-sample properties of methods, that have not been investigated yet, with the properties of two established benchmark methods through an extensive Monte Carlo study. In the first group, there are the symmetric JPR of [Wolf and Wunderli \(2015\)](#), the asymmetric, ‘equal-tailed’ JPR of [Wolf and Wunderli \(2015\)](#) and the adjusted Bonferroni JPR of [Lütkepohl et al. \(2015\)](#). The group of benchmark methods consists on the one hand of the JPR of [Staszewska-Bystrova \(2011\)](#), because several Monte Carlo studies¹ have shown its reliable performance in various scenarios, and on the other hand of the standard Bonferroni JPR, because this allows to compare the performance of the adjusted Bonferroni JPR to its unadjusted counterpart.

The methods of [Jordà and Marcellino \(2010\)](#) and [Staszewska-Bystrova and Winker \(2013\)](#) are omitted for the following reasons: First, it has already been demonstrated in various Monte Carlo studies² that the method [Jordà and Marcellino \(2010\)](#) suffers from severe undercoverage in many scenarios³. Second, the performance of the threshold accepting optimization heuristic of [Staszewska-Bystrova and Winker \(2013\)](#) is, although the method is computationally very demanding, generally not superior to the one of [Staszewska-Bystrova \(2011\)](#); see [Staszewska-Bystrova and Winker \(2013, Section 4\)](#).

The Monte Carlo study is designed to primarily focus on the following issues regarding their effect on the finite-sample properties of the various JPRs: estimation of the lag order

¹See [Staszewska-Bystrova \(2011\)](#) and [Staszewska-Bystrova and Winker \(2013\)](#)

²See [Staszewska-Bystrova \(2011, 2013\)](#), [Staszewska-Bystrova and Winker \(2013\)](#) and [Wolf and Wunderli \(2015\)](#).

³[Staszewska-Bystrova \(2013\)](#) proposes an modification of the joint prediction region of [Jordà and Marcellino \(2010\)](#). The simulation study of [Staszewska-Bystrova \(2013\)](#) indicates that the modification improves the performances but there is still severe undercoverage for some scenarios.

of the VAR, stationarity characteristics of the underlying data generating processes, non-normal error distributions, the dimension of the VAR process and model misspecification.

The remainder of the paper is organized as follows. Section 2.2 introduces vector autoregressive processes, Section 2.3 presents the different methods of constructing joint prediction regions, Section 4H describes the employed bootstrap algorithm, Section 2.5 describes in detail the Monte Carlo study and presents the results of the simulation study, Section 2.6 presents an empirical application, and Section 2.7 concludes.

2.2 The Model

2.2.1 Vector Autoregression

Consider a k -dimensional VAR(p) process:

$$y_t = \nu + A_1 y_{t-1} + \dots + A_p y_{t-p} + \epsilon_t , \quad (2.1)$$

where y_t is a k -dimensional random vector, the A_i are fixed $k \times k$ coefficient matrices, ν is a k -dimensional vector of fixed intercept terms, and $\{\epsilon_t\}$ is a k -dimensional i.i.d. process with $\mathbb{E}[\epsilon_t] = 0$ and $\mathbb{E}[\epsilon_t \epsilon_t'] = \Sigma_\epsilon$. The covariance matrix Σ_ϵ is assumed to be positive definite with finite elements. Any VAR(p) process has a kp -dimensional VAR(1) representation

$$Y_t = V + \mathbf{A} Y_{t-1} + U_t ,$$

where

$$Y_t := \begin{bmatrix} y_t \\ y_{t-1} \\ \vdots \\ y_{t-p+1} \end{bmatrix}, V := \begin{bmatrix} \nu \\ 0 \\ \vdots \\ 0 \end{bmatrix}, \mathbf{A} := \begin{bmatrix} A_1 & A_2 & \cdots & A_{p-1} & A_p \\ I_k & 0 & \cdots & 0 & 0 \\ 0 & I_k & \cdots & 0 & 0 \\ \vdots & \vdots & \ddots & \vdots & \vdots \\ 0 & 0 & \cdots & I_k & 0 \end{bmatrix} \text{ and } U_t := \begin{bmatrix} \epsilon_t \\ 0 \\ \vdots \\ 0 \end{bmatrix} .$$

A VAR(p) process is stable and stationary if

$$\det(I_k - A_1 z^1 - \dots - A_p z^p) \neq 0 \quad \text{for } z \in \mathbb{C}, |z| \leq 1 .$$

A stationary VAR(p) process admits a Wold vector moving average (VMA) representation of the following form

$$y_t = \mu + \sum_{i=0}^{+\infty} \phi_i \epsilon_{t-i} ,$$

where $\mu := \mathbb{E}[y_t] = (I_k - A_1 - \dots - A_p)^{-1} \nu$ and the ϕ_i are fixed $k \times k$ VMA-coefficient matrices.

2.2.2 Estimation and Finite-Sample Bias

The parameters of a VAR(p) process, $\beta := \text{vec}(\nu, A_1, \dots, A_p)$, are consistently estimated by the standard procedure of least squares (LS). The LS estimator can be written in the following closed form expression $\hat{\beta}_{LS} = ((ZZ')Z \otimes I_k)y$, where $Z = [Z_0, \dots, Z_T]_{[(kp+1) \times T]}$ with $Z'_t := [1 \ y'_t \dots y'_{t-p+1}]$ and $y := \text{vec}((y_1, \dots, y_T))$.

The number of lags, if unknown, is estimated by minimizing the Bayesian information criterion⁴ (BIC) over a compact set of lag orders $S \subset \mathbb{N}_{>0}$

$$\hat{p}_{BIC} \in \arg \min_{m \in S \subset \mathbb{N}_{>0}} \text{BIC}(m) = \log \left(\left| \hat{\Sigma}_\epsilon(m) \right| \right) + \frac{\log(T)}{T} m k^2 ,$$

where $|\hat{\Sigma}_\epsilon(m)|$ denotes the determinant of the estimated covariance matrix of ϵ_t based on a VAR(m) process. The BIC is a consistent order selection criterion, that is, $\hat{p}_{BIC} \xrightarrow{p} p$, where \xrightarrow{p} denotes convergence in probability as $T \rightarrow \infty$. A more detailed discussion about parameter estimation and the order selection in vector autoregressions can be found in [Lütkepohl \(2005, Sections 3–4\)](#).

It is a well-known fact that the presence of lagged endogenous variables in vector autoregressions entails that the LS estimator of β is biased in finite samples, that is, $\mathbb{E}[\hat{\beta}_{LS}] \neq \beta$. As a consequence, correcting the LS estimator $\hat{\beta}_{LS}$ for its bias is desirable.

⁴Alternatively, the lag order can be estimated using the Akaike information criterion (AIC) or the corrected Akaike information criterion (AICc) of [Hurvich and Tsai \(1993\)](#). However, using the BIC results in a more parsimonious model.

The literature offers two basic approaches of estimating the finite-sample bias of the least squares estimator: bias estimators based on closed-form formulas and bias estimators based on bootstrap techniques.

Closed-form formulas have been derived by [Yamamoto and Kunitomo \(1981\)](#), [Nicholls and Pope \(1988\)](#) and [Pope \(1990\)](#)⁵. The closed-form formulas are all based on asymptotic approximations of the finite-sample distribution of the least squares estimator. Using asymptotic approximations removes the bias up to first order; for details see [Yamamoto and Kunitomo \(1981\)](#) or [Pope \(1990\)](#). [Engsted and Pedersen \(2014\)](#) show that the formula of [Yamamoto and Kunitomo \(1981\)](#) and [Pope \(1990\)](#) are, although independently developed, in fact numerically identical. From a computational point of view these closed-form solutions are easy to implement and fast in terms of execution time.

A nonparametric bootstrap procedure to estimate the bias can be found in [Kilian \(1998\)](#). This bootstrap procedure removes the first-order bias of the LS estimator; see [Kilian \(1998\)](#) for details. The bootstrap procedure is also straightforward to implement, but the computational burden is substantial, which makes it less practical for a Monte Carlo study⁶.

Taking into account the trade-off between fast execution and accuracy of parameter estimates, the choice falls on the bias correction of [Pope \(1990\)](#). Choosing the closed-form formulas of [Pope \(1990\)](#) can be justified by the simulation study of [Engsted and Pedersen \(2014\)](#), which shows for one thing that both approaches indeed yield a significant reduction in bias in finite samples and for another thing that the performance in terms of bias reduction of both approaches is very similar for stationary processes.

[Pope \(1990\)](#) derives the following approximation for the bias of $\hat{\mathbf{A}}$:

$$\text{Bias}(\hat{\mathbf{A}}) = -\frac{b}{T} + \mathcal{O}(T^{-\frac{3}{2}}), \quad (2.2)$$

⁵[Pope \(1990\)](#) presents the same bias formula as [Nicholls and Pope \(1988\)](#) but shows that it is still valid under milder assumptions than in the work of [Nicholls and Pope \(1988\)](#).

⁶[Bauer et al. \(2012\)](#) propose a refined nonparametric bootstrap approach, the so-called “inverse bootstrap bias correction”. In their simulation study it is shown that the inverse bootstrap method yields a slightly more accurate bias estimate than the bootstrap method of [Kilian \(1998\)](#) and the closed-form solution of [Pope \(1990\)](#). However, this improvement comes at the cost of an even greater computational burden than the bootstrap procedure of [Kilian \(1998\)](#).

where

$$b := \Sigma_U \left[(I_{kp} - \mathbf{A})^{-1} + \mathbf{A}' \left(I_{kp} - (\mathbf{A}')^2 \right)^{-1} + \sum_{i=1}^k \lambda_i (I_{kp} - \lambda_i \mathbf{A}')^{-1} \right] \Sigma_Y^{-1} .$$

Here, I_{kp} denotes the $kp \times kp$ identity matrix, λ_i denotes the i -th eigenvalue of \mathbf{A} , Σ_Y denotes the covariance matrix of Y_t and Σ_U denotes the covariance matrix of U_t . Neglecting higher-order terms and replacing true parameters by its LS estimators yields the following estimator for the finite-sample bias of $\hat{\mathbf{A}}$ and \hat{V}

$$\widehat{\text{Bias}}(\hat{\mathbf{A}}) := -\frac{1}{T} \hat{\Sigma}_U \left[\left(I_{kp} - \hat{\mathbf{A}} \right)^{-1} + \hat{\mathbf{A}}' \left(I_{kp} - (\hat{\mathbf{A}}')^2 \right)^{-1} + \sum_{i=1}^k \hat{\lambda}_i \left(I_{kp} - \hat{\lambda}_i \hat{\mathbf{A}}' \right)^{-1} \right] \hat{\Sigma}_Y^{-1}$$

$$\widehat{\text{Bias}}(\hat{V}) := -\widehat{\text{Bias}}(\hat{\mathbf{A}}) \left(I_{kp} - \hat{\mathbf{A}} \right)^{-1} \hat{V} .$$

The bias-corrected parameter estimators are then given by

$$\hat{\mathbf{A}}^{BC} := \hat{\mathbf{A}}_{LS} - \widehat{\text{Bias}}(\hat{\mathbf{A}}) \quad \text{and} \quad \hat{V}^{BC} := \hat{V}_{LS} - \widehat{\text{Bias}}(\hat{V}) ,$$

and $\hat{\beta}_{LS}^{BC} := \text{vec}(\hat{V}^{BC}, \hat{A}_1^{BC}, \dots, \hat{A}_p^{BC})$.

Remark 2.2.1 It is in general possible that the parameter estimate is pushed into the non-stationarity region through the bias-correction, that is, the process corresponding to $\hat{\mathbf{A}}_{LS}$ is stationary, whereas the process corresponding to $\hat{\mathbf{A}}^{BC}$ is non-stationary. In order to avoid such scenarios, [Kilian \(1998\)](#) proposes a stationarity correction that shrinks the bias estimate until the estimated process is stationary; for more details see [Kilian \(1998, p.220\)](#). This stationarity correction is applied in the Monte Carlo simulation. ■

2.2.3 Path Forecast and Prediction Error

A path forecast of length H for the i -th variable of a $\text{VAR}(p)$ process, based on an observed time series of length T , consists of the concatenation of H individual point forecasts and is denoted by

$$\hat{Y}_{T,i}(H) := (\hat{y}_{T,i}(1), \dots, \hat{y}_{T,i}(H))', \quad \text{for } i = 1, \dots, k .$$

Given an estimator $\tilde{\beta}$ for the parameters of the VAR(p) process, the individual point forecasts are computed via the following standard forecasting recursion:

$$\hat{y}_T(h) = \tilde{\nu} + \tilde{A}_1 \hat{y}_T(h-1) + \cdots + \tilde{A}_p \hat{y}_T(h-p), \quad \text{for } h = 1, \dots, H, \quad (2.3)$$

where $\hat{y}_T(j) = y_{T-j}$ if $j \leq 0$. Using the bias-corrected LS estimators $\hat{\beta}_{LS}^{BC}$ yields the path forecast $\hat{Y}_{T,i}^{BC}(H)$, which will be used in the Monte Carlo simulation throughout.

The estimated prediction error for $h \in \{1, \dots, H\}$ is given by $\hat{u}_{T+h} := y_{T+h} - \hat{y}_T(h)$. Following the standard literature⁷, there are two estimators of the covariance matrix of \hat{u}_{T+h} :

$$\hat{\Sigma}_y(h) = \sum_{i=0}^{h-1} \hat{\phi}_i \hat{\Sigma}_\epsilon \hat{\phi}_i' \quad \text{and} \quad \hat{\Sigma}_{\hat{y}}(h) = \sum_{i=0}^{h-1} \hat{\phi}_i \hat{\Sigma}_\epsilon \hat{\phi}_i' + \frac{\hat{\Omega}(h)}{T},$$

where an explicit formula for $\hat{\Omega}(h)$ can be found in [Lütkepohl \(2005, Section 3.5.2\)](#). $\hat{\Sigma}_{\hat{y}}(h)$ incorporates the uncertainty originated from the estimation of the parameters. Thus, there are four different estimators of the forecast error covariance matrix

$$\hat{\Sigma}_y(h) \quad , \quad \hat{\Sigma}_y^{BC}(h) \quad , \quad \hat{\Sigma}_{\hat{y}}(h) \quad \text{and} \quad \hat{\Sigma}_{\hat{y}}^{BC}(h). \quad (2.4)$$

2.3 Joint Prediction Regions

2.3.1 Bonferroni-type JPRs

The Bonferroni joint prediction region for $Y_{T,H,i}$ consists of the Cartesian product of the marginal prediction intervals for each horizon $h \in \{1, \dots, H\}$. The nominal coverage level of the marginal intervals is equal to $(1 - \alpha/H)$, determined according to Bonferroni's inequality to ensure that the joint coverage level is asymptotically at least at the pre-specified level $(1 - \alpha)$. Thus, the rectangular Bonferroni joint prediction region is given by

$$\text{JPR}_{\text{Bon}}^{(1-\alpha)} := [q_{1,\alpha/2H}^*, q_{1,1-\alpha/2H}^*] \times \cdots \times [q_{H,\alpha/2H}^*, q_{H,1-\alpha/2H}^*], \quad (2.5)$$

⁷See for example [Lütkepohl \(2005, Section 3.5\)](#).

where $q_{h,\alpha/2H}^*$ and $q_{h,1-\alpha/2H}^*$ denote the $\alpha/2H$ quantile and the $1 - \alpha/2H$ quantile, respectively, of the bootstrap predictive distribution at horizon $h \in \{1, \dots, H\}$.

Lütkepohl et al. (2015) propose an adjustment procedure that reduces the volume of Bonferroni confidence bands for structural impulse response function in order to obtain an asymptotic coverage that is closer to $(1 - \alpha)$. Apparently, the construction of the Bonferroni-JPR is conceptually identical to the construction of Bonferroni confidence bands, and hence the adjustment of Lütkepohl et al. (2015) can be applied to narrow the Bonferroni-JPR and reduce the asymptotic coverage bias.

The procedure of Lütkepohl et al. (2015) works as follows: First, construct the envelope of all bootstrap continuations $Y_{T,H,i,b}^* := (y_{T+1,i,b}^*, \dots, y_{T+H,i,b}^*)'$ that are completely covered by the Bonferroni joint prediction region (2.5) and denote their number by N_B ⁸. Second, apply a sequential procedure that removes $N_B - (1 - \alpha) \times B$ bootstrap continuations. More specifically, in each step, the bootstrap continuations that provide at least one point on the current (adjusted) joint prediction region are identified⁹. The continuation that contributes the most to the volume of the current joint prediction region is removed and the new joint prediction region is the envelope of the remaining continuations. The procedure terminates when there are exactly $(1 - \alpha) \times B$ continuations left. Thus, the rectangular Adjusted-Bonferroni joint prediction region for $Y_{T,i,H}$ is given by

$$\text{JPR}_{\text{Adj.-Bon}}^{(1-\alpha)} := [l_{1,(1-\alpha)}^*, u_{1,(1-\alpha)}^*] \times \dots \times [l_{H,(1-\alpha)}^*, u_{H,(1-\alpha)}^*] , \quad (2.6)$$

where $l_{i,(1-\alpha)}^*$ denotes the lower bound of the envelope of the remaining $(1 - \alpha) \times B$ bootstrap continuations at forecast horizon $i \in \{1, \dots, H\}$ and $u_{i,(1-\alpha)}^*$ denotes the corresponding upper bound.

2.3.2 Bootstrap JPR

The method of Wolf and Wunderli (2015) is based on the bootstrap distribution of the vector of standardized prediction errors

$$\hat{S}_{T,b,i}^*(H) := (\hat{u}_{T,i,b}^*(1)/\hat{\sigma}_{T,i,b}^*(1), \dots, \hat{u}_{T,i,b}^*(H)/\hat{\sigma}_{T,i,b}^*(H))' ,$$

⁸By construction of $\text{JPR}_{\text{Bonf}}^{(1-\alpha)}$, N_B is larger than $(1 - \alpha) \times B$.

⁹There are at most $2H$ such continuations.

where $\hat{u}_{T,i,b}^*(h) := \hat{y}_{T,i,b}^*(h) - y_{T+h,i,b}^*$, $\hat{y}_{T,i,b}^*(h)$ denotes the forecast at horizon h based on $\hat{\beta}_{LS}^{*,BC}$ and $\hat{\sigma}_{T,b}^*(h)$ denotes the prediction standard error at forecast horizon $h \in \{1, \dots, H\}$ based on the b -th bootstrap sample. Subsequently, obtain the empirical distribution of $\max_{H,b}^{\|\cdot\|,*} := \|\hat{S}_{T,b,i}^*(H)\|_\infty$, where $\|\cdot\|_\infty$ denotes the maximum norm¹⁰. The symmetric and rectangular joint prediction region of [Wolf and Wunderli \(2015\)](#) with a nominal coverage of $(1 - \alpha)$ is then given by

$$\text{JPR}_{\text{Sym-WW}}^{(1-\alpha)} := \left[\hat{y}_{T,i}(1) \pm \hat{d}_{|\cdot|,(1-\alpha)}^{\max,*} \cdot \hat{\sigma}_{T,i}^{BC}(1) \right] \times \dots \times \left[\hat{y}_{T,i}(H) \pm \hat{d}_{|\cdot|,(1-\alpha)}^{\max,*} \cdot \hat{\sigma}_{T,i}^{BC}(H) \right], \quad (2.7)$$

where $\hat{y}_{T,i}(h)$ denotes the point forecast at horizon $h \in \{1, \dots, H\}$, $\hat{d}_{|\cdot|,(1-\alpha)}^{\max,*}$ denotes the $(1 - \alpha)$ quantile of the empirical distribution of $\max_{H,b}^{\|\cdot\|,*}$ and $\hat{\sigma}_{T,i}(h)$ denotes the prediction standard error at forecast period $h \in \{1, \dots, H\}$. The bootstrap procedure incorporates the estimation uncertainty through parameter re-estimation. Thus, $\hat{\sigma}_{T,i}(h)$ is given by the square root of the (i, i) -th element of the estimator of the variance matrix of the prediction error that does not incorporate the estimation uncertainty, that is, $\hat{\Sigma}_y^{BC}(h)$.

Furthermore, the method of [Wolf and Wunderli \(2015\)](#) allows the construction of an asymmetric, ‘equal-tailed’ joint prediction region for $Y_{T,H,i}$. More specifically, the asymmetric joint prediction region is given as the intersection of a one-sided lower joint prediction region and a one-sided upper joint prediction region, that is,

$$\text{JPR}_{\text{Asy-WW}}^{(1-\alpha)} := \text{JPR}_{\text{lower}}^{(1-\alpha/2)} \cap \text{JPR}_{\text{upper}}^{(1-\alpha/2)}. \quad (2.8)$$

Using the formulas in [Wolf and Wunderli \(2015, p.358\)](#), the asymmetric joint prediction region in (2.8) can be rewritten as

$$\text{JPR}_{\text{Asy-WW}}^{(1-\alpha)} = \left[\hat{y}_{T,i}(1) - \hat{d}_{(1-\alpha/2)}^{\max,*} \cdot \hat{\sigma}_{T,i}^{BC}(1), \hat{y}_{T,i}(1) - \hat{d}_{\alpha/2}^{\min,*} \cdot \hat{\sigma}_{T,i}^{BC}(1) \right] \times \dots \times \left[\hat{y}_{T,i}(H) - \hat{d}_{(1-\alpha/2)}^{\max,*} \cdot \hat{\sigma}_{T,i}^{BC}(H), \hat{y}_{T,i}(H) - \hat{d}_{\alpha/2}^{\min,*} \cdot \hat{\sigma}_{T,i}^{BC}(H) \right], \quad (2.9)$$

where $\hat{d}_{(1-\alpha/2)}^{\max,*}$ denotes the $(1 - \alpha/2)$ quantile of the empirical distribution of $\max_{H,b}^* := \max \left(\hat{S}_{T,b,i}^*(H) \right)$, $\hat{d}_{\alpha/2}^{\min,*}$ denotes the $\alpha/2$ quantile of the empirical distribution of $\min_{H,b}^* :=$

¹⁰For $x \in \mathbb{R}^d$, the maximum norm is defined as $\|x\|_\infty := \max \{|x_1|, \dots, |x_d|\}$.

$\min \left(\hat{S}_{T,b,i}^*(H) \right)$ and $\hat{\sigma}_{T,i}^{BC}(h)$ is the same estimator as in the symmetric case, that is, $\hat{\sigma}_{T,i}^{BC}(h) = \sqrt{\hat{\Sigma}_y^{BC}(h)_{ii}}$.

Remark 2.3.1 In general, the method of [Wolf and Wunderli \(2015\)](#) allows the construction of a joint prediction region for $Y_{T,H,i}$ that controls the generalized familywise error k -FWE $:= \mathbb{P}(\text{at least } k \text{ of the } y_{T+h,i} \text{ are not contained in the JPR})$. In other words, such a JPR then covers at least $H - k + 1$ elements of the path forecast with probability $(1 - \alpha)$, for more details see [Wolf and Wunderli \(2015, p.356\)](#). However, for the sake of comparability with the other methods of constructing a joint prediction region, only the case $k = 1$, that is all elements of $Y_{T,H,i}$ are covered with a prespecified probability $(1 - \alpha)$, is included in the Monte Carlo study. ■

2.3.3 Neighbouring Path JPR

The neighbouring path (NP) method of [Staszewska-Bystrova \(2011\)](#) is based on the bootstrap distribution of $Y_{T,H,i}^*$. The transformation of the predictive bootstrap distribution into a joint prediction region is then made by the following heuristic iterative procedure: Remove the particular bootstrap path $Y_{T,H,i,b}^*$ that is the furthest away from the path forecast $\hat{Y}_{T,i}^{BC}(H)$, where the distance is measured by the (squared) Euclidean norm¹¹. Repeat this procedure until a total of $\alpha \times B$ bootstrap paths are removed. The NP joint prediction region for $Y_{T,H,i}$ with a nominal coverage of $(1 - \alpha)$ is then given by the envelope of the remaining $(1 - \alpha) \times B$ paths, that is

$$\text{JPR}_{\text{NP}} := [l_{1,(1-\alpha)}^*, u_{1,(1-\alpha)}^*] \times \cdots \times [l_{H,(1-\alpha)}^*, u_{H,(1-\alpha)}^*], \quad (2.10)$$

where $l_{h,(1-\alpha)}^*$ denotes the lower bound of the envelope of the remaining $(1 - \alpha) \times B$ bootstrap paths at forecast horizon $h \in \{1, \dots, H\}$ and $u_{h,(1-\alpha)}^*$ denotes the corresponding upper bound. Note that the joint prediction region of [Staszewska-Bystrova \(2011\)](#) is not symmetric about $\hat{Y}_{T,i}^{BC}$ and has a jagged shape due to its way of construction. A further discussion about the NP method is found in [Wolf and Wunderli \(2015, Section 3.3\)](#).

¹¹Alternatively, [Staszewska-Bystrova \(2011\)](#) suggests the L_1 -norm, that is $\sum_{h=1}^H |\hat{y}_{T,i}(h) - y_{T+h,i}^*|$. However, the Euclidian norm seems to work better according to the simulation study in [Staszewska-Bystrova \(2011\)](#).

Remark 2.3.2 The method of [Staszewska-Bystrova and Winker \(2013\)](#) basically replaces the heuristic iterative elimination procedure of [Staszewska-Bystrova \(2011\)](#) by a sophisticated threshold accepting optimization heuristic. However, the computational burden of the proposed threshold accepting method is enormous and the extensive simulation study of [Staszewska-Bystrova and Winker \(2013\)](#) demonstrates that the NP Heuristic method of [Staszewska-Bystrova \(2011\)](#) generally outperforms the method of [Staszewska-Bystrova and Winker \(2013\)](#). Thus, in order to be able to conduct the simulation study within a reasonable amount of time, the threshold accepting method is omitted. ■

2.4 Bootstrap Details

Bootstrap data $\{y_1^*, \dots, y_T^*\}$ and $\{y_{T+1}^*, \dots, y_{T+H}^*\}$ are generated by the following four-step bootstrap algorithm of [Fresoli et al. \(2015\)](#):

1. Given \hat{p}_{BIC} , $\hat{\beta}_{LS}^{BC}$, $\{y_t\}_{t=1}^T$ and the corresponding series of centered and rescaled¹² residuals $\{\hat{\epsilon}_t\}_{t=p+1}^T$, generate a bootstrap sample $\{y_1^*, \dots, y_T^*\}$ via the following recursion

$$y_t^* = \begin{cases} y_t & \text{if } t = 1, \dots, p \\ \hat{\nu}^{BC} + \hat{A}_1^{BC} y_{t-1}^* + \dots + \hat{A}_p^{BC} y_{t-p}^* + e_t^* & \text{if } t = p+1, \dots, T \end{cases}, \quad (2.11)$$

where e_t^* is a random draw with replacement from the empirical distribution of $\{\hat{\epsilon}_t\}_{t=p+1}^T$.

2. Re-estimate the lag order \hat{p}_{BIC}^* and obtain $\hat{\beta}_{LS}^{*,BC} := (\hat{\nu}^{*,BC}, \hat{A}_1^{*,BC}, \dots, \hat{A}_{\hat{p}^*}^{*,BC})$ by fitting a $\text{VAR}(\hat{p}_{BIC}^*)$ model to the bootstrap sample $\{y_1^*, \dots, y_T^*\}$.
3. Generate $\{y_{T+1}^*, \dots, y_{T+H}^*\}$ conditional on $\{y_1, \dots, y_T\}$ via

$$y_{T+h}^* = \nu^* + \hat{A}_1^* y_{T+h-1}^* + \dots + \hat{A}_{\hat{p}^*}^* y_{T+h-p}^* + e_h^*, \quad \text{for } h = 1, \dots, H,$$

where $y_{T+j}^* = y_{T+j}$ if $j \leq 0$ and e_h^* is a random draw with replacement from the empirical distribution of $\{\hat{\epsilon}_t\}_{t=p+1}^T$.

4. Repeat steps 1–3 B times.

¹²The centering and rescaling is carried out as suggested in [Stine \(1987\)](#).

The bootstrap algorithm of [Fresoli et al. \(2015\)](#) is asymptotically valid under some regularity conditions, that is, $\hat{Y}_{T,H,i}^* := (y_{T+1,i}^*, \dots, y_{T+H,i}^*)'$ conditional on $\{y_1, \dots, y_T\}$ converges weakly in probability to $Y_{T,H,i}$ as $T \rightarrow \infty$; for the proof see [Fresoli et al. \(2015, p.839\)](#).

Remark 2.4.1 The previously outlined bootstrap algorithm differs from the original algorithm in [Fresoli et al. \(2015\)](#) in two minor aspects. First, the LS parameter estimates are corrected for their finite-sample bias using the bias formula of [Pope \(1990\)](#). Second, the lag order is endogenized in the sense that p_{BIC}^* is re-estimated for each bootstrap sample. However, both modifications do not affect the asymptotic validity of the bootstrap algorithm. ■

Remark 2.4.2 In [Staszewska-Bystrova \(2011\)](#), the bootstrap data is actually generated using the bootstrap-after-bootstrap procedure of [Kim \(2001\)](#). In contrast to the previously outlined procedure of [Fresoli et al. \(2015\)](#), the procedure of [Kim \(2001\)](#) is based on the backward representation of a VAR(p) model. However, using the backward representation for generating bootstrap predictive distributions has some serious disadvantages; for a discussion see [Fresoli et al. \(2015, Section 1\)](#). The similar finite-sample performance of both approaches justifies the use of the [Fresoli et al. \(2015\)](#) bootstrap instead of the bootstrap-after-bootstrap procedure. ■

2.5 Monte Carlo Simulation

2.5.1 Data Generating Processes

Bivariate VAR(1) Models

The basis data generating process (DGP) is the following bivariate VAR(1) process previously used in [Amihud and Hurvich \(2004\)](#), [Amihud et al. \(2009\)](#), and [Engsted and Pedersen \(2014\)](#):

$$\text{DGP-1: } y_t = \begin{pmatrix} 1 \\ 1 \end{pmatrix} + \begin{pmatrix} 0.80 & 0.10 \\ 0.10 & 0.85 \end{pmatrix} y_{t-1} + \epsilon_t . \quad (2.12)$$

The characteristic roots of the process in (3.2) are $\rho_1 = (1.385, 1.077)'$. Thus, the process is stationary but persistent since the smallest root is close to unity. Furthermore, in order to cover a broader range of stationarity characteristics, the DGP's corresponding to the following slope coefficient matrices are investigated:

$$A_2 := \begin{pmatrix} -0.80 & 0.10 \\ 0.10 & -0.85 \end{pmatrix}, \quad A_3 := \begin{pmatrix} 0.30 & 0.10 \\ 0.10 & 0.35 \end{pmatrix},$$

$$A_4 := \begin{pmatrix} -0.30 & 0.10 \\ 0.10 & -0.35 \end{pmatrix}, \quad A_5 := \begin{pmatrix} 1.00 & 0.00 \\ 0.10 & 0.85 \end{pmatrix},$$

where DGP- i corresponds to A_i , $i \in \{2, \dots, 5\}$. The characteristic roots of all five DGP's are presented in Table 2.1. The roots of DGP-1–DGP-4 are all within the stationary

DGP	Roots
1	(1.385, 1.077)
2	(-1.385, -1.077)
3	(2.336, 4.506)
4	(-2.336, -4.506)
5	(1.000, 1.177)

Table 2.1: Characteristic roots of DGP1–DGP5.

region, but DGP-5 has an exact unit root and is therefore non-stationary. The consequences of the unit root are far-reaching, for example, the LS estimator of β is no longer consistent and the bootstrap procedure of [Fresoli et al. \(2015\)](#) is no longer asymptotically valid. However, in the Monte Carlo simulation the presence of the unit root in DGP-5 is ignored and the same methodology as for DGP-1–DGP-4 is applied.

Trivariate VAR(4) Model

DGP-6 is a more realistic trivariate VAR(4) process previously considered in [Staszewska-Bystrova \(2011\)](#) and [Jordà and Marcellino \(2010\)](#). More specifically, the parameters are the estimates of a model of inflation, the unemployment rate and the federal fund rate¹³

¹³For more details about the used data set, see [Staszewska-Bystrova \(2011\)](#) or [Jordà and Marcellino \(2010\)](#).

using US quarterly data from 1960Q1 through 2004Q1. The DGP is given by

$$\text{DGP-6: } y_t = \nu + \tilde{A}_1 y_{t-1} + \tilde{A}_2 y_{t-2} + \tilde{A}_3 y_{t-3} + \tilde{A}_4 y_{t-4} + \epsilon_t, \quad (2.13)$$

where

$$\tilde{A}_1 := \begin{pmatrix} 0.549 & -0.965 & 0.164 \\ 0.029 & 1.480 & 0.003 \\ 0.084 & -1.567 & 0.962 \end{pmatrix}, \quad \tilde{A}_2 := \begin{pmatrix} 0.118 & 1.506 & -0.128 \\ -0.013 & -0.494 & 0.043 \\ 0.197 & 1.763 & -0.364 \end{pmatrix},$$

$$\tilde{A}_3 := \begin{pmatrix} 0.060 & -0.954 & 0.054 \\ 0.002 & -0.029 & -0.024 \\ -0.070 & -0.848 & 0.333 \end{pmatrix}, \quad \tilde{A}_4 := \begin{pmatrix} 0.261 & 0.250 & -0.098 \\ -0.012 & -0.014 & 0.008 \\ -0.046 & 0.563 & -0.010 \end{pmatrix},$$

and $\nu := (1.076, 0.125, 0.347)'$.

Six-variate VAR(2) Model

DGP-7 is a six-variate VAR(2) process previously considered in the Monte Carlo study of [Staszewska-Bystrova and Winker \(2013\)](#). The process is based on an empirical model for corporate bond spreads presented in the financial stability report of the Deutsche Bundesbank (2005, p.145ff)¹⁴. The data set is provided by [Staszewska-Bystrova and Winker \(2013\)](#)¹⁵ and consists of monthly data from January 1999 through December 2007. The population parameters are estimated by bias-corrected least squares and the resulting coefficient matrices are provided in Appendix [2A](#).

Error Processes

The error process $\{\epsilon_t\}$ is assumed to be an independent and identically distributed (i.i.d.) process according to one of the following three distributions:

- $\epsilon_t \sim \mathcal{N}(0, \Sigma_\epsilon)$. A multivariate normal distribution with covariance matrix Σ_ϵ .

¹⁴[Staszewska-Bystrova and Winker \(2014\)](#) studied the same model with regard to its forecasting performance.

¹⁵The data set of [Staszewska-Bystrova and Winker \(2013\)](#) differs in some minor aspects from the original data set of the Deutsche Bundesbank, for details see [Staszewska-Bystrova and Winker \(2013\)](#) and [Staszewska-Bystrova and Winker \(2014\)](#).

- $\epsilon_t := \frac{1}{\sqrt{3}} \times \tilde{\epsilon}$, where $\tilde{\epsilon}_t$ follows a multivariate t -distribution with 3 degrees of freedom and scale matrix Σ_ϵ . The variance of ϵ_t is then given by Σ_ϵ . In the following, this distribution of ϵ_t is just called $t(3)$ -distribution.
- $\epsilon_t := C \left(\frac{1}{\sqrt{6}} \times (\tilde{\epsilon}_t - 3_{[k \times 1]}) \right)$. $\tilde{\epsilon}_t$ is a k -dimensional vector, where each component is χ^2 distributed with 3 degrees of freedom. The pre-multiplication of the centered and rescaled $\tilde{\epsilon}_t$ with the Cholesky decomposition of Σ_ϵ , denoted by C , ensures that the variance of ϵ_t is Σ_ϵ . In the following, this distribution of ϵ_t is just called χ_3^2 -distribution.

In DGP1–DGP5, the covariance matrices of the error terms, ϵ_t , are given by the 2×2 identity matrix for simplicity and in DGP6, the covariance matrix is given by

$$\Sigma_\epsilon^6 := \begin{pmatrix} 0.962 & -0.018 & 0.166 \\ -0.018 & 0.049 & -0.087 \\ 0.116 & -0.087 & 0.693 \end{pmatrix},$$

where Σ_ϵ^6 is, as in [Staszewska-Bystrova \(2011\)](#), the maximum likelihood estimate of the variance based on the same data as the slope coefficients in DGP-6. The coefficients of the covariance matrix of ϵ_t in DGP-7 is provided in [Appendix 2A](#).

Misspecified Models

The assumption about the underlying true data generating process is crucial in applied work. However, it is an assumption that is not verifiable in practice. It is therefore instructive to investigate the finite-sample performance of each of the five joint prediction regions if the model is misspecified. More specifically, the data is generated by either a vector moving average (VMA) process or a threshold vector autoregressive (TVAR) process. The joint prediction regions are then computed with the *same* methodology as in the previous section, that is, based on a $\text{VAR}(\hat{p})$ model, where the lag order is estimated using the BIC.

The basis data generating process is a VMA(1) process used in [Galbraith et al. \(2002\)](#):

$$\text{DGP-8: } y_t = \begin{pmatrix} 1 \\ 1 \end{pmatrix} + \underbrace{\begin{pmatrix} 0.20 & 0.10 \\ 0.10 & 0.60 \end{pmatrix}}_{:=M_7} \epsilon_{t-1} + \epsilon_t. \quad (2.14)$$

The characteristic roots in (2.14), that is the roots of $\det(I_2 + M_7 z)$, are given by $\rho_7 := (-5.669, -1.604)'$. In order to cover a broader range of process characteristics, the VMA(1) processes corresponding to the following slope coefficient matrices are investigated:

$$M_9 := \begin{pmatrix} -0.20 & 0.10 \\ 0.10 & 0.60 \end{pmatrix}, \quad M_{10} := \begin{pmatrix} -0.80 & 0.10 \\ 0.10 & -0.60 \end{pmatrix}, \quad M_{11} := \begin{pmatrix} 1.20 & 0.10 \\ 0.10 & 0.90 \end{pmatrix},$$

where DGP- i corresponds to M_i , $i \in \{8, 9, 10\}$. The characteristic roots of these processes are given by $\rho_8 := (-1.633, 4.710)'$, $\rho_9 := (1.189, 1.790)'$ and $\rho_{11} := (-1.150, -0.813)'$, respectively.

Remark 2.5.1 A VMA(q) process has a pure VAR(∞) representation if $\det(I_k + M_1 z^1 + \dots + M_q z^q) \neq 0$ for $z \in \mathbb{C}, |z| \leq 1$. Thus, DGP-8, DGP-9 and DGP-10 exhibit a VAR(∞) representation, whereas DGP-11 does not. This implies that only the processes in DGP-8, DGP-9 and DGP-10 can be approximated by a finite VAR process. ■

For simplicity, it is assumed that $\{\epsilon_t\}$ is an i.i.d. process with $\epsilon_t \sim \mathcal{N}(0, \Sigma_\epsilon)$, where the variance matrix Σ_ϵ is taken from Galbraith et al. (2002) and is given by

$$\Sigma_\epsilon^{8,9,10,11} := \begin{pmatrix} 1.00 & 0.50 \\ 0.50 & 1.00 \end{pmatrix}.$$

Furthermore, the last considered data generating process is a non-linear TVAR(1) process already used by Tsay (1998). The process is given by

$$\text{DGP-12: } y_t = \begin{cases} A_1^{(1)} y_{t-1} + \epsilon_t^{(1)}, & \text{if } y_{1,t-1} < 0 \\ A_1^{(2)} y_{t-1} + \epsilon_t^{(2)}, & \text{if } y_{1,t-1} \geq 0 \end{cases}, \quad (2.15)$$

where

$$A_1^{(1)} := \begin{pmatrix} 0.70 & 0.00 \\ 0.30 & 0.70 \end{pmatrix} \quad \text{and} \quad A_1^{(2)} := \begin{pmatrix} -0.70 & 0.00 \\ -0.30 & -0.70 \end{pmatrix}.$$

The error process is assumed to be an i.i.d. process with $\epsilon_t^{(i)} \sim \mathcal{N}(0, \Sigma_i)$ $i \in \{1, 2\}$. The corresponding regime-dependent covariance matrices of ϵ_t are also taken from Tsay

(1998) and are given by

$$\Sigma_1 := \begin{pmatrix} 1.00 & 0.20 \\ 0.20 & 1.00 \end{pmatrix} \quad \text{and} \quad \Sigma_2 := \begin{pmatrix} 1.00 & -0.30 \\ -0.30 & 1.00 \end{pmatrix}.$$

2.5.2 Design

The nominal coverage probability of each of the joint prediction regions is 90%. The empirical coverage of a particular joint prediction region is computed in the usual way, that is, as the number of continuations that are completely covered by a joint prediction region divided by the total number of continuations. In particular, 2,000 time series samples $\{y_1, \dots, y_T\}$ are generated according to the specified data generating processes, each with 100 independent continuations $\{y_{T+1}, \dots, y_{T+H}\}$. As a result, the empirical coverages are computed based on 200,000 continuations and are therefore very accurate.

The forecast horizon is $H \in \{6, 12, 24\}$ and the sample size is $T \in \{100, 200, 400\}$. The number of bootstrap samples is $B = 2,000$ throughout. The lag order is, if assumed to be unknown, determined using the BIC. The maximum lag order is determined using the rule of thumb proposed by [Schwert \(1989\)](#)¹⁶. According to this rule, the maximum lag is given by the integer part of $12(T/100)^{0.25}$. Thus, the maximum lag order is given by 12, 14 and 16 for sample sizes of 100, 200 and 400, respectively.

In order to be able to compare the volume of the joint prediction regions, the geometric-mean volume width is computed in each of the 2,000 Monte Carlo repetitions. More specifically, each of the joint prediction regions can be characterized by the Cartesian product of H individual prediction intervals, $\text{PI}_h = [l_h, u_h] \subset \mathbb{R}$, where u_h and l_h denote the upper and the lower bound of the joint prediction region at a given forecast horizon $h \in \{1, \dots, H\}$. The geometric-mean volume is then computed by $w_{\text{geo}} := (\prod_{i=1}^H w_i)^{\frac{1}{H}}$, where $w_i := u_h - l_h$. The empirical volume of the m -th method of constructing a joint prediction region is then computed by taking the mean, that is

$$\bar{V}_{\text{geo},m} := \frac{1}{2000} \sum_{j=1}^{2000} \left(\prod_{i=1}^H w_{m,j,i} \right)^{\frac{1}{H}}, \quad (2.16)$$

¹⁶[Staszewska-Bystrova and Winker \(2013\)](#) also use the rule of [Schwert \(1989\)](#) to determine the maximum lag order.

where $w_{m,j,i} := u_{m,j,i} - l_{m,j,i}$. The geometric-mean volume (instead of the arithmetic mean) is reported because the geometric-mean volume can be interpreted as the length of a ‘representative’ marginal prediction interval in the sense that the volume of an artificial joint prediction region constructed by the Cartesian product of H of the representative intervals yields the same aggregate volume as the actual obtained aggregate volume $\prod_{i=1}^H w_i$.

2.5.3 Results

Bivariate VAR(1) Models

The tables with the simulation results can be found in Appendices [2C](#), [2D](#), [2E](#) and [2F](#). The following general conclusions can be drawn from the simulation results:

- Estimating the lag order has no considerable effect on the finite-sample performance (measured by the empirical coverage and the volume) of all methods compared to the scenario where the true lag order is known.
- The characteristics of the data generating process and the distribution of the error terms have an effect on the finite-sample performance of all methods. The direction and the magnitude of the effect is method-specific and depends on the sample size and the forecasting horizon; see Figure [2A.1](#) for a graphical illustration.

The main method-specific results can be summarized as follows:

- The finite-sample performance of the symmetric WW-JPR of [Wolf and Wunderli \(2015\)](#) is strictly increasing in the sample size T and decreasing in the forecasting horizon H . More specifically, for the stationary processes (DGP-1–DGP-4) and a sample size of $T = 100$, the WW-JPR is only reliable for $H \in \{6, 12\}$. There is considerable undercoverage for some scenarios with fat-tailed and skewed errors when $H = 24$. However, increasing the sample size to $T = 200$ reduces the downward coverage bias in a substantial way especially for the large forecasting horizon $H = 24$. For $T = 400$, the empirical coverages are close to 90% even with non-normal errors and $H = 24$, which renders the WW-JPR the most robust method in these scenarios. For the unit root process (DGP-5), the coverage bias is more pronounced compared to the stationary processes, independently of the sample size and the forecasting horizon.

- The performance of the asymmetric WW-JPR, in comparison with its symmetric counterpart, ranges between comparable and inferior for the scenarios with normal or fat-tailed errors (t -distribution). In the scenarios with skewed errors (χ_3^2 -distribution), the asymmetric outperforms the symmetric WW-JPR only in 25 out of 90 scenarios.
- The finite-sample performance of the Bonferroni-JPR depends mainly on the process characteristics. For the persistent processes (DGP-1, DGP-2), the method exhibits the expected upward coverage bias, practically independent of the error distribution. But for the less persistent processes (DGP-3, DGP-4), the Bonferroni-JPR features mild to substantial undercoverage for the longer forecast horizons $H \in \{12, 24\}$. The phenomenon is even more pronounced with fat-tailed errors (in contrast to the normal and the χ_3^2 -distribution) but can be mitigated by increasing the sample size. For the unit root process (DGP-5) and $T = 100$, the Bonferroni-JPR exhibits an empirical coverage close to 90%, but increasing the sample size results in an upward coverage bias. The volume of the Bonferroni-JPR is in general larger than the volume of the competing methods.
- The adjustment procedure of [Lütkepohl et al. \(2015\)](#) reduces the volume and the empirical coverage throughout all scenarios. Thus, the coverage bias is only diminished in the scenarios where the Bonferroni-JPR exhibits overcoverage (DGP-1, DGP-2, DGP-5). However, the reduction of volume and the resulting reduction in the coverage rate is by far not sufficient to eliminate the positive coverage bias. Thus, the previously presented properties of the Bonferroni-JPR inherently apply to the Adjusted Bonferroni-JPR.
- The NP-JPR of [Staszewska-Bystrova \(2011\)](#) exhibits good and robust performances for the short forecast horizon $H = 6$. For $H \in \{12, 24\}$, the performance depends substantially on the process characteristics and the error distribution. More specifically, for the scenarios with normal errors, the performance is good for the persistent processes (DGP-1, DGP-2), but there is mild to substantial undercoverage for the less persistent processes (DGP-3, DGP-4) and the unit root process (DGP-5). The NP-JPR lacks robustness with respect to the error distribution be-

cause non-normality of the errors causes the empirical coverages to substantially deteriorate especially when $H = 24$.

In addition to the previously presented results that depend on specific population characteristics, which are unknown in any application, it is instructive to analyze the *overall* performance of the various methods of constructing a joint prediction region. Thus, given a sample size $T \in \{100, 200, 400\}$, the simulation results (with BIC lag selection) are condensed into the following two key figures: The (overall) mean absolute deviation of the empirical coverages from its nominal value and the average volume. More specifically, the mean absolute deviation (MAD) for a sample size of T is computed as

$$\text{MAD}_T = \frac{1}{90} \sum_k \sum_d \sum_{dgp} \sum_H |EC_{k,d,H,dgp,T} - 90| , \quad (2.17)$$

where EC denotes the empirical coverage, $k \in \{1, 2\}$, $d \in \{\text{Normal}, t(3), \chi^2\}$, $H \in \{6, 12, 24\}$ and $dgp \in \{\text{DGP-1}, \text{DGP-2}, \text{DGP-3}, \text{DGP-4}, \text{DGP-5}\}$. In other words, the MAD_T is the average deviation (of the empirical coverage from the nominal coverage) over all variables, all data generating processes, all error distributions and all forecast horizons. The average volume is computed analogously as

$$\bar{V}_T = \frac{1}{90} \sum_k \sum_{dist} \sum_{dgp} \sum_H \bar{V}_{k,d,H,dgp,T} , \quad (2.18)$$

where \bar{V} denotes the volume. The performance of a particular prediction region is obviously decreasing in the MAD and the volume. Measuring the performance by means of two attributes allows the graphical analysis in the (MAD, \bar{V}) space. Figure 2A.2 displays the (MAD, \bar{V}) -combination for each method and various sample sizes. The main findings about the overall performances are as follows:

- The symmetric WW-JPR outperforms all competing methods in terms of coverage for the larger sample sizes $T = 200, 400$ and is among the best for $T = 100$.
- The asymmetric WW-JPR exhibits about the same volume as the symmetric WW-JPR, but is inferior to its symmetric counterpart in terms of coverage.
- The Bonferroni-JPR exhibits the largest volume for all sample sizes. For $T = 100$,

the Bonferroni JPR exhibits the smallest coverage bias but for the other considered sample sizes it is outperformed by at least one other method.

- The adjustment of [Lütkepohl et al. \(2015\)](#) improves the finite-sample performance (in terms of coverage bias and volume) for $T = 200, 400$. However, for $T = 100$, the volume is reduced but the coverage bias is increased.
- The NP-JPR outperforms the other methods in terms of the volume but exhibits a substantially larger coverage bias than the best performing method (WW-JPR).

Trivariate VAR(4) Model

The tables with the simulations result are found in Appendix [2G](#). The trivariate VAR(4) model is stationary and persistent and therefore exhibits similar stationarity characteristics like the bivariate VAR(1) models of DGP-1 and DGP-2. However, the complexity of DGP-6 is substantially larger compared to the VAR(1) models¹⁷. Thus, given a sample size, there are more parameters to estimate or in other words there are less degrees of freedom. The results give some indication about how the increased complexity affects the finite-sample properties of the various JPRs. The main conclusions can be summarized as follows:

- For $T = 100$, the increased complexity of the underlying model (compared to the bivariate VAR(1) models) substantially distorts the coverage rate of the symmetric WW-JPR especially when $H = 24$. Additionally, there are systematic differences in the coverage rates among the different variables of the system (y_1, y_2, y_3) , where $EC_{y_1} > EC_{y_2}, EC_{y_3}$. However, the coverage distortion as well as the differences in the performance of the variables are substantially reduced for a sample size of $T = 200$. For $T = 400$, the empirical coverage is close to the nominal coverage of 90%. Furthermore, the symmetric WW-JPR is robust with respect to the distribution of the errors (for all sample sizes).
- The difference between the symmetric and the asymmetric WW-JPR in terms of performance is effectively small but in favor of the symmetric version for almost all scenarios. Furthermore, the differences (in coverage rates and volumes) between the

¹⁷The true model in DGP-6 consists of 39 parameters (without the covariance parameters), whereas the true models in DGP-1 and DGP-2 only consist of 6 parameters each.

two JPRs based on [Wolf and Wunderli \(2015\)](#) decrease with increasing sample size. Thus, the previously presented properties of the symmetric WW-JPR inherently apply also to the asymmetric WW-JPR.

- The Bonferroni-JPR exhibits coverage rates that are larger than the nominal coverage rate, independently of the forecasting horizon and the sample size. The amount of the upward coverage bias depends on the error distribution and is less pronounced for scenarios with fat-tailed errors (see Figure [2A.3](#)). There are also systematic differences in the coverage rates among the different variables of the system. However, similar to the WW-JPRs, the performance variation among the variables decreases with increasing sample size. More specifically, the Bonferroni-JPR is the largest of all competing methods in all scenarios.
- The adjustment of [Lütkepohl et al. \(2015\)](#) reduces the volume and the coverage bias of the Bonferroni-JPR. However, the coverage rate of the Adjusted Bonferroni-JPR is still substantially above the nominal coverage. This result is illustrated in Figure [2A.3](#) which shows the coverage rates of the Bonferroni-JPR (red) and the Adjusted Bonferroni-JPR (blue) for various sample sizes and forecasting horizons.
- Despite the increased complexity of model (compared to the VAR(1) models), the NP-JPR exhibits good performances even for $T = 100$. The coverage rates systematically vary among the variables of the system and the performance is affected by the error distribution, where the fat-tailed errors reduce the coverage rates especially for $H = 24$. However, both effects diminish with an increasing sample size. The NP-JPR is strictly smaller than the Bonferroni-type JPRs but weakly larger than the WW-JPRs.

Similar to the bivariate VAR(1) models, the method-specific results depend on population characteristics. Thus, it is in turn instructive to analyze the *overall* performance by means of the mean absolute deviation and the average volume. The MAD is computed over all variables, all error distributions and all forecast horizons¹⁸. Figure [2A.4](#) displays the (MAD, \bar{V}) -combinations for each method and various sample sizes. The analysis of the overall performance allows the following conclusions:

¹⁸ $\text{MAD}_T = \frac{1}{27} \sum_k \sum_d \sum_H |EC_{k,d,H,T} - 90|$ and $\bar{V}_T = \frac{1}{27} \sum_k \sum_d \sum_H \bar{V}_{k,d,H,T}$.

- The empirical coverage of the WW-JPR is distorted for $T = 100$. However, increasing the sample size to $T = 200$ eliminates around 80% of the coverage bias. For $T = 400$, the WW-JPR exhibits even the smallest volume and the smallest bias.
- The asymmetric WW-JPR exhibits about the same volume as the symmetric WW-JPR but a larger coverage bias. However, the difference shrinks with increasing sample size and is almost negligible for $T = 400$.
- The Adjusted Bonferroni-JPR exhibits superior finite-sample performances compared to the Bonferroni-JPR. However, the (absolute) performance of the Bonferroni-type JPR's improves when the sample size is increased from $T = 100$ to $T = 200$, but deteriorates when the sample size is further increased to $T = 400$.
- The NP-JPR exhibits the smallest coverage bias for $T = 100, 200$ and is even with the symmetric WW-JPR for $T = 400$. The NP-JPR is smaller than the Bonferroni-type JPRs.

Six-variate VAR(2) Model

The tables with the simulations result are found in Appendix 2H. DGP-7 is also stationary and persistent but more complex than DGP-6. More specifically, the true model consists of 78 parameters (without the covariance parameters) vs. 39 parameters of the model in DGP-6. Thus, the results give an indication about the performance of the JPRs in scenarios with a large number of parameters to estimate from a given sample size. The main conclusions can be summarized as follows:

- For $T = 100$, the symmetric WW-JPR exhibits mild to severe undercoverage. The coverage bias increases with the forecasting horizon and varies substantially among the six variables of the system (see Figure 2A.5). Increasing the sample size reduces on the one hand the coverage bias and on the other hand the variation of the coverage rates among the variables. However, even for $T = 400$, there is still small to substantial undercoverage depending on the forecasting horizon and the specific variable of the system (see Figure 2A.6). The symmetric WW-JPR is smaller than the Bonferroni-type JPRs and the NP-JPR. Furthermore, the volume of the symmetric WW-JPR is constant over all sample sizes.

- The asymmetric WW-JPR is virtually identical to the symmetric WW-JPR and exhibits therefore the same coverage and volume properties.
- The Bonferroni-JPR exhibits undercoverage for $T = 100$ and all $H \in \{6, 12, 24\}$. The downward bias substantially varies among the variables and ranges between small and serious (see Figure 2A.5). Increasing the sample size causes the coverage rate to increase resulting eventually in overcoverage for some of the variables (see Figure 2A.6). The Bonferroni-JPR is larger than all other JPRs. The Adjusted Bonferroni-JPR has only marginally smaller volume than the Bonferroni-JPR and exhibits smaller coverage rates.
- For $T = 100$, the NP-JPR also suffers from small to serious undercoverage, where the amount of bias depends on the forecasting horizon and the specific variable of the system (see Figure 2A.5). However, increasing the sample size substantially reduces the coverage distortion and the coverage variation among the variables (see Figure 2A.6). The NP-JPR has smaller volume than the Bonferroni-type JPRs but larger volume than the WW-JPRs.
- Figure 2A.7 provides a graphical illustration of the finite-sample performances in terms of the mean absolute deviation over all variables and all forecast horizons and the corresponding average volumes. The figure highlights the fact that the coverage bias is seriously reduced by increasing the sample size, especially the JPR's based on [Wolf and Wunderli \(2015\)](#) improve substantially from an increase in the sample size.

Misspecified Models

The tables with the simulation results can be found in Appendices 2I and 2J. The main conclusions can be summarized as follows:

- The symmetric WW-JPR exhibits small to mild undercoverage for all scenarios with VMA processes (DGP-8–DGP-11). The downward coverage bias is increasing in the forecast horizon and decreasing in the sample size. For the TVAR model (DGP-12), the coverage rates of the symmetric WW-JPR systematically vary among the two variables. More specifically, the JPR for y_1 exhibits mild undercoverage for $T = 100$ but small overcoverage for $T = 200, 400$, whereas the JPR for y_2 exhibits

overcoverage especially for $T = 200, 400$. The volume of the symmetric WW-JPR is comparable with the volume of the Bonferroni-JPR throughout.

- The performance in terms of the coverage rates of the asymmetric WW-JPR is inferior to the symmetric WW-JPR. However, the difference between the two methods based on [Wolf and Wunderli \(2015\)](#) diminishes with increasing sample size. The volume is about the same as the volume of its symmetric counterpart.
- For $H = 6$, the Bonferroni-JPR exhibits coverage rates (for the VMA processes) that are close to the nominal level. For $H \in \{12, 24\}$, the method is less robust with respect to the underlying process characteristics (DGP-8–DGP-11). However, the variation in the coverage rates among the variables is diminishing with a larger sample size. For the TVAR model (DGP-12), the Bonferroni-JPR exhibits similar properties as the symmetric WW-JPR. The Adjusted Bonferroni-JPR features the same properties because the adjustment reduces the volume and the coverage rate only marginally.
- For the scenarios with the VMA processes, the NP-JPR exhibits mild undercoverage for the short forecast horizon $H = 6$ and $T = 100$. The coverage bias increases in the forecast horizon and decreases in the sample size. Similar to the Bonferroni-type JPRs, the NP-JPR lacks robustness with respect to the underlying process characteristics and exhibits a larger bias for DGP-8 and DGP-9 than for DGP-10 and DGP-11. For the TVAR model (DGP-12), the coverage rates systematically vary among the two variables and are between substantial undercoverage ($T = 100, H = 24, y_1$) and mild overcoverage ($T = 400, H = 24, y_2$).

2.5.4 Summary of Simulation Evidence

- There is evidence that a higher complexity of the underlying VAR (that is less degrees of freedom) potentially results in JPRs with finite-sample coverage rates that are severely downward biased especially for large forecast horizons. Thus, given a small sample size relative to the size of the model, indeed a common scenario in applied work, the JPRs (based on the considered methods) for a path forecast should be suspected to underestimate the uncertainty about the future path.

- The simulations show that there is not a particular method that uniformly exhibits the best finite-sample performance throughout all scenarios.
- The symmetric WW-JPR based on [Wolf and Wunderli \(2015\)](#) performs well in terms of coverage and robustness in scenarios where either the model is small and/or the sample size is large (relative to the model). Furthermore, the symmetric WW-JPR is well-behaved in the sense that the coverage bias is strictly decreasing in the sample size.
- The asymmetric WW-JPR based on [Wolf and Wunderli \(2015\)](#) is inferior compared with its symmetric counterpart even in most of the scenarios with a skewed error distribution. Thus, the asymmetric WW-JPR can not be recommended for the use in practice.
- The Bonferroni-JPR and the NP-JPR exhibit less downward coverage bias in scenarios with low degrees of freedom than the symmetric WW-JPR.
- The adjustment of [Lütkepohl et al. \(2015\)](#) reduces the volume of the Bonferroni-JPR and as a consequence the coverage rate, but the effect is in general very small. Thus, the adjustment does not substantially improve the finite-sample properties of the Bonferroni-JPR. This is in contrast to the results of the simulation study of [Lütkepohl et al. \(2015\)](#) in the context of the confidence sets for impulse response functions, where the effect (in terms of coverage) of the adjustment is much stronger.

2.6 Empirical Application

The various JPRs are illustrated using the reduced-form VAR(12) model of the global oil market of [Baumeister and Kilian \(2015\)](#)¹⁹. The purpose of the model is to produce accurate path forecasts for the real oil price. The four-dimensional VAR(12) model includes the following key variables relevant to the determination of the real price of oil²⁰:

- $\Delta prod_t$: The percent change in global crude oil production

¹⁹The reduced-form model of [Baumeister and Kilian \(2015\)](#) is based on the structural VAR model of [Kilian and Murphy \(2014\)](#).

²⁰More details about the specific computation of the variables are found in [Baumeister and Kilian \(2015\)](#) and [Kilian and Murphy \(2014\)](#).

- $real_t$: A business cycle index of global real activity constructed
- r_t^{oil} : The log of the real oil price
- Δinv_t : The change in global crude oil inventories.

The monthly data set from February 1973 through August 2009 is downloaded from the homepage of the Journal of Applied Econometrics²¹. The parameters of the VAR(12) model (with intercept) are estimated with the same methodology as in the Monte Carlo simulation using the entire sample of 439 observations, that is $\{y_1, \dots, y_{439}\}$, where $y_t := (\Delta prod_t, real_t, r_t^{oil}, \Delta inv_t)'$. The paths forecasts for each of the four variables of the model are computed based on the estimated model $\widehat{VAR}(12)$ with a forecast horizon of 6, 12 and 24, respectively. This corresponds to the period of

- (a) September 2009 through February 2010 ($H = 6$)
- (b) September 2009 through August 2010 ($H = 12$)
- (c) September 2009 through August 2011 ($H = 24$).

The JPRs (based on all five methods) with a nominal coverage level of 90% are computed for each of the paths forecasts using 2000 bootstrap replications.

Table 2.2 contains the volumes of the resulting 90% JPRs for $\Delta prod_t$, $real_t$, r_t^{oil} and Δinv_t and all forecast horizons $H \in \{6, 12, 24\}$. The table confirms the following volume-related results obtained from the Monte Carlo simulations. First, the adjustment of Lütkepohl et al. (2015) only marginally reduces the volume of the Bonferroni-JPR. Second, the symmetric WW-JPR and the asymmetric WW-JPR almost coincide for larger models and as a consequence exhibit a similar volume. Third, the NP-JPR is smaller than the Bonerroni-type JPRs but larger than the WW-JPRs.

Figure 2.1 displays the path forecast for r_t^{oil} (solid black line), the variable of interest in the analysis of Baumeister and Kilian (2015), and the 90% symmetric WW-JPR (red dotted lines), the asymmetric 90% WW-JPR (blue dotted lines)²², the 90% Bonferroni-JPR (brown dashed-dotted lines), the 90% Adjusted Bonferroni-JPR (orange dashed-dotted lines) and the 90% NP-JPR (green dashed lines)²³. The figure nicely illustrates

²¹<http://onlinelibrary.wiley.com/doi/10.1002/jae.2322/abstract>

²²The symmetric WW-JPR and the asymmetric WW-JPR effectively coincide. Thus, red dotted line corresponding to the symmetric WW-JPR is almost not visible.

²³The corresponding figures for the variables $real_t$, $\Delta prod_t$ and Δinv_t are found in Appendix 2B.

		Method				
Horizon	Variable	Sym-WW	Asy-WW	NP	Bon	Adj-Bon
$H = 6$	$\Delta prod_t$	10.68	10.66	10.43	10.90	10.89
	$real_t$	47.40	47.19	56.33	64.51	64.02
	r_t^{oil}	59.39	59.50	71.91	79.27	78.38
	Δinv_t	99.31	101.88	112.00	113.66	113.31
$H = 12$	$\Delta prod_t$	12.30	11.95	12.28	12.38	12.38
	$real_t$	68.85	68.98	80.00	94.10	91.50
	r_t^{oil}	89.91	89.95	107.34	122.13	119.90
	Δinv_t	114.22	117.45	126.37	127.84	127.66
$H = 24$	$\Delta prod_t$	14.33	13.59	13.69	13.81	13.77
	$real_t$	95.81	95.85	109.25	126.53	122.57
	r_t^{oil}	131.83	131.76	151.97	176.22	171.66
	Δinv_t	132.00	133.85	143.61	142.47	142.21

Table 2.2: Volume of the JPR’s for various forecasting horizons.

the different volumes and the different shapes of the various JPRs. The NP-JPR and the Bonferroni-type-JPR have a jagged shape whereas the WW-JPR’s are smooth by construction.

2.7 Conclusion

Path forecasts, defined as sequences of individual forecasts, generated by vector autoregressions are widely used in applied work. It has been recognized that a rigorous econometric analysis often requires, besides the path forecast, a joint prediction region that contains the entire future path with a prespecified coverage probability. This paper investigates the finite-sample performance of a number of different methods to construct a joint prediction region in various scenarios through an extensive Monte Carlo study.

The simulations show that there is not a particular method that uniformly exhibits the best finite-sample performance throughout all scenarios. The symmetric JPR based on [Wolf and Wunderli \(2015\)](#) outperforms the other competing methods in scenarios with high degrees of freedom. Its strong points are the robustness concerning the distribution of the errors, large forecast horizons and model misspecification. The performance of the

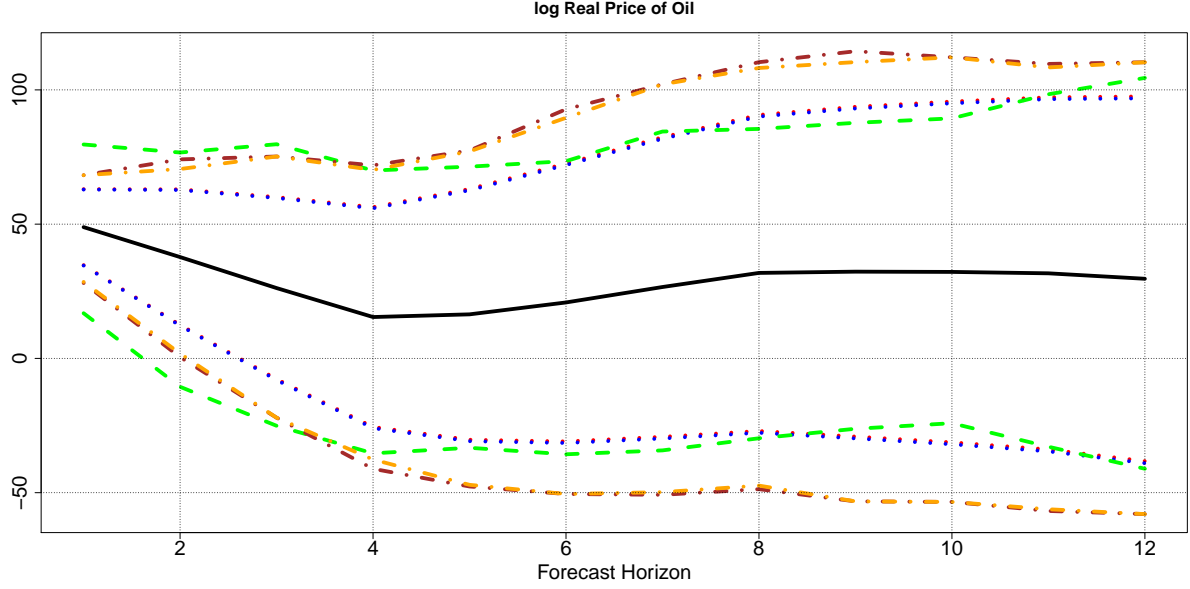


Figure 2.1: Path forecast (solid black) for the log real price of oil over the period 9/2009 through 8/2010, the 90% symmetric WW-JPR (red dotted), the 90% asymmetric WW-JPR (blue dotted), the 90% Bonferroni-JPR (brown dashed-dotted), the 90% Adjusted Bonferroni-JPR (orange dashed-dotted) and the 90% NP-JPR (green dashed lines).

asymmetric JPR based on [Wolf and Wunderli \(2015\)](#) is in general inferior compared to its symmetric counterpart and can therefore not be recommended for the use in practice. The adjustment of [Lütkepohl et al. \(2015\)](#) reduces the volume and the coverage rate of the Bonferroni-JPR, but the adjustment does not substantially improve the finite-sample properties. Furthermore, the simulation results provide evidence that in scenarios with low degrees of freedom, a common scenario in applied work, the JPRs based on all the considered methods should be suspected of underestimating the uncertainty about the future path especially for large forecast horizons.

References

- Amihud, Y. and Hurvich, C. M. (2004). Predictive regressions: A reduced-bias estimation method. *Journal of Financial and Quantitative Analysis*, 39(04):813–841.
- Amihud, Y., Hurvich, C. M., and Wang, Y. (2009). Multiple-predictor regressions: Hypothesis testing. *Review of Financial Studies*, 22(1):413–434.
- Bauer, M. D., Rudebusch, G. D., and Wu, J. C. (2012). Correcting estimation bias in dynamic term structure models. *Journal of Business & Economic Statistics*, 30(3):454–467.
- Baumeister, C. and Kilian, L. (2015). Forecasting the real price of oil in a changing world: A forecast combination approach. *Journal of Business & Economic Statistics*, 33(3):338–351.
- Bowden, D. C. (1970). Simultaneous confidence bands for linear regression models. *Journal of the American Statistical Association*, 65(329):413–421.
- Engsted, T. and Pedersen, T. Q. (2014). Bias-correction in vector autoregressive models: A simulation study. *Econometrics*, 2(1):45–71.
- Fresoli, D., Ruiz, E., and Pascual, L. (2015). Bootstrap multi-step forecasts of non-Gaussian VAR models. *International Journal of Forecasting*, 31(3):834–848.
- Galbraith, J., Ullah, A., and Zinde-Walsh, V. (2002). Estimation of the vector moving average model by vector autoregression. *Econometric Reviews*, 21(2):205–219.
- Hurvich, C. M. and Tsai, C.-L. (1993). A corrected Akaike information criterion for vector autoregressive model selection. *Journal of Time Series Analysis*, 14(3):271–279.
- Jordà, O. and Marcellino, M. (2010). Path forecast evaluation. *Journal of Applied Econometrics*, 25(4):635–662.
- Kilian, L. (1998). Small-sample confidence intervals for impulse response functions. *The Review of Economics and Statistics*, 80(2):218–230.

- Kilian, L. and Murphy, D. P. (2014). The role of inventories and speculative trading in the global market for crude oil. *Journal of Applied Econometrics*, 29(3):454–478.
- Kim, J. H. (2001). Bootstrap-after-bootstrap prediction intervals for autoregressive models. *Journal of Business & Economic Statistics*, 19(1):117–128.
- Lütkepohl, H. (2005). *New Introduction to Multiple Time Series Analysis*. Springer, Berlin.
- Lütkepohl, H., Staszewska-Bystrova, A., and Winker, P. (2015). Comparison of methods for constructing joint confidence bands for impulse response functions. *International Journal of Forecasting*, 31(3):782–798.
- Nicholls, D. F. and Pope, A. L. (1988). Bias in the estimation of multivariate autoregressions. *Australian Journal of Statistics*, 30A(12):296–309.
- Pope, A. L. (1990). Biases of estimators in multivariate non-gaussian autoregressions. *Journal of Time Series Analysis*, 11(3):249–258.
- Scheffé, H. (1953). A method for judging all contrasts in the analysis of variance. *Biometrika*, 40(1-2):87–110.
- Scheffé, H. (1959). *The Analysis of Variance*. John Wiley & Sons, New York.
- Schwert, G. W. (1989). Tests for unit roots: A monte carlo investigation. *Journal of Business & Economic Statistics*, 7(2):147–159.
- Sims, C. A. (1980). Macroeconomics and reality. *Econometrica*, 48(1):1–48.
- Staszewska-Bystrova, A. (2011). Bootstrap prediction bands for forecast paths from vector autoregressive models. *Journal of Forecasting*, 30(8):721–735.
- Staszewska-Bystrova, A. (2013). Modified Scheffé prediction bands. *Journal of Economics and Statistics (Jahrbuecher fuer Nationaloekonomie und Statistik)*, 233(5-6):680–690.
- Staszewska-Bystrova, A. and Winker, P. (2013). Constructing narrowest pathwise bootstrap prediction bands using threshold accepting. *International Journal of Forecasting*, 29(2):221–233.

- Staszewska-Bystrova, A. and Winker, P. (2014). Measuring forecast uncertainty of corporate bond spreads by Bonferroni-type prediction bands. *Central European Journal of Economic Modelling and Econometrics*, 2:89–104.
- Stine, R. A. (1987). Estimating properties of autoregressive forecasts. *Journal of the American Statistical Association*, 82(400):1072–1078.
- Stock, J. H. and Watson, M. W. (2001). Vector autoregressions. *Journal of Economic Perspectives*, 15(4):101–115.
- Tsay, R. S. (1998). Testing and modeling multivariate threshold models. *Journal of the American Statistical Association*, 93:1188–1202.
- Wolf, M. and Wunderli, D. (2015). Bootstrap joint prediction regions. *Journal of Time Series Analysis*, 36(3):352–376.
- Yamamoto, T. and Kunitomo, N. (1981). Asymptotic bias of ordinary least squares estimator for multivariate autoregressive models. *Annals of the Institute of Statistical Mathematics*, 36(504):419–430.

Appendix

2A Six-variate VAR(2) Model

The coefficient matrices and the covariance matrix are given by

$$A_1 := \begin{pmatrix} 0.805 & 0.037 & 3.363 & 9.488 & -0.877 & 2.469 \\ 0.386 & 1.064 & -106.444 & 27.825 & -32.667 & 21.498 \\ -0.001 & -0.001 & 0.456 & 0.0215 & 0.139 & -0.014 \\ 0.006 & -0.001 & -0.040 & 1.331 & 0.106 & -0.224 \\ 0.005 & 0.003 & 0.008 & -0.0148 & 0.713 & 0.134 \\ -0.003 & 0.001 & 0.082 & -0.301 & 0.145 & 1.028 \end{pmatrix},$$

$$A_2 := \begin{pmatrix} 0.136 & -0.059 & 10.202 & -8.191 & 3.720 & -2.150 \\ -0.494 & -0.092 & 75.699 & -19.392 & 21.442 & -12.982 \\ 0.001 & 0.000 & -0.064 & -0.041 & -0.111 & -0.004 \\ -0.003 & 0.001 & 0.219 & -0.402 & -0.085 & 0.120 \\ -0.007 & -0.002 & 0.533 & 0.072 & 0.112 & -0.053 \\ 0.002 & -0.001 & -0.375 & 0.342 & -0.086 & -0.029 \end{pmatrix},$$

$$\Sigma_\epsilon := \begin{pmatrix} 7.692 & 16.944 & -0.025 & 0.007 & 0.057 & -0.007 \\ 16.944 & 216.793 & -0.299 & -0.110 & 0.694 & 0.198 \\ -0.025 & -0.299 & 0.001 & -0.001 & -0.004 & -0.001 \\ 0.007 & -0.110 & -0.001 & 0.021 & 0.012 & -0.006 \\ 0.057 & 0.694 & -0.004 & 0.012 & 0.034 & 0.001 \\ -0.007 & 0.198 & -0.001 & -0.006 & 0.001 & .0102 \end{pmatrix},$$

and the intercept ν is given by $(-8.239, 8.025, 0.005, 0.211, 0.190, -0.192)'$.

2B Figures

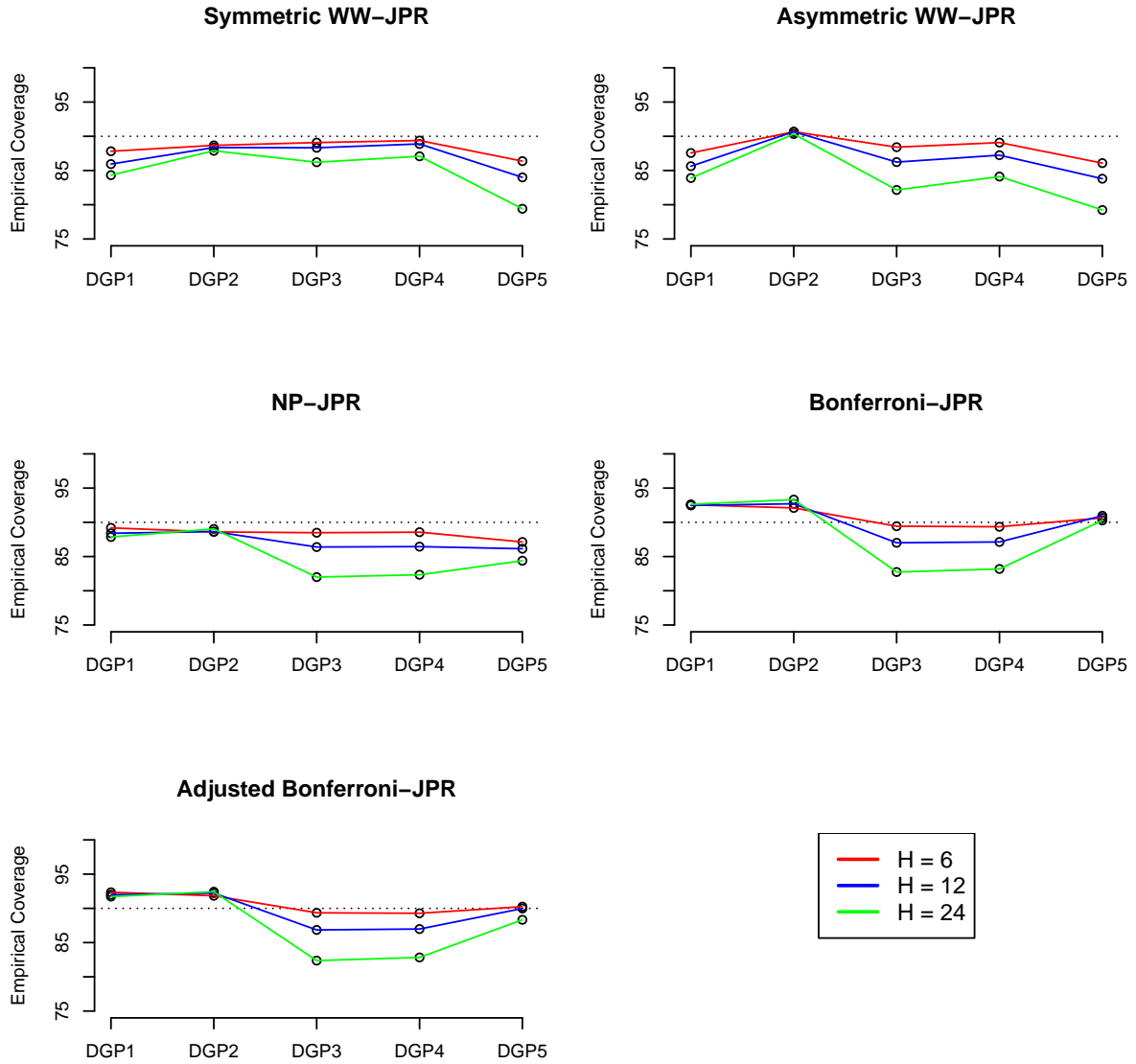


Figure 2A.1: Empirical coverages of various 90% JPR's for the first variable y_1 : $H \in \{6, 12, 24\}$, $T = 100$, $\epsilon_t \sim \mathcal{N}(0, \Sigma)$ and BIC lag selection.

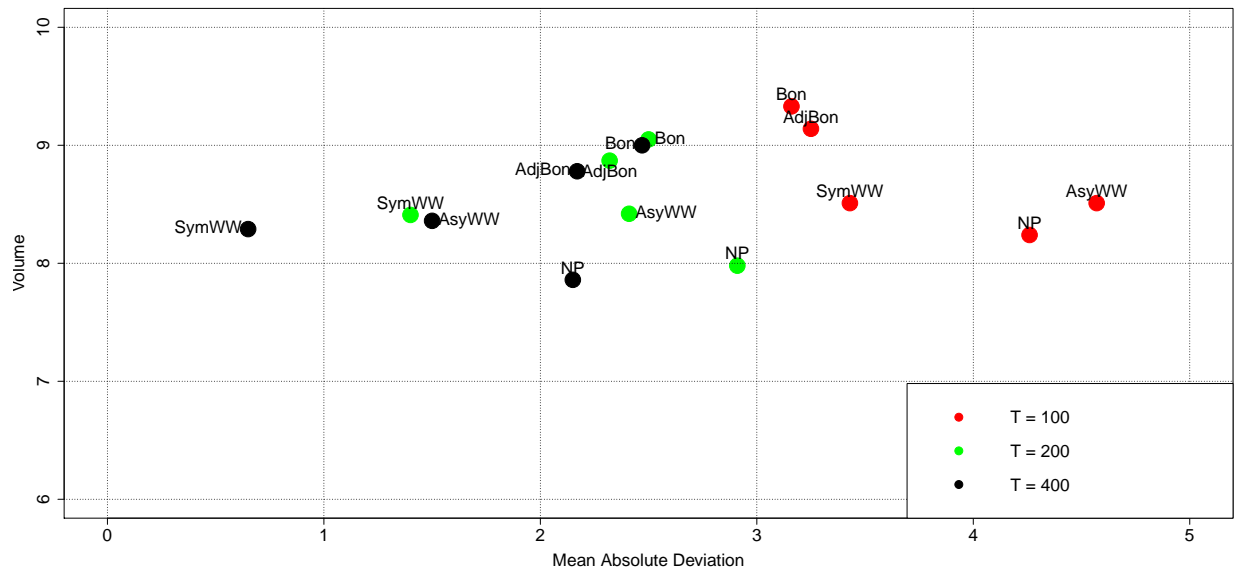


Figure 2A.2: Overall performance analysis for the bivariate VAR(1) models (DGP-1–DGP-5): (MAD, \bar{V}) -combination of the symmetric WW-JPR (SymWW), the asymmetric WW-JPR (AsyWW), the Bonferroni-JPR (Bon), the Adjusted Bonferroni-JPR (AdjBon) and the NP-JPR (NP) for $T \in \{100, 200, 400\}$.

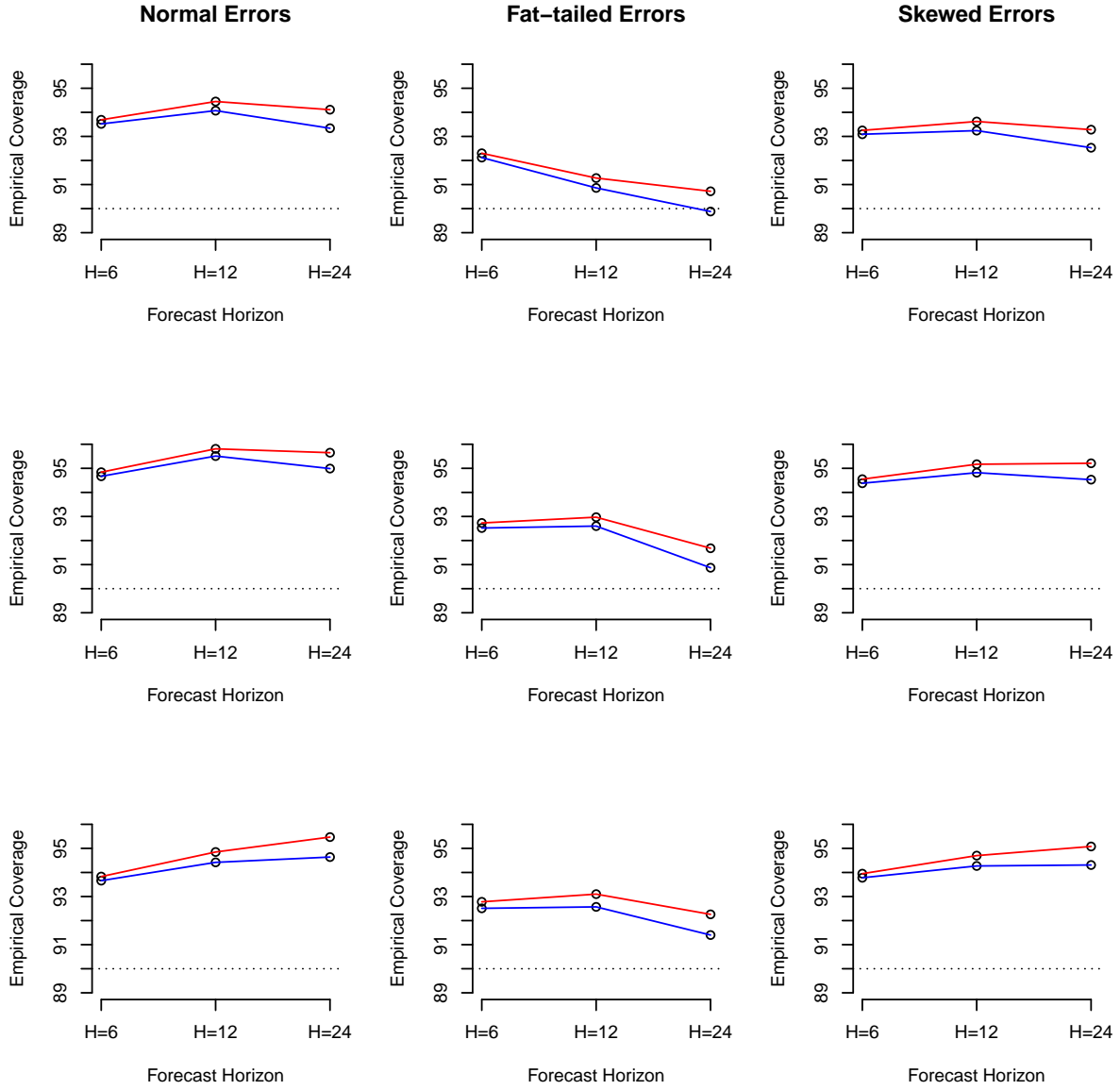


Figure 2A.3: DGP-6: Empirical coverages of the Bonferroni-JPR (red) and the Adjusted Bonferroni-JPR (blue) for the first variable y_1 with $(1 - \alpha)\% = 90\%$. The top row of subfigures corresponds to $T = 100$, the middle row to $T = 200$ and the bottom row to $T = 400$, respectively.

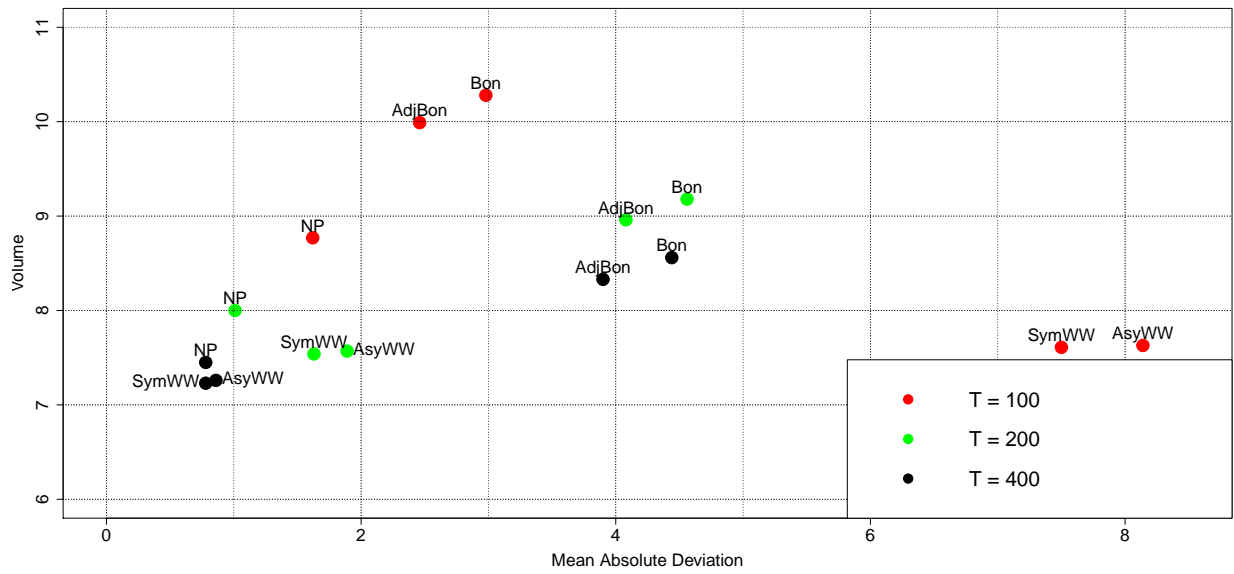


Figure 2A.4: Overall performance analysis for the trivariate VAR(4) model (DGP-6): (MAD, \bar{V})-combination of the symmetric WW-JPR (SymWW), the asymmetric WW-JPR (AsyWW), the Bonferroni-JPR (Bon), the Adjusted Bonferroni-JPR (AdjBon) and the NP-JPR (NP) for $T \in \{100, 200, 400\}$.

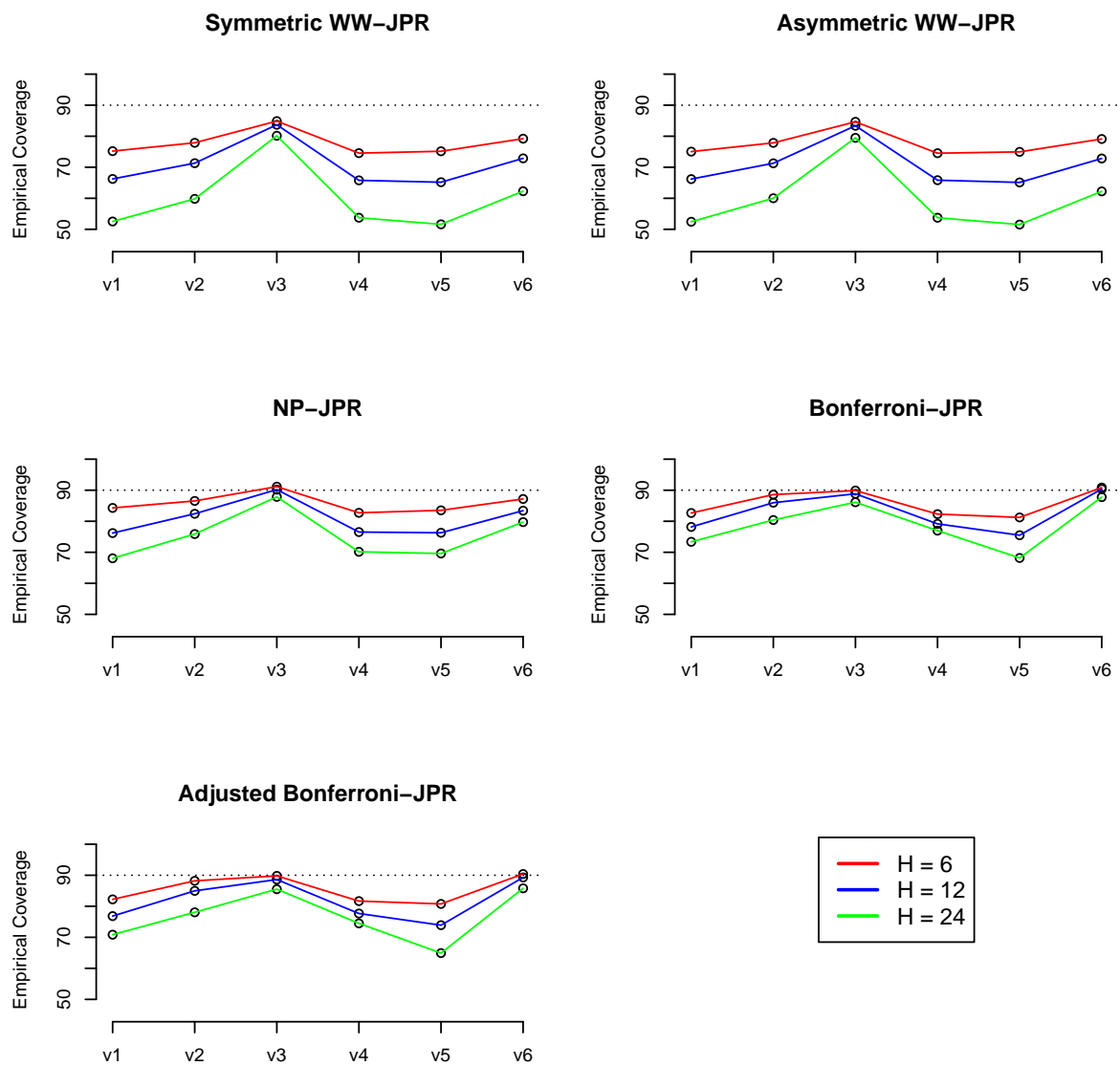


Figure 2A.5: Empirical coverages of various 90% JPRs for all six variables: $H \in \{6, 12, 24\}$, $T = 100$, $\epsilon_t \sim \mathcal{N}(0, \Sigma_7)$ and BIC lag selection.

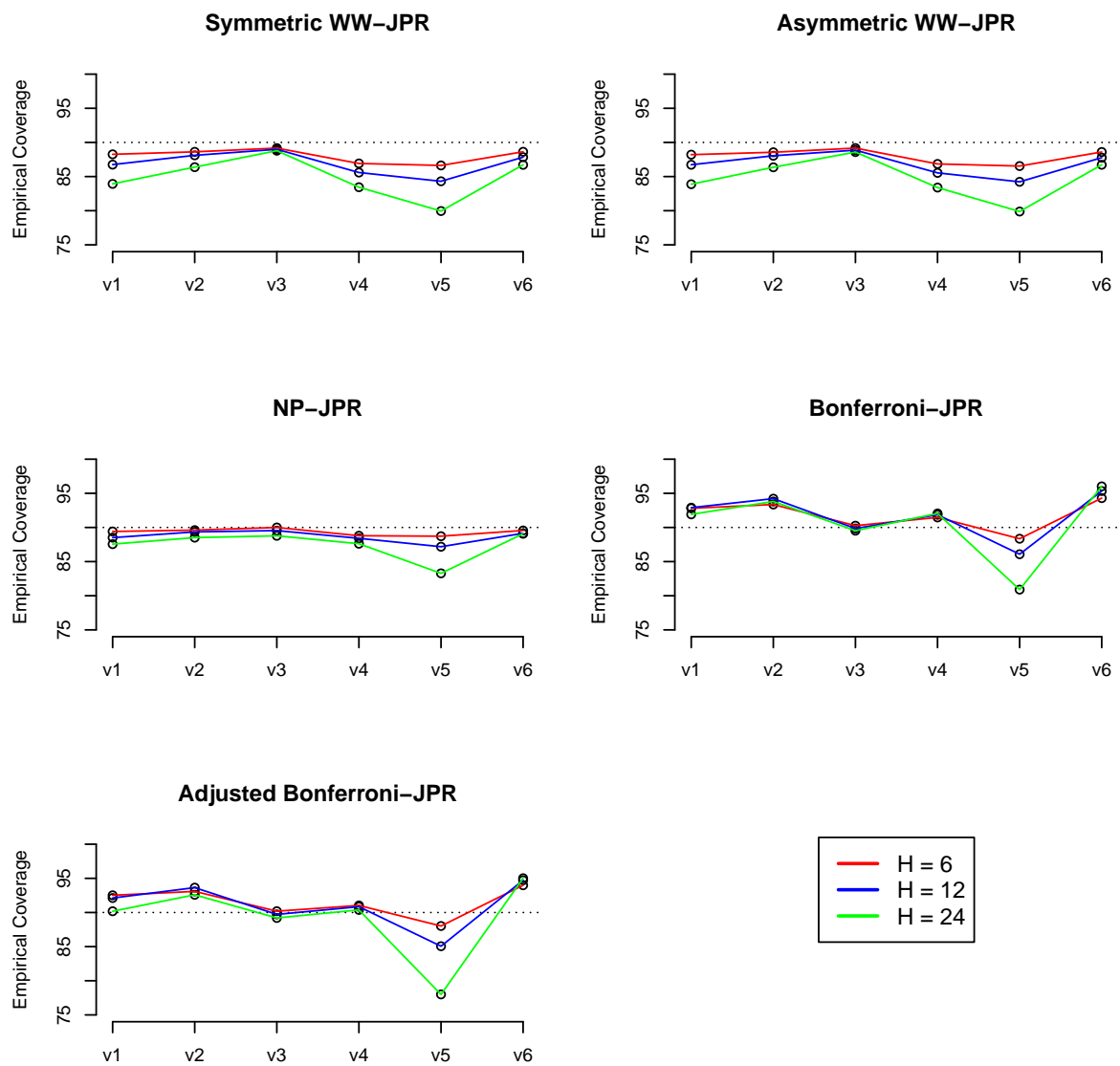


Figure 2A.6: Empirical Coverages of various 90% JPRs for all six variables: $H \in \{6, 12, 24\}$, $T = 400$, $\epsilon_t \sim \mathcal{N}(0, \Sigma_\epsilon^7)$ and BIC lag selection.

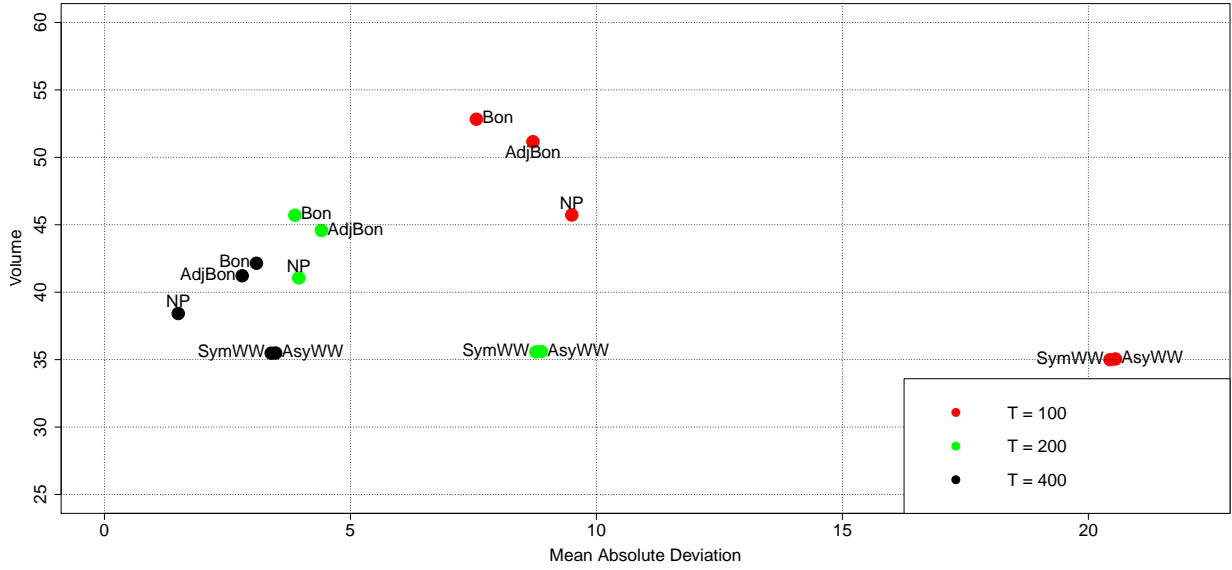


Figure 2A.7: Overall performance analysis for the six-variate VAR(2) model (DGP-7): (MAD, \bar{V})-combination of the symmetric WW-JPR (SymWW), the asymmetric WW-JPR (AsyWW), the Bonferroni-JPR (Bon), the Adjusted Bonferroni-JPR (AdjBon) and the NP-JPR (NP) for $T \in \{100, 200, 400\}$.

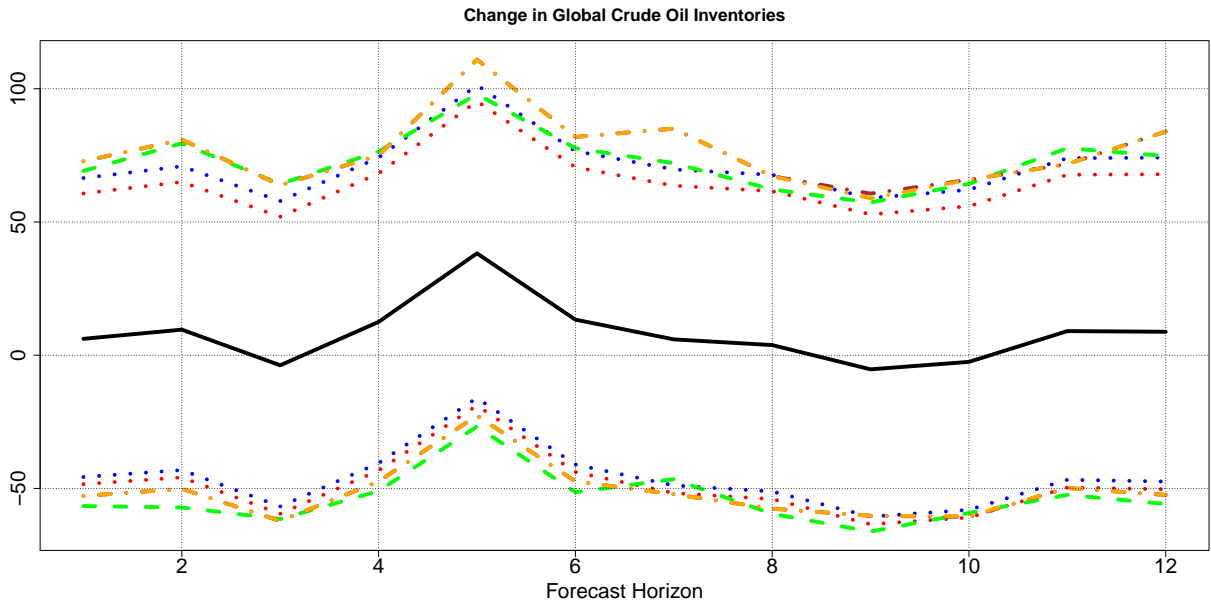


Figure 2A.8: Path forecast (solid black) for the change in global crude oil inventories over the period 9/2009 through 8/2010, the 90% symmetric WW-JPR (red dotted), the 90% asymmetric WW-JPR (blue dotted), the 90% Bonferroni-JPR (brown dashed-dotted), the 90% Adjusted Bonferroni-JPR (orange dashed-dotted) and the 90% NP-JPR (green dashed lines).

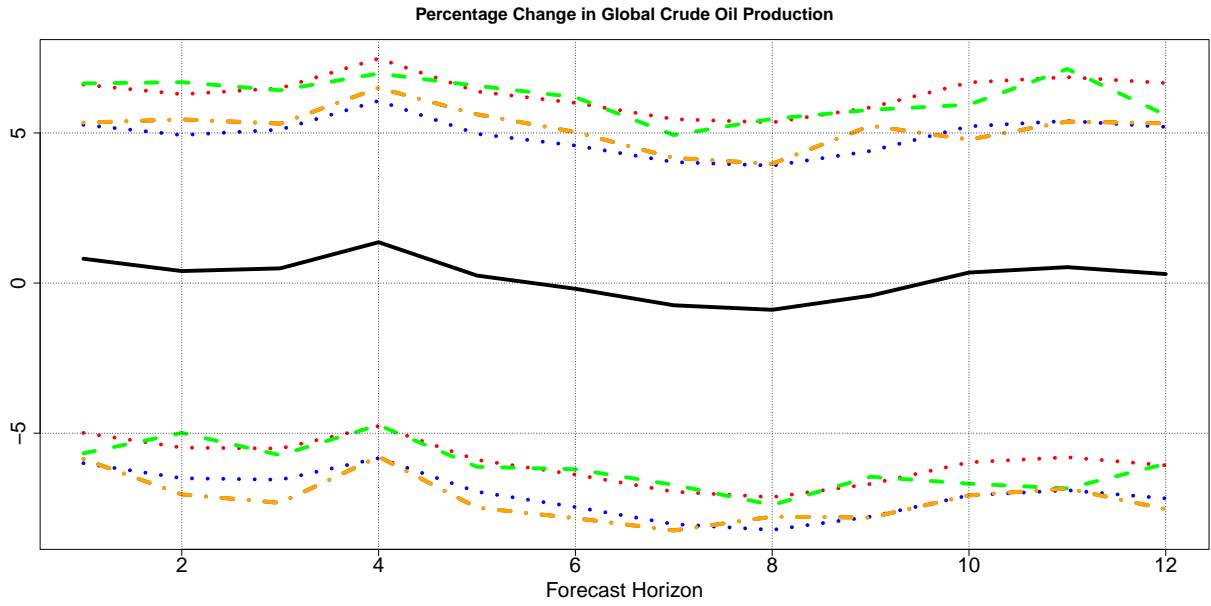


Figure 2A.9: Path forecast (solid black) for the percentage change in global crude oil production over the period 9/2009 through 8/2010, the 90% symmetric WW-JPR (red dotted), the 90% asymmetric WW-JPR (blue dotted), the 90% Bonferroni-JPR (brown dashed-dotted), the 90% Adjusted Bonferroni-JPR (orange dashed-dotted) and the 90% NP-JPR (green dashed lines).

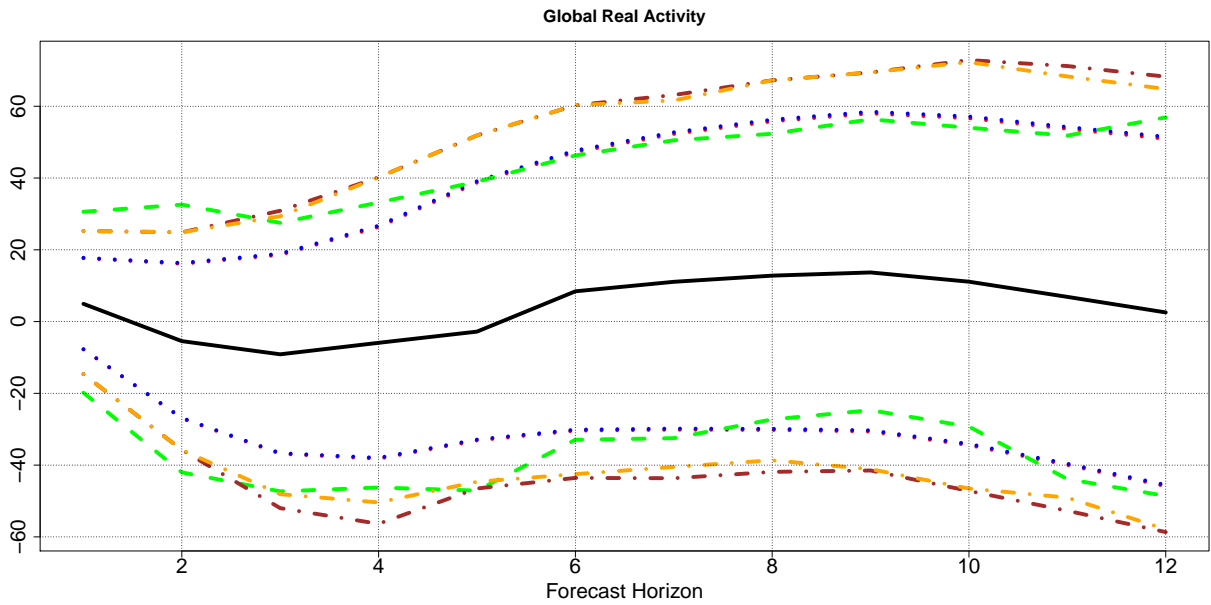


Figure 2A.10: Path forecast (solid black) for the global real activity over the period 9/2009 through 8/2010, the 90% symmetric WW-JPR (red dotted), the 90% asymmetric WW-JPR (blue dotted), the 90% Bonferroni-JPR (brown dashed-dotted), the 90% Adjusted Bonferroni-JPR (orange dashed-dotted) and the 90% NP-JPR (green dashed lines).

2C Empirical Coverages for DGP-1–5 with Known Lag Order

		$\mathcal{N}(0, \Sigma)$ Distribution					
	Method	$H = 6$		$H = 12$		$H = 24$	
		$v = 1$	$v = 2$	$v = 1$	$v = 2$	$v = 1$	$v = 2$
DGP-1	Sym-WW	87.19	87.26	86.96	86.21	84.86	84.20
	Asy-WW	86.97	87.02	86.58	85.92	84.52	83.82
	NP	88.53	88.57	89.33	88.81	88.74	88.25
	Bon	91.93	92.25	93.15	93.31	93.14	93.57
	Adj-Bon	91.71	92.03	92.68	92.85	92.32	92.68
DGP-2	Sym-WW	88.96	88.86	88.37	88.31	87.68	87.76
	Asy-WW	90.94	91.06	90.66	90.84	90.15	90.52
	NP	88.92	88.83	88.70	88.70	88.83	89.12
	Bon	92.30	92.43	92.62	93.23	93.13	93.78
	Adj-Bon	92.07	92.20	92.15	92.73	92.20	92.84
DGP-3	Sym-WW	88.99	88.90	88.37	88.69	86.80	87.04
	Asy-WW	88.28	88.25	86.08	86.74	83.23	83.70
	NP	88.44	88.48	86.39	87.05	83.02	83.53
	Bon	89.25	89.49	87.01	87.78	83.82	84.50
	Adj-Bon	89.18	89.40	86.85	87.61	83.44	84.13
DGP-4	Sym-WW	89.04	89.09	88.87	88.83	87.13	87.12
	Asy-WW	88.74	88.93	87.27	87.62	84.23	84.64
	NP	88.22	88.27	86.45	86.58	82.43	82.74
	Bon	89.00	89.27	87.12	87.56	83.35	83.93
	Adj-Bon	88.92	89.18	86.98	87.39	83.02	83.50
DGP-5	Sym-WW	86.82	85.53	84.09	82.16	79.11	77.28
	Asy-WW	86.62	85.26	83.97	81.89	78.91	76.93
	NP	87.60	86.70	86.12	85.35	84.52	83.99
	Bon	90.91	90.52	90.97	90.18	89.99	89.05
	Adj-Bon	90.54	90.25	90.00	89.44	88.03	87.23

Table 2.3: Known Lag, $T = 100$: Empirical coverages for the v -th variable.

		$\mathcal{N}(\mathbf{0}, \Sigma)$ Distribution					
	Method	$H = 6$		$H = 12$		$H = 24$	
		$v = 1$	$v = 2$	$v = 1$	$v = 2$	$v = 1$	$v = 2$
DGP-1	Sym-WW	88.94	88.88	88.62	88.43	87.92	87.46
	Asy-WW	88.78	88.73	88.46	88.28	87.73	87.32
	NP	88.94	88.86	88.82	88.63	88.33	88.08
	Bon	92.40	92.63	93.09	93.38	93.35	93.78
	Adj-Bon	92.19	92.38	92.59	92.84	92.38	92.80
DGP-2	Sym-WW	89.29	89.66	89.57	89.33	89.00	89.01
	Asy-WW	91.35	91.89	91.87	91.91	91.46	91.76
	NP	88.98	89.32	89.13	88.94	88.68	88.81
	Bon	92.41	93.03	93.39	93.67	93.52	94.17
	Adj-Bon	92.17	92.78	92.89	93.10	92.58	93.18
DGP-3	Sym-WW	89.53	89.23	89.10	89.18	88.14	88.23
	Asy-WW	89.09	88.88	88.38	88.45	85.96	86.16
	NP	88.87	88.72	87.61	87.73	84.68	84.88
	Bon	89.80	89.81	88.54	88.87	85.50	85.88
	Adj-Bon	89.72	89.72	88.38	88.71	85.21	85.59
DGP-4	Sym-WW	89.54	89.66	89.30	89.61	88.74	88.71
	Asy-WW	89.58	89.83	88.75	89.29	86.92	87.23
	NP	88.67	88.92	87.39	87.89	84.73	84.87
	Bon	89.68	89.99	88.40	88.93	85.70	86.07
	Adj-Bon	89.60	89.90	88.25	88.76	85.41	85.75
DGP-5	Sym-WW	88.36	87.72	87.11	86.36	84.54	84.15
	Asy-WW	88.20	87.56	86.94	86.23	84.46	84.06
	NP	88.20	87.81	87.14	86.98	85.60	85.83
	Bon	92.26	91.69	92.83	91.94	92.68	91.59
	Adj-Bon	91.93	91.42	92.00	91.28	91.07	90.09

Table 2.4: Known Lag, $T = 200$: Empirical coverages for the v -th variable.

		$\mathcal{N}(\mathbf{0}, \Sigma)$ Distribution					
	Method	$H = 6$		$H = 12$		$H = 24$	
		$v = 1$	$v = 2$	$v = 1$	$v = 2$	$v = 1$	$v = 2$
DGP-1	Sym-WW	89.47	89.47	89.20	89.36	88.87	88.88
	Asy-WW	89.34	89.34	89.11	89.22	88.75	88.79
	NP	89.15	89.19	88.67	88.91	88.01	88.19
	Bon	92.56	92.92	93.05	93.60	93.30	94.08
	Adj-Bon	92.34	92.67	92.54	93.08	92.28	93.03
DGP-2	Sym-WW	89.72	89.83	89.70	89.63	89.57	89.50
	Asy-WW	91.77	92.07	92.11	92.28	92.07	92.29
	NP	89.37	89.39	88.90	88.88	88.30	88.33
	Bon	92.65	93.09	93.27	93.71	93.47	94.08
	Adj-Bon	92.42	92.84	92.74	93.15	92.51	93.07
DGP-3	Sym-WW	89.82	89.61	89.51	89.41	89.23	88.90
	Asy-WW	89.65	89.40	89.06	88.95	88.29	88.04
	NP	89.19	89.05	88.07	87.99	86.15	85.97
	Bon	90.22	90.22	89.15	89.24	87.22	87.19
	Adj-Bon	90.15	90.15	88.99	89.06	86.93	86.88
DGP-4	Sym-WW	89.92	89.68	89.41	89.81	89.04	89.14
	Asy-WW	90.16	90.06	89.45	89.80	88.49	88.83
	NP	89.23	88.98	87.93	88.28	85.90	86.11
	Bon	90.21	90.16	89.03	89.49	87.03	87.47
	Adj-Bon	90.15	90.07	88.88	89.32	87.76	87.14
DGP-5	Sym-WW	89.03	88.96	88.37	88.19	87.28	87.43
	Asy-WW	88.95	88.84	88.27	88.09	87.19	87.36
	NP	88.65	88.59	87.64	87.73	86.66	86.98
	Bon	92.92	92.37	93.85	92.71	94.32	93.10
	Adj-Bon	92.61	92.11	93.09	92.12	92.85	91.80

Table 2.5: Known Lag, $T = 400$: Empirical coverages for the v -th variable.

		$t(3)$ Distribution					
	Method	$H = 6$		$H = 12$		$H = 24$	
		$v = 1$	$v = 2$	$v = 1$	$v = 2$	$v = 1$	$v = 2$
DGP-1	Sym-WW	88.70	88.59	87.18	87.23	84.54	84.65
	Asy-WW	87.77	87.68	85.38	85.44	81.57	82.12
	NP	87.85	87.98	86.29	86.56	83.27	84.00
	Bon	90.70	91.21	89.61	90.31	88.02	89.38
	Adj-Bon	90.50	91.01	89.13	89.81	86.98	88.36
DGP-2	Sym-WW	89.52	89.39	88.40	88.26	86.13	86.67
	Asy-WW	91.37	91.53	89.92	90.23	87.51	88.52
	NP	87.99	87.90	86.64	86.84	84.27	85.38
	Bon	91.28	92.20	90.68	91.27	88.79	90.37
	Adj-Bon	91.57	91.92	90.24	90.83	87.95	89.40
DGP-3	Sym-WW	88.96	88.68	87.38	87.69	82.33	81.94
	Asy-WW	87.97	87.73	83.54	84.05	75.28	75.16
	NP	86.49	86.30	82.74	83.39	73.34	73.47
	Bon	87.66	87.61	82.26	82.83	71.91	72.19
	Adj-Bon	87.56	87.50	82.18	82.75	71.70	71.97
DGP-4	Sym-WW	89.11	89.43	87.42	87.58	82.30	82.84
	Asy-WW	88.98	89.25	84.30	84.80	77.18	77.84
	NP	86.52	86.86	82.53	83.03	74.04	74.55
	Bon	88.27	88.61	82.71	83.38	73.81	74.73
	Adj-Bon	88.13	88.45	82.60	83.25	73.60	74.46
DGP-5	Sym-WW	88.04	87.52	86.78	85.97	82.13	81.82
	Asy-WW	87.15	86.44	85.49	83.63	80.42	79.10
	NP	86.83	86.06	85.53	83.86	82.84	80.88
	Bon	90.47	89.39	90.00	87.84	88.70	86.03
	Adj-Bon	90.13	89.17	89.13	87.17	86.86	84.44

Table 2.6: Known Lag, $T = 100$: Empirical coverages for the v -th variable.

		$t(3)$ Distribution					
	Method	$H = 6$		$H = 12$		$H = 24$	
		$v = 1$	$v = 2$	$v = 1$	$v = 2$	$v = 1$	$v = 2$
DGP-1	Sym-WW	89.75	89.90	89.32	89.38	87.82	87.70
	Asy-WW	89.22	89.41	88.52	88.53	85.73	85.95
	NP	88.43	88.60	87.60	87.75	84.93	85.31
	Bon	91.99	92.47	81.26	91.98	88.94	90.13
	Adj-Bon	91.68	92.15	90.82	91.49	88.04	89.11
DGP-2	Sym-WW	90.05	90.12	89.22	89.56	88.16	88.34
	Asy-WW	92.28	92.57	91.38	91.97	89.90	90.44
	NP	88.62	88.77	87.36	87.87	85.76	86.42
	Bon	92.75	93.21	92.11	93.04	90.62	91.76
	Adj-Bon	92.47	92.92	91.53	92.48	89.76	90.84
DGP-3	Sym-WW	89.98	89.82	88.90	88.97	87.17	87.53
	Asy-WW	89.30	89.17	87.91	87.87	82.31	83.01
	NP	88.10	87.88	85.25	85.56	78.89	80.85
	Bon	89.06	89.09	86.67	86.82	80.34	81.05
	Adj-Bon	88.89	88.90	86.44	86.59	80.18	80.88
DGP-4	Sym-WW	89.82	89.83	89.01	88.95	87.56	87.44
	Asy-WW	89.76	90.03	88.67	88.82	83.25	83.71
	NP	87.79	87.97	85.32	85.42	80.22	80.42
	Bon	89.05	89.44	87.22	87.47	81.33	81.83
	Adj-Bon	88.91	89.29	86.94	87.12	81.08	81.56
DGP-5	Sym-WW	89.75	89.53	88.45	88.32	86.79	86.61
	Asy-WW	89.28	89.06	87.74	87.51	85.61	85.19
	NP	88.55	88.04	86.93	86.46	84.97	83.90
	Bon	93.07	92.03	92.65	90.83	91.80	89.20
	Adj-Bon	92.78	91.74	91.90	90.28	90.34	87.89

Table 2.7: Known Lag, $T = 200$: Empirical coverages for the v -th variable.

		$t(3)$ Distribution					
	Method	$H = 6$		$H = 12$		$H = 24$	
		$v = 1$	$v = 2$	$v = 1$	$v = 2$	$v = 1$	$v = 2$
DGP-1	Sym-WW	90.04	90.06	89.72	89.90	89.39	89.54
	Asy-WW	89.82	89.83	89.23	89.38	88.52	88.68
	NP	88.94	88.98	87.97	88.21	86.64	86.92
	Bon	92.95	93.39	92.38	93.14	91.02	92.06
	Adj-Bon	92.66	93.07	91.78	92.53	90.14	91.12
DGP-2	Sym-WW	90.13	90.24	90.17	90.05	89.53	89.34
	Asy-WW	92.58	92.97	92.62	92.90	91.92	92.01
	NP	88.88	89.07	88.33	88.22	86.88	87.04
	Bon	93.32	93.84	93.47	94.01	92.37	93.07
	Adj-Bon	93.05	93.55	92.85	93.41	91.42	92.10
DGP-3	Sym-WW	89.97	90.04	89.62	89.55	88.24	88.54
	Asy-WW	89.62	89.71	88.85	88.92	87.48	87.60
	NP	88.61	88.67	86.96	86.99	83.36	83.66
	Bon	89.70	8.990	88.12	88.43	84.95	85.26
	Adj-Bon	89.59	89.78	87.86	88.14	84.55	84.82
DGP-4	Sym-WW	90.16	90.04	89.54	89.73	88.83	88.62
	Asy-WW	90.46	90.49	89.38	89.81	88.25	88.38
	NP	88.74	88.71	86.90	87.18	83.78	83.71
	Bon	90.02	90.11	88.36	88.82	85.63	85.89
	Adj-Bon	89.91	90.00	88.11	88.54	85.23	85.43
DGP-5	Sym-WW	89.98	89.94	89.50	89.52	88.52	88.85
	Asy-WW	89.73	89.68	89.14	89.10	87.93	88.15
	NP	88.88	88.69	87.96	87.59	86.49	85.95
	Bon	94.19	93.06	94.48	92.65	94.11	91.74
	Adj-Bon	93.88	92.76	93.83	92.03	92.91	90.60

Table 2.8: Known Lag, $T = 400$: Empirical coverages for the v -th variable.

		χ_3^2 Distribution					
	Method	$H = 6$		$H = 12$		$H = 24$	
		$v = 1$	$v = 2$	$v = 1$	$v = 2$	$v = 1$	$v = 2$
DGP-1	Sym-WW	88.49	88.35	87.46	87.34	86.23	85.67
	Asy-WW	87.87	87.60	86.62	86.23	84.25	83.63
	NP	89.34	89.18	89.02	88.83	87.95	87.54
	Bon	93.46	93.47	93.49	93.81	93.12	93.11
	Adj-Bon	93.26	93.27	93.05	93.33	92.26	92.24
DGP-2	Sym-WW	88.66	88.90	88.70	88.67	87.72	87.50
	Asy-WW	91.34	91.78	91.11	91.40	90.12	90.13
	NP	88.20	88.46	88.25	88.45	87.68	87.77
	Bon	92.52	93.10	92.65	93.28	92.53	92.97
	Adj-Bon	92.25	92.81	92.19	92.75	91.62	92.03
DGP-3	Sym-WW	88.76	88.67	87.68	87.29	83.60	83.95
	Asy-WW	91.83	91.36	90.31	89.91	86.74	86.89
	NP	88.57	88.64	87.22	86.92	82.86	83.28
	Bon	92.40	92.30	90.08	89.94	85.23	85.74
	Adj-Bon	92.31	92.22	89.99	89.81	85.03	85.50
DGP-4	Sym-WW	88.77	88.90	87.80	87.30	83.59	83.50
	Asy-WW	91.45	91.25	89.57	88.90	85.39	83.17
	NP	88.66	88.74	87.28	86.79	82.35	82.08
	Bon	91.54	91.33	88.94	88.36	83.27	83.31
	Adj-Bon	91.39	91.18	88.79	88.19	82.97	82.94
DGP-5	Sym-WW	88.45	87.09	85.93	85.46	81.72	81.63
	Asy-WW	82.20	83.36	78.52	79.43	73.76	73.31
	NP	86.16	86.11	84.16	84.16	83.53	82.46
	Bon	86.65	90.08	87.58	89.69	87.92	88.33
	Adj-Bon	86.13	89.78	86.30	88.85	85.69	86.47

Table 2.9: Known Lag, $T = 100$: Empirical coverages for the v -th variable.

		χ_3^2 Distribution					
	Method	$H = 6$		$H = 12$		$H = 24$	
		$v = 1$	$v = 2$	$v = 1$	$v = 2$	$v = 1$	$v = 2$
DGP-1	Sym-WW	89.46	89.55	89.12	88.90	88.32	88.20
	Asy-WW	89.17	89.16	88.48	87.96	86.83	87.01
	NP	89.39	89.50	88.98	88.59	87.69	88.01
	Bon	93.56	93.54	93.73	93.90	93.13	93.92
	Adj-Bon	93.34	93.62	93.24	93.36	92.16	92.93
DGP-2	Sym-WW	89.71	89.81	89.19	89.46	88.71	88.86
	Asy-WW	92.60	92.79	92.09	92.48	91.49	91.85
	NP	89.11	89.24	88.54	88.78	87.75	88.21
	Bon	93.61	93.97	93.37	94.04	92.98	93.99
	Adj-Bon	93.36	93.71	92.86	93.47	92.07	92.95
DGP-3	Sym-WW	89.24	89.56	88.59	88.82	87.61	87.44
	Asy-WW	91.34	91.32	91.55	91.22	89.77	89.50
	NP	88.97	89.29	87.82	88.17	85.85	85.93
	Bon	92.16	92.32	91.53	91.43	88.85	88.84
	Adj-Bon	92.08	92.23	91.36	91.27	88.62	88.58
DGP-4	Sym-WW	89.17	89.38	88.33	88.47	87.37	87.26
	Asy-WW	91.30	91.51	90.78	90.49	88.30	88.27
	NP	88.79	89.12	87.55	87.48	85.02	84.95
	Bon	91.41	91.76	90.25	90.10	87.01	87.06
	Adj-Bon	91.29	91.62	89.98	89.78	86.61	86.59
DGP-5	Sym-WW	89.62	88.99	88.45	88.27	86.51	86.96
	Asy-WW	84.71	86.08	82.94	84.10	79.62	80.70
	NP	86.93	87.74	85.36	86.23	84.00	84.30
	Bon	88.02	91.49	89.39	91.60	90.05	91.01
	Adj-Bon	87.55	91.25	88.28	90.88	88.00	89.40

Table 2.10: Known Lag, $T = 200$: Empirical coverages for the v -th variable.

		χ_3^2 Distribution					
	Method	$H = 6$		$H = 12$		$H = 24$	
		$v = 1$	$v = 2$	$v = 1$	$v = 2$	$v = 1$	$v = 2$
DGP-1	Sym-WW	89.55	89.70	89.47	89.56	89.28	89.20
	Asy-WW	89.62	89.53	89.08	89.30	88.87	88.60
	NP	89.38	89.39	88.86	89.02	88.34	88.12
	Bon	93.43	93.70	93.62	94.22	93.75	94.12
	Adj-Bon	93.21	93.46	93.11	93.68	92.79	93.07
DGP-2	Sym-WW	89.78	89.76	89.81	89.53	89.13	89.37
	Asy-WW	92.79	92.91	92.79	92.67	92.16	92.50
	NP	89.34	89.24	88.84	88.54	87.73	88.02
	Bon	93.79	94.03	93.83	94.13	93.21	94.14
	Adj-Bon	93.53	93.77	93.30	93.54	92.17	93.10
DGP-3	Sym-WW	89.72	89.71	89.24	89.28	88.54	88.67
	Asy-WW	90.91	90.84	91.09	90.83	91.31	91.02
	NP	89.30	89.33	88.48	88.50	86.90	87.03
	Bon	91.82	92.01	91.31	91.33	90.17	90.18
	Adj-Bon	91.73	91.90	91.15	91.17	89.83	89.85
DGP-4	Sym-WW	89.56	89.71	89.37	89.33	88.23	88.71
	Asy-WW	91.57	91.78	91.29	91.31	90.15	90.84
	NP	89.10	89.27	88.33	88.28	86.05	86.55
	Bon	91.81	92.03	90.96	91.03	88.71	89.43
	Adj-Bon	91.68	91.89	90.68	90.72	88.19	88.83
DGP-5	Sym-WW	90.28	89.57	89.60	89.59	88.77	89.07
	Asy-WW	86.91	87.96	85.51	86.78	83.92	85.00
	NP	87.96	88.60	86.52	87.50	85.16	85.82
	Bon	89.69	92.58	90.61	92.72	91.72	92.56
	Adj-Bon	89.30	92.32	89.67	92.07	89.96	91.09

Table 2.11: Known Lag, $T = 400$: Empirical coverages for the v -th variable.

2D Volumes for DGP-1–5 with Known Lag Order

		$\mathcal{N}(\mathbf{0}, \Sigma)$ Distribution					
	Method	$H = 6$		$H = 12$		$H = 24$	
		$v = 1$	$v = 2$	$v = 1$	$v = 2$	$v = 1$	$v = 2$
DGP-1	Sym-WW	6.44	6.69	8.12	8.63	9.90	10.77
	Asy-WW	6.44	6.69	8.12	8.62	9.89	10.76
	NP	6.76	7.06	8.69	9.30	10.98	12.00
	Bon	7.23	7.61	9.69	10.55	13.50	15.27
	Adj-Bon	7.19	7.56	9.53	10.34	12.94	14.58
DGP-2	Sym-WW	6.49	6.74	8.11	8.67	9.90	10.86
	Asy-WW	6.79	7.08	8.49	9.13	10.36	11.44
	NP	6.63	6.91	8.33	8.93	10.30	11.33
	Bon	7.08	7.40	9.10	9.87	11.70	13.14
	Adj-Bon	7.03	7.36	8.97	9.72	11.35	12.70
DGP-3	Sym-WW	5.03	5.08	5.62	5.71	6.08	6.21
	Asy-WW	5.04	5.10	5.56	5.66	5.95	6.09
	NP	5.01	5.08	5.55	5.66	5.94	6.09
	Bon	5.15	5.22	5.63	5.76	5.99	6.16
	Adj-Bon	5.14	5.21	5.62	5.74	5.97	6.14
DGP-4	Sym-WW	5.02	5.08	5.60	5.67	6.07	6.17
	Asy-WW	5.07	5.14	5.58	5.67	5.98	6.10
	NP	4.98	5.04	5.51	5.59	5.90	6.02
	Bon	5.11	5.19	5.58	5.68	5.94	6.08
	Adj-Bon	5.10	5.18	5.57	5.67	5.92	6.05
DGP-5	Sym-WW	7.52	6.61	10.63	8.59	15.24	11.55
	Asy-WW	7.52	6.61	10.63	8.59	15.23	11.54
	NP	8.00	6.99	11.54	9.34	17.36	13.13
	Bon	8.63	7.42	13.05	10.12	21.07	14.86
	Adj-Bon	8.55	7.37	12.75	9.97	20.15	14.35

Table 2.12: Known Lag, $T = 100$: Volumes for the v -th variable.

		$\mathcal{N}(\mathbf{0}, \Sigma)$ Distribution					
	Method	$H = 6$		$H = 12$		$H = 24$	
		$v = 1$	$v = 2$	$v = 1$	$v = 2$	$v = 1$	$v = 2$
DGP-1	Sym-WW	6.40	6.65	8.00	8.51	9.67	10.52
	Asy-WW	6.40	6.65	8.00	8.51	9.67	10.52
	NP	6.56	6.85	8.22	8.77	9.99	10.89
	Bon	6.94	7.28	8.90	9.62	11.10	12.36
	Adj-Bon	6.90	7.23	8.79	9.47	10.81	11.99
DGP-2	Sym-WW	6.41	6.69	8.03	8.54	9.66	10.55
	Asy-WW	6.70	7.03	8.39	8.99	10.08	11.09
	NP	6.54	6.85	8.16	8.70	9.84	10.76
	Bon	6.91	7.28	8.82	9.52	10.87	12.16
	Adj-Bon	6.87	7.23	8.71	9.38	10.60	11.80
DGP-3	Sym-WW	4.99	5.03	5.54	5.63	6.05	6.14
	Asy-WW	5.00	5.03	5.56	5.64	6.00	6.10
	NP	4.97	5.02	5.51	5.61	5.95	6.06
	Bon	5.07	5.13	5.60	5.70	5.99	6.11
	Adj-Bon	5.06	5.12	5.58	5.69	5.97	6.08
DGP-4	Sym-WW	4.99	5.04	5.55	5.64	6.06	6.15
	Asy-WW	5.03	5.10	5.59	5.69	6.03	6.14
	NP	4.96	5.02	5.50	5.60	5.94	6.04
	Bon	5.06	5.13	5.58	5.69	5.98	6.09
	Adj-Bon	5.05	5.12	5.57	5.67	5.96	6.07
DGP-5	Sym-WW	7.50	6.62	10.58	8.61	15.10	11.49
	Asy-WW	7.50	6.62	10.57	8.61	15.09	11.49
	NP	7.83	6.86	11.06	9.01	16.01	12.26
	Bon	8.42	7.24	12.44	9.71	18.91	13.54
	Adj-Bon	8.34	7.20	12.18	9.57	18.18	13.15

Table 2.13: Known Lag, $T = 200$: Volumes for the v -th variable.

		$\mathcal{N}(\mathbf{0}, \Sigma)$ Distribution					
	Method	$H = 6$		$H = 12$		$H = 24$	
		$v = 1$	$v = 2$	$v = 1$	$v = 2$	$v = 1$	$v = 2$
DGP-1	Sym-WW	6.40	6.64	7.94	8.48	9.54	10.41
	Asy-WW	6.39	6.64	7.94	8.48	9.54	10.41
	NP	6.54	6.82	8.09	8.65	9.68	10.57
	Bon	6.88	7.21	8.66	9.39	10.54	11.75
	Adj-Bon	6.84	7.16	8.56	9.26	10.30	11.44
DGP-2	Sym-WW	6.41	6.65	7.96	8.48	9.56	10.43
	Asy-WW	6.69	6.98	8.32	8.92	9.98	10.95
	NP	6.53	6.81	8.07	8.62	9.63	10.51
	Bon	6.87	7.20	8.64	9.34	10.47	11.65
	Adj-Bon	6.83	7.15	8.53	9.20	10.23	11.35
DGP-3	Sym-WW	4.97	5.03	5.51	5.59	6.03	6.11
	Asy-WW	4.98	5.03	5.52	5.60	6.04	6.11
	NP	4.95	5.02	5.49	5.58	5.97	6.06
	Bon	5.04	5.12	5.55	5.65	6.01	6.09
	Adj-Bon	5.04	5.11	5.54	5.63	5.99	6.07
DGP-4	Sym-WW	4.98	8.02	5.52	5.61	6.02	6.11
	Asy-WW	5.20	5.07	5.56	5.65	6.05	6.14
	NP	4.96	5.00	5.49	5.59	5.95	6.05
	Bon	5.05	5.10	5.56	5.65	5.99	6.09
	Adj-Bon	5.04	5.09	5.54	5.64	5.67	6.07
DGP-5	Sym-WW	7.48	6.63	10.58	8.60	15.13	11.49
	Asy-WW	7.48	6.63	10.58	8.60	15.13	11.49
	NP	7.77	6.82	10.89	8.85	15.51	11.90
	Bon	8.34	7.18	12.24	9.49	18.32	13.05
	Adj-Bon	8.27	7.14	11.98	9.36	17.62	12.70

Table 2.14: Known Lag, $T = 400$: Volumes for the v -th variable.

		$t(3)$ Distribution					
	Method	$H = 6$		$H = 12$		$H = 24$	
		$v = 1$	$v = 2$	$v = 1$	$v = 2$	$v = 1$	$v = 2$
DGP-1	Sym-WW	6.88	7.08	9.43	9.80	11.88	12.55
	Asy-WW	7.13	7.34	9.60	10.00	11.81	12.82
	NP	6.72	6.99	9.24	9.75	11.54	12.45
	Bon	8.07	8.50	10.60	11.46	14.15	15.92
	Adj-Bon	8.00	8.41	10.42	11.21	13.58	15.19
DGP-2	Sym-WW	7.05	7.19	9.49	9.90	12.07	12.76
	Asy-WW	8.12	8.30	10.62	11.27	13.44	14.20
	NP	6.68	6.91	9.08	9.56	11.43	12.24
	Bon	8.57	8.86	10.66	11.45	13.12	14.44
	Adj-Bon	8.37	8.64	10.48	11.23	12.71	13.92
DGP-3	Sym-WW	6.06	6.07	8.15	8.43	9.30	9.20
	Asy-WW	6.53	6.50	7.85	8.16	8.68	8.60
	NP	5.51	5.53	7.01	7.19	7.66	7.65
	Bon	6.63	6.64	7.50	7.78	7.67	7.67
	Adj-Bon	6.58	6.59	7.49	7.76	7.65	7.65
DGP-4	Sym-WW	6.17	6.19	8.23	8.27	9.71	9.60
	Asy-WW	6.84	6.80	8.05	8.16	9.57	9.32
	NP	5.55	5.62	7.07	7.17	7.98	7.96
	Bon	6.82	6.81	7.67	7.75	8.04	8.06
	Adj-Bon	6.70	6.68	7.64	7.72	8.02	8.02
DGP-5	Sym-WW	7.64	7.05	11.45	9.89	16.53	13.47
	Asy-WW	7.85	7.31	11.74	10.04	16.84	13.60
	NP	7.75	6.95	11.66	9.76	17.26	13.48
	Bon	9.40	8.19	14.03	11.01	21.76	15.49
	Adj-Bon	9.28	8.11	13.65	10.83	20.64	14.94

Table 2.15: Known Lag, $T = 100$: Volumes for the v -th variable.

		$t(3)$ Distribution					
	Method	$H = 6$		$H = 12$		$H = 24$	
		$v = 1$	$v = 2$	$v = 1$	$v = 2$	$v = 1$	$v = 2$
DGP-1	Sym-WW	6.74	6.93	9.10	9.63	11.68	11.42
	Asy-WW	6.86	7.04	9.49	9.95	11.76	12.58
	NP	6.53	6.77	8.68	9.18	11.01	11.79
	Bon	8.16	8.57	10.63	11.44	12.60	13.91
	Adj-Bon	7.78	8.22	10.40	11.18	12.27	13.47
DGP-2	Sym-WW	6.75	6.95	8.99	9.37	11.83	12.46
	Asy-WW	7.65	7.96	10.38	10.84	13.17	14.04
	NP	6.51	6.76	8.61	9.08	11.21	11.90
	Bon	8.10	8.56	10.96	11.68	13.24	14.44
	Adj-Bon	7.79	8.25	10.54	11.25	12.86	13.95
DGP-3	Sym-WW	5.95	5.94	7.62	7.75	10.41	10.45
	Asy-WW	6.13	6.09	8.33	8.43	9.82	9.92
	NP	5.53	5.53	6.78	6.92	8.34	8.46
	Bon	6.16	6.18	8.13	8.28	9.30	9.40
	Adj-Bon	6.08	6.07	8.04	8.17	9.27	9.38
DGP-4	Sym-WW	5.93	5.91	7.75	7.77	10.38	10.31
	Asy-WW	6.24	6.25	8.60	8.71	9.91	9.93
	NP	5.49	5.50	6.86	6.89	8.37	8.41
	Bon	6.11	6.12	8.26	8.40	9.40	9.43
	Adj-Bon	6.06	6.06	8.08	8.14	9.29	9.33
DGP-5	Sym-WW	7.65	6.80	10.79	9.34	15.71	13.01
	Asy-WW	7.46	6.87	10.88	9.49	15.92	13.49
	NP	7.48	6.73	10.91	9.23	15.79	12.88
	Bon	9.92	8.37	14.66	11.65	20.86	15.60
	Adj-Bon	9.59	8.07	14.10	11.06	19.84	14.98

Table 2.16: Known Lag, $T = 200$: Volumes for the v -th variable.

		$t(3)$ Distribution					
	Method	$H = 6$		$H = 12$		$H = 24$	
		$v = 1$	$v = 2$	$v = 1$	$v = 2$	$v = 1$	$v = 2$
DGP-1	Sym-WW	6.58	6.77	8.74	9.16	11.40	11.97
	Asy-WW	6.64	6.82	8.89	9.29	11.94	12.44
	NP	6.46	6.68	8.51	8.99	10.82	11.49
	Bon	8.01	8.44	10.70	11.53	13.21	14.23
	Adj-Bon	7.79	8.10	10.11	10.92	12.76	13.72
DGP-2	Sym-WW	6.63	6.80	8.93	9.28	11.39	11.97
	Asy-WW	7.47	7.74	10.19	10.70	13.26	14.04
	NP	6.46	6.69	8.59	8.99	10.83	11.46
	Bon	7.90	8.33	11.15	12.10	13.79	15.01
	Adj-Bon	7.72	8.11	10.38	11.15	13.07	14.18
DGP-3	Sym-WW	5.82	5.84	7.51	7.54	9.54	9.65
	Asy-WW	5.90	5.93	7.72	7.78	10.55	10.66
	NP	5.51	5.54	6.86	6.91	8.30	8.38
	Bon	5.98	6.06	7.72	7.86	9.78	9.94
	Adj-Bon	5.94	6.01	7.57	7.66	9.60	9.73
DGP-4	Sym-WW	5.80	5.82	7.45	7.51	9.77	9.73
	Asy-WW	6.02	6.07	7.83	7.94	10.86	11.00
	NP	5.50	5.53	6.85	6.91	8.44	8.42
	Bon	5.96	6.01	7.66	7.77	9.95	10.06
	Adj-Bon	5.93	6.00	7.56	7.65	9.69	9.72
DGP-5	Sym-WW	7.41	6.80	10.79	9.34	15.71	13.01
	Asy-WW	7.46	6.87	10.88	9.49	15.92	13.49
	NP	7.48	6.73	10.91	9.23	15.79	12.88
	Bon	9.92	8.37	14.66	11.65	220.86	15.60
	Adj-Bon	9.59	8.07	14.10	11.06	19.84	14.98

Table 2.17: Known Lag, $T = 400$: Volumes for the v -th variable.

		χ^2_3 Distribution					
	Method	$H = 6$		$H = 12$		$H = 24$	
		$v = 1$	$v = 2$	$v = 1$	$v = 2$	$v = 1$	$v = 2$
DGP-1	Sym-WW	6.78	6.99	8.83	9.25	11.09	11.83
	Asy-WW	6.61	6.85	8.39	8.90	10.35	11.23
	NP	6.57	6.86	8.59	9.20	10.99	12.01
	Bon	7.32	7.70	9.74	10.60	13.53	15.32
	Adj-Bon	7.27	7.64	9.57	10.39	12.97	14.63
DGP-2	Sym-WW	6.95	7.19	8.98	9.48	11.02	11.80
	Asy-WW	7.49	7.81	9.54	10.22	11.57	12.58
	NP	6.76	7.7	8.76	9.35	10.79	11.66
	Bon	7.57	7.94	9.75	10.57	12.33	13.65
	Adj-Bon	7.48	7.85	9.60	10.38	11.95	13.18
DGP-3	Sym-WW	5.99	6.00	7.35	7.34	8.25	8.28
	Asy-WW	5.34	5.37	5.95	6.01	6.40	6.50
	NP	4.91	4.98	5.67	5.74	6.11	6.23
	Bon	5.41	5.46	5.88	5.97	6.20	6.34
	Adj-Bon	5.40	5.45	5.87	5.96	6.18	6.31
DGP-4	Sym-WW	6.06	6.11	7.39	7.34	8.35	8.31
	Asy-WW	5.58	5.70	6.33	6.42	6.91	7.05
	NP	5.05	5.15	5.92	6.01	6.49	6.62
	Bon	5.57	5.69	6.20	6.29	6.60	6.74
	Adj-Bon	5.53	5.64	6.17	6.26	6.56	6.71
DGP-5	Sym-WW	7.61	6.92	10.99	9.30	15.81	12.47
	Asy-WW	7.61	6.75	10.88	8.92	15.62	11.92
	NP	7.57	6.79	11.17	9.27	16.90	12.98
	Bon	8.64	7.48	13.03	10.25	20.68	14.78
	Adj-Bon	8.56	7.43	12.73	10.09	19.80	14.29

Table 2.18: Known Lag, $T = 100$: Volumes for the v -th variable.

		χ^2_3 Distribution					
	Method	$H = 6$		$H = 12$		$H = 24$	
		$v = 1$	$v = 2$	$v = 1$	$v = 2$	$v = 1$	$v = 2$
DGP-1	Sym-WW	6.69	6.87	8.70	9.05	10.77	11.48
	Asy-WW	6.51	6.74	8.26	8.73	10.04	10.90
	NP	6.24	6.49	8.08	8.57	9.98	10.87
	Bon	7.01	7.33	9.01	9.68	11.23	12.50
	Adj-Bon	6.96	7.27	8.89	9.52	10.94	12.13
DGP-2	Sym-WW	6.90	7.10	8.78	9.25	10.75	11.53
	Asy-WW	7.46	7.75	9.37	10.00	11.32	12.32
	NP	6.70	6.98	8.56	9.11	10.47	11.32
	Bon	7.51	7.85	9.56	10.32	11.70	12.96
	Adj-Bon	7.43	7.76	9.38	10.11	11.39	12.56
DGP-3	Sym-WW	5.94	5.99	7.20	7.25	8.59	8.55
	Asy-WW	5.16	5.25	5.95	6.02	6.50	6.57
	NP	4.75	4.84	5.44	5.53	6.09	6.19
	Bon	5.20	5.30	5.92	6.01	6.39	6.47
	Adj-Bon	5.19	5.29	5.91	5.99	6.37	6.45
DGP-4	Sym-WW	5.96	6.02	7.18	7.27	8.55	8.58
	Asy-WW	5.40	5.56	6.28	6.47	6.96	7.19
	NP	4.89	5.01	5.68	5.85	6.49	6.67
	Bon	5.37	5.52	6.18	6.37	6.80	7.02
	Adj-Bon	5.34	5.49	6.12	6.30	6.75	6.96
DGP-5	Sym-WW	7.48	6.88	10.80	9.17	15.68	12.39
	Asy-WW	7.49	3.72	10.72	8.82	15.50	11.86
	NP	7.25	6.55	10.58	8.83	15.68	12.18
	Bon	8.40	7.30	12.49	9.80	19.09	13.65
	Adj-Bon	8.31	7.25	12.20	9.66	18.33	13.26

Table 2.19: Known Lag, $T = 200$: Volumes for the v -th variable.

		χ^2_3 Distribution					
	Method	$H = 6$		$H = 12$		$H = 24$	
		$v = 1$	$v = 2$	$v = 1$	$v = 2$	$v = 1$	$v = 2$
DGP-1	Sym-WW	6.64	6.81	8.60	9.01	10.66	11.29
	Asy-WW	6.45	6.69	8.17	8.67	9.95	10.72
	NP	6.11	6.36	7.88	8.40	9.71	10.49
	Bon	6.90	7.23	8.80	9.48	10.80	11.88
	Adj-Bon	6.85	7.17	8.68	9.33	10.54	11.55
DGP-2	Sym-WW	6.85	7.02	8.74	9.14	10.58	11.36
	Asy-WW	7.39	7.65	9.32	9.88	11.17	12.15
	NP	6.64	6.89	8.50	8.99	10.26	11.11
	Bon	7.43	7.75	9.46	10.13	11.38	12.57
	Adj-Bon	7.35	7.66	9.29	9.93	11.08	12.18
DGP-3	Sym-WW	5.91	5.92	7.17	7.20	8.47	8.50
	Asy-WW	5.10	5.16	5.83	5.90	6.62	6.70
	NP	4.66	4.72	5.33	5.42	5.97	6.07
	Bon	5.14	5.21	5.82	5.91	6.48	6.57
	Adj-Bon	5.13	5.20	5.81	5.89	6.45	6.55
DGP-4	Sym-WW	5.95	6.00	7.22	7.22	8.40	8.52
	Asy-WW	5.35	5.50	6.24	6.38	7.05	7.34
	NP	4.83	4.95	5.65	5.78	6.39	6.64
	Bon	5.33	5.47	6.18	6.31	6.86	7.14
	Adj-Bon	5.31	5.44	6.12	6.24	6.77	7.03
DGP-5	Sym-WW	7.44	6.82	10.72	9.14	15.52	12.36
	Asy-WW	7.46	6.67	10.65	8.80	15.35	11.83
	NP	7.11	6.40	10.34	8.62	15.02	11.81
	Bon	8.35	7.20	12.28	9.60	18.35	13.18
	Adj-Bon	8.26	7.15	12.00	9.46	17.62	12.82

Table 2.20: Known Lag, $T = 400$: Volumes for the v -th variable.

2E Empirical Coverages for DGP-1–5 with BIC Lag Selection

		$\mathcal{N}(0, \Sigma)$ Distribution					
	Method	$H = 6$		$H = 12$		$H = 24$	
		$v = 1$	$v = 2$	$v = 1$	$v = 2$	$v = 1$	$v = 2$
DGP-1	Sym-WW	87.81	87.59	85.94	86.16	84.23	83.16
	Asy-WW	87.56	87.35	85.63	85.88	83.90	82.81
	NP	89.19	89.15	88.40	88.57	87.86	87.02
	Bon	92.56	92.77	92.47	93.14	92.62	92.51
	Adj-Bon	92.35	92.55	91.99	92.60	91.72	91.52
DGP-2	Sym-WW	88.67	88.96	88.35	88.48	87.88	88.09
	Asy-WW	90.66	91.17	90.66	91.10	90.33	90.81
	NP	88.60	88.94	88.64	88.93	89.03	89.58
	Bon	92.10	92.66	92.71	93.33	93.32	94.03
	Adj-Bon	91.84	92.41	92.23	92.81	92.43	93.13
DGP-3	Sym-WW	89.08	89.03	88.32	88.39	86.21	86.49
	Asy-WW	88.41	88.28	86.23	85.56	82.16	82.97
	NP	88.48	88.52	86.39	86.74	82.00	82.78
	Bon	89.43	89.52	87.01	87.55	82.74	83.78
	Adj-Bon	89.35	89.43	86.85	87.38	82.37	83.39
DGP-4	Sym-WW	89.38	89.16	88.88	88.94	87.08	87.34
	Asy-WW	89.08	89.02	87.24	87.60	84.12	84.85
	NP	88.56	88.37	86.45	86.68	82.34	82.76
	Bon	89.35	89.36	87.13	87.54	83.19	84.05
	Adj-Bon	89.28	89.28	86.98	87.37	82.83	83.68
DGP-5	Sym-WW	86.37	85.35	84.00	82.26	79.41	77.15
	Asy-WW	86.08	85.12	83.80	81.95	79.23	77.00
	NP	87.13	86.60	86.14	85.32	84.89	84.06
	Bon	90.65	90.46	90.96	90.05	90.28	89.12
	Adj-Bon	90.25	90.20	89.98	89.33	88.33	87.28

Table 2.21: BIC order selection, $T = 100$: Empirical coverages for the v -th variable.

		$\mathcal{N}(\mathbf{0}, \Sigma)$ Distribution					
	Method	$H = 6$		$H = 12$		$H = 24$	
		$v = 1$	$v = 2$	$v = 1$	$v = 2$	$v = 1$	$v = 2$
DGP-1	Sym-WW	88.89	88.79	88.28	88.45	87.66	87.69
	Asy-WW	88.79	88.64	88.14	88.26	87.44	87.54
	NP	89.00	88.86	88.44	88.62	88.11	88.29
	Bon	92.33	92.67	92.79	93.42	93.16	93.89
	Adj-Bon	92.12	92.45	92.28	92.88	92.21	92.91
DGP-2	Sym-WW	89.41	89.39	89.32	89.12	88.83	88.66
	Asy-WW	91.43	91.63	91.71	91.71	91.35	91.43
	NP	89.12	89.12	89.01	88.81	88.48	88.41
	Bon	92.42	92.82	93.26	93.56	93.46	93.95
	Adj-Bon	92.20	92.58	92.74	93.03	92.53	92.93
DGP-3	Sym-WW	89.36	89.63	89.10	89.18	87.96	88.42
	Asy-WW	88.94	89.26	88.24	88.44	85.70	86.43
	NP	88.74	89.03	87.42	87.75	84.44	85.17
	Bon	89.69	90.12	88.50	88.86	85.27	86.18
	Adj-Bon	89.61	90.03	88.34	88.70	84.97	85.84
DGP-4	Sym-WW	89.67	89.61	89.37	89.54	88.40	88.96
	Asy-WW	89.71	89.76	88.92	89.27	86.47	87.54
	NP	88.88	88.94	87.59	87.82	84.24	85.22
	Bon	89.84	89.85	88.55	88.96	85.21	86.41
	Adj-Bon	89.76	89.77	88.38	88.79	84.90	86.12
DGP-5	Sym-WW	88.36	87.63	87.02	86.24	84.70	84.13
	Asy-WW	88.31	87.50	86.93	86.08	84.58	83.96
	NP	88.30	87.66	87.08	86.85	85.60	85.75
	Bon	92.25	91.50	92.78	91.72	92.59	91.43
	Adj-Bon	91.92	91.25	91.94	91.05	90.92	89.97

Table 2.22: BIC order selection, $T = 200$: Empirical coverages for the v -th variable.

		$\mathcal{N}(\mathbf{0}, \Sigma)$ Distribution					
	Method	$H = 6$		$H = 12$		$H = 24$	
		$v = 1$	$v = 2$	$v = 1$	$v = 2$	$v = 1$	$v = 2$
DGP-1	Sym-WW	89.49	89.44	89.38	89.15	88.83	88.78
	Asy-WW	89.36	89.31	89.27	89.06	88.72	88.69
	NP	89.21	89.24	88.87	88.71	87.95	88.12
	Bon	92.65	92.87	93.22	93.49	93.16	93.92
	Adj-Bon	92.40	92.64	92.72	92.97	92.18	92.85
DGP-2	Sym-WW	89.51	89.67	89.63	89.54	89.50	89.31
	Asy-WW	91.62	91.94	91.95	92.17	91.99	92.17
	NP	89.10	89.29	88.82	88.86	88.20	88.18
	Bon	92.51	92.98	93.19	93.71	89.39	93.97
	Adj-Bon	92.28	92.74	92.70	93.15	92.39	92.86
DGP-3	Sym-WW	89.66	89.78	89.63	89.37	89.01	88.95
	Asy-WW	89.47	89.59	89.22	89.03	88.12	88.19
	NP	89.11	89.19	88.22	88.12	86.02	86.12
	Bon	90.07	90.38	89.26	89.24	87.15	87.38
	Adj-Bon	89.99	90.31	89.11	89.07	86.87	87.05
DGP-4	Sym-WW	89.81	89.84	89.62	89.64	89.17	89.27
	Asy-WW	90.08	90.24	89.52	89.73	88.63	88.89
	NP	89.14	89.18	88.07	88.18	86.04	86.21
	Bon	90.16	90.36	89.08	89.41	87.16	87.48
	Adj-Bon	90.09	90.29	88.95	89.26	86.87	87.17
DGP-5	Sym-WW	89.26	88.85	88.63	88.26	87.28	87.12
	Asy-WW	89.20	88.78	88.52	88.19	87.19	87.11
	NP	88.80	88.60	87.92	87.82	86.60	86.75
	Bon	93.09	92.36	93.90	92.77	94.17	92.83
	Adj-Bon	92.77	92.11	93.14	92.16	92.70	91.53

Table 2.23: BIC order selection, $T = 400$: Empirical coverages for the v -th variable.

		$t(3)$ Distribution					
	Method	$H = 6$		$H = 12$		$H = 24$	
		$v = 1$	$v = 2$	$v = 1$	$v = 2$	$v = 1$	$v = 2$
DGP-1	Sym-WW	88.53	88.55	87.03	87.30	84.11	84.59
	Asy-WW	87.66	87.69	85.40	85.79	81.30	82.07
	NP	87.87	88.13	86.33	87.04	83.19	84.17
	Bon	90.76	91.30	89.65	90.67	87.90	89.31
	Adj-Bon	90.55	91.08	89.21	90.21	86.90	88.32
DGP-2	Sym-WW	89.38	89.22	87.94	88.14	86.02	86.55
	Asy-WW	91.20	91.28	89.56	90.09	87.50	88.45
	NP	87.79	87.72	86.24	86.64	84.30	85.25
	Bon	91.66	91.94	90.37	91.18	88.89	90.25
	Adj-Bon	91.38	91.67	89.92	90.71	87.98	89.36
DGP-3	Sym-WW	88.78	88.67	86.90	86.47	82.02	82.54
	Asy-WW	87.98	87.76	82.83	82.77	75.01	75.59
	NP	86.42	86.22	82.15	82.14	73.04	73.90
	Bon	87.69	87.53	81.50	81.59	71.54	72.53
	Adj-Bon	87.59	87.41	81.42	81.49	71.34	72.32
DGP-4	Sym-WW	88.92	88.80	87.43	87.65	81.76	82.57
	Asy-WW	88.71	88.78	84.47	84.90	76.34	77.87
	NP	86.37	86.31	82.81	83.15	83.23	74.65
	Bon	88.02	88.13	82.93	83.47	73.01	74.70
	Adj-Bon	87.87	87.97	82.82	83.34	72.77	74.45
DGP-5	Sym-WW	88.23	87.60	86.14	85.68	81.48	81.32
	Asy-WW	87.42	86.66	84.61	84.10	79.54	78.65
	NP	87.03	86.26	84.77	84.10	82.22	80.10
	Bon	90.51	89.42	89.56	88.14	88.22	85.24
	Adj-Bon	90.17	89.16	88.66	87.52	86.32	86.32

Table 2.24: BIC order selection, $T = 100$: Empirical coverages for the v -th variable.

		$t(3)$ Distribution					
	Method	$H = 6$		$H = 12$		$H = 24$	
		$v = 1$	$v = 2$	$v = 1$	$v = 2$	$v = 1$	$v = 2$
DGP-1	Sym-WW	89.70	89.75	89.23	89.34	87.96	87.65
	Asy-WW	89.17	89.33	88.36	88.45	86.11	85.92
	NP	88.49	88.52	87.43	87.58	85.26	85.42
	Bon	91.98	92.41	91.14	91.87	89.23	90.14
	Adj-Bon	91.68	92.11	90.67	91.31	88.34	89.16
DGP-2	Sym-WW	89.79	90.09	89.32	89.64	88.24	88.41
	Asy-WW	92.13	96.51	91.41	92.03	89.94	90.58
	NP	88.45	88.80	87.46	87.88	85.97	86.43
	Bon	92.70	93.22	92.15	92.98	90.70	91.86
	Adj-Bon	92.37	92.94	91.61	92.46	89.87	90.92
DGP-3	Sym-WW	89.93	90.09	88.82	88.54	87.00	87.14
	Asy-WW	89.24	89.39	88.15	87.81	82.38	82.83
	NP	87.94	88.24	85.40	85.22	79.77	80.28
	Bon	89.01	89.27	86.82	86.75	80.30	80.92
	Adj-Bon	88.85	89.10	86.62	86.51	80.17	80.75
DGP-4	Sym-WW	89.75	89.58	88.78	89.15	86.89	87.70
	Asy-WW	89.78	89.74	88.46	88.80	83.00	83.89
	NP	87.83	87.73	85.13	85.71	79.69	80.93
	Bon	89.10	89.10	87.03	87.49	81.08	82.02
	Adj-Bon	88.99	88.96	86.77	87.23	80.86	81.77
DGP-5	Sym-WW	89.51	89.46	88.47	88.28	86.50	86.65
	Asy-WW	89.03	89.06	87.72	87.50	85.39	85.05
	NP	88.21	88.09	86.70	86.37	84.62	83.76
	Bon	92.84	91.93	92.53	90.77	91.65	89.21
	Adj-Bon	92.49	91.61	91.79	90.24	90.19	87.90

Table 2.25: BIC order selection, $T = 200$: Empirical coverages for the v -th variable.

		$t(3)$ Distribution					
	Method	$H = 6$		$H = 12$		$H = 24$	
		$v = 1$	$v = 2$	$v = 1$	$v = 2$	$v = 1$	$v = 2$
DGP-1	Sym-WW	90.02	90.01	89.98	89.91	89.37	89.36
	Asy-WW	89.77	89.75	89.48	89.47	88.51	88.55
	NP	88.94	88.90	88.25	88.36	86.56	86.73
	Bon	92.95	93.27	92.60	93.17	90.91	91.85
	Adj-Bon	92.65	92.96	92.03	92.62	90.03	90.92
DGP-2	Sym-WW	90.10	90.11	89.98	89.95	89.34	89.57
	Asy-WW	92.59	92.72	92.43	92.70	91.77	92.22
	NP	88.97	88.92	88.24	88.29	86.67	87.36
	Bon	93.25	93.62	92.37	92.90	92.20	93.23
	Adj-Bon	92.98	93.35	92.70	93.26	91.24	92.23
DGP-3	Sym-WW	89.93	90.18	89.45	89.23	88.28	88.57
	Asy-WW	89.63	89.85	88.86	88.50	87.35	87.61
	NP	88.59	88.82	86.97	86.70	83.28	83.66
	Bon	89.63	90.10	88.19	87.97	84.85	85.29
	Adj-Bon	89.52	89.89	87.93	87.69	84.49	84.93
DGP-4	Sym-WW	90.03	89.89	89.60	89.52	88.89	88.58
	Asy-WW	90.33	90.35	89.50	89.46	88.55	88.38
	NP	88.57	88.50	86.94	86.94	83.90	83.74
	Bon	89.87	89.95	88.37	88.49	85.94	85.86
	Adj-Bon	89.77	89.84	88.15	88.21	85.30	85.39
DGP-5	Sym-WW	89.81	89.82	89.46	89.50	88.35	88.92
	Asy-WW	89.61	89.56	89.07	89.10	88.23	88.30
	NP	88.67	88.55	87.83	87.48	86.73	86.09
	Bon	94.01	92.99	94.31	92.64	94.34	91.93
	Adj-Bon	93.71	92.70	93.65	92.02	93.14	90.78

Table 2.26: BIC order selection, $T = 400$: Empirical coverages for the v -th variable.

		χ^2_3 Distribution					
	Method	$H = 6$		$H = 12$		$H = 24$	
		$v = 1$	$v = 2$	$v = 1$	$v = 2$	$v = 1$	$v = 2$
DGP-1	Sym-WW	88.40	88.25	87.62	87.55	85.89	85.93
	Asy-WW	87.17	87.32	85.57	85.86	83.62	83.90
	NP	88.84	88.85	88.36	88.47	87.63	87.82
	Bon	92.74	93.18	92.75	93.21	92.92	93.59
	Adj-Bon	92.52	92.96	92.29	92.76	92.02	92.74
DGP-2	Sym-WW	88.88	89.16	88.30	88.59	87.48	87.55
	Asy-WW	91.54	91.98	90.84	91.32	89.88	90.27
	NP	88.42	88.82	88.00	88.30	87.58	87.99
	Bon	92.73	93.35	92.50	93.20	92.32	93.22
	Adj-Bon	92.49	93.08	92.02	92.68	91.42	92.24
DGP-3	Sym-WW	88.50	88.68	87.46	87.42	83.81	83.44
	Asy-WW	91.62	91.52	90.17	89.94	86.88	86.59
	NP	88.41	88.59	86.98	87.15	83.06	82.87
	Bon	92.25	92.41	89.94	90.00	85.41	85.33
	Adj-Bon	92.18	92.33	89.85	89.90	85.22	85.09
DGP-4	Sym-WW	88.81	88.47	87.53	87.66	83.64	83.52
	Asy-WW	91.40	90.80	89.33	89.13	85.44	85.10
	NP	88.65	88.25	87.09	87.15	82.40	82.08
	Bon	91.47	90.93	88.60	88.62	83.30	83.18
	Adj-Bon	91.32	90.76	88.46	88.44	83.01	82.82
DGP-5	Sym-WW	88.59	87.57	85.90	85.51	81.12	81.88
	Asy-WW	82.53	83.73	87.09	78.79	73.02	73.43
	NP	86.60	86.60	84.16	83.87	83.14	82.77
	Bon	87.33	90.57	87.46	89.28	88.09	88.58
	Adj-Bon	86.82	90.28	86.17	88.40	85.77	86.74

Table 2.27: BIC order selection, $T = 100$: Empirical coverages for the v -th variable.

		χ_3^2 Distribution					
	Method	$H = 6$		$H = 12$		$H = 24$	
		$v = 1$	$v = 2$	$v = 1$	$v = 2$	$v = 1$	$v = 2$
DGP-1	Sym-WW	89.62	89.47	89.04	89.12	88.37	88.33
	Asy-WW	89.01	89.14	88.18	88.17	87.14	87.12
	NP	89.42	89.32	88.70	88.88	88.08	88.08
	Bon	93.48	93.94	93.59	94.09	93.42	94.01
	Adj-Bon	93.25	93.68	93.09	93.54	92.46	92.98
DGP-2	Sym-WW	89.54	89.58	89.27	89.33	88.75	89.01
	Asy-WW	92.45	92.61	92.14	92.31	91.60	91.89
	NP	89.06	89.08	88.49	88.59	87.89	88.33
	Bon	93.48	93.79	93.41	93.95	93.15	93.95
	Adj-Bon	93.26	93.54	92.90	93.40	92.18	92.99
DGP-3	Sym-WW	89.38	89.27	88.69	88.57	87.72	87.39
	Asy-WW	91.32	91.05	91.40	91.14	89.95	89.53
	NP	89.05	89.00	88.01	87.94	86.08	85.78
	Bon	92.17	92.10	91.38	91.40	89.05	88.82
	Adj-Bon	92.09	92.01	91.23	91.23	88.80	88.57
DGP-4	Sym-WW	89.48	89.36	88.32	88.55	87.69	87.63
	Asy-WW	91.52	91.60	90.52	90.71	88.74	88.63
	NP	89.11	89.00	87.42	87.56	85.33	85.33
	Bon	91.69	91.87	90.08	90.35	87.42	87.40
	Adj-Bon	91.54	91.72	89.78	90.01	87.02	86.93
DGP-5	Sym-WW	89.83	88.97	88.76	88.40	86.50	87.14
	Asy-WW	84.80	86.21	83.08	83.98	80.92	80.26
	NP	87.02	87.76	85.58	86.15	84.08	84.01
	Bon	88.27	91.83	89.45	91.43	89.96	90.61
	Adj-Bon	87.81	91.54	88.33	90.69	87.96	88.93

Table 2.28: BIC order selection, $T = 200$: Empirical coverages for the v -th variable.

		χ^2_3 Distribution					
	Method	$H = 6$		$H = 12$		$H = 24$	
		$v = 1$	$v = 2$	$v = 1$	$v = 2$	$v = 1$	$v = 2$
DGP-1	Sym-WW	89.68	89.77	89.53	89.53	89.24	89.21
	Asy-WW	89.69	89.52	89.36	89.46	88.59	88.70
	NP	88.46	89.50	89.11	89.06	88.11	88.24
	Bon	93.46	93.69	93.79	94.34	93.53	94.22
	Adj-Bon	93.22	93.44	93.27	93.80	92.58	93.18
DGP-2	Sym-WW	89.77	89.90	89.79	89.65	89.53	89.34
	Asy-WW	92.76	93.04	92.77	92.86	92.49	92.48
	NP	89.17	89.45	88.85	88.74	88.03	87.83
	Bon	93.80	94.12	93.89	94.34	93.42	94.03
	Adj-Bon	93.54	93.86	93.37	93.77	92.48	93.00
DGP-3	Sym-WW	89.61	89.70	89.27	89.26	88.58	88.44
	Asy-WW	90.76	90.80	91.06	90.75	91.10	90.71
	NP	89.26	89.34	88.48	88.45	87.00	86.86
	Bon	91.71	91.96	91.37	92.21	90.03	89.88
	Adj-Bon	91.63	91.88	91.20	91.01	89.68	89.54
DGP-4	Sym-WW	89.73	89.79	89.40	89.20	88.48	88.50
	Asy-WW	91.71	91.84	91.44	91.29	90.64	90.53
	NP	89.33	89.35	88.49	88.20	86.42	86.34
	Bon	91.94	92.10	91.13	91.03	89.12	89.14
	Adj-Bon	91.81	91.95	90.84	90.71	88.59	88.54
DGP-5	Sym-WW	90.25	89.42	89.74	89.43	88.68	89.26
	Asy-WW	86.65	88.00	85.39	86.84	83.57	84.83
	NP	87.69	88.49	86.36	87.46	84.93	85.62
	Bon	89.46	92.55	90.79	92.71	91.52	92.46
	Adj-Bon	89.08	92.30	89.82	92.05	89.76	90.96

Table 2.29: BIC order selection, $T = 400$: Empirical coverages for the v -th variable.

2F Volumes for DGP-1–5 with BIC Lag Selection

		$\mathcal{N}(0, \Sigma)$ Distribution					
	Method	$H = 6$		$H = 12$		$H = 24$	
		$v = 1$	$v = 2$	$v = 1$	$v = 2$	$v = 1$	$v = 2$
DGP-1	Sym-WW	6.47	6.71	8.07	8.63	9.83	10.68
	Asy-WW	6.47	6.71	8.07	8.63	9.82	10.67
	NP	6.79	7.10	8.64	8.29	10.83	11.85
	Bon	7.28	7.66	9.63	10.54	13.24	14.97
	Adj-Bon	7.23	7.60	9.47	10.33	12.70	14.30
DGP-2	Sym-WW	6.46	6.75	8.11	8.69	9.89	10.87
	Asy-WW	6.75	7.09	8.49	9.16	10.35	11.45
	NP	6.60	6.92	8.33	8.95	10.30	11.35
	Bon	7.04	7.42	9.10	9.91	11.69	13.16
	Adj-Bon	7.00	7.37	8.97	9.75	11.34	12.72
DGP-3	Sym-WW	5.04	5.09	5.59	5.68	6.06	6.17
	Asy-WW	5.06	5.11	5.54	5.64	5.93	6.06
	NP	5.03	5.09	5.53	5.64	5.91	6.06
	Bon	5.17	5.24	5.61	5.73	5.97	6.13
	Adj-Bon	5.16	5.23	5.60	5.72	5.94	6.10
DGP-4	Sym-WW	5.05	5.08	5.60	5.68	6.07	6.20
	Asy-WW	5.10	5.15	5.58	5.68	5.98	6.12
	NP	5.00	5.05	5.51	5.60	5.90	6.03
	Bon	5.14	5.19	5.59	5.69	5.94	6.10
	Adj-Bon	5.14	5.18	5.57	5.68	5.92	6.07
DGP-5	Sym-WW	7.49	6.60	10.63	8.61	15.22	11.52
	Asy-WW	7.49	6.60	10.63	8.60	15.22	11.51
	NP	7.97	6.98	11.54	9.35	17.35	13.11
	Bon	8.59	7.42	13.06	10.14	20.98	14.83
	Adj-Bon	8.52	7.37	12.76	9.98	20.07	14.32

Table 2.30: BIC order selection, $T = 100$: Empirical coverages for the v -th variable.

		$\mathcal{N}(\mathbf{0}, \Sigma)$ Distribution					
	Method	$H = 6$		$H = 12$		$H = 24$	
		$v = 1$	$v = 2$	$v = 1$	$v = 2$	$v = 1$	$v = 2$
DGP-1	Sym-WW	6.40	6.65	7.97	8.52	9.66	10.53
	Asy-WW	6.40	6.65	7.97	8.52	9.66	10.53
	NP	6.57	6.85	8.19	8.77	9.98	10.91
	Bon	6.95	7.29	8.85	9.61	11.10	12.40
	Adj-Bon	6.91	7.24	8.74	9.47	10.81	12.03
DGP-2	Sym-WW	6.42	6.68	8.01	8.53	9.63	10.51
	Asy-WW	6.71	7.01	8.38	8.97	10.06	11.05
	NP	6.55	6.84	8.16	8.70	9.81	10.72
	Bon	6.93	7.27	8.81	9.52	10.83	12.09
	Adj-Bon	6.89	7.22	8.70	9.38	10.57	11.75
DGP-3	Sym-WW	4.97	5.06	5.55	5.63	6.04	6.16
	Asy-WW	4.98	5.06	5.56	5.64	5.99	6.12
	NP	4.96	5.04	5.51	5.61	5.94	6.07
	Bon	5.06	5.16	5.60	5.70	5.98	6.12
	Adj-Bon	5.06	5.15	5.58	5.69	5.97	6.10
DGP-4	Sym-WW	4.99	5.04	5.55	5.64	6.04	6.17
	Asy-WW	5.03	5.10	5.59	5.69	6.00	6.15
	NP	4.96	5.02	5.50	5.60	5.91	6.05
	Bon	5.06	5.13	5.59	5.69	5.95	6.10
	Adj-Bon	5.05	5.12	5.57	5.68	5.94	6.08
DGP-5	Sym-WW	7.50	6.61	10.59	8.60	15.13	11.49
	Asy-WW	7.49	6.61	10.59	8.60	15.12	11.49
	NP	7.83	6.85	11.07	9.00	16.04	12.25
	Bon	8.41	7.22	12.45	9.70	18.96	13.53
	Adj-Bon	8.34	7.18	12.19	9.56	18.23	13.14

Table 2.31: BIC order selection, $T = 200$: Empirical coverages for the v -th variable.

		$\mathcal{N}(\mathbf{0}, \Sigma)$ Distribution					
	Method	$H = 6$		$H = 12$		$H = 24$	
		$v = 1$	$v = 2$	$v = 1$	$v = 2$	$v = 1$	$v = 2$
DGP-1	Sym-WW	6.40	6.65	7.6	8.48	9.55	10.40
	Asy-WW	6.39	6.64	7.96	8.47	9.55	10.41
	NP	6.54	6.83	8.10	8.65	9.69	10.57
	Bon	6.88	7.21	8.68	9.37	10.54	11.74
	Adj-Bon	6.84	7.17	8.58	9.24	10.30	11.43
DGP-2	Sym-WW	6.39	6.64	7.95	8.48	9.55	10.41
	Asy-WW	6.67	6.97	8.30	8.91	9.96	10.94
	NP	6.51	6.80	8.05	8.61	9.62	10.49
	Bon	6.85	7.19	8.62	9.33	10.45	11.64
	Adj-Bon	6.81	7.14	8.51	9.19	10.22	11.33
DGP-3	Sym-WW	4.97	5.03	5.52	5.60	6.02	6.11
	Asy-WW	4.98	5.04	5.52	5.60	6.04	6.12
	NP	4.95	5.02	5.50	5.59	5.97	6.07
	Bon	5.04	5.12	5.56	5.65	6.00	6.11
	Adj-Bon	5.04	5.11	5.55	5.64	5.98	6.09
DGP-4	Sym-WW	4.97	5.03	5.52	5.60	6.02	6.12
	Asy-WW	5.01	5.09	5.55	5.64	6.04	6.15
	NP	4.95	5.02	5.49	5.58	5.95	6.06
	Bon	5.04	5.11	5.56	5.65	5.99	6.10
	Adj-Bon	5.03	5.11	5.54	5.63	5.97	6.08
DGP-5	Sym-WW	7.50	6.62	10.60	8.62	15.15	11.49
	Asy-WW	7.49	6.62	10.60	8.62	15.14	11.49
	NP	7.78	6.82	10.91	8.87	15.54	11.90
	Bon	8.35	7.17	12.26	9.51	18.33	13.05
	Adj-Bon	8.28	7.12	12.01	9.39	17.64	12.70

Table 2.32: BIC order selection, $T = 400$: Empirical coverages for the v -th variable.

		$t(3)$ Distribution					
	Method	$H = 6$		$H = 12$		$H = 24$	
		$v = 1$	$v = 2$	$v = 1$	$v = 2$	$v = 1$	$v = 2$
DGP-1	Sym-WW	6.88	7.12	9.18	9.68	11.97	12.82
	Asy-WW	7.13	7.34	9.31	9.84	11.97	12.87
	NP	6.76	7.07	99.07	9.71	11.56	12.59
	Bon	8.07	8.51	10.38	11.37	14.21	16.08
	Adj-Bon	8.00	8.43	10.20	11.13	13.62	15.35
DGP-2	Sym-WW	7.01	7.19	9.42	9.82	12.17	12.86
	Asy-WW	8.06	8.30	10.64	11.29	13.75	14.75
	NP	6.63	6.84	9.01	9.49	11.46	12.22
	Bon	8.46	8.83	10.57	11.34	13.14	14.38
	Adj-Bon	8.24	8.59	10.39	11.12	12.73	13.87
DGP-3	Sym-WW	6.08	6.11	7.94	7.97	9.56	9.66
	Asy-WW	6.57	6.56	7.67	7.81	9.15	9.29
	NP	5.52	5.53	6.87	6.89	7.76	7.89
	Bon	6.65	6.66	7.30	7.37	7.78	7.92
	Adj-Bon	6.60	6.61	7.29	7.36	7.76	7.90
DGP-4	Sym-WW	6.11	6.10	8.18	8.21	9.41	9.87
	Asy-WW	6.73	6.73	8.12	8.21	9.07	10.01
	NP	5.50	5.52	7.04	7.08	7.73	8.12
	Bon	6.72	6.72	7.60	7.71	7.80	8.22
	Adj-Bon	6.58	6.58	7.57	7.67	7.77	8.18
DGP-5	Sym-WW	7.77	7.11	11.24	9.81	16.36	13.44
	Asy-WW	7.97	7.41	11.58	10.00	16.55	13.62
	NP	7.79	6.94	11.49	9.64	17.15	13.39
	Bon	9.47	8.26	13.70	10.84	21.35	15.29
	Adj-Bon	9.35	8.18	13.34	10.66	20.34	14.76

Table 2.33: BIC order selection, $T = 100$: Empirical coverages for the v -th variable.

		$t(3)$ Distribution					
	Method	$H = 6$		$H = 12$		$H = 24$	
		$v = 1$	$v = 2$	$v = 1$	$v = 2$	$v = 1$	$v = 2$
DGP-1	Sym-WW	6.73	6.89	9.15	9.53	11.84	12.38
	Asy-WW	6.85	7.01	9.50	9.86	11.94	12.54
	NP	6.54	6.75	8.74	9.18	11.10	11.78
	Bon	8.08	8.46	10.67	11.36	12.72	13.87
	Adj-Bon	7.78	8.17	10.47	11.10	12.40	13.43
DGP-2	Sym-WW	6.77	7.02	8.97	9.41	11.83	12.43
	Asy-WW	7.70	8.04	10.28	10.91	13.19	14.12
	NP	6.51	6.78	8.61	9.10	11.18	11.87
	Bon	8.14	8.61	10.83	11.72	13.22	14.41
	Adj-Bon	7.81	8.23	10.44	11.28	12.84	13.92
DGP-3	Sym-WW	5.95	5.99	7.69	7.65	10.34	10.30
	Asy-WW	6.12	6.16	8.40	8.29	9.77	9.79
	NP	5.52	5.58	6.85	6.84	8.27	8.35
	Bon	6.14	6.23	8.17	8.12	9.24	9.29
	Adj-Bon	6.06	6.14	8.08	8.02	9.21	9.26
DGP-4	Sym-WW	5.90	5.91	7.64	7.76	10.33	10.43
	Asy-WW	6.20	6.25	8.50	8.63	9.92	10.06
	NP	5.48	5.52	6.78	6.90	8.29	8.49
	Bon	6.08	6.13	8.18	8.32	9.35	9.48
	Adj-Bon	6.03	6.08	7.97	8.07	9.26	9.38
DGP-5	Sym-WW	7.54	6.96	11.03	9.46	16.06	13.16
	Asy-WW	7.63	7.08	11.24	9.79	16.35	13.33
	NP	7.59	6.81	11.09	9.30	16.27	12.97
	Bon	9.74	8.49	14.08	11.15	20.46	14.89
	Adj-Bon	9.53	8.13	13.67	10.92	19.52	14.41

Table 2.34: BIC order selection, $T = 200$: Empirical coverages for the v -th variable.

		$t(3)$ Distribution					
	Method	$H = 6$		$H = 12$		$H = 24$	
		$v = 1$	$v = 2$	$v = 1$	$v = 2$	$v = 1$	$v = 2$
DGP-1	Sym-WW	6.62	6.77	8.85	9.21	11.48	12.06
	Asy-WW	6.68	6.83	8.99	9.33	12.08	12.58
	NP	6.49	6.69	8.59	9.01	10.85	11.55
	Bon	8.05	8.46	10.85	11.60	13.30	14.37
	Adj-Bon	7.74	8.13	10.25	10.92	12.85	13.85
DGP-2	Sym-WW	6.63	6.79	8.84	9.15	11.60	12.16
	Asy-WW	7.47	7.70	10.06	10.46	13.80	14.21
	NP	6.48	6.68	8.57	8.97	10.79	11.57
	Bon	7.87	8.24	10.91	11.63	14.34	15.15
	Adj-Bon	7.70	8.40	10.30	10.93	13.51	14.32
DGP-3	Sym-WW	5.79	5.84	7.44	7.39	9.58	9.66
	Asy-WW	5.87	5.92	7.68	7.61	10.51	10.62
	NP	5.50	5.55	6.86	6.86	8.31	8.40
	Bon	5.95	6.04	7.68	7.66	9.76	9.92
	Adj-Bon	5.92	6.00	7.56	7.53	9.61	9.73
DGP-4	Sym-WW	5.82	5.81	7.50	7.46	9.76	9.60
	Asy-WW	6.04	6.07	7.88	7.84	10.95	10.72
	NP	5.50	5.51	6.88	6.89	8.41	8.40
	Bon	5.96	6.01	7.71	7.71	10.00	9.88
	Adj-Bon	5.93	5.97	7.61	7.59	9.73	9.59
DGP-5	Sym-WW	7.37	6.77	11.02	9.48	15.83	13.00
	Asy-WW	7.41	6.83	11.05	9.57	16.04	13.48
	NP	7.45	6.69	10.94	9.23	15.87	12.88
	Bon	9.71	8.32	14.91	11.81	20.99	15.61
	Adj-Bon	9.41	8.02	14.27	11.14	19.96	14.99

Table 2.35: BIC order selection, $T = 400$: Empirical coverages for the v -th variable.

		χ^2_3 Distribution					
	Method	$H = 6$		$H = 12$		$H = 24$	
		$v = 1$	$v = 2$	$v = 1$	$v = 2$	$v = 1$	$v = 2$
DGP-1	Sym-WW	6.76	6.97	8.87	9.30	11.01	11.83
	Asy-WW	6.57	6.84	8.40	8.95	10.28	11.23
	NP	6.51	6.85	8.58	9.22	10.94	12.04
	Bon	7.26	7.66	9.71	10.61	13.47	15.35
	Adj-Bon	7.21	7.60	9.55	10.40	12.92	14.65
DGP-2	Sym-WW	6.97	7.23	8.96	9.44	11.08	11.88
	Asy-WW	7.50	7.87	9.51	10.16	11.64	12.68
	NP	6.77	7.12	8.74	9.29	10.84	11.75
	Bon	7.59	8.00	9.74	10.50	12.40	13.76
	Adj-Bon	7.51	7.90	9.58	10.31	12.02	13.28
DGP-3	Sym-WW	5.96	6.01	7.29	7.32	8.26	8.30
	Asy-WW	5.29	8.37	5.91	5.99	6.41	6.51
	NP	4.91	4.98	5.65	5.73	6.12	6.22
	Bon	5.37	5.46	5.85	5.94	6.21	6.34
	Adj-Bon	5.36	5.45	5.83	5.93	6.18	6.31
DGP-4	Sym-WW	6.07	6.03	7.36	7.42	8.29	8.29
	Asy-WW	5.58	5.65	6.30	6.48	6.88	7.03
	NP	5.05	5.09	5.91	6.05	6.46	6.60
	Bon	5.57	5.63	6.15	6.34	6.56	6.73
	Adj-Bon	5.53	5.58	6.13	6.31	6.53	6.69
DGP-5	Sym-WW	7.42	6.81	10.74	9.15	15.54	12.39
	Asy-WW	7.60	6.77	10.85	8.89	15.59	11.97
	NP	7.58	6.81	11.15	9.22	16.90	13.04
	Bon	8.65	7.52	12.99	10.21	20.75	14.85
	Adj-Bon	8.56	7.47	12.69	10.05	19.86	14.36

Table 2.36: BIC order selection, $T = 100$: Empirical coverages for the v -th variable.

		χ^2_3 Distribution					
	Method	$H = 6$		$H = 12$		$H = 24$	
		$v = 1$	$v = 2$	$v = 1$	$v = 2$	$v = 1$	$v = 2$
DGP-1	Sym-WW	6.72	6.89	8.67	9.09	10.77	11.44
	Asy-WW	6.53	6.77	8.24	8.75	10.05	10.88
	NP	6.25	6.52	8.06	8.60	10.00	10.85
	Bon	7.02	7.37	8.99	9.70	11.28	12.49
	Adj-Bon	6.97	7.31	8.87	9.55	10.98	12.11
DGP-2	Sym-WW	6.89	7.08	8.79	9.23	10.76	11.54
	Asy-WW	7.44	7.72	9.38	9.96	11.34	12.34
	NP	6.69	6.96	8.57	9.09	10.48	11.34
	Bon	7.49	7.83	9.57	10.28	11.72	12.99
	Adj-Bon	7.41	7.74	9.40	10.07	11.40	12.58
DGP-3	Sym-WW	5.94	5.94	7.23	7.25	8.59	8.57
	Asy-WW	5.15	5.20	5.94	6.04	6.51	6.58
	NP	4.76	4.81	5.45	5.53	6.10	6.18
	Bon	5.19	5.26	5.91	6.03	6.39	6.47
	Adj-Bon	5.18	5.25	5.89	6.00	6.37	6.45
DGP-4	Sym-WW	6.01	6.03	7.18	7.25	8.61	8.60
	Asy-WW	5.43	5.56	6.26	6.49	7.04	7.19
	NP	4.91	5.20	5.67	5.84	6.53	6.69
	Bon	5.40	5.52	6.17	6.40	6.86	7.02
	Adj-Bon	5.37	5.49	6.11	6.32	6.81	6.96
DGP-5	Sym-WW	7.49	6.84	10.84	9.23	15.62	12.43
	Asy-WW	7.51	6.69	10.76	8.88	15.45	11.90
	NP	7.26	6.53	10.62	8.88	15.63	12.20
	Bon	8.42	7.28	12.54	9.86	19.02	13.68
	Adj-Bon	8.33	7.23	12.25	9.71	18.26	13.29

Table 2.37: BIC order selection, $T = 200$: Empirical coverages for the v -th variable.

		χ_3^2 Distribution					
	Method	$H = 6$		$H = 12$		$H = 24$	
		$v = 1$	$v = 2$	$v = 1$	$v = 2$	$v = 1$	$v = 2$
DGP-1	Sym-WW	6.64	6.83	8.59	9.00	10.62	11.27
	Asy-WW	6.46	6.70	8.16	8.67	9.90	10.70
	NP	6.11	6.38	7.89	8.41	9.66	10.47
	Bon	6.91	7.25	8.79	9.49	10.73	11.84
	Adj-Bon	6.86	7.20	8.67	9.34	10.49	11.52
DGP-2	Sym-WW	6.83	7.04	8.74	9.13	10.62	11.32
	Asy-WW	7.37	7.69	9.32	9.88	11.20	12.12
	NP	6.62	6.91	8.50	8.99	10.31	11.08
	Bon	7.42	7.79	9.46	10.15	11.41	12.53
	Adj-Bon	7.34	7.70	9.29	9.94	11.11	12.14
DGP-3	Sym-WW	5.88	5.91	7.15	7.20	8.44	8.43
	Asy-WW	5.07	5.15	5.82	5.89	6.60	6.64
	NP	4.65	4.72	5.32	5.42	5.96	6.05
	Bon	5.12	5.20	5.82	5.91	6.46	6.52
	Adj-Bon	5.11	5.19	5.80	5.89	6.43	6.49
DGP-4	Sym-WW	5.97	6.01	7.22	7.22	8.44	8.47
	Asy-WW	5.38	5.51	6.24	6.38	7.11	7.30
	NP	4.84	4.95	5.65	5.78	6.41	6.60
	Bon	5.36	5.48	6.17	6.31	6.91	7.10
	Adj-Bon	5.33	5.46	6.11	6.25	6.81	7.00
DGP-5	Sym-WW	7.42	6.81	10.74	9.15	15.54	12.39
	Asy-WW	7.45	6.67	10.67	8.80	15.38	11.86
	NP	7.10	6.39	10.35	8.63	15.05	11.83
	Bon	8.33	7.20	12.31	9.61	18.41	13.22
	Adj-Bon	8.24	7.15	12.2	9.47	17.68	12.85

Table 2.38: BIC order selection, $T = 400$: Empirical coverages for the v -th variable.

2G Results for DGP-6 with BIC Lag Selection

		$\mathcal{N}(0, \Sigma)$ Distribution								
EC	Method	$H = 6$			$H = 12$			$H = 24$		
		$v = 1$	$v = 2$	$v = 3$	$v = 1$	$v = 2$	$v = 3$	$v = 1$	$v = 2$	$v = 3$
T=100	Sym-WW	86.05	81.76	83.49	84.16	81.46	81.59	80.62	77.98	78.78
	Asy-WW	85.80	81.61	83.33	83.93	81.42	81.41	80.39	78.18	78.79
	NP	91.64	87.02	89.36	90.95	89.50	89.28	89.26	90.71	89.35
	Bon	93.69	92.28	93.22	94.45	94.06	93.86	94.11	94.61	94.15
	Adj-Bon	93.52	91.98	92.95	94.07	93.53	93.32	93.34	93.77	93.24
T=200	Sym-WW	90.31	88.24	87.93	90.12	87.95	87.84	88.34	87.58	87.46
	Asy-WW	90.12	88.18	87.81	89.86	87.93	87.77	88.27	87.80	87.39
	NP	93.02	90.06	90.37	92.71	90.47	90.76	91.24	91.41	91.28
	Bon	94.84	94.72	94.01	95.81	95.33	95.20	95.65	96.03	95.82
	Adj-Bon	94.67	94.45	93.75	95.51	94.82	94.71	94.99	95.28	95.08
T=400	Sym-WW	90.21	88.87	88.94	90.06	88.69	88.61	89.71	88.74	88.62
	Asy-WW	90.10	88.83	88.93	89.96	88.86	88.52	89.60	89.00	88.58
	NP	91.67	89.53	89.91	91.29	89.44	89.35	90.64	89.96	89.71
	Bon	93.83	94.35	93.82	94.85	94.81	94.56	95.47	95.49	95.36
	Adj-Bon	93.66	94.07	93.55	94.42	94.25	94.04	94.64	94.59	94.42
Volume										
T=100	Sym-WW	6.69	2.09	7.08	8.67	3.07	9.88	10.92	4.47	12.97
	Asy-WW	6.69	2.09	7.09	8.66	3.08	9.88	10.92	4.48	12.99
	NP	7.69	2.44	8.23	10.15	3.65	11.70	13.14	5.55	15.80
	Bon	8.22	2.67	8.94	11.40	4.12	13.34	15.89	6.55	19.22
	Adj-Bon	8.16	2.64	8.85	11.18	4.04	13.06	15.24	6.31	18.45
T=200	Sym-WW	6.58	2.13	7.13	8.58	3.08	9.86	10.73	4.46	12.81
	Asy-WW	6.58	2.13	7.13	8.58	3.09	9.87	10.73	4.48	12.82
	NP	7.08	2.33	7.74	9.25	3.35	10.70	11.64	4.94	14.00
	Bon	7.45	2.52	8.30	10.13	3.71	11.91	13.29	5.52	16.08
	Adj-Bon	7.40	2.58	8.23	9.97	3.65	11.69	12.87	5.36	15.57
T=400	Sym-WW	6.21	2.11	6.96	7.99	3.03	9.58	10.10	4.35	12.41
	Asy-WW	6.21	2.11	6.96	7.98	3.04	9.58	10.10	4.38	12.41
	NP	6.53	2.25	7.40	8.38	3.18	10.16	10.53	4.62	12.96
	Bon	6.79	2.43	7.84	9.02	3.50	11.06	11.74	5.10	14.62
	Adj-Bon	6.76	2.40	7.78	8.89	3.45	10.87	11.41	4.97	14.20

Table 2.39: BIC Lag Selection: Empirical coverages and volumes for the v -th variable.

		$t(3)$ Distribution								
EC		$H = 6$			$H = 12$			$H = 24$		
		$v = 1$	$v = 2$	$v = 3$	$v = 1$	$v = 2$	$v = 3$	$v = 1$	$v = 2$	$v = 3$
T=100	Sym-WW	87.11	84.94	85.51	84.68	82.60	82.37	81.35	80.86	80.19
	Asy-WW	86.34	84.41	85.08	82.98	81.92	81.25	78.76	80.03	78.81
	NP	90.06	87.45	88.79	87.83	87.18	86.79	85.53	88.10	86.50
	Bon	92.30	92.50	92.51	91.27	91.97	91.35	90.72	92.69	91.70
	Adj-Bon	92.12	92.23	92.26	90.86	91.42	90.83	89.88	91.83	90.75
T=200	Sym-WW	89.48	89.06	88.69	89.02	88.57	88.24	87.16	87.88	87.09
	Asy-WW	89.06	88.66	88.32	88.30	88.33	87.77	85.50	87.62	86.08
	NP	90.41	89.36	89.49	89.60	89.13	89.19	87.20	89.12	88.30
	Bon	92.73	94.27	93.52	92.97	94.04	93.62	91.68	93.93	93.06
	Adj-Bon	92.52	94.02	93.27	92.60	93.49	93.10	90.87	93.12	92.22
T=400	Sym-WW	89.64	89.63	89.55	89.63	89.49	89.37	89.05	89.08	88.95
	Asy-WW	89.41	89.48	89.32	89.25	89.50	89.06	88.16	89.28	88.42
	NP	89.67	89.28	89.42	89.30	88.95	88.91	87.85	88.62	88.09
	Bon	92.78	94.83	94.08	93.10	94.62	94.18	92.26	94.35	93.61
	Adj-Bon	92.51	94.52	93.81	92.57	94.09	93.67	91.40	93.52	92.67
Volume										
T=100	Sym-WW	7.04	2.12	7.22	9.54	3.19	10.35	12.50	4.82	13.96
	Asy-WW	7.28	2.17	7.39	9.71	3.28	10.58	12.44	4.92	14.06
	NP	7.75	2.42	8.16	10.47	3.65	11.77	13.54	5.63	15.96
	Bon	8.94	2.95	9.74	11.96	4.33	13.91	16.63	6.82	19.83
	Adj-Bon	8.85	2.90	9.60	11.72	4.23	13.57	15.91	6.55	18.99
T=200	Sym-WW	6.79	2.09	7.10	9.21	9.17	10.24	12.40	4.87	14.15
	Asy-WW	6.88	2.11	7.16	9.50	3.27	10.48	12.60	5.01	14.37
	NP	7.00	2.26	7.56	9.54	3.35	10.77	12.50	5.16	14.69
	Bon	8.29	2.86	9.31	11.28	4.22	13.28	14.61	6.19	17.71
	Adj-Bon	8.05	2.79	9.09	11.04	4.09	12.92	14.13	5.96	17.07
T=400	Sym-WW	6.41	2.05	6.89	8.74	3.10	9.97	11.57	4.60	13.42
	Asy-WW	6.46	2.06	6.94	8.86	3.16	10.08	11.97	4.76	13.79
	NP	6.47	2.19	7.23	8.83	3.21	10.28	11.54	4.77	13.60
	Bon	7.65	2.82	8.99	10.68	4.24	13.21	13.76	5.97	16.94
	Adj-Bon	7.43	2.71	8.69	10.17	4.07	12.64	13.26	5.72	16.26

Table 2.40: BIC Lag Selection: Empirical coverages and volumes for the v -th variable.

		χ^2_3 Distribution								
EC	Method	$H = 6$			$H = 12$			$H = 24$		
		$v = 1$	$v = 2$	$v = 3$	$v = 1$	$v = 2$	$v = 3$	$v = 1$	$v = 2$	$v = 3$
T=100	Sym-WW	86.40	83.45	84.06	84.94	81.67	81.53	82.08	78.73	79.17
	Asy-WW	85.64	82.63	83.72	83.99	81.22	81.01	80.59	78.62	78.48
	NP	90.68	87.55	88.67	89.80	88.41	87.91	88.17	89.66	88.21
	Bon	93.25	93.23	92.67	93.62	93.54	92.59	93.28	93.92	92.99
	Adj-Bon	93.09	92.95	92.41	93.24	92.96	92.01	92.53	93.10	92.08
T=200	Sym-WW	89.73	88.43	88.13	89.21	88.30	87.95	88.53	88.03	87.45
	Asy-WW	90.28	87.84	87.89	89.44	88.18	87.60	88.36	88.13	87.05
	NP	92.13	89.81	89.94	91.61	90.41	90.08	90.65	91.36	90.43
	Bon	94.55	95.24	93.74	95.17	95.84	94.67	95.21	96.31	95.17
	Adj-Bon	94.38	94.96	93.50	94.82	95.35	94.16	94.53	95.58	94.38
T=400	Sym-WW	89.77	89.25	89.21	89.45	89.08	88.77	89.44	89.02	88.72
	Asy-WW	90.36	89.07	89.03	89.89	88.87	88.62	89.57	89.43	88.57
	NP	91.11	89.79	89.03	90.82	89.49	89.28	90.24	89.91	89.34
	Bon	93.95	95.22	93.91	94.70	95.40	94.50	95.08	95.93	94.95
	Adj-Bon	93.78	94.96	93.60	94.27	94.88	93.96	94.31	95.08	93.98
Volume										
T=100	Sym-WW	7.05	2.11	7.31	9.26	3.13	10.18	11.86	4.64	13.37
	Asy-WW	6.99	2.13	7.32	9.07	3.12	10.19	11.51	4.61	13.38
	NP	7.78	2.44	8.40	10.27	3.62	11.82	13.34	5.57	15.93
	Bon	8.51	2.75	9.27	11.64	4.14	13.57	16.19	6.60	19.41
	Adj-Bon	8.44	2.72	9.17	11.41	4.05	13.27	15.52	6.35	18.62
T=200	Sym-WW	6.85	2.10	7.35	9.09	3.15	10.24	11.51	4.63	13.33
	Asy-WW	6.78	2.12	7.34	8.93	3.12	10.24	11.24	4.58	13.34
	NP	7.04	2.22	7.92	9.39	3.29	11.00	11.86	4.99	14.34
	Bon	7.66	2.55	8.68	10.45	3.77	12.40	13.61	5.59	16.58
	Adj-Bon	7.60	2.51	8.59	10.27	3.69	12.15	13.17	5.43	16.04
T=400	Sym-WW	6.53	2.07	7.22	8.57	3.08	9.97	10.91	4.52	12.95
	Asy-WW	6.41	2.10	7.20	8.35	3.06	9.97	10.58	4.47	12.96
	NP	6.44	2.12	7.60	8.53	3.10	10.42	10.76	4.59	13.39
	Bon	7.01	2.46	8.30	9.36	3.55	11.63	12.06	5.20	15.24
	Adj-Bon	6.97	2.43	8.21	9.21	3.49	11.40	11.72	5.04	14.76

Table 2.41: BIC Lag Selection: Empirical coverages and volumes for the v -th variable.

2H Results for DGP-7 with BIC Lag Selection

		$\mathcal{N}(0, \Sigma)$ Distribution					
EC	Method	$H = 6$					
		$v = 1$	$v = 2$	$v = 3$	$v = 4$	$v = 5$	$v = 6$
T=100	Sym-WW	75.20	77.88	84.87	74.55	75.15	79.21
	Asy-WW	75.04	77.86	84.64	74.53	74.96	79.11
	NP	84.29	86.55	91.15	82.72	83.52	87.18
	Bon	82.66	88.59	89.89	82.30	81.24	90.86
	Adj-Bon	82.23	88.20	89.80	81.67	80.76	90.40
T=200	Sym-WW	85.12	85.91	87.88	82.45	82.09	86.09
	Asy-WW	84.99	85.77	87.80	82.36	81.99	86.01
	NP	88.48	89.02	90.46	86.82	86.82	89.04
	Bon	90.51	92.31	90.11	87.27	84.02	93.42
	Adj-Bon	90.19	91.99	90.04	86.70	83.62	93.07
T=400	Sym-WW	88.26	88.62	89.17	86.92	86.63	88.63
	Asy-WW	88.21	88.56	89.17	86.85	86.54	88.60
	NP	89.41	89.61	90.00	88.79	88.72	89.56
	Bon	92.81	93.36	90.26	91.47	88.35	94.30
	Adj-Bon	92.52	93.09	90.19	91.03	88.02	93.99
Volume							
T=100	Sym-WW	22.90	151.86	0.21	1.52	1.27	0.94
	Asy-WW	22.91	115.91	0.21	1.52	1.27	0.94
	NP	29.28	143.49	0.24	2.15	1.68	1.33
	Bon	30.82	154.68	0.24	2.15	1.68	1.33
	Adj-Bon	30.82	154.68	0.24	2.12	1.66	1.31
T=200	Sym-WW	22.92	116.82	0.21	1.48	1.22	0.93
	Asy-WW	22.92	116.82	0.21	1.48	1.22	0.93
	NP	26.27	129.98	0.22	1.74	1.40	1.05
	Bon	27.39	138.62	0.22	1.87	1.44	1.14
	Adj-Bon	27.16	137.43	0.22	1.84	1.43	1.13
T=400	Sym-WW	22.90	116.67	0.20	1.48	1.21	0.93
	Asy-WW	22.89	116.62	0.20	1.48	1.21	0.93
	NP	24.93	124.31	0.21	1.64	1.32	1.00
	Bon	25.88	131.89	0.21	1.77	1.36	1.09
	Adj-Bon	25.68	130.88	0.21	1.75	1.35	1.08

Table 2.42: BIC Lag Selection: Empirical coverages and volumes for the v -th variable.

		$\mathcal{N}(\mathbf{0}, \Sigma)$ Distribution					
EC	Method	$H = 12$					
		$v = 1$	$v = 2$	$v = 3$	$v = 4$	$v = 5$	$v = 6$
T=100	Sym-WW	66.24	71.31	83.70	65.78	68.18	72.87
	Asy-WW	66.19	71.28	83.38	65.83	65.11	72.82
	NP	76.19	82.41	90.20	76.52	76.29	83.41
	Bon	78.17	85.98	88.85	79.16	75.50	90.38
	Adj-Bon	76.84	84.97	88.61	77.67	73.91	89.29
T=200	Sym-WW	80.84	84.15	87.41	78.74	75.95	84.53
	Asy-WW	80.75	84.08	87.16	78.70	75.84	84.44
	NP	85.66	88.24	89.94	84.82	81.99	88.69
	Bon	88.89	92.54	89.79	86.75	79.28	94.69
	Adj-Bon	87.85	91.84	89.63	85.42	77.88	93.96
T=400	Sym-WW	86.75	88.11	88.99	85.59	84.31	87.84
	Asy-WW	86.73	88.05	88.87	85.54	84.23	87.77
	NP	88.51	89.35	89.54	88.41	87.18	89.14
	Bon	92.90	94.22	89.85	91.86	86.08	95.34
	Adj-Bon	92.12	93.64	89.72	90.85	85.06	94.72
Volume							
T=100	Sym-WW	36.01	157.68	0.24	2.43	1.66	1.46
	Asy-WW	36.02	157.86	0.24	2.43	1.66	1.46
	NP	47.55	198.49	0.27	3.22	2.13	1.89
	Bon	54.13	225.37	0.28	3.82	2.37	2.29
	Adj-Bon	52.64	219.99	0.27	3.70	2.32	2.22
T=200	Sym-WW	37.00	159.00	0.23	2.30	1.59	1.46
	Asy-WW	37.00	159.05	0.23	2.43	1.59	1.46
	NP	43.68	178.37	0.25	2.94	1.88	1.66
	Bon	48.40	196.96	0.25	3.34	2.00	1.93
	Adj-Bon	47.27	193.32	0.25	3.26	1.96	1.88
T=400	Sym-WW	37.31	158.31	0.23	2.43	1.57	1.45
	Asy-WW	37.30	158.32	0.23	2.43	1.57	1.45
	NP	41.02	168.34	0.24	2.74	1.74	1.56
	Bon	44.85	183.82	0.24	3.08	1.82	1.79
	Adj-Bon	43.93	180.83	0.24	3.00	1.79	1.75

Table 2.43: BIC Lag Selection: Empirical coverages and volumes for the v -th variable.

		$\mathcal{N}(\mathbf{0}, \Sigma)$ Distribution					
EC	Method	$H = 24$					
		$v = 1$	$v = 2$	$v = 3$	$v = 4$	$v = 5$	$v = 6$
T=100	Sym-WW	52.53	59.81	80.15	53.74	51.61	62.28
	Asy-WW	52.44	60.02	79.84	53.73	51.54	62.23
	NP	68.07	75.88	87.86	70.15	69.61	79.73
	Bon	73.37	80.40	86.13	76.98	68.17	87.78
	Adj-Bon	70.85	78.06	85.51	74.49	64.92	85.79
T=200	Sym-WW	73.63	79.99	87.09	73.51	66.48	80.21
	Asy-WW	73.60	80.00	86.50	73.55	66.42	80.12
	NP	80.87	86.12	89.42	81.84	74.62	87.60
	Bon	85.23	90.56	89.33	86.16	71.64	93.84
	Adj-Bon	83.09	89.00	88.96	84.04	68.09	92.59
T=400	Sym-WW	83.93	86.38	88.79	83.44	79.95	86.72
	Asy-WW	83.88	86.36	88.59	83.39	79.88	86.73
	NP	87.56	88.51	88.78	87.62	83.28	89.08
	Bon	91.92	93.80	89.53	92.05	80.90	96.02
	Adj-Bon	90.18	92.59	89.20	90.38	78.00	95.02
Volume							
T=100	Sym-WW	58.48	220.77	0.28	3.88	2.18	2.29
	Asy-WW	58.54	221.26	0.28	3.88	2.18	2.29
	NP	82.41	297.22	0.32	5.58	3.07	3.25
	Bon	102.01	352.43	0.32	7.06	3.64	4.17
	Adj-Bon	97.31	337.13	0.32	6.73	3.47	3.96
T=200	Sym-WW	63.40	223.10	0.26	4.06	2.80	2.27
	Asy-WW	63.42	223.44	0.26	4.06	2.08	2.27
	NP	77.82	261.09	0.28	5.08	2.58	2.70
	Bon	93.04	293.68	0.28	6.15	2.86	3.29
	Adj-Bon	89.23	284.04	0.28	5.90	2.75	3.16
T=400	Sym-WW	63.85	221.49	0.26	4.08	2.03	2.24
	Asy-WW	63.81	221.73	0.26	4.08	2.03	2.24
	NP	71.73	241.04	0.27	4.67	2.32	2.44
	Bon	83.33	266.37	0.27	5.52	2.48	2.92
	Adj-Bon	80.18	258.55	0.27	5.31	2.40	2.81

Table 2.44: BIC Lag Selection: Empirical coverages and volumes for the v -th variable.

2I Empirical Coverages for DGP-8–12 with BIC Lag Selection

		$\mathcal{N}(0, \Sigma)$ Distribution					
	Method	$H = 6$		$H = 12$		$H = 24$	
		$v = 1$	$v = 2$	$v = 1$	$v = 2$	$v = 1$	$v = 2$
DGP-8	Sym-WW	88.58	88.42	88.38	88.18	86.30	86.98
	Asy-WW	87.81	87.89	85.71	86.91	81.85	98.64
	NP	87.79	88.21	86.00	87.16	81.44	84.42
	Bon	88.48	89.55	86.29	88.50	81.82	85.93
	Adj-Bon	88.42	89.45	86.16	88.25	81.48	85.47
DGP-9	Sym-WW	88.90	88.75	88.39	88.20	86.04	87.20
	Asy-WW	88.28	88.12	85.61	86.78	81.21	84.94
	NP	87.66	88.39	85.06	86.97	79.82	84.55
	Bon	88.36	89.65	85.20	88.17	79.84	85.93
	Adj-Bon	88.31	89.53	85.10	87.94	79.57	85.46
DGP-10	Sym-WW	88.36	88.89	88.52	88.70	88.16	87.94
	Asy-WW	88.87	89.08	88.51	88.20	87.58	86.70
	NP	87.93	88.34	87.24	87.09	85.50	84.68
	Bon	89.45	89.55	88.83	88.25	87.26	86.19
	Adj-Bon	89.35	89.45	88.59	88.05	86.79	85.76
DGP-11	Sym-WW	87.34	87.17	87.51	87.43	87.04	87.26
	Asy-WW	87.05	86.89	86.74	86.60	85.57	85.81
	NP	87.58	87.43	87.12	87.12	85.33	85.56
	Bon	89.20	89.09	88.42	88.41	86.76	87.14
	Adj-Bon	89.09	88.94	88.16	88.13	86.27	86.62
DGP-12	Sym-WW	89.50	91.16	88.72	91.05	86.77	90.30
	Asy-WW	88.79	90.95	87.14	90.16	83.93	88.56
	NP	89.05	90.98	87.36	90.33	83.93	88.56
	Bon	89.88	91.95	88.08	90.90	83.63	88.87
	Adj-Bon	89.79	91.87	87.90	90.76	84.23	88.56

Table 2.45: BIC Lag Selection, $T = 100$: Empirical coverages for the v -th variable.

		$\mathcal{N}(0, \Sigma)$ Distribution					
	Method	$H = 6$		$H = 12$		$H = 24$	
		$v = 1$	$v = 2$	$v = 1$	$v = 2$	$v = 1$	$v = 2$
DGP-8	Sym-WW	89.38	88.72	89.26	88.86	87.93	88.27
	Asy-WW	88.89	88.45	88.38	88.38	85.28	87.11
	NP	88.66	88.35	87.40	87.67	83.86	85.61
	Bon	89.42	89.80	88.31	89.16	84.50	87.09
	Adj-Bon	89.35	89.69	88.17	88.93	84.27	86.66
DGP-9	Sym-WW	89.49	88.97	89.19	88.69	88.16	88.52
	Asy-WW	89.19	88.76	88.21	88.17	84.62	87.42
	NP	88.59	88.49	86.69	87.47	82.69	85.83
	Bon	89.26	89.90	87.56	88.95	83.28	87.18
	Adj-Bon	89.20	89.79	87.44	88.73	83.11	86.80
DGP-10	Sym-WW	88.73	89.40	89.10	89.44	89.15	89.10
	Asy-WW	89.58	89.88	89.60	89.63	89.30	88.59
	NP	88.22	88.85	87.74	87.96	86.47	86.08
	Bon	89.96	90.13	89.46	89.42	88.24	87.48
	Adj-Bon	89.84	90.03	89.23	89.23	87.81	87.11
DGP-11	Sym-WW	88.28	87.91	88.32	88.33	88.76	88.58
	Asy-WW	88.23	87.83	87.97	88.09	88.07	87.91
	NP	88.04	87.83	87.47	87.56	86.67	86.48
	Bon	89.88	89.55	88.91	89.20	88.10	87.98
	Adj-Bon	89.74	89.42	88.69	88.95	87.71	87.56
DGP-12	Sym-WW	90.11	92.02	89.82	93.11	88.84	93.48
	Asy-WW	89.67	91.97	89.09	92.85	87.28	92.54
	NP	89.53	91.66	88.47	92.20	85.88	91.39
	Bon	90.51	92.79	89.52	93.18	86.97	92.10
	Adj-Bon	90.42	92.71	89.35	93.05	86.66	91.86

Table 2.46: BIC Lag Selection, $T = 200$: Empirical coverages for the v -th variable.

		$\mathcal{N}(0, \Sigma)$ Distribution					
	Method	$H = 6$		$H = 12$		$H = 24$	
		$v = 1$	$v = 2$	$v = 1$	$v = 2$	$v = 1$	$v = 2$
DGP-8	Sym-WW	89.60	89.02	89.56	89.27	88.82	89.04
	Asy-WW	89.46	89.03	89.05	89.15	87.83	88.63
	NP	88.99	88.52	88.02	88.04	85.62	86.51
	Bon	89.88	90.09	88.93	89.56	86.54	88.02
	Adj-Bon	89.81	89.97	88.77	89.35	86.29	87.63
DGP-9	Sym-WW	89.79	89.25	89.48	89.29	88.63	89.09
	Asy-WW	89.69	89.22	89.03	89.17	87.55	88.72
	NP	89.02	88.72	87.65	88.10	84.81	86.55
	Bon	89.71	90.26	88.51	89.65	85.74	87.99
	Adj-Bon	89.66	90.15	88.38	89.43	85.50	87.59
DGP-10	Sym-WW	89.02	89.61	89.29	89.86	89.45	89.46
	Asy-WW	90.03	90.22	90.08	90.33	89.98	89.53
	NP	88.52	89.11	88.16	88.58	87.04	86.79
	Bon	90.25	90.42	89.84	89.92	88.68	88.27
	Adj-Bon	90.12	90.31	89.61	89.75	88.29	87.93
DGP-11	Sym-WW	88.87	88.63	89.22	89.19	89.19	89.27
	Asy-WW	88.81	88.65	89.14	89.18	88.94	89.09
	NP	88.51	88.24	88.22	88.23	86.92	87.12
	Bon	90.25	90.18	89.81	89.94	88.46	88.73
	Adj-Bon	90.14	90.05	89.58	89.72	88.02	88.31
DGP-12	Sym-WW	90.40	92.29	90.73	94.05	90.40	94.97
	Asy-WW	90.18	92.22	90.30	93.92	89.77	94.65
	NP	89.81	92.08	89.42	93.07	87.74	93.07
	Bon	90.90	92.92	90.47	93.94	88.92	94.05
	Adj-Bon	90.81	92.83	90.31	93.80	88.64	93.84

Table 2.47: BIC Lag Selection, $T = 400$: Empirical coverages for the v -th variable.

2J Volumes for DGP-8–12 with BIC Lag Selection

		$\mathcal{N}(0, \Sigma)$ Distribution					
	Method	$H = 6$		$H = 12$		$H = 24$	
		$v = 1$	$v = 2$	$v = 1$	$v = 2$	$v = 1$	$v = 2$
DGP-8	Sym-WW	4.91	5.47	5.52	6.25	5.94	6.83
	Asy-WW	4.94	5.48	5.45	6.23	5.79	6.76
	NP	4.88	5.49	5.43	6.25	5.76	6.78
	Bon	5.01	5.66	5.49	6.40	5.78	6.90
	Adj-Bon	5.00	5.65	5.48	6.37	5.77	6.86
DGP-9	Sym-WW	4.87	5.57	5.42	6.25	5.81	6.83
	Asy-WW	4.92	5.58	5.34	6.23	5.65	6.77
	NP	4.81	5.59	5.27	6.23	5.57	6.77
	Bon	4.94	5.76	5.31	6.37	5.58	6.89
	Adj-Bon	4.94	5.75	5.31	6.35	5.56	6.85
DGP-10	Sym-WW	5.78	5.38	6.53	6.02	7.19	6.59
	Asy-WW	5.89	5.46	6.60	6.06	7.21	6.57
	NP	5.78	5.37	6.50	5.97	7.12	6.48
	Bon	5.97	5.52	6.67	6.09	7.25	6.57
	Adj-Bon	5.95	5.51	6.64	6.07	7.20	6.54
DGP-11	Sym-WW	7.30	6.27	8.32	7.15	9.16	7.90
	Asy-WW	7.33	6.29	8.32	7.15	9.11	7.86
	NP	7.40	6.36	8.38	7.21	9.17	7.92
	Bon	7.63	6.56	8.59	7.39	9.34	8.08
	Adj-Bon	7.61	6.55	8.55	7.36	9.28	8.02
DGP-12	Sym-WW	5.52	7.89	6.18	9.03	6.70	9.92
	Asy-WW	5.54	7.94	6.14	9.01	6.58	9.79
	NP	5.52	7.87	6.14	8.95	6.58	9.72
	Bon	5.69	8.21	9.26	9.17	6.68	9.89
	Adj-Bon	5.68	8.19	6.24	9.14	6.64	9.84

Table 2.48: BIC Lag Selection, $T = 100$: Volumes each the v -th variable.

		$\mathcal{N}(0, \Sigma)$ Distribution					
	Method	$H = 6$		$H = 12$		$H = 24$	
		$v = 1$	$v = 2$	$v = 1$	$v = 2$	$v = 1$	$v = 2$
DGP-8	Sym-WW	4.99	5.50	5.47	6.19	5.93	6.77
	Asy-WW	4.93	5.51	5.49	6.20	5.86	6.76
	NP	4.89	5.51	5.42	6.18	5.80	6.72
	Bon	4.99	5.65	5.50	6.31	5.83	6.80
	Adj-Bon	4.98	5.64	5.49	6.28	5.82	6.77
DGP-9	Sym-WW	4.85	5.50	5.36	6.17	5.84	6.79
	Asy-WW	4.88	5.51	5.40	6.17	5.74	6.78
	NP	4.81	5.50	5.28	6.16	5.64	6.73
	Bon	4.90	5.64	5.37	6.27	5.68	6.80
	Adj-Bon	4.89	5.63	5.36	6.25	5.67	6.77
DGP-10	Sym-WW	5.71	5.33	6.46	5.96	7.11	6.54
	Asy-WW	5.82	5.40	6.55	6.02	7.16	6.56
	NP	5.72	5.32	6.45	5.94	7.05	6.46
	Bon	5.87	5.44	6.57	6.03	7.13	6.52
	Adj-Bon	5.86	5.43	6.55	6.01	7.10	6.49
DGP-11	Sym-WW	7.24	6.21	8.21	7.07	9.10	7.83
	Asy-WW	7.27	6.23	8.23	7.09	9.11	7.83
	NP	7.30	6.27	8.24	7.10	9.07	7.80
	Bon	7.49	6.42	8.40	7.24	9.18	7.90
	Adj-Bon	7.47	6.41	8.37	7.21	9.13	7.86
DGP-12	Sym-WW	5.47	7.83	6.13	9.04	6.71	10.05
	Asy-WW	5.47	7.85	6.15	9.09	6.66	10.03
	NP	5.45	7.79	6.10	8.97	6.60	9.87
	Bon	5.58	8.05	6.22	9.21	6.67	10.01
	Adj-Bon	5.57	8.03	6.20	9.18	6.64	9.96

Table 2.49: BIC Lag Selection, $T = 200$: Volumes each the v -th variable.

		$\mathcal{N}(0, \Sigma)$ Distribution					
	Method	$H = 6$		$H = 12$		$H = 24$	
		$v = 1$	$v = 2$	$v = 1$	$v = 2$	$v = 1$	$v = 2$
DGP-8	Sym-WW	4.90	5.46	5.23	6.14	5.90	6.75
	Asy-WW	4.91	5.48	5.44	6.16	5.92	6.76
	NP	4.88	5.48	5.40	6.14	5.83	6.72
	Bon	4.96	5.60	5.46	6.23	5.86	6.77
	Adj-Bon	4.96	5.59	5.45	6.21	5.85	6.74
DGP-9	Sym-WW	4.84	5.47	5.34	6.14	5.79	6.75
	Asy-WW	4.86	5.48	5.36	6.16	5.83	6.76
	NP	4.81	5.48	5.29	6.14	5.69	6.71
	Bon	4.88	5.60	5.35	6.23	5.74	6.76
	Adj-Bon	4.88	5.59	5.34	6.21	5.72	6.73
DGP-10	Sym-WW	5.68	5.29	6.42	5.94	7.07	6.50
	Asy-WW	5.79	5.37	6.51	6.00	7.14	6.54
	NP	5.70	5.29	6.41	5.93	7.04	6.45
	Bon	5.83	5.40	6.52	6.00	7.10	6.49
	Adj-Bon	5.82	5.39	6.49	5.99	7.07	6.47
DGP-11	Sym-WW	7.22	6.18	8.20	7.04	9.02	7.78
	Asy-WW	7.23	6.20	8.22	7.05	9.04	7.79
	NP	7.27	6.23	8.22	7.05	9.00	7.76
	Bon	7.43	6.37	8.35	7.17	9.07	7.83
	Adj-Bon	7.42	6.36	8.32	7.15	9.03	7.79
DGP-12	Sym-WW	5.43	7.82	6.10	9.03	6.71	10.12
	Asy-WW	5.44	7.84	6.11	9.06	6.72	10.15
	NP	5.42	7.79	6.08	8.96	6.64	9.98
	Bon	5.54	8.02	6.17	9.16	6.70	10.11
	Adj-Bon	5.53	8.00	6.15	9.13	6.67	10.06

Table 2.50: BIC Lag Selection, $T = 400$: Volumes each the v -th variable.

Chapter 3

Balanced Bootstrap Joint Confidence Bands for Structural Impulse Responses

This chapter is jointly written with Michael Wolf. A version of this chapter is forthcoming in the *Journal of Time Series Analysis*.

Abstract

Constructing joint confidence bands for structural impulse response functions based on a VAR model is a difficult task because of the non-linear nature of such functions. We propose new joint confidence bands that cover the entire true structural impulse response function up to a chosen maximum horizon with a prespecified probability $(1 - \alpha)$, at least asymptotically. Such bands are based on a certain bootstrap procedure from the multiple testing literature. We compare the finite-sample properties of our method with those of existing methods via extensive Monte Carlo simulations. We also investigate the effect of endogenizing the lag order in our bootstrap procedure on the finite-sample properties. Furthermore, an empirical application to a real data set is provided.

JEL classification: C12, C32

Keywords: Bootstrap; impulse response functions; joint confidence bands; vector autoregressive process.

3.1 Introduction

Impulse response analysis based on low-dimensional structural vector autoregressions (VARs) is still a popular tool in applied work; for example, see [Barsky and Sims \(2011\)](#), [Kurmman and Otrok \(2013\)](#), and [Bian and Gete \(2015\)](#). In practice, the impulse response functions have to be estimated from the data and it is standard in the literature to report the corresponding estimation uncertainty in the form of confidence bands.

It is by now a well-known fact that simply connecting individual marginal confidence intervals with nominal confidence level $(1 - \alpha)$ does not result in confidence bands that cover the *entire* true impulse response function with the prespecified confidence level $(1 - \alpha)$. Instead, such a procedure results in joint confidence bands that are too narrow and hence cover the true impulse responses with probability less than the desired level.¹ Consequently, the literature has proposed a substantial number of methods to construct ‘proper’ joint confidence bands that are designed to actually cover the entire true impulse response function with a prespecified probability; for example, see [Staszewska \(2007\)](#), [Jordà \(2009\)](#), and [Lütkepohl et al. \(2015a,b\)](#).

The finite-sample properties of the existing methods are compared in [Lütkepohl et al. \(2015a,b\)](#) via extensive Monte Carlo experiments. They find that the traditional Bonferroni bands and the Wald bands of [Lütkepohl et al. \(2015b\)](#) mostly exhibit empirical coverage rates close to or above the nominal level but that the bands can be excessively wide. In contrast, the bands of the other competing methods — namely, the bands of [Staszewska \(2007\)](#) and [Jordà \(2009\)](#) as well as the size-adjusted Bonferroni and Wald bands of [Lütkepohl et al. \(2015a,b\)](#) — are narrower but suffer from finite-sample coverage rates below the nominal level in certain scenarios. Consequently, there is no method so far that produces joint confidence bands for impulse response functions that enjoys both (i) robust empirical coverage rates close to the nominal confidence level and (ii) moderate volumes compared to the Bonferroni and Wald bands.

We propose new joint confidence bands for impulse response functions that are based on the methodology of [Romano and Wolf \(2010\)](#) who provide a bootstrap-based method to construct rectangular joint confidence bands for a generic parameter $\theta \in \mathbb{R}^d$. Furthermore,

¹This property is obvious from a theoretical point of view; in addition, for example, see [Lütkepohl et al. \(2015a\)](#) for Monte Carlo evidence.

they prove that, under weak regularity conditions, their proposed joint confidence bands have asymptotically the correct coverage probability and are also asymptotically balanced. The resulting joint confidence bands are subsequently labeled as balanced bootstrap (BB) bands.

In addition, we conduct a Monte Carlo experiment to compare the finite-sample properties of the proposed BB bands with those of a set of competing methods. We find that the BB bands are smaller than the Bonferroni and the Wald bands. Furthermore, the BB confidence bands seem to work reliably in scenarios where the ratio of the sample size to the number of coefficients is not small (that is, in medium to high-degrees-of-freedom scenarios), even when the maximum propagation horizon is large.

The remainder of the paper is organized as follows. Section 3.2 reviews impulse response functions of structural vector autoregressions. Section 3.3 presents the new confidence bands. Section 4.4 briefly describes the competing methods to construct confidence bands. Section 3.5 describes the Monte Carlo experiment and presents the empirical findings. Section 3.6 presents an empirical application. Section 3.7 concludes. The Appendix contains additional details about the estimation of impulse response functions, an algorithm to construct the BB bands, boxplots describing the finite-sample properties of the various methods, figures corresponding to the Monte Carlo simulations and the empirical application and tables with the simulation results.

3.2 Structural Impulse Response Functions

Consider an m -dimensional reduced-form VAR(p) process of the form

$$y_t = \nu + A_1 y_{t-1} + \dots + A_p y_{t-p} + u_t , \quad (3.1)$$

where y_t is an m -dimensional random vector, the A_i are $m \times m$ coefficient matrices, ν is an m -dimensional intercept vector, and $\{u_t\}$ is an m -dimensional independent and identically distributed (i.i.d.) process with $\mathbb{E}[u_t] = 0$ and positive-definite covariance matrix $\Sigma_u :=$

$\mathbb{E}[u_t u_t']$. The process in (3.1) is stable and stationary if and only if

$$\det(I_m - A_1 z^1 - \dots - A_p z^p) \neq 0 \quad \text{for all } z \in \mathbb{C} \text{ with } |z| \leq 1 .$$

A stationary VAR(p) process admits a Wold vector moving average (VMA) representation of the form

$$y_t = \mu + \sum_{i=0}^{+\infty} \phi_i u_{t-i} , \quad (3.2)$$

where $\mu := \mathbb{E}[y_t] = (I_m - A_1 - \dots - A_p)^{-1} \nu$ and the ϕ_i are fixed $m \times m$ VMA-coefficient matrices that satisfy $\phi_0 = I_m$ and $\phi_s = \sum_{j=1}^s \phi_{s-j} A_j$, for $s \in \mathbb{N}_+$.

The structural representation of (3.1) is given by

$$B_0^{-1} y_t = B_0^{-1} \nu + B_0^{-1} A_1 y_{t-1} + \dots + B_0^{-1} A_p y_{t-p} + B_0^{-1} u_t , \quad (3.3)$$

where $B_0^{-1} \in \mathbb{R}^{m \times m}$ is a non-singular linear mapping that transforms the reduced-form errors u_t into the structural shocks ε_t , that is, $\varepsilon_t := B_0^{-1} u_t$. The key restriction on B_0^{-1} (or equivalently on B_0) emerges from imposing that the structural shocks are instantaneously uncorrelated and have unit variance². Thus, B_0 needs to satisfy the following equation:

$$\Sigma_u = B_0 B_0' . \quad (3.4)$$

Simple accounting reveals that there are $m(m-1)/2$ degrees of freedom in specifying B_0 , and hence further restrictions are needed to achieve identification³. The literature offers a wide variety of different identification strategies; for example, see [Lütkepohl \(2005, Section 9.1\)](#) for a brief overview.

However, we will be agnostic about the particular identification procedure, as our goal is to provide new joint confidence bands with good finite-sample properties rather than to propose a new identification procedure. Thus, at this point, we only assume that the structural VAR is exactly identified via an arbitrary identification procedure.

²This implies that the covariance matrix of the ε_t is equal to the m -dimensional identity matrix, that is, $\mathbb{E}[\varepsilon_t \varepsilon_t'] = I_m$.

³[Rubio-Ramirez et al. \(2010\)](#) provide a necessary and sufficient condition for global (exact) identification of structural VARs; in particular, the necessary condition of [Rubio-Ramirez et al. \(2010\)](#) is equivalent to the widely used (necessary) rank condition of [Rothenberg \(1971\)](#).

The identification of the impact matrix B_0 allows one to exactly express the reduced-form VAR(p) process $\{y_t\}$ as a structural vector moving average process

$$y_t = \mu + \sum_{i=0}^{+\infty} \Theta_i \varepsilon_{t-i} , \quad (3.5)$$

where $\Theta_h := \phi_h B_0$. The (i, j) -th structural impulse response function with a maximum propagation horizon $H \in \mathbb{N}$, denoted by $\Theta_{ij,H}$, measures the partial effect of a one-standard-deviation shock⁴ in the j -th variable on the i -th variable over $H + 1$ periods and is given by the vector that collects the (i, j) -th element of the corresponding structural vector moving average (VMA) coefficient matrices, that is,

$$\Theta_{ij,H} := \begin{pmatrix} \frac{\partial y_{t,i}}{\partial \varepsilon_{t,j}} \\ \vdots \\ \frac{\partial y_{t+H,i}}{\partial \varepsilon_{t,j}} \end{pmatrix} = \begin{pmatrix} \Theta_{ij,0} \\ \vdots \\ \Theta_{ij,H} \end{pmatrix} \quad \text{for } i, j = 1, \dots, m . \quad (3.6)$$

The structural VMA coefficient matrices at propagation horizon $h \in \{0, \dots, H\}$ can be obtained as $\Theta_h = (JA^h J')B_0$, where $J := [I_m : 0 : \dots : 0] \in \mathbb{R}^{m \times mp}$ is a selector matrix and A denotes the reduced-form coefficient matrix of the mp -dimensional companion form of a VAR(p) process. Thus, the structural impulse response function $\Theta_{ij,H}$ is a non-linear function of the reduced-form model coefficients (A_1, \dots, A_p) and the impact matrix B_0 , that is,

$$\Theta_{ij,H} = \Theta_{ij,H}(A_1, \dots, A_p, B_0) . \quad (3.7)$$

The reduced-form coefficient matrices (A_1, \dots, A_p) are usually estimated by a standard procedure such as least squares (LS). The impact matrix B_0 is in general a function of the reduced-form coefficient matrices $(A_1, \dots, A_p, \Sigma_u)$ and a set of identifying restrictions. An estimator for B_0 , denoted by \hat{B}_0 , is found by replacing the true coefficient matrices by corresponding estimators (and by imposing the identifying restrictions). Thus, a plug-in estimator of the impulse response function is obtained as

$$\hat{\Theta}_{ij,H} := \Theta_{ij,H}(\hat{A}_1, \dots, \hat{A}_p, \hat{B}_0) . \quad (3.8)$$

⁴Given the normalization $\mathbb{E}[\varepsilon_t \varepsilon_t'] = I_m$, a one-standard-deviation shock is equivalent to a unit shock.

The estimator in (3.8) is consistent if the estimators $(\hat{A}_1, \dots, \hat{A}_p, \hat{B}_0)$ are consistent because $\Theta_{ij,H}(\cdot)$ is a continuous function.

3.3 New Joint Confidence Bands

3.3.1 Motivation and Notation

Romano and Wolf (2010) propose a method to construct joint confidence bands for a generic parameter $\theta \in \mathbb{R}^d$. For them, this method is just a means to an end, where the end is stepwise multiple testing procedure that controls the familywise error rate. But we can adapt this method to our ‘direct’ end of constructing joint confidence bands for impulse response functions. The method of Romano and Wolf (2010) is based on the availability of a consistent estimator for the parameter of interest and a bootstrap procedure that estimates the sampling distribution of the aforementioned estimator. Therefore, it can be used one-to-one to construct joint confidence bands for impulse response functions of structural vector autoregressions because both a consistent estimator for $\Theta_{ij,H}$ and such a bootstrap procedure are available; for example, see Kilian (1998b).

The asymptotic properties of the generic bands hinge on a set of regularity conditions about the asymptotic distribution of the estimator (of the parameter of interest) and the bootstrap; see Romano and Wolf (2010, Theorem 3.1). A discussion of the validity of the regularity conditions in the present context — that is, the construction of joint confidence bands for impulse response functions of structural vector autoregressions — is found in Section 3.3.3 below.

The bands of Romano and Wolf (2010) are rectangular by construction in contrast to methods that produce joint confidence sets of a non-rectangular shape in first place, from which then rectangular joint confidence bands are obtained by projection on the axes; an example of the latter approach are the Wald bands of Lütkepohl et al. (2015b). Such projection methods usually result in conservative joint confidence bands, even asymptotically, which are excessive in volume and thus leads to a loss in information.

Furthermore, the method of Romano and Wolf (2010) is attractive from a computational point of view, since it involves only the computation of the estimator of the impulse response function $\Theta_{ij,H}$ and an estimator (via the bootstrap) of the sampling distribution of the statistic $\max \sqrt{T} |\hat{\Theta}_{ij,H} - \Theta_{ij,H}|$, where T denotes the sample size and both the

maximum and the absolute value of a vector are understood to be element-wise operators. Both quantities are straightforward to compute and do not contain any sort of potential numerical difficulties such as, for example, the inversion of a large-dimensional matrix.

In contrast, the construction of the size-adjusted Wald joint confidence bands of [Lütkepohl et al. \(2015b\)](#) requires on the one hand the computation and the inversion of the (potentially large-dimensional) asymptotic covariance matrix of the vectorized estimators of $(A_1, \dots, A_p, \Sigma_u)$ and on the other hand an iterative procedure to decrease the volume of the confidence bands; see Section 3.4.3.

Next, the following notation is introduced:

- Let $\left\{ \sqrt{T} \left| \hat{\Theta}_{ij,h,b}^* - \hat{\Theta}_{ij,h} \right| \right\}_{b=1}^B$ denote the marginal bootstrap distribution at propagation horizon $h \in \{0, \dots, H\}$ based on B bootstrap replications.
- Let $\hat{H}_h^*(t)$, $h \in \{0, \dots, H\}$, denote the following empirical distribution function

$$\forall t \in \mathbb{R}, \quad \hat{H}_h^*(t) := \frac{1}{B} \sum_{b=1}^B \mathbb{1} \left\{ \sqrt{T} |\hat{\Theta}_{ij,h,b}^* - \hat{\Theta}_{ij,h}| \leq t \right\},$$

and the corresponding empirical quantile function is then given by

$$\hat{H}_h^{*,-1}(q) := \inf \left\{ t : \hat{H}_h^*(t) \geq q \right\}.$$

- Let $\hat{L}^*(t)$ denote the following empirical distribution function

$$\forall t \in \mathbb{R}, \quad \hat{L}^*(t) := \frac{1}{B} \sum_{b=1}^B \mathbb{1} \left\{ \max_{h \in \tilde{S}_{ij}} \left\{ \hat{H}_h^*(\sqrt{T} |\hat{\Theta}_{ij,h,b}^* - \hat{\Theta}_{ij,h}|) \right\} \leq t \right\},$$

where $\tilde{S}_{ij} \subseteq \{0, \dots, H\}$ denotes the propagation horizons when $\sqrt{T} |\hat{\Theta}_{ij,h} - \Theta_{ij,h}|$ exhibits a non-degenerate distribution; see Remark 3.3.1. The corresponding empirical quantile function is then given by

$$\hat{L}^{*,-1}(q) := \inf \left\{ t : \hat{L}^*(t) \geq q \right\}.$$

Remark 3.3.1 Identifying restrictions may predetermine the response at one or multiple propagation horizons \tilde{h} , that is, for some known constant $c_{\tilde{h}} \in \mathbb{R}$, $\hat{\Theta}_{ij,\tilde{h}} = c_{\tilde{h}}$ and

also $\hat{\Theta}_{ij,\tilde{h},b}^* = c_{\tilde{h}}$ for all b . Consequently, $\hat{H}_{\tilde{h}}^*(t) = \mathbb{1}_{[0,\infty)}(t)$ with probability one, and hence the empirical distribution of $\max_{h \in \{0, \dots, H\}} \left\{ \hat{H}_h^* \left(\sqrt{T} \left| \hat{\Theta}_{ij,h,b}^* - \hat{\Theta}_{ij,h} \right| \right) \right\}$ is degenerate at one (with probability one). Defining $\hat{L}^*(t)$ as the empirical distribution function of the aforementioned distribution would result in joint confidence bands that are excessively wide because $\hat{L}^{*, -1}(1 - \alpha) = 1$ for all $\alpha \in [0, 1)$; see formula (3.9). Hence, $\hat{L}^*(t)$ is defined as the empirical distribution function of $\max_{h \in \tilde{S}_{ij}} \left\{ \hat{H}_h^* \left(\sqrt{T} \left| \hat{\Theta}_{ij,h,b}^* - \hat{\Theta}_{ij,h} \right| \right) \right\}$. ■

3.3.2 Balanced Bootstrap Joint Confidence Bands

Based on equation (3.7) in Romano and Wolf (2010), we define the balanced bootstrap (BB) joint confidence bands for $\Theta_{ij,H}$ with nominal coverage probability $(1 - \alpha)$ as the Cartesian product of the following $(H + 1)$ marginal intervals:

$$\left[\hat{\Theta}_{ij,h} - \frac{1}{\sqrt{T}} \hat{H}_h^{*, -1} \left(\hat{L}^{*, -1}(1 - \alpha) \right), \hat{\Theta}_{ij,h} + \frac{1}{\sqrt{T}} \hat{H}_h^{*, -1} \left(\hat{L}^{*, -1}(1 - \alpha) \right) \right] \quad \text{for } h = 0, \dots, H . \quad (3.9)$$

A detailed algorithm for the construction of the BB bands is found in Appendix 3C. In the following, the BB bands for $\Theta_{ij,H}$ with a nominal coverage of $(1 - \alpha)$ are denoted by $\text{CB}_{\text{BB}, ij}^{(1-\alpha)}$. It is worth providing some further discussion about the BB joint confidence bands.

As is evident from (3.9), the BB bands are based on the estimated sampling distributions of the non-studentized roots $\sqrt{T} |\hat{\Theta}_{ij,h} - \Theta_{ij,h}|$. Often confidence intervals based on studentized roots are preferred from a higher-order asymptotic point of view; for example, see Hinkley and Wei (1984). However, under the assumption of stationarity of $\{y_t\}$, the standard deviations of the scaled estimator $\sqrt{T} \hat{\Theta}_{ij,h}$, denoted by σ_h , are decreasing in the propagation horizon (for fixed T), that is, $\sigma_h \rightarrow 0$, and the same is true for the standard errors $\hat{\sigma}_h$; for example, see Lütkepohl (1990). As a consequence, using the estimated sampling distributions of the studentized roots $\sqrt{T} |\hat{\Theta}_{ij,h} - \Theta_{ij,h}| / \hat{\sigma}_h$ results in joint confidence bands that can have excessively large volume, as pointed out by Lütkepohl et al. (2015a).

The construction of the BB bands involves the pre-pivoting transformation of Beran (1987); that is, the roots that underlie the joint confidence bands are monotonically transformed by their estimated empirical distribution function \hat{H}_h^* . Beran (1987) argues that

the prepivoting transformation reduces the coverage bias of marginal confidence intervals and also results in improved higher-order properties, similar to studentized roots. Consequently, using the prepivoting transformation results in BB joint confidence bands with good coverage properties but without excessive volume; see the Monte Carlo simulations in Section 3.5.

The BB bands are symmetric around the estimated impulse response function. The methodology of Romano and Wolf (2010) also allows the construction of asymmetric, ‘equal-tailed’ joint confidence bands based on the estimated distribution of the one-sided roots $\sqrt{T}(\hat{\Theta}_{ij,h} - \Theta_{ij,h})$. But simulation results (not reported here) suggest that the symmetric bands are superior to the asymmetric bands in terms of finite-sample coverage properties.

Remark 3.3.2 In the absence of any ‘favoritism’ of certain propagation horizons, the property of balance is a desirable one, as has previously been argued by Beran (1987, 1988) and Romano and Wolf (2010) in more general contexts: Balanced confidence bands spread out the probability of missing at least one element of the impulse response function evenly over the individual propagation horizons (up to the maximum propagation horizon H considered).

Another way to look at this issue is the following. If the property of balance were considered completely irrelevant, it would be easy to construct joint confidence bands with coverage $(1 - \alpha)$: Construct a marginal confidence interval for the impulse response function at propagation horizon one with coverage $(1 - \alpha)$ and take the Cartesian product of it with the Cartesian product of $H - 1$ times the real line. The resulting Cartesian product then trivially results in valid joint confidence bands with maximum propagation horizon H , for any H . Such joint confidence bands are extremely unbalanced and are of no use in practice.

Of course, this example is perverse, since all but the first intervals are unbounded. However, it can be considered as a limiting case for a non-perverse example where all but the first interval have individual coverage probabilities that are close to one (but less than one) and where the first interval has individual coverage probability close to $(1 - \alpha)$ (but greater than $1 - \alpha$), in a way such that the coverage probability of the confidence bands are equal to $(1 - \alpha)$. Clearly, such imbalanced bands are also not desirable from a

practical point of view.

Last but not least, it can be expected that imposing the property of balance, at least asymptotically, will result in joint confidence bands with small volume; though it may well be possible to find joint confidence bands with even smaller volume if the property of balance is abandoned, a topic which is left to future research.

If certain propagation horizons are ‘favored’ over others, then it is desirable to construct imbalanced joint confidence bands such that the marginal coverage probabilities at the favored propagation horizons are suitably higher compared to the other propagation horizons. An explicit construction of this sort is beyond the scope of this paper. However, the solution in such a case can certainly not be to employ joint confidence bands whose balance properties are unknown and which do not adapt to any ‘favored’ propagation horizons, either, such as the Wald-type bands of [Lütkepohl et al. \(2015b\)](#). ■

Remark 3.3.3 [Cao and Sun \(2011\)](#) derive the asymptotic distribution of structural impulse response functions of short panel vector autoregressions. Furthermore, [Cao and Sun \(2011\)](#) compare the finite-sample coverage properties of marginal confidence for individual responses based on the asymptotic distribution with the properties of various bootstrap intervals, but joint confidence bands for the entire impulse response function are not considered in their study. We expect that our proposed method can also be applied to construct joint confidence bands for impulse response functions of short panel vector autoregressions. However, a detailed analysis of this topic is beyond the scope of this paper. ■

3.3.3 Asymptotic Properties

The regularity conditions underlying Theorem 3.1 of [Romano and Wolf \(2010\)](#), which states the asymptotic properties of the generic bootstrap joint confidence bands, involve the asymptotic distribution of the estimator of the impulse response function and the asymptotic validity of the bootstrap. Thus, for the sake of completeness, both assumptions are subsequently reviewed.

Under standard assumptions and when LS is used for the estimation of $(A_1, \dots, A_p, \Sigma_u)$, the asymptotic distribution of $\sqrt{T}(\hat{\Theta}_{ij,H} - \Theta_{ij,H})$ is generally derived via an application of the delta method; for example, see [Lütkepohl \(1990\)](#). Thus, the asymptotic distribu-

tion of the (standardized) estimator of the impulse response function is typically normal because the (vectorized) LS estimator of $(A_1, \dots, A_p, \Sigma_u)$ is asymptotically normal under weak high-level assumptions: for example, see [Lütkepohl \(2005, Section 3.7\)](#). However, [Lütkepohl \(1989\)](#) and [Benkwitz et al. \(2000\)](#) note that the asymptotic covariance matrix, denoted by $\Sigma_{\hat{\Theta}}$, is singular in certain scenarios; hence, in such scenarios, the limiting distribution of $\sqrt{T}(\hat{\Theta}_{ij,H} - \Theta_{ij,H})$ is not normal, but degenerate normal instead.

This characteristic of the asymptotic distribution of the estimated impulse response function (that is, normal versus degenerate normal) has an impact on the consistency of the bootstrap for the joint sampling distribution of $\sqrt{T}(\hat{\Theta}_{ij,H} - \Theta_{ij,H})$. More specifically, in case the asymptotic distribution is non-degenerate normal, the bootstrap is consistent because the usual smoothness conditions underlying the bootstrap are satisfied; for example, see [Horowitz \(2001\)](#). However, the bootstrap may not be consistent when the asymptotic distribution is degenerate normal; for example, see [Benkwitz et al. \(2000\)](#).

It is evident that assumptions B1–B4 of [Romano and Wolf \(2010, p. 607\)](#) are satisfied if the asymptotic distribution of $\hat{\Theta}_{ij,H}$ is non-degenerate normal, which is the case if $\Sigma_{\hat{\Theta}}$ is positive definite. Thus, the asymptotic properties of $\text{CB}_{\text{BB},ij}^{(1-\alpha)}$ can then be deduced from Theorem 3.1 of [Romano and Wolf \(2010\)](#). More specifically, it holds that

$$\lim_{T \rightarrow \infty} \mathbb{P} \left(\Theta_{ij,H} \in \text{CB}_{\text{BB},ij}^{(1-\alpha)} \right) = (1 - \alpha) , \quad (3.10)$$

if $\Sigma_{\hat{\Theta}}$ is positive definite. Furthermore, let $\text{CB}_{\text{BB},ij,h}^{(1-\alpha)}$ denote the h -th marginal confidence interval for $\Theta_{ij,h}$, then it holds that

$$\lim_{T \rightarrow \infty} \mathbb{P} \left(\Theta_{ij,h} \in \text{CB}_{\text{BB},ij,h}^{(1-\alpha)} \right) = \rho \in (0, 1) \quad \forall h \in \{0, \dots, H\} , \quad (3.11)$$

if $\Sigma_{\hat{\Theta}}$ is positive definite. Summarizing, under the condition of a positive definite covariance matrix $\Sigma_{\hat{\Theta}}$, the BB joint confidence bands have asymptotically the correct coverage rate and are asymptotically balanced in the sense that coverage rate of the marginal intervals $\text{CB}_{\text{BB},ij,h}^{(1-\alpha)}$ are asymptotically independent of $h \in \{0, \dots, H\}$.

Data generating processes that give rise to a singular asymptotic covariance matrix $\Sigma_{\hat{\Theta}}$ are included in the Monte Carlo experiment in [Section 3.5](#) to gain some simulation-based insights about the properties of the BB bands in scenarios with an asymptotic degenerate

normal distribution.

Remark 3.3.4 The traditional Bonferroni bands and the size-adjusted Bonferroni bands of [Lütkepohl et al. \(2015a\)](#) have a similar handicap: These joint confidence bands are also only proven to work if the bootstrap is consistent for all marginal distributions $\sqrt{T}(\hat{\Theta}_{ij,h} - \Theta_{ij,h})$, which is the case if $\sqrt{T}(\hat{\Theta}_{ij,h} - \Theta_{ij,h})$ converges to a non-degenerate normal distribution for all $h \in \{0, \dots, H\}$; for more details, see [Lütkepohl et al. \(2015b, p. 9\)](#). ■

The simultaneous test of $H_{0,h} : \Theta_{ij,h} = 0, h \in \{0, \dots, H\}$, is of great interest in applied work. Such a test can be carried out by ‘inverting’ the joint confidence bands for $\Theta_{ij,H}$. In particular, any $H_{0,h}$ is rejected for which zero is not contained in the marginal confidence interval $\text{CB}_{\text{BB},ij,h}^{(1-\alpha)}$. It follows from Corollary 3.1 of [Romano and Wolf \(2010\)](#) that such a testing procedure asymptotically controls the probability of falsely rejecting at least one true hypothesis $H_{0,h}$, that is,

$$\limsup_{T \rightarrow \infty} \mathbb{P}(\text{reject at least one true hypothesis } H_{0,h}) \leq \alpha, \quad (3.12)$$

at least as long as $\Sigma_{\hat{\Theta}}$ is positive definite. In other words, for all $h \in \{0, \dots, H\}$ for which zero is not contained in the corresponding marginal confidence interval, one can be jointly confident that the true impulse response $\Theta_{ij,h}$ is non-zero; that is, the confidence holds jointly for all such h and not just individually (for a given such h).

3.4 Competing Methods

In order to assess the finite-sample performance of our proposed method, we compare its finite-sample properties with those of relevant competing methods in the literature. More specifically, the list of the competing bands consists of the Naïve bands, the traditional Bonferroni bands, and the recently proposed Wald and Adjusted-Wald bands of [Lütkepohl et al. \(2015b\)](#). In the following, each of the four competing methods is briefly outlined; more details are found in the corresponding references.

3.4.1 Naïve Confidence Bands

The Naïve confidence bands for $\Theta_{ij,H}$, as defined in [Lütkepohl et al. \(2015a\)](#), are given by the collection of the $(H + 1)$ marginal confidence intervals with individual confidence level $(1 - \alpha)$, that is,

$$\text{CB}_{\text{Naïve},ij}^{(1-\alpha)} := \left[q_{0,\frac{\alpha}{2}}^{*,ij}, q_{0,(1-\frac{\alpha}{2})}^{*,ij} \right] \times \cdots \times \left[q_{H,\frac{\alpha}{2}}^{*,ij}, q_{H,(1-\frac{\alpha}{2})}^{*,ij} \right], \quad (3.13)$$

where $q_{h,\frac{\alpha}{2}}^{*,ij}$ and $q_{h,(1-\frac{\alpha}{2})}^{*,ij}$ denote the $\frac{\alpha}{2}$ and $1 - \frac{\alpha}{2}$ quantiles of the bootstrap distribution of the estimated impulse response coefficient at horizon $h \in \{0, \dots, H\}$.

3.4.2 Bonferroni Joint Confidence Bands

The Bonferroni joint confidence bands for $\Theta_{ij,H}$ consist of the Cartesian product of $(H + 1)$ marginal confidence intervals for the individual responses $\Theta_{ij,h}$, $h \in \{0, \dots, H\}$, where the nominal confidence level of the marginal intervals is adjusted via Bonferroni's inequality in order to ensure that the joint coverage probability is, asymptotically, at least $(1 - \alpha)$. (Of course, this can only be guaranteed if the underlying bootstrap method is consistent.) More specifically, the adjusted marginal nominal confidence level is equal to $(1 - \beta)$, where $\beta := \alpha / (H + 1)$ ⁵. The rectangular Bonferroni joint confidence bands for $\Theta_{ij,H}$, as defined in [Lütkepohl et al. \(2015a\)](#), are given by

$$\text{CB}_{\text{B},ij}^{(1-\alpha)} := \left[q_{0,\frac{\beta}{2}}^{*,ij}, q_{0,(1-\frac{\beta}{2})}^{*,ij} \right] \times \cdots \times \left[q_{H,\frac{\beta}{2}}^{*,ij}, q_{H,(1-\frac{\beta}{2})}^{*,ij} \right], \quad (3.14)$$

where $q_{h,\frac{\beta}{2}}^{*,ij}$ and $q_{h,(1-\frac{\beta}{2})}^{*,ij}$ denote the $\frac{\beta}{2}$ and $1 - \frac{\beta}{2}$ quantiles of the bootstrap distribution of the estimated impulse response coefficient at horizon $h \in \{0, \dots, H\}$.

3.4.3 Wald and Adjusted-Wald Joint Confidence Bands

The Wald joint confidence bands for $\Theta_{ij,H}$ of [Lütkepohl et al. \(2015b\)](#) are constructed in a two-step fashion. First, the bootstrap Wald test for the relevant reduced-form parameters of the underlying VAR is inverted to obtain a joint confidence ellipse. Second, the ellipse is projected onto the axes of the impulse response space, resulting in rectangular joint confidence bands for $\Theta_{ij,H}$.

⁵In case the initial response is zero by construction, β is equal to α/H .

More specifically, the Wald joint confidence ellipse for the relevant reduced-form coefficients, denoted by θ , with a nominal confidence level of $(1 - \alpha)$ is given by

$$\mathcal{W}_{(1-\alpha)}^\theta = \left\{ \theta : T \left(\hat{\theta} - \theta \right)' \left(\hat{\Sigma}_\theta \right)^{-1} \left(\hat{\theta} - \theta \right) \leq w_{(1-\alpha)}^* \right\} ,$$

where $\hat{\theta}$ denotes a consistent estimator for θ , $\hat{\Sigma}_\theta$ denotes a consistent estimator of the asymptotic variance of $\hat{\theta}$, and $w_{(1-\alpha)}^*$ denotes the $(1 - \alpha)$ quantile of the bootstrap distribution of the Wald statistic⁶. The bootstrap impulse responses are ordered according to the set of increasing bootstrap Wald statistics $\{w_1^* \leq \dots \leq w_B^*\}$ in the sense that $\hat{\Theta}_{ij,H,n}^*$ corresponds to w_n^* . Finally, the rectangular Wald joint confidence bands for $\Theta_{ij,H}$ with nominal confidence level $(1 - \alpha)$ are given as the envelope of the ordered set of bootstrap impulse response functions $\left\{ \hat{\Theta}_{ij,H,1}^*, \dots, \hat{\Theta}_{ij,H,(1-\alpha) \times B}^* \right\}$, that is,

$$\text{CB}_{\text{Wald},ij}^{(1-\alpha)} := [l_{ij,0}^*, u_{ij,0}^*] \times \dots \times [l_{ij,H}^*, u_{ij,H}^*] , \quad (3.15)$$

where $l_{ij,s}^* := \min \left\{ \hat{\Theta}_{ij,b,n}^* : n = 1, \dots, (1 - \alpha) \times B \right\}$, and $u_{ij,s}^*$ is defined as the corresponding upper bound; we assume here tacitly that $(1 - \alpha) \times B$ is an integer, otherwise take the smallest integer larger than $(1 - \alpha) \times B$.

Lütkepohl et al. (2015b) point out that the Wald bands are conservative by construction, and hence usually cover more than $(1 - \alpha) \times B$ of the bootstrap impulse response functions. Thus, a volume adjustment of the Wald bands can be considered and Lütkepohl et al. (2015b) propose the following iterative adjustment⁷: remove iteratively the last element in the set of ordered bootstrap impulse responses until the bootstrap coverage of the envelope of the remaining functions is greater than or equal to $(1 - \alpha)$. The resulting rectangular Adjusted-Wald joint confidence bands for $\Theta_{ij,H}$ with a nominal confidence level $(1 - \alpha)$ are given as the envelope of the remaining bootstrap impulse responses, that is,

$$\text{CB}_{\text{Adj-W},ij}^{(1-\alpha)} := [\tilde{l}_{ij,0}^*, \tilde{u}_{ij,0}^*] \times \dots \times [\tilde{l}_{ij,H}^*, \tilde{u}_{ij,H}^*] , \quad (3.16)$$

⁶This is the empirical distribution of $w_b^* := T \left(\hat{\theta}_b^* - \theta \right)' \left(\hat{\Sigma}_\theta^* \right)^{-1} \left(\hat{\theta}_b^* - \theta \right)$, $b = 1, \dots, B$, where $\hat{\theta}_b^*$ and $\hat{\Sigma}_\theta^*$ are estimators based on bootstrap data $\{y_1^*, \dots, y_T^*\}$.

⁷Lütkepohl et al. (2015b) also propose another adjustment procedure and the resulting joint confidence bands are called Bonferroni-adjusted Wald bands, see Lütkepohl et al. (2015b, p. 11).

where $\tilde{l}_{ij,h}^* := \min \left\{ \hat{\Theta}_{ij,b,h}^* : b = 1, \dots, \tilde{B} \right\}$, and \tilde{B} denotes index of the first bootstrap impulse response that is not removed, and $\tilde{u}_{ij,H}^*$ is defined as the corresponding upper bound.

3.5 Monte Carlo Simulation

3.5.1 Lag Selection and Estimation of Impulse Responses

The lag order is selected using the Akaike information Criterion (AIC), as [Kilian \(2001\)](#) provides simulation evidence that confidence intervals (for individual responses) based on the AIC exhibit superior finite-sample coverage properties compared to confidence intervals based on the Schwarz Information Criterion and the Hannan-Quinn Criterion. The maximum lag order p_{\max} is determined endogenously using the rule of thumb proposed in [Schwert \(1989\)](#). According to this rule, the maximum lag order is given by

$$p_{\max} := \lfloor 12(T/100)^{0.25} \rfloor, \quad (3.17)$$

where $\lfloor \cdot \rfloor$ denotes the integer part of a real number and T denotes the sample size. Thus, the maximum lag order is given by 12, 14, and 16 for sample sizes of 100, 200, and 400, respectively. In the following, \hat{p} denotes the lag order selected by the AIC, that is, $\hat{p} := \hat{p}_{\text{AIC}}$.

We estimate the reduced-form coefficients $(\nu, A_1, \dots, A_{\hat{p}})$ of the VAR model by least squares; see [Lütkepohl \(2005, Section 3.2\)](#) for more details. It is well known that the LS estimator is biased in finite samples due to the presence of lagged endogenous variables. Thus, we correct for the finite-sample bias using the closed-form bias estimator of [Pope \(1990\)](#); see Appendix [3A](#) for details. The corresponding bias-corrected estimators of the slope coefficients are given by

$$\hat{A}_i^{\text{BC}} := \hat{A}_{\text{LS},i} - \widehat{\text{Bias}}(\hat{A}_{\text{LS},i}), \quad \text{for } i = 1, \dots, \hat{p},$$

where $\hat{A}_{\text{LS},i}$ denotes the LS estimator of A_i and $\widehat{\text{Bias}}(\hat{A}_{\text{LS},i})$ denotes Pope's corresponding bias estimator. Furthermore, in scenarios where the bias correction causes nonstationarity — that is, where the process corresponding to $(\nu, \hat{A}_{\text{LS},1}, \dots, \hat{A}_{\text{LS},\hat{p}})$ is stationary but

the process corresponding to $(\nu^{\text{BC}}, \hat{A}_1^{\text{BC}}, \dots, \hat{A}_{\hat{p}}^{\text{BC}})$ is non-stationary — the stationarity correction of Kilian (1998b) is applied instead; see Appendix 3B for details.

We assume a recursive structure of the structural VAR model, that is, the impact matrix B_0 is given by the lower-triangular Cholesky decomposition of Σ_u . The corresponding estimator is naturally given by

$$\hat{B}_0 := \text{chol} \left(\hat{\Sigma}_u^{\text{BC}} \right) ,$$

where $\hat{\Sigma}_u^{\text{BC}}$ denotes the estimated residual covariance matrix based on the bias-corrected VAR coefficient estimators. Summarizing, the estimated structural impulse response functions $\hat{\Theta}_{ij,H}$ are obtained as

$$\hat{\Theta}_{ij,H} := \Theta_{ij,H} \left(\hat{A}_1^{\text{BC}}, \dots, \hat{A}_{\hat{p}}^{\text{BC}}, \text{chol} \left(\hat{\Sigma}_u^{\text{BC}} \right) \right) . \quad (3.18)$$

3.5.2 Bootstrap Details

The bootstrap distribution of the estimator of the structural impulse response functions is generated by the following nonparametric bootstrap procedure of Kilian (1998b):

- a) Given $\{y_t\}_{t=1}^T$, \hat{p} , $(\hat{\nu}^{\text{BC}}, \hat{A}_1^{\text{BC}}, \dots, \hat{A}_{\hat{p}}^{\text{BC}})$ and the corresponding series of residuals $\{\hat{u}_t\}_{t=\hat{p}+1}^T$, generate a bootstrap sample $\{y_1^*, \dots, y_T^*\}$ via the following recursion

$$y_t^* = \begin{cases} y_t , & t = 1, \dots, \hat{p} \\ \hat{\nu}^{\text{BC}} + \hat{A}_1^{\text{BC}} y_{t-1}^* + \dots + \hat{A}_{\hat{p}}^{\text{BC}} y_{t-\hat{p}}^* + e_t^* , & t = \hat{p} + 1, \dots, T \end{cases} , \quad (3.19)$$

where e_t^* is a random draw with replacement from the empirical distribution of the residuals that are rescaled and centered to have mean zero⁸.

- b) Obtain $(\hat{A}_1^{*,\text{BC}}, \dots, \hat{A}_{\hat{p}}^{*,\text{BC}})$ and $\hat{\Sigma}_u^{*,\text{BC}}$ by fitting a VAR(\hat{p}) model to $\{y_t^*\}_{t=1}^T$.

- c) Obtain $\hat{\Theta}_{ij,H}^* = \Theta_{ij,H} \left(\hat{A}_1^{*,\text{BC}}, \dots, \hat{A}_{\hat{p}}^{*,\text{BC}}, \text{chol} \left(\hat{\Sigma}_u^{*,\text{BC}} \right) \right)$.

- d) Repeat steps a) to c) B times resulting in the bootstrap sample $\left\{ \hat{\Theta}_{ij,H,b}^* \right\}_{b=1}^B$.

⁸The centering and rescaling is carried out as suggested in Stine (1987).

The previously outlined bootstrap algorithm is subsequently referred to as the *exogenous bootstrap* because the lag order is *not* re-estimated based on the bootstrap sample $\{y_1^*, \dots, y_T^*\}$.

The Wald-type joint confidence bands of Lütkepohl et al. (2015b) can only be constructed using the exogenous bootstrap because the computation of the bootstrap Wald statistic requires that the vector of the estimator of the slope coefficients $(\hat{A}_1, \dots, \hat{A}_{\hat{p}})$ and the bootstrap analogues $(\hat{A}_1^*, \dots, \hat{A}_{\hat{p}^*}^*)$ have the same dimension and hence the same lag order, that is, $\hat{p} = \hat{p}^*$. Therefore, a fair comparison of the finite-sample performance of the BB bands with the competing methods should be based on the exogenous bootstrap.

Remark 3.5.1 The exogenous bootstrap algorithm differs from the original algorithm in Kilian (1998b) in one minor aspect. The LS parameter estimates of the reduced-form coefficients are corrected for their finite-sample bias using the closed-form bias formula of Pope (1990) instead of a bootstrap-based bias correction as in Kilian (1998b). This modification can be justified, on the one hand, since both procedures remove only the first-order bias and, on the other hand, since both procedure exhibit a similar finite-sample performance, as is shown in the Monte Carlo study by Engsted and Pedersen (2014). ■

Kilian (1998a) provides simulation-based evidence that endogenizing the lag order selection in the bootstrap procedure results in an improved coverage accuracy of marginal bootstrap intervals for impulse responses of structural vector autoregressions. In order to investigate whether a similar effect can be observed for joint confidence bands, the BB bands, the Naïve bands, and the Bonferroni bands will be additionally constructed based on the endogenous bootstrap procedure of Kilian (1998a).

Remark 3.5.2 Our suggested bootstrap procedure is an extension of previous proposals for univariate finite-order ARMA models to multivariate finite-order VAR models, where the order is determined in a data-dependent fashion as opposed to being assumed known; in particular, we follow Kilian (2001) in using the AIC to select the order. As stated before, the maximum order considered is allowed to tend to infinity together with the sample size T ; see (3.17). Therefore, our bootstrap procedure can also be considered a sieve bootstrap, whose validity in more general models — that is, in models more general than a finite-order VAR model — is studied in Meyer and Kreiss (2015).

There are recent bootstrap procedures — such as the hybrid bootstrap of [Jentsch and Kreiss \(2010\)](#) and the linear process bootstrap of [Jentsch and Politis \(2015\)](#) — which can be applied in the present context to generate the bootstrap data $\{y_1^*, \dots, y_T^*\}$. However, an in-depth analysis of the effect of employing different bootstrap procedures on the finite-sample performances of confidence bands for structural impulse response functions is beyond the scope of this paper. ■

3.5.3 Data Generating Processes

We first consider the bivariate data generating processes from [Kilian \(1998b\)](#), which were previously considered in [Lütkepohl et al. \(2015a\)](#) and [Lütkepohl et al. \(2015b\)](#) in the context of joint confidence bands for structural impulse response functions, that is,

$$\text{DGP-1} \quad y_t = \begin{pmatrix} \rho & 0.0 \\ 0.5 & 0.5 \end{pmatrix} y_{t-1} + u_t, \quad (3.20)$$

with $\rho \in \{0.95, 0.9, 0.5, 0, -0.5, -0.9, -0.95\}$. The specific variants of DGP-1 will be denoted by DGP-1*i*, $i \in \{a, \dots, g\}$, depending on the specific value of ρ . The characteristic roots of the processes are presented in [Table 3.1](#).

DGP	Roots
1a	(2.000, 1.053)
1b	(2.000, 1.111)
1c	(2.000, 2.000)
1d	(2.000)
1e	(2.000, -2.000)
1f	(2.000, -1.111)
1g	(2.000, -1.053)

Table 3.1: Characteristic roots of the various variants of DGP-1.

Some properties of DGP-1 are worth mentioning: First, all processes are stationary but some are persistent (DGP-1a, DGP-1g). Second, independently of ρ , the true response of the first variable to a shock in the second variable is zero at all propagation horizons, that is $\Theta_{12,H} = 0 \in \mathbb{R}^{H+1}$, and hence the asymptotic distribution of the estimator is degenerate normal as noted in [Benkwitz et al. \(2000\)](#). Third, for $\rho = 0$ (DGP-1d), the true response

of the first variable to a shock in the first variable is also zero at all propagation horizons, that is, $\Theta_{11,H} = 0$, and hence the estimator is also asymptotically degenerate normal.

Furthermore, we use $u_t \stackrel{\text{i.i.d.}}{\sim} \mathcal{N}(0, \Sigma_u^1)$, where the population covariance matrix is given by

$$\Sigma_u^1 = \begin{pmatrix} 1.00 & 0.30 \\ 0.30 & 1.00 \end{pmatrix}.$$

In the Monte Carlo simulation, data samples of length $T \in \{100, 400\}$ are generated for each variant of DGP-1 and the propagation horizon is $H \in \{10, 20\}$; [Lütkepohl et al. \(2015a,b\)](#) use the same choices of T and H .

DGP-2 is a trivariate VAR(4) model previously considered in [Staszewska-Bystrova \(2011\)](#). More specifically, the population parameters of DGP-2 are the estimates of a model of the inflation rate, the unemployment rate, and the federal fund rate using US quarterly data from 1960-Q1 through 2004-Q1; for more details about the data set, see [Stock and Watson \(2001\)](#) or [Staszewska-Bystrova \(2011\)](#). The DGP is given by

$$\textbf{DGP-2} \quad y_t = \nu + A_1 y_{t-1} + A_2 y_{t-2} + A_3 y_{t-3} + A_4 y_{t-4} + u_t, \quad (3.21)$$

where

$$A_1 := \begin{pmatrix} 0.549 & -0.965 & 0.164 \\ 0.029 & 1.480 & 0.003 \\ 0.084 & -1.567 & 0.962 \end{pmatrix}, \quad A_2 := \begin{pmatrix} 0.118 & 1.506 & -0.128 \\ -0.013 & -0.494 & 0.043 \\ 0.197 & 1.763 & -0.364 \end{pmatrix},$$

$$A_3 := \begin{pmatrix} 0.060 & -0.954 & 0.054 \\ 0.002 & -0.029 & -0.024 \\ -0.070 & -0.848 & 0.333 \end{pmatrix}, \quad A_4 := \begin{pmatrix} 0.261 & 0.250 & -0.098 \\ -0.012 & -0.014 & 0.008 \\ -0.046 & 0.563 & -0.010 \end{pmatrix},$$

and $\nu := (1.076, 0.125, 0.347)'$. Furthermore, we use $u_t \stackrel{\text{i.i.d.}}{\sim} \mathcal{N}(0, \Sigma_u^2)$, where the population covariance matrix of DGP-2 is the covariance estimate based on the same data as the

intercept and the slope coefficients and is given by

$$\Sigma_u^2 := \begin{pmatrix} 0.962 & -0.018 & 0.116 \\ -0.018 & 0.049 & -0.087 \\ 0.116 & -0.087 & 0.693 \end{pmatrix} .$$

In the Monte Carlo study, data samples of length $T \in \{100, 400\}$ are generated and the maximum propagation horizon is $H \in \{4, 8, 12, 16, 20, 24, 28\}$. The choices of H reflect the fact that DGP-2 is an empirical DGP based on quarterly data and hence the considered values of the maximum propagation horizon H correspond to impulse responses over one up to seven years.

3.5.4 Simulation Parameters and Performance Evaluation

The nominal confidence level of the various joint confidence bands is 90%. The number of bootstrap replications is $B = 2000$ throughout and the number of Monte Carlo replications is also 2000. The finite-sample performance of the various bands is evaluated via the empirical volume and the empirical coverage rate. More specifically, the empirical coverage rate is calculated in the usual way, that is,

$$EC := \frac{1}{2000} \sum_{m=1}^{2000} \mathbb{1}_{\{\Theta_{ij,H} \in \text{CB}_{m,ij}\}} ,$$

where $\text{CB}_{m,ij}$ denotes particular joint confidence bands for $\Theta_{ij,H}$ and $\mathbb{1}_{\{A\}}$ denotes the indicator function of an event A . The empirical volume of particular joint confidence bands for $\Theta_{ij,H}$ is computed as the average of the sum of the lengths of the corresponding marginal intervals, that is,

$$V := \frac{1}{2000} \sum_{m=1}^{2000} \sum_{h=0}^H (u_{m,h} - l_{m,h}) ,$$

where $u_{m,h}$ denotes the upper bound of the h -th marginal interval of the bands in the m -th Monte Carlo repetition and $l_{m,h}$ denotes the corresponding lower bound.

3.5.5 Results

DGP-1: Bivariate VAR(1) Models

The tables with the simulation results are found in Appendix 3I. Boxplots summarizing the performance of the various methods across different scenarios are found in Appendices 3D and 3E. The focus is on the finite-sample performance of the BB bands because the performance of the competing methods have already been investigated individually for this specific DGP in Lütkepohl et al. (2015a,b). The main conclusions are as follows:

- For $T = 100$ and $H = 10$, the BB bands exhibit coverage rates close to or mildly below the nominal level of 90% except in the scenarios where the asymptotic distribution of the estimator of the impulse response function is degenerate normal (that is, joint confidence bands for $\Theta_{1,1}$ of DGP-1d and $\Theta_{1,2}$ of all processes) and the scenario where joint confidence bands are constructed for $\Theta_{1,1}$ of DGP-1g. The bands of the former scenarios exhibit coverage rates above the nominal level, whereas the bands for the latter scenario exhibit substantial undercoverage. Furthermore, the BB bands are robust with respect to the propagation horizon. Overall, the coverage bias of the BB bands is substantially reduced for the large sample size of $T = 400$; see Figures 3A.1 and 3A.2.
- In general, the coverage bias of the BB bands is comparable to that of the Adjusted-Wald bands, but smaller than the coverage bias of the Naïve bands, the Bonferroni bands, and the Wald bands.
- In all scenarios, the BB bands are smaller than the Bonferroni bands, where the excess volume (vis-à-vis the volume of the BB bands) of the Bonferroni bands ranges from 0.7% to 55%. Overall, the excess volume tends to increase with the sample size T and the maximum propagation horizon H . However, there does not seem to be a clear pattern between the stationary characteristics of the processes and the excess volume of the Bonferroni bands.
- In 108 out of the 112 scenarios, the BB bands exhibit a smaller volume than the conservative Wald bands. In these scenarios, the volume of the Wald bands is substantially larger and the excess volume (vis-à-vis the volume of the BB bands)

ranges from 24.5% to 82.9%. Furthermore, the excess volume decreases with the maximum propagation horizon H and the sample size T in almost all scenarios.

- In 98 out of the 112 scenarios, the volume of the Adjusted-Wald bands is smaller than the volume of the BB bands. However, the difference is usually small. As expected, the BB bands are larger than the Naïve bands which completely ignore the inherent simultaneity in the construction of the bands.

DGP-2: Trivariate VAR(1) Model

The complexity of DGP-2 is substantially larger compared to the bivariate VAR(1) models of DGP-1. The true impulse response functions of DGP-2 depend on 42 population reduced-form coefficients (compared to 7 population coefficients in DGP-1). Thus, the results for $T = 100$ give some indication about the performance of the joint confidence bands in scenarios where the ratio of the sample size to the number of coefficients is small (that is, low degrees of freedom)⁹. The tables with the simulation results are found in Appendices 3J and 3K. Boxplots summarizing the performance of the various methods across different scenarios are found in Appendices 3F and 3G. The main conclusions are as follows:

- For $T = 100$, there are systematic differences in the coverage rates of the BB bands, that is the bands for $\Theta_{1,1}, \Theta_{1,3}, \Theta_{3,3}$ perform worse than the bands for the other impulse responses; see Figure 3A.9. More specifically, the bands for $\Theta_{1,1}, \Theta_{1,3}, \Theta_{3,3}$ exhibit substantial undercoverage whereas the bands for the remaining impulse responses exhibit only mild under- and overcoverage, even for large H . Overall, the coverage distortion as well as the variation in coverage rates are substantially reduced for a sample size of $T = 200$, except the coverage rates of the bands for $\Theta_{1,1}$ which are still seriously below 90%. For $T = 400$, the coverage rates of the BB bands are consistently close to the nominal coverage of 90%, even for large H ; see Figure 3A.10.
- In principle, the BB bands are smaller than the two conservative bands (Bonferroni and Wald) and larger than the Naïve bands. Interestingly, the BB bands are even smaller than the Adjusted-Wald bands in 172 out of 189 scenarios. In general,

⁹For $T = 100$, there are 300 individual data points to estimate the 42 coefficients.

the volume of the BB bands is strictly decreasing in the sample size, but strictly increasing in the propagation horizon.

- For $T = 100$, there are systematic differences in the coverage rates of the Bonferroni bands. The Bonferroni bands for $\Theta_{1,1}$, $\Theta_{1,3}$, $\Theta_{3,3}$ exhibit massive to substantial undercoverage in some scenarios, whereas the bands for the other impulse responses exhibit only mild under- and overcoverage. For a larger sample size of $T = 200$, the coverage rates are close or above the nominal level of 90% except the coverage rates of the bands for $\Theta_{1,1}$, which are still seriously below 90%. For $T = 400$, all coverage rates are above the nominal level.
- The coverage rates of the Wald bands are markedly above the nominal level of 90% in 173 out of 189 scenarios. Overall, the positive coverage bias is enhanced with the sample size; see Figures N.1 and N.2 in the Supplementary Material. In all scenarios, the Wald bands exhibit the largest volume and are substantially larger than the Bonferroni bands.
- For $T = 100$, the Adjusted-Wald bands exhibit coverage rates that are substantially distorted and systematically differ among the different impulse response functions; see Figure 3A.9. Nevertheless, the coverage distortions and the systematic variation in coverage rates are mitigated as the sample size increases; see Figure 3A.10.
- The Naïve bands massively under-represent the joint estimation uncertainty in all scenarios. The empirical coverage rate falls below 40% in some scenarios with $T = 100$. Thus, these results provide additional evidence that the Naïve bands should not be used in practice, at least not when joint confidence bands are desired.

Empirical Balance

From a theoretical point of view, the BB bands, the Naïve bands and the Bonferroni bands are asymptotically balanced, that is, the marginal coverage probability is (asymptotically) independent of the propagation horizon $h \in \{0, \dots, H\}$. The Wald-type bands of Lütkepohl et al. (2015b) have not been theoretically investigated in terms of asymptotic balance.

Table 3.2 presents the mean absolute deviations (MAD) from the mean of the marginal empirical coverage rates for DGP-2, $H = 20$ and $T \in \{100, 400\}$. For the small sample

size $T = 100$, the (unadjusted) Wald bands exhibit the smallest deviations from balance, followed closely by the Bonferroni bands. The third place is shared by the BB bands and the Adjusted-Wald bands and the last place goes to the Naïve bands. Increasing the sample size to $T = 400$ reduces the MAD of all methods in all scenarios. The first two places are again awarded to the Wald and the Bonferroni bands, respectively. However, the BB bands exhibit the smaller MAD in six out of nine scenarios when compared to the Adjusted-Wald bands and in seven out of nine scenarios when compared to the Naïve bands, respectively, resulting in the third place. The last place is shared by the Adjusted-Wald and the Naïve bands.

DGP2	Method	$\Theta_{1,1}$	$\Theta_{1,2}$	$\Theta_{1,3}$	$\Theta_{2,1}$	$\Theta_{2,2}$	$\Theta_{2,3}$	$\Theta_{3,1}$	$\Theta_{3,2}$	$\Theta_{3,3}$
$T = 100$	Naïve	7.97	1.63	5.61	2.46	1.44	0.51	3.41	3.44	2.91
	BB	1.95	0.95	4.35	0.73	1.02	0.47	1.39	2.20	0.64
	Bonferroni	2.26	0.44	3.73	0.47	0.57	0.31	0.47	1.32	0.75
	Wald	1.32	0.35	2.58	0.28	0.43	0.30	0.35	0.72	0.53
	Adj-Wald	3.15	0.70	5.35	1.64	0.61	0.74	1.77	1.27	1.35
$T = 400$	Naïve	0.37	0.38	0.54	0.70	0.58	0.65	0.95	0.69	0.72
	BB	0.51	0.43	0.32	0.13	0.27	0.22	0.66	0.52	0.27
	Bonferroni	0.20	0.20	0.13	0.19	0.29	0.15	0.41	0.14	0.30
	Wald	0.11	0.08	0.07	0.16	0.15	0.08	0.22	0.13	0.12
	Adj-Wald	0.82	0.36	1.04	0.21	0.25	0.42	1.28	0.32	0.80

Table 3.2: MAD of the empirical marginal coverage rates (from their mean) of nominal 90% confidence bands with $H = 20$, normal errors, and AIC lag selection.

Exogenous vs. Endogenous Bootstrap

The tables with the simulation results for the Naïve bands, the Bonferroni bands, and the BB bands based on the endogenous bootstrap are found in the Appendices [3L](#), [3M](#) and [3N](#). The main conclusions are as follows:

- The simulation results for the bivariate VAR(1) models show that endogenizing the lag uncertainty in general results in an upward shift of the coverage rates of the BB bands for both $T = 100$ and $T = 400$; see Figure [3A.11](#). The effect on the coverage rates of endogenizing the lag uncertainty is ambiguous as there are scenarios where the coverage bias is reduced (for example, bands for $\Theta_{1,1}$ of DGP-1g), but also scenarios where the opposite is true (for example, bands for $\Theta_{1,1}$ of

DGP-1e). However, the BB bands based on the endogenous bootstrap are larger than the BB bands based on the exogenous bootstrap.

- The results for the trivariate VAR(4) model show that the coverage rates of the BB bands based on the endogenous bootstrap are surprisingly inferior to those of the BB bands based on exogenous bootstrap for $T = 100$; see Figure 3A.12. For $T = 200, 400$, there are scenarios where the BB bands based on the endogenous bootstrap are superior, but in the majority of the scenarios, the bands based on the exogenous bootstrap are superior. For $T = 100$, endogenizing the lag uncertainty results in bands that are smaller than the bands based on the exogenous bootstrap. The same is true for the majority of the scenarios with $T = 200, 400$, although the differences are decreasing in the sample size.
- The results for the the bivariate VAR(1) models show that the coverage rates of the Bonferroni bands based on the endogenous bootstrap are larger than those of the Bonferroni bands based on the exogenous bootstrap in the majority of the scenarios, although the differences tend to decrease with the sample size. Hence, endogenizing the lag uncertainty increases the coverage bias of the Bonferroni bands, as the Bonferroni bands based on the exogenous bands exhibit coverage rates above the nominal level.
- The simulation results for the trivariate VAR(4) model show that the effect of endogenizing the lag uncertainty on the Bonferroni bands is ambiguous (for all sample sizes); there are scenarios where the bands based on the endogenous bootstrap are superior but also scenarios where the opposite is true. The Bonferroni bands based on the endogenous bootstrap are smaller than the Bonferroni bands based on the exogenous bootstrap in almost all scenarios.

3.5.6 Summary of simulation Evidence

We have conducted a Monte Carlo simulation to compare the finite-sample properties of the BB bands with a number of competing methods. We have included several bivariate VAR(1) models and an empirical trivariate VAR(4) model in the set of data generating processes.

The simulation results of the bivariate VAR(1) models show that the BB bands and the Adjusted-Wald bands exhibit both a smaller coverage bias and a smaller volume than the Bonferroni and the Wald bands. Both methods are robust with respect to the maximum propagation horizon and also produce reasonable joint confidence bands when the true impulse response is zero and hence the asymptotic distribution of the estimator is degenerate.

The simulation results of the trivariate VAR(4) model show that the coverage rates of the BB bands, the Bonferroni bands, and the Adjusted-Wald bands are potentially downward biased in low-degrees-of-freedom scenarios. In such scenarios, the Wald bands may be preferred to avoid the use of bands that underestimate the estimation uncertainty, but the price to pay is the large volume of the Wald bands, especially for large maximum propagation horizons. For $T = 400$, the BB bands exhibit the smallest coverage bias and at the same time the smallest volume among all joint confidence bands (except for the Naïve bands).

Overall, both the Adjusted-Wald bands and the BB bands work reliably in small models. However, the simulation results of the trivariate VAR(4) model show that the BB bands generally outperform the Adjusted-Wald bands in more complex models.

Endogenizing the lag uncertainty reduces the coverage bias of the BB bands only in particular scenarios. However, in the majority of the scenarios, the BB bands based on the exogenous bootstrap are superior in that regard. The effect on the volume is ambiguous and depends on the data generating process; the same holds for the Bonferroni bands. Based on these findings, we do not promote the endogenous bootstrap.

Furthermore, the results of the trivariate VAR(4) model confirm two of the main empirical findings in [Lütkepohl et al. \(2015b\)](#). First, the Wald bands tend to exhibit a larger volume than the Bonferroni bands. Second, the volume-adjustment of the Wald bands can result in coverage rates markedly below the nominal level in low-degrees-of-freedom scenarios.

3.6 Empirical Application

We illustrate the BB joint confidence bands and the competing methods using the structural VAR model of [Kilian \(2009\)](#). The three-dimensional VAR model of [Kilian](#) includes

the following three variables:

- $\Delta prod_t$: the percentage change in global crude oil production
- $real_t$: a business cycle index of global real activity (expressed in logs)
- rpo_t : the real price of oil (expressed in logs)

The monthly data set from 1973-01 through 2007-12 is downloaded from the homepage of the American Economic Review¹⁰. We estimate the parameters of the reduced-form VAR(3) model (as suggested by the AIC) by the same methodology as in the Monte Carlo simulation. Following Kilian (2009), we use a recursive identification scheme where B_0 is the lower-triangular Cholesky decomposition of the reduced-form residual covariance matrix and the maximum propagation horizon is $H = 18$. The 90% joint confidence bands are constructed based on the bootstrap procedure of ? with $B = 2000$ replications.

	BB	Bon	Wald	A-Wald	Naïve
Θ_{11}	31.77	35.69	42.63	34.50	20.25
Θ_{21}	23.06	27.77	33.72	24.09	16.24
Θ_{31}	21.25	25.27	32.03	21.82	14.48
Θ_{12}	41.73	54.35	62.56	44.54	31.99
Θ_{22}	59.99	73.66	94.45	64.41	44.67
Θ_{32}	45.72	62.34	75.75	44.79	34.25
Θ_{13}	65.61	88.09	107.61	65.31	51.12
Θ_{23}	89.19	114.63	128.32	95.58	67.83
Θ_{33}	85.05	115.42	133.36	87.68	64.98

Table 3.3: Volume of joint confidence bands for $H = 18$.

Table 3.3 presents the volumes of the 90% joint confidence bands of all impulse responses with a maximum propagation horizon of $H = 18$. The Wald and the Bonferroni bands exhibit the largest volumes in all scenarios. The BB bands have the smallest volume (of the proper joint confidence bands) in seven out of nine scenarios. These findings are completely in line with the simulation-based findings about the volumes of the various joint confidence bands.

Figure 3.1 displays the estimated structural response of $\Delta prod_t$ to a one-standard-deviation shock in $\varepsilon_{t,2}$ over a maximum propagation horizon of $H = 18$ (that is, $\hat{\Theta}_{12,18}$)

¹⁰<https://www.aeaweb.org/articles?id=10.1257/aer.99.3.1053>

and the corresponding nominal 90% joint confidence bands¹¹. The figure illustrates the

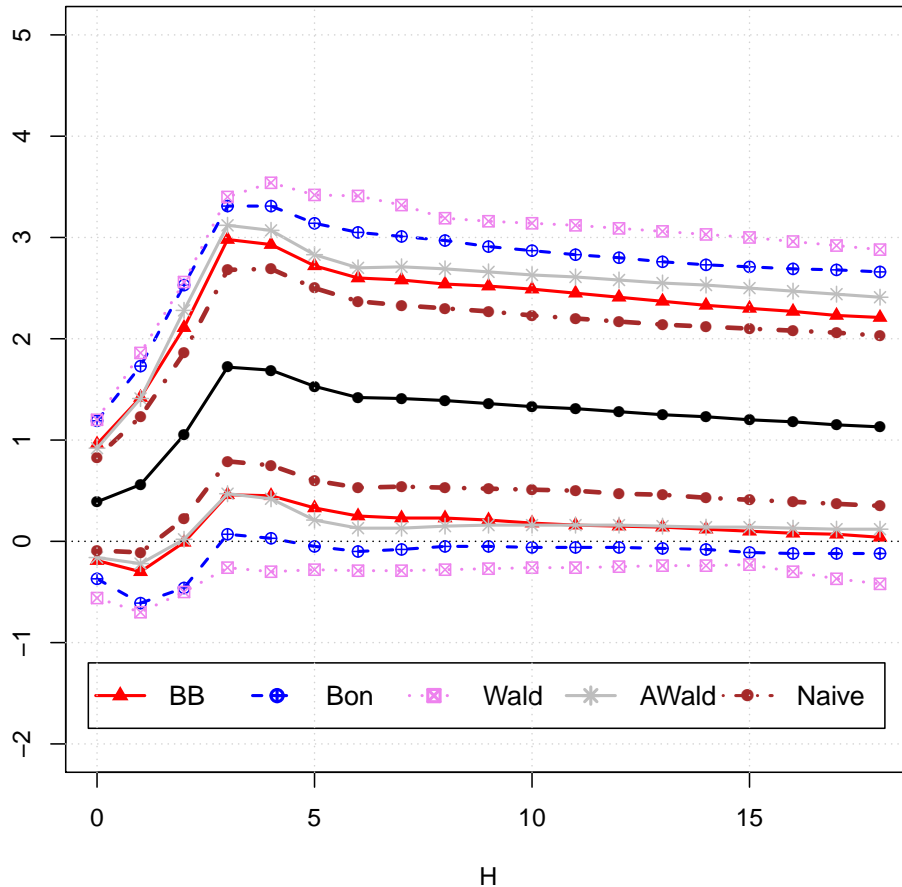


Figure 3.1: Estimated impulse response of $\Delta prod_t$ to a one-standard-deviation shock in $\varepsilon_{t,2}$ over a maximum propagation horizon of $H = 18$ (solid line with circles) and the corresponding nominal 90% joint confidence bands.

different shapes and volumes of the joint confidence bands. Inference based on the BB bands results in rejecting the null hypothesis of a zero response for propagation horizons $h = 4-18$ (as the marginal intervals do not cover zero). Inverting the other confidence bands results in different conclusions about the simultaneous test of the $H+1$ hypotheses. More specifically, inference based on the Bonferroni bands results in rejecting the null hypothesis of a zero response for only two propagation horizons ($h = 3, 4$), inference based the Wald bands results in accepting the null hypothesis of a zero response at all propagation horizons $h \in \{0, \dots, 18\}$, and inference based on the Adjusted-Wald bands

¹¹The figures of the remaining eight impulse responses are relegated to the Supplementary Material for the sake of clarity.

results in rejecting the null hypothesis of a zero response for propagation horizons $h = 3$ – 18 .

3.7 Conclusion

Impulse response analysis based on low-dimensional structural vector autoregressions is still a popular tool in applied work. It is standard in applications to equip the estimated impulse response function with confidence bands that indicate the underlying estimation uncertainty. The literature has proposed several methods to construct joint confidence bands designed to cover the entire true impulse response function with a prespecified probability. The so far existing methods suffer from deficiencies: They can exhibit empirical coverage rates substantially below the desired nominal level in certain scenarios or they can be excessively large in terms of the aggregate volume.

We have proposed new joint confidence bands for impulse response functions of structural vector autoregressions based on multiple testing methodology of [Romano and Wolf \(2010\)](#). Under weak regularity conditions, these balanced bootstrap (BB) bands have asymptotically the desired coverage probability and are also asymptotically balanced.

We have compared the finite-sample properties of the BB bands to those of existing bands by means of a Monte Carlo simulation. The BB bands (i) have smaller volume than the two conservative bands — the traditional Bonferroni bands and the Wald bands of [Lütkepohl et al. \(2015b\)](#) — and (ii) have similar volume compared to the Adjusted-Wald bands of [Lütkepohl et al. \(2015b\)](#). In terms of coverage probability, the performance of the BB bands is overall the best.

Nevertheless, the BB bands — just like the Adjusted-Wald bands — can suffer from undercoverage for small sample sizes. It stands to reason that this problem can be fixed, or at least mitigated, by a double-bootstrap approach. However, studying the finite-sample properties of such an approach via Monte Carlo simulations does not seem feasible given currently available computing power.

References

- Barsky, R. B. and Sims, E. R. (2011). News shocks and business cycles. *Journal of Monetary Economics*, 58(3):273–289.
- Benkwitz, A., Neumann, M. H., and Lütkepohl, H. (2000). Problems related to confidence intervals for impulse responses of autoregressive processes. *Econometric Reviews*, 19(1):69–103.
- Beran, R. (1987). Prepivoting to reduce level error of confidence sets. *Biometrika*, 74(3):457–468.
- Beran, R. (1988). Balanced simultaneous confidence sets. *Journal of the American Statistical Association*, 83(403):pp. 679–686.
- Bian, T. Y. and Gete, P. (2015). What drives housing dynamics in China? A sign restrictions VAR approach. *Journal of Macroeconomics*, 46:96–112.
- Cao, B. and Sun, Y. (2011). Asymptotic distributions of impulse response functions in short panel vector autoregressions. *Journal of Econometrics*, 163(2):127 – 143.
- Engsted, T. and Pedersen, T. Q. (2014). Bias-correction in vector autoregressive models: A simulation study. *Econometrics*, 2(1):45–71.
- Hinkley, D. and Wei, B.-C. (1984). Improvements of jackknife confidence limit methods. *Biometrika*, 71(2):331–339.
- Horowitz, J. L. (2001). The bootstrap. In *Handbook of Econometrics*, volume 5, chapter 52, pages 3159–3228. Elsevier, 1 edition.
- Jentsch, C. and Kreiss, J.-P. (2010). The multiple hybrid bootstrap: Resampling multivariate linear processes. *Journal of Multivariate Analysis*, 101(10):2320–2345.
- Jentsch, C. and Politis, D. N. (2015). Covariance matrix estimation and linear process bootstrap for multivariate time series of possibly increasing dimension. *Annals of Statistics*, 43(3):1117–1140.

- Jordà, O. (2009). Simultaneous confidence regions for impulse responses. *Review of Economics and Statistics*, 91(3):629–647.
- Kilian, L. (1998a). Accounting for lag order uncertainty in autoregressions: the endogenous lag order bootstrap algorithm. *Journal of Time Series Analysis*, 19(5):531–548.
- Kilian, L. (1998b). Small-sample confidence intervals for impulse response functions. *Review of Economics and Statistics*, 80(2):218–230.
- Kilian, L. (2001). Impulse response analysis in vector autoregressions with unknown lag order. *Journal of Forecasting*, 20(3):161–179.
- Kilian, L. (2009). Not all oil price shocks are alike: Disentangling demand and supply shocks in the crude oil market. *American Economic Review*, 99(3):1053–1069.
- Kurmann, A. and Otrok, C. (2013). News shocks and the slope of the term structure of interest rates. *American Economic Review*, 103(6):2612–2632.
- Lütkepohl, H. (1989). A note on the asymptotic distribution of impulse response functions of estimated var models with orthogonal residuals. *Journal of Econometrics*, 42(3):371–376.
- Lütkepohl, H. (1990). Asymptotic distributions of impulse response functions and forecast error variance decompositions of vector autoregressive models. *Review of Economics and Statistics*, 72(1):116–125.
- Lütkepohl, H. (2005). *New Introduction to Multiple Time Series Analysis*. Springer, Berlin.
- Lütkepohl, H., Staszewska-Bystrova, A., and Winker, P. (2015a). Comparison of methods for constructing joint confidence bands for impulse response functions. *International Journal of Forecasting*, 31(3):782–798.
- Lütkepohl, H., Staszewska-Bystrova, A., and Winker, P. (2015b). Confidence bands for impulse responses: Bonferroni vs. Wald. *Oxford Bulletin of Economics and Statistics*, 77(6):800–821.

- Meyer, M. and Kreiss, J.-P. (2015). On the vector autoregressive sieve bootstrap. *Journal of Time Series Analysis*, 36(3):377–397.
- Pope, A. L. (1990). Biases of estimators in multivariate non-Gaussian autoregressions. *Journal of Time Series Analysis*, 11(3):249–258.
- Romano, J. P. and Wolf, M. (2010). Balanced control of generalized error rates. *Annals of Statistics*, 38(1):pp. 598–633.
- Rothenberg, T. J. (1971). Identification in parametric models. *Econometrica*, 39(3):577–591.
- Rubio-Ramirez, J. F., Waggoner, D. F., and Zha, T. (2010). Structural vector autoregressions: Theory of identification and algorithms for inference. *Review of Economic Studies*, 77(2):665–696.
- Schwert, G. W. (1989). Tests for unit roots: A Monte Carlo investigation. *Journal of Business & Economic Statistics*, 7(2):147–159.
- Staszewska, A. (2007). Representing uncertainty about response paths: The use of heuristic optimisation methods. *Computational Statistics & Data Analysis*, 52(1):121–132.
- Staszewska-Bystrova, A. (2011). Bootstrap prediction bands for forecast paths from vector autoregressive models. *Journal of Forecasting*, 30(8):721–735.
- Stine, R. A. (1987). Estimating properties of autoregressive forecasts. *Journal of the American Statistical Association*, 82(400):1072–1078.
- Stock, J. H. and Watson, M. W. (2001). Vector autoregressions. *Journal of Economic Perspectives*, 15(4):101–115.

Appendix

3A Bias Correction

Let A denote the matrix of the true slope coefficients of the VAR(1) representation of a general VAR(p) process. Under some regularity conditions, [Pope \(1990\)](#) derives the following approximation for the finite-sample bias of the least squares (LS) estimator of A :

$$\text{Bias}(\hat{A}) = -\frac{b}{T} + \mathcal{O}(T^{-\frac{3}{2}}),$$

where

$$b := \Sigma_U \left[(I_{kp} - A')^{-1} + A' (I_{kp} - (A')^2)^{-1} + \sum_{i=1}^k \lambda_i (I_{kp} - \lambda_i A')^{-1} \right] \Sigma_Y^{-1}.$$

Here, I_{kp} denotes the $kp \times kp$ identity matrix, λ_i denotes the i -th eigenvalue of A , Σ_Y denotes the covariance matrix of $Y_t := (y'_t, y'_{t-1}, \dots, y'_{t-p+1})'$ and Σ_U denotes the covariance matrix of $U_t := (u_t, 0, \dots, 0)'$. Neglecting higher order terms and replacing true parameters by their LS estimators yields the following estimator for the finite-sample bias of \hat{A} :

$$\widehat{\text{Bias}}(\hat{A}) := -\frac{1}{T} \hat{\Sigma}_U \left[(I_{kp} - \hat{A}')^{-1} + \hat{A}' (I_{kp} - (\hat{A}')^2)^{-1} + \sum_{i=1}^k \hat{\lambda}_i (I_{kp} - \hat{\lambda}_i \hat{A}')^{-1} \right] \hat{\Sigma}_Y^{-1}.$$

Thus, the bias-corrected LS estimator is given by

$$\hat{A}^{\text{BC}} := \hat{A} - \widehat{\text{Bias}}(\hat{A}).$$

3B Stationary Correction

In order to prevent that stationary parameter estimates are pushed outside the stationary region by the bias correction, [Kilian \(1998b\)](#) proposes the following adjustment procedure:

- a) Calculate the modulus of the largest root of the (uncorrected) LS estimate \hat{A} and denote this quantity by $r(\hat{A})$. If $r(\hat{A}) \geq 1$, set $\hat{\hat{A}} := \hat{A}$. If $r(\hat{A}) < 1$, construct the bias-corrected estimator $\hat{A}^{\text{BC}} := \hat{A} - \widehat{\text{Bias}}(\hat{A})$.

- b) If $r(\hat{A}^{\text{BC}}) \geq 1$, obtain $\tilde{A}_i := \hat{A} - \delta_i \widehat{\text{Bias}}(\hat{A})$ with $\delta_1 = 1$ and $\delta_i = \delta_{i-1} - 0.01$.
- c) Repeat step b) until $r(\tilde{A}_i) < 1$.
- d) Set $\hat{\hat{A}} := \tilde{A}_i$.

3C Construction of BB bands

The following algorithm provides a step-by-step instruction for the construction of the BB bands with nominal confidence level of $(1-\alpha)$ for an arbitrary identification procedure.

1. Fit a $\text{VAR}(\hat{p})$ model to the the observed time series $\{y_1, \dots, y_T\}$, where \hat{p} denotes the estimated lag order.
2. Compute the impact matrix \hat{B}_0 according to the chosen approach of identification.
3. Estimate the structural impulse response function of interest with maximum propagation horizon H , that is,

$$\hat{\Theta}_{ij,H} := \Theta_{ij,H} \left(\hat{A}_1, \dots, \hat{A}_{\hat{p}}, \hat{B}_0 \right) ,$$

where the $\hat{A}_1, \dots, \hat{A}_{\hat{p}}$ are the estimated reduced-form coefficients.

4. Generate a bootstrap sample $\left\{ \sqrt{T} \left| \hat{\Theta}_{ij,H,b}^* - \hat{\Theta}_{ij,H} \right| \right\}_{b=1}^B$. The number B of bootstrap replications should be at least 2000, if feasible.
5. Compute the following $(H+1)$ empirical distribution functions

$$\hat{H}_h^*(t) := \frac{1}{B} \sum_{b=1}^B \mathbb{1}_{\left\{ \sqrt{T} \left| \hat{\Theta}_{ij,h,b}^* - \hat{\Theta}_{ij,h} \right| \leq t \right\}} \quad \text{for } h = 0, \dots, H .$$

Statistical software packages usually provide a built-in function for computing the empirical distribution function; for example, the function `ecdf` in the software package R.

6. Compute the following bootstrap sample $\left\{ \max_{h \in \tilde{S}} \left\{ \hat{H}_h^* \left(\sqrt{T} \left| \hat{\Theta}_{ij,h,b}^* - \hat{\Theta}_{ij,h} \right| \right) \right\} \right\}_{b=1}^B$ and the corresponding $(1-\alpha)$ quantile. Statistical software packages usually provide a built-in function for computing empirical quantiles; for example, the function `quantile` in the software package R.

7. Construct the BB confidence bands for $\Theta_{ij,H}$ with nominal confidence level $(1 - \alpha)$ by computing $(H + 1)$ marginal intervals

$$\left[\hat{\Theta}_{ij,h} \pm \frac{1}{\sqrt{T}} \hat{H}_h^{*,-1} \left(\hat{L}^{-1}(1 - \alpha) \right) \right] \quad \text{for } h = 0, \dots, H ,$$

where $\hat{H}_h^{*,-1}(q) := \inf \left\{ t : \hat{H}_h^*(t) \geq q \right\}$ and $\hat{L}^{-1}(1 - \alpha)$ denotes the $(1 - \alpha)$ quantile from step 6.

Remark 3.7.1 The methodology of [Romano and Wolf \(2010\)](#) allows one to construct joint confidence bands that do not cover all but ‘only’ at least $H - k + 2$, $k \geq 2$, of the elements of $\Theta_{ij,H}$ with nominal confidence level $1 - \alpha$. Step 6. in the previous algorithm has to be modified to construct such bands. More specifically, one has to compute the empirical $(1 - \alpha)$ quantile of

$$\left\{ k\text{-max}_{h \in \tilde{S}} \left\{ \hat{H}_h \left(\sqrt{T} \left| \hat{\Theta}_{ij,h,b}^* - \hat{\Theta}_{ij,h} \right| \right) \right\} \right\}_{b=1}^B ,$$

where $k\text{-max}$ is the function that returns the k -th largest element of a vector. ■

3D DGP-1: Empirical Coverages

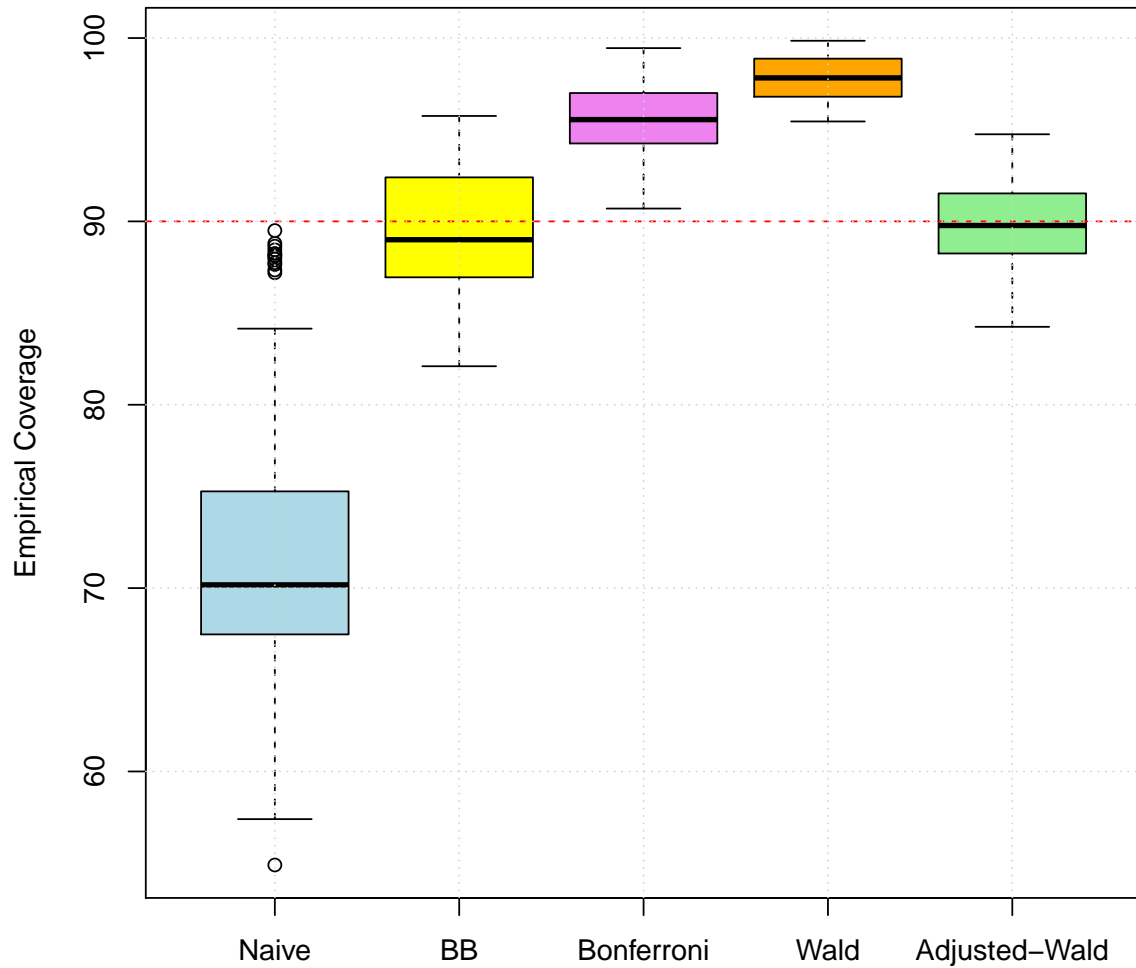


Figure 3A.1: DGP-1: Boxplots of the empirical coverages across all variants of DGP-1, all impulse responses and all maximum propagation horizons (56 parameter constellations in total) of nominal 90% joint confidence bands for $T = 100$.

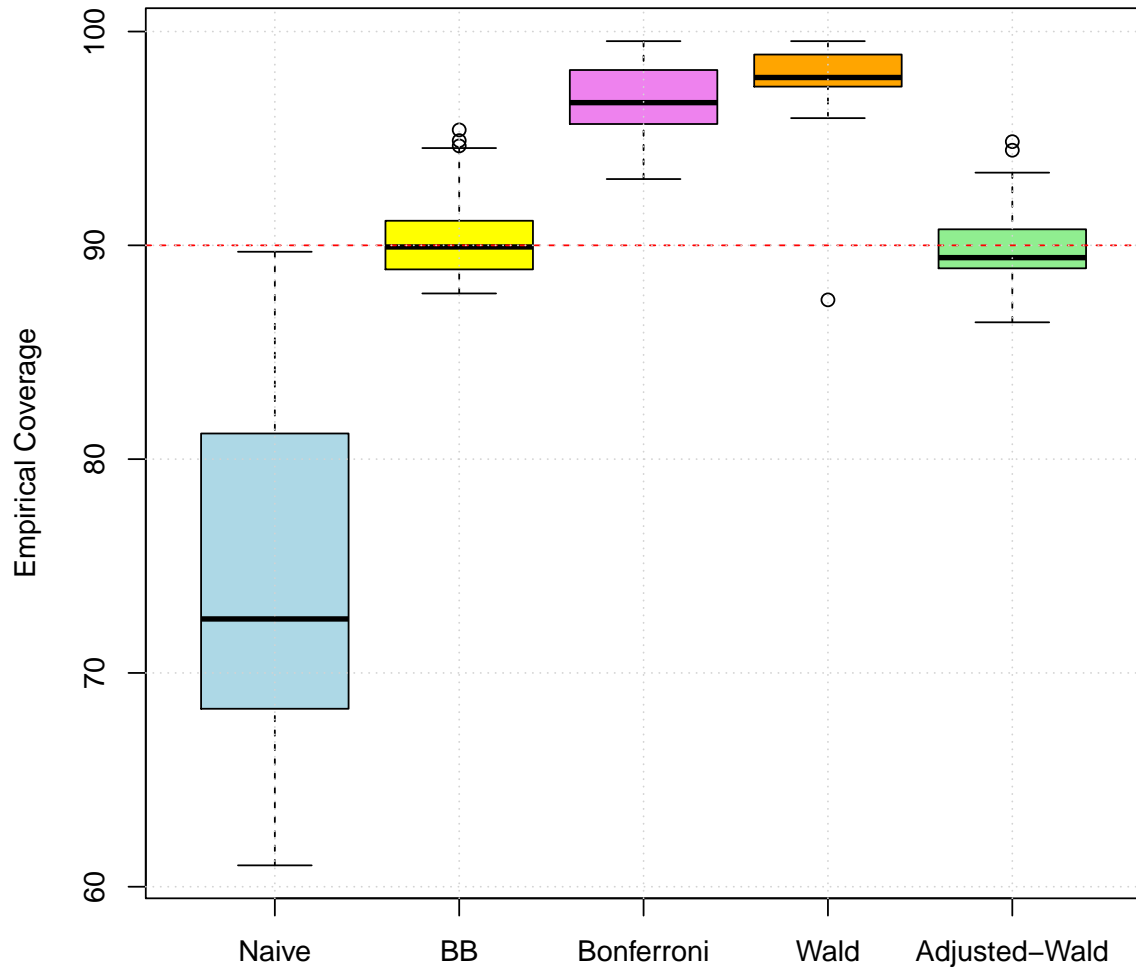


Figure 3A.2: DGP-1: Boxplots of the empirical coverages across all variants of DGP-1, all impulse responses and all maximum propagation horizons (56 parameter constellations in total) of nominal 90% joint confidence bands for $T = 400$.

3E DGP-1: Volumes

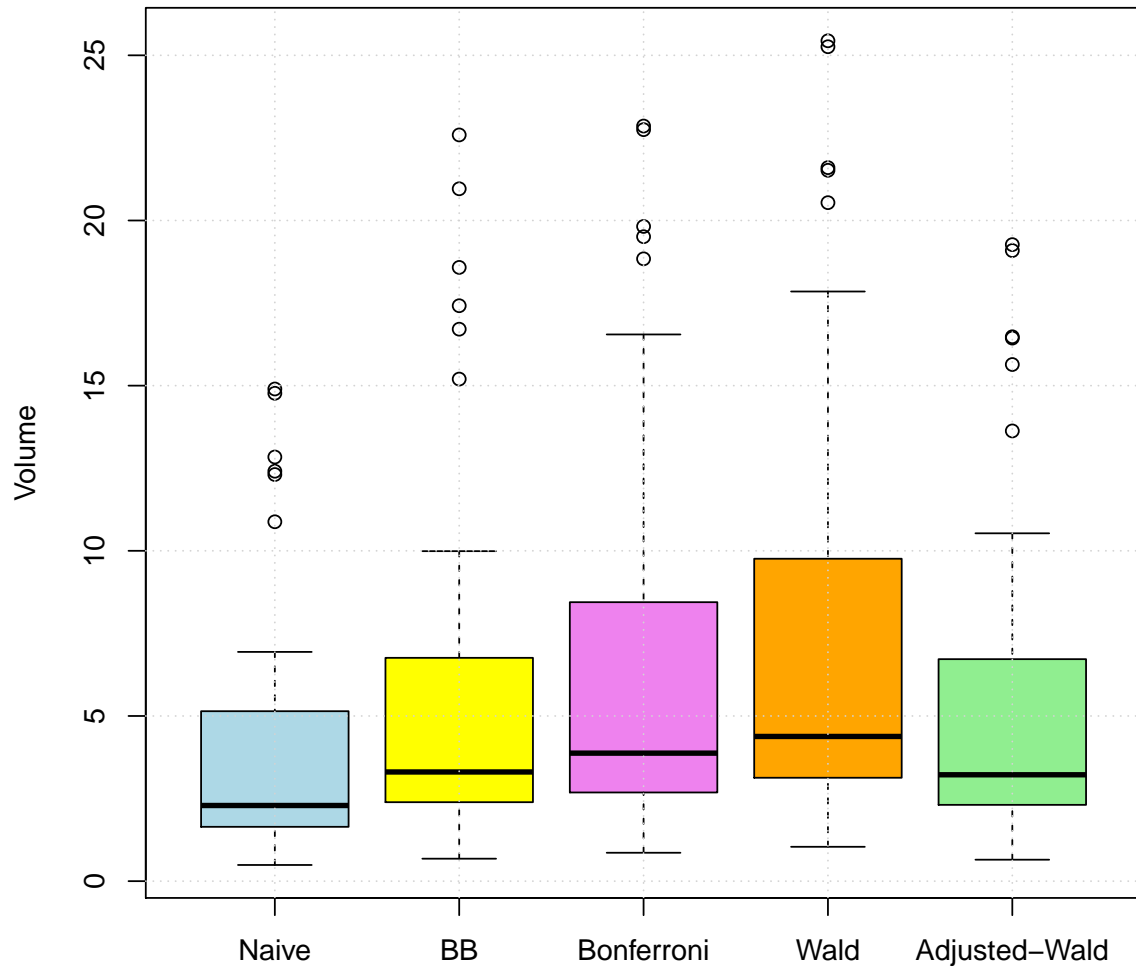


Figure 3A.3: DGP-1: Boxplots of the volumes across all variants of DGP-1, all impulse responses and all maximum propagation horizons (56 parameter constellations in total) of nominal 90% joint confidence bands for $T = 100$.

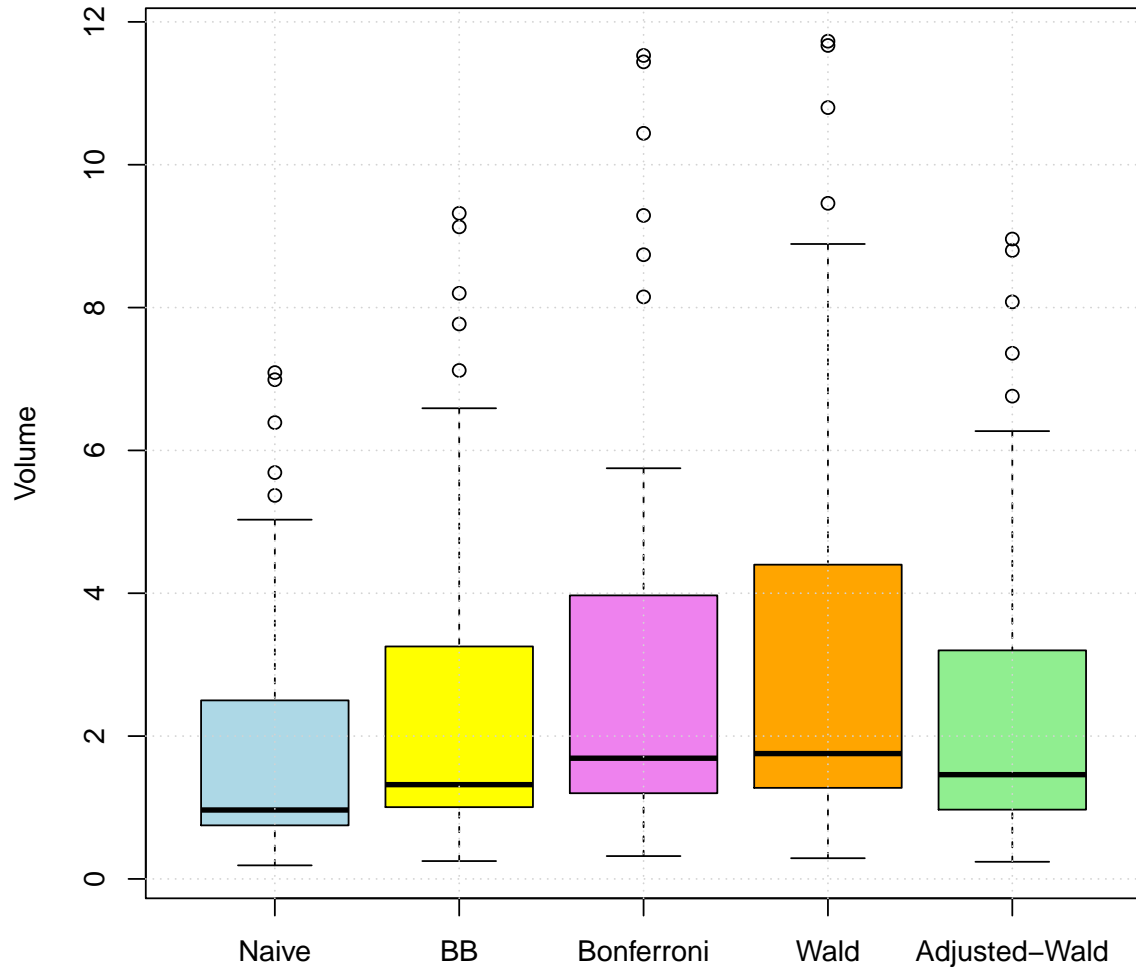


Figure 3A.4: DGP-1: Boxplots of the volumes across all variants of DGP-1, all impulse responses and all maximum propagation horizons (56 parameter constellations in total) of nominal 90% joint confidence bands for $T = 400$.

3F DGP-2: Empirical Coverages

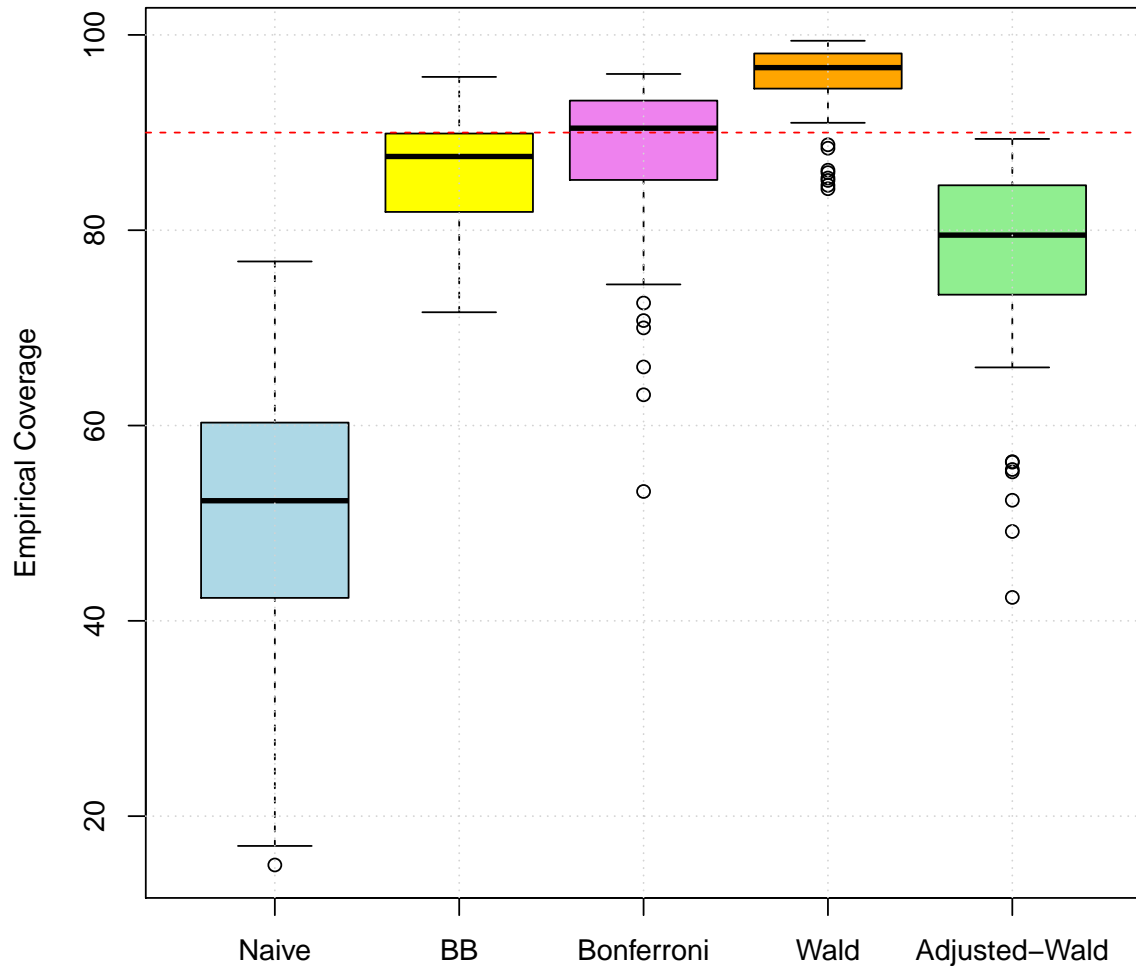


Figure 3A.5: DGP-2: Boxplots of the empirical coverages across all impulse responses and all maximum propagation horizons (63 parameter constellations in total) of nominal 90% joint confidence bands for $T = 100$.

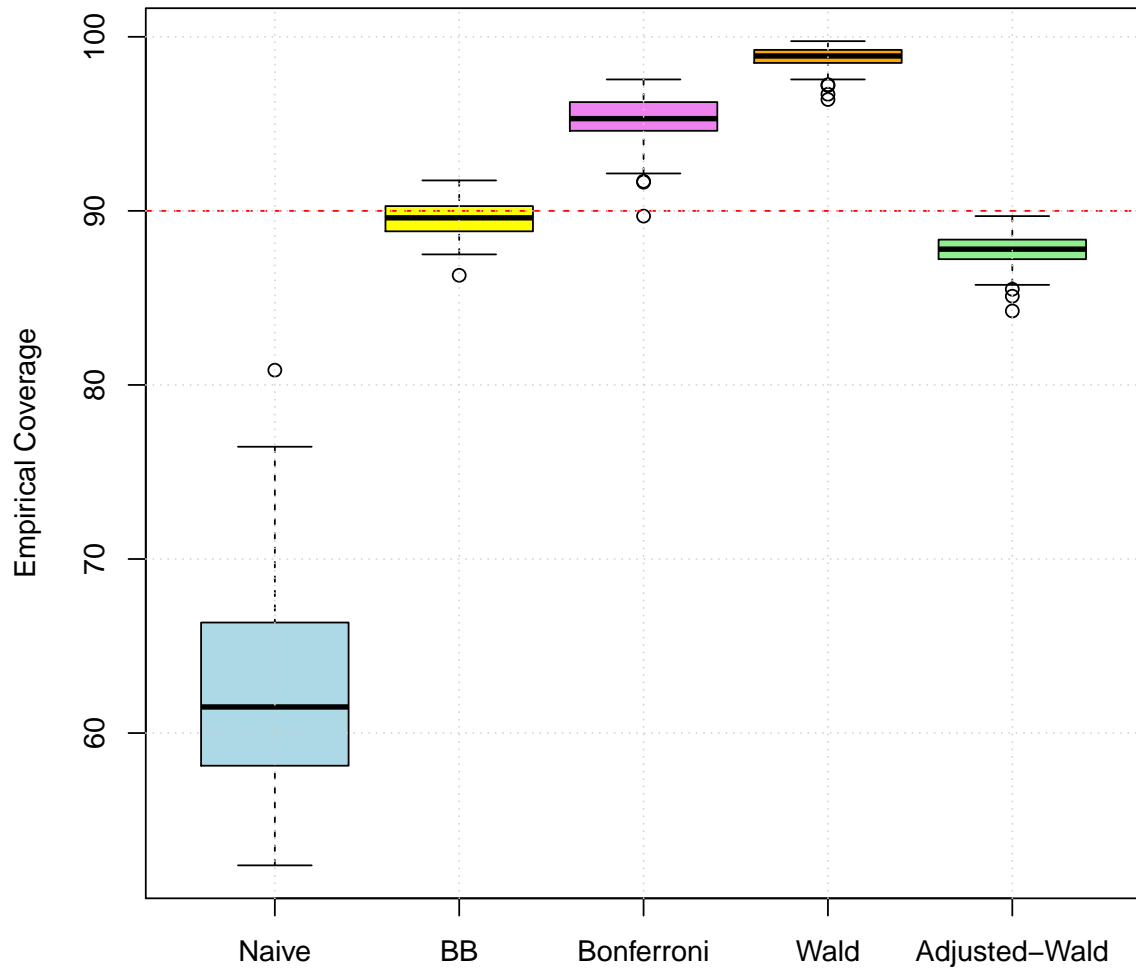


Figure 3A.6: DGP-2: Boxplots of the empirical coverages across all impulse responses and all maximum propagation horizons (63 parameter constellations in total) of nominal 90% joint confidence bands for $T = 400$.

3G DGP-2: Volumes

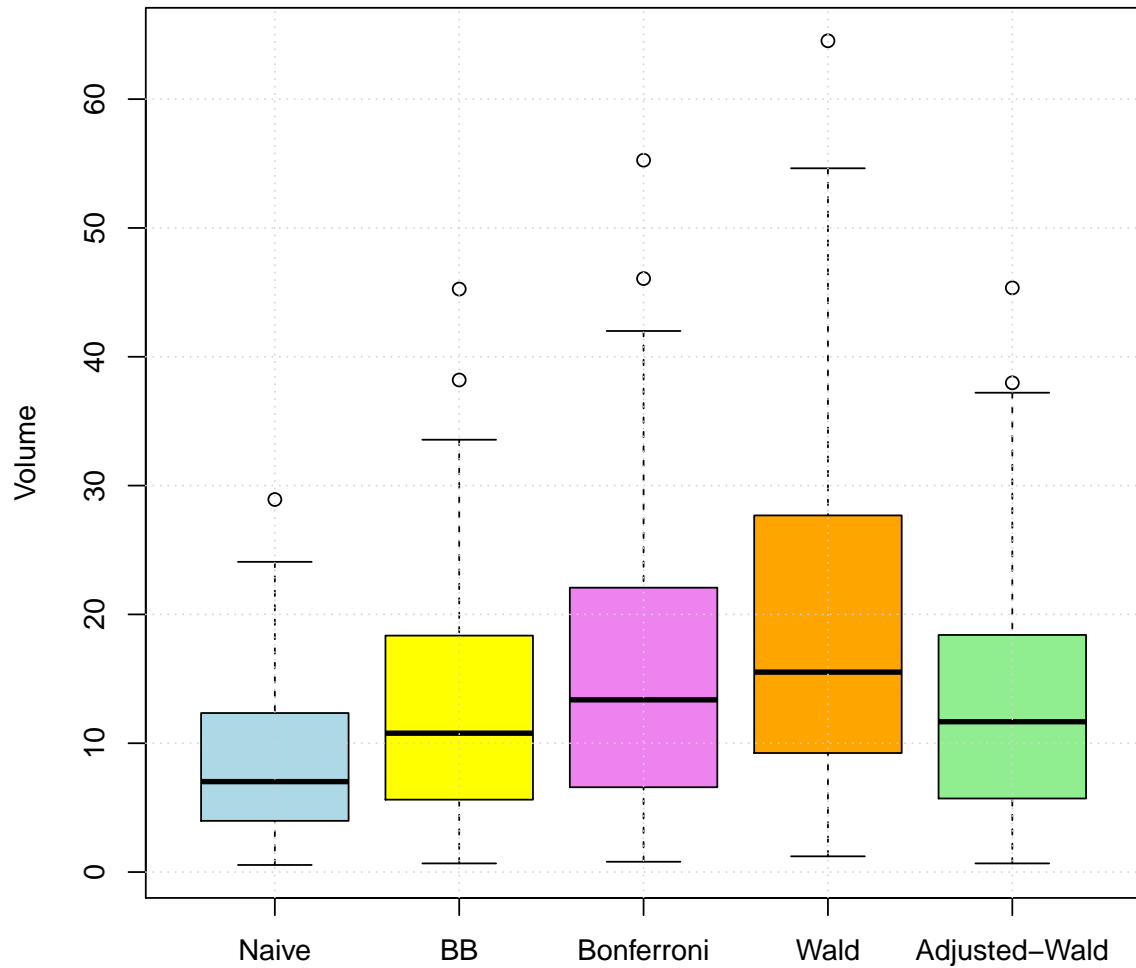


Figure 3A.7: DGP-2: Boxplots of the volumes across all impulse responses and all maximum propagation horizons (63 parameter constellations in total) of nominal 90% joint confidence bands for $T = 100$.

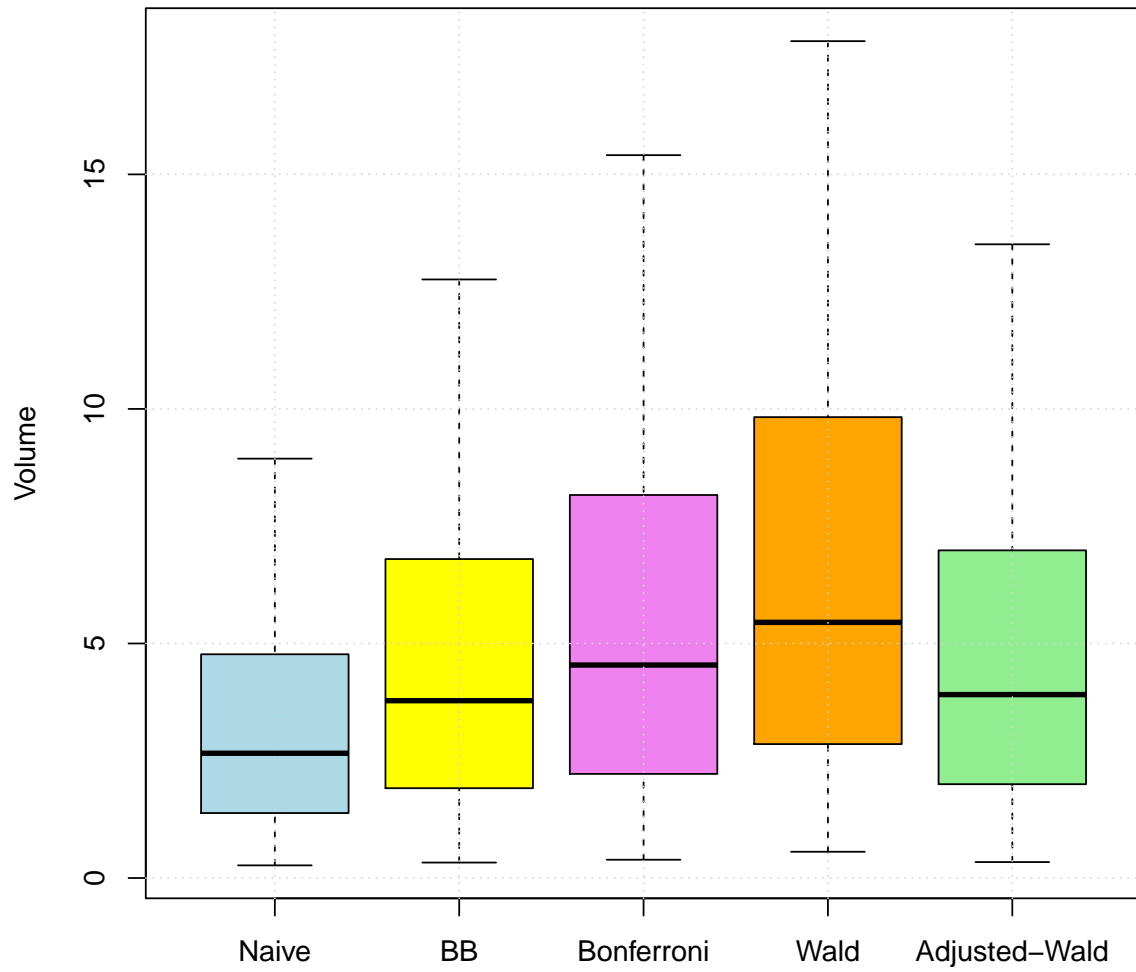


Figure 3A.8: DGP-2: Boxplots of the volumes across all impulse responses and all maximum propagation horizons (63 parameter constellations in total) of nominal 90% joint confidence bands for $T = 400$.

3H Figures

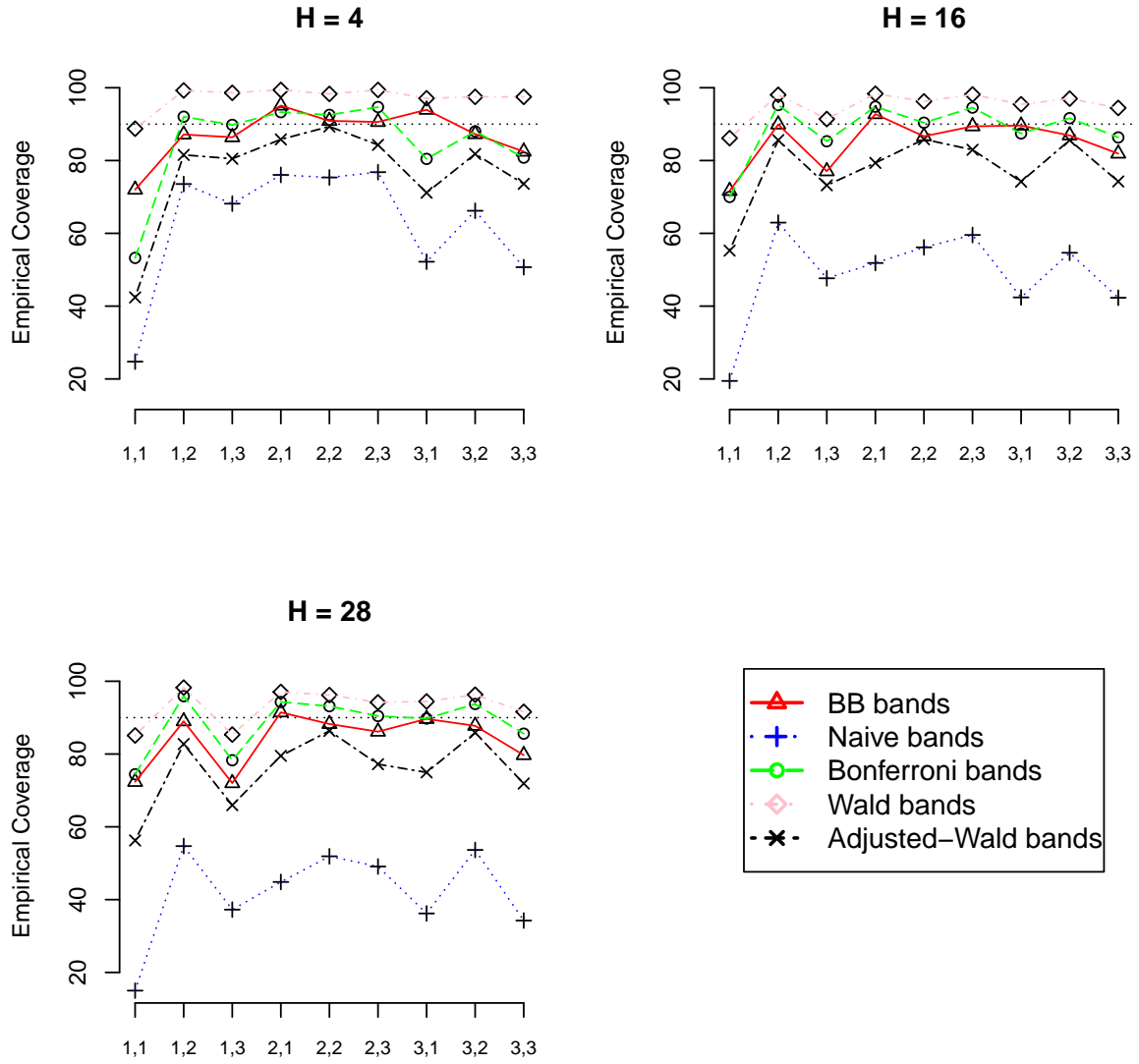


Figure 3A.9: DGP-2: Empirical coverage rates of nominal 90% joint confidence bands for $\Theta_{i,j}$, where $i, j \in \{1, 2, 3\}$. The sample size is $T = 100$ and the maximum propagation horizon is $H \in \{4, 16, 28\}$.

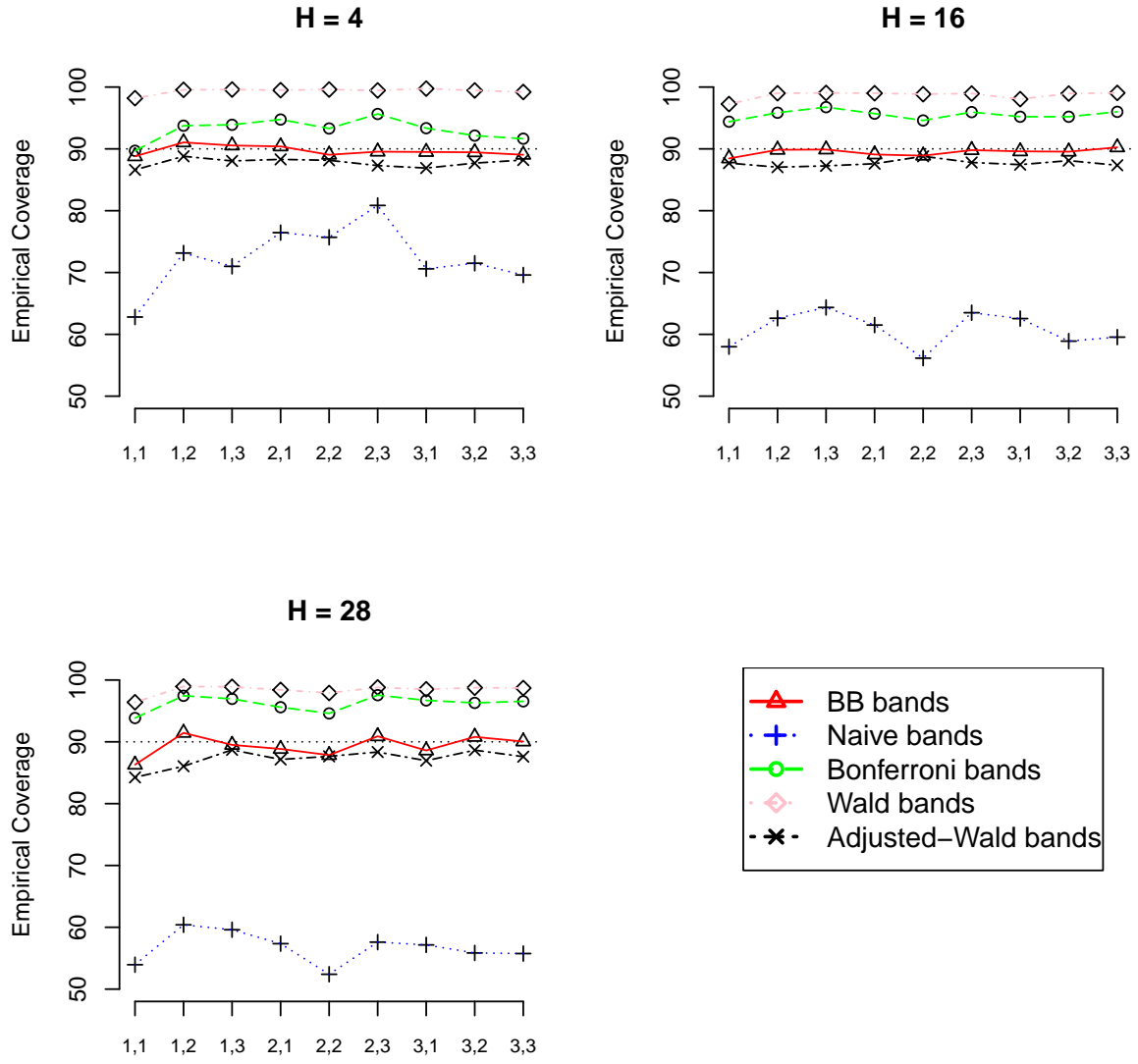


Figure 3A.10: DGP-2: Empirical coverage rates of nominal 90% joint confidence bands for $\Theta_{i,j}$, where $i, j \in \{1, 2, 3\}$. The sample size is $T = 400$ and the maximum propagation horizon is $H \in \{4, 16, 28\}$.

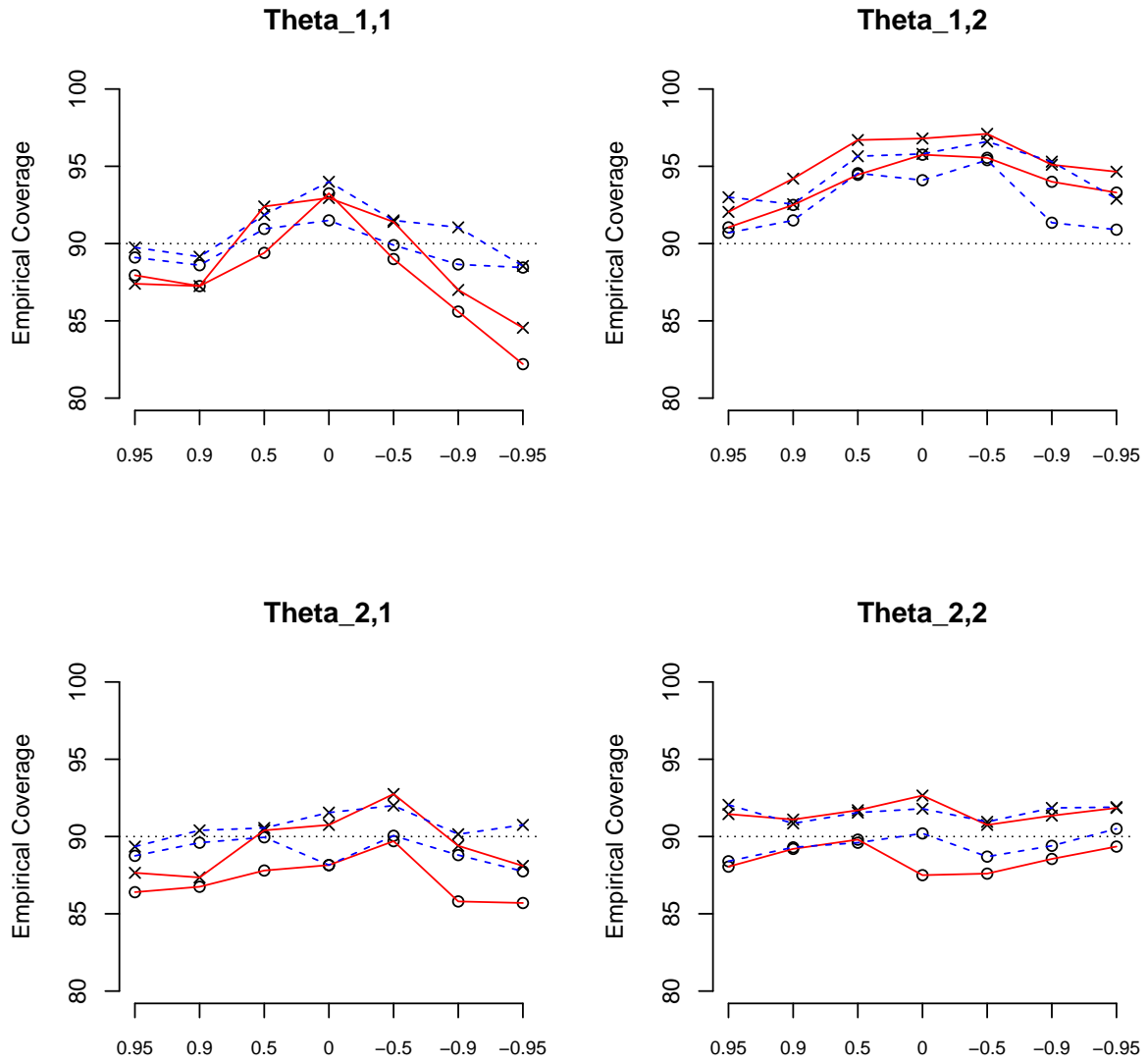


Figure 3A.11: DGP-1: Empirical coverages of the BB bands with a maximum propagation horizon of $H = 10$ with $T = 100$ and exogenous bootstrap (solid line, circle), with $T = 400$ and exogenous bootstrap (dashed line, circle), with $T = 100$ and endogenous bootstrap (solid line, cross) and with $T = 400$ and endogenous bootstrap (dashed line, cross).

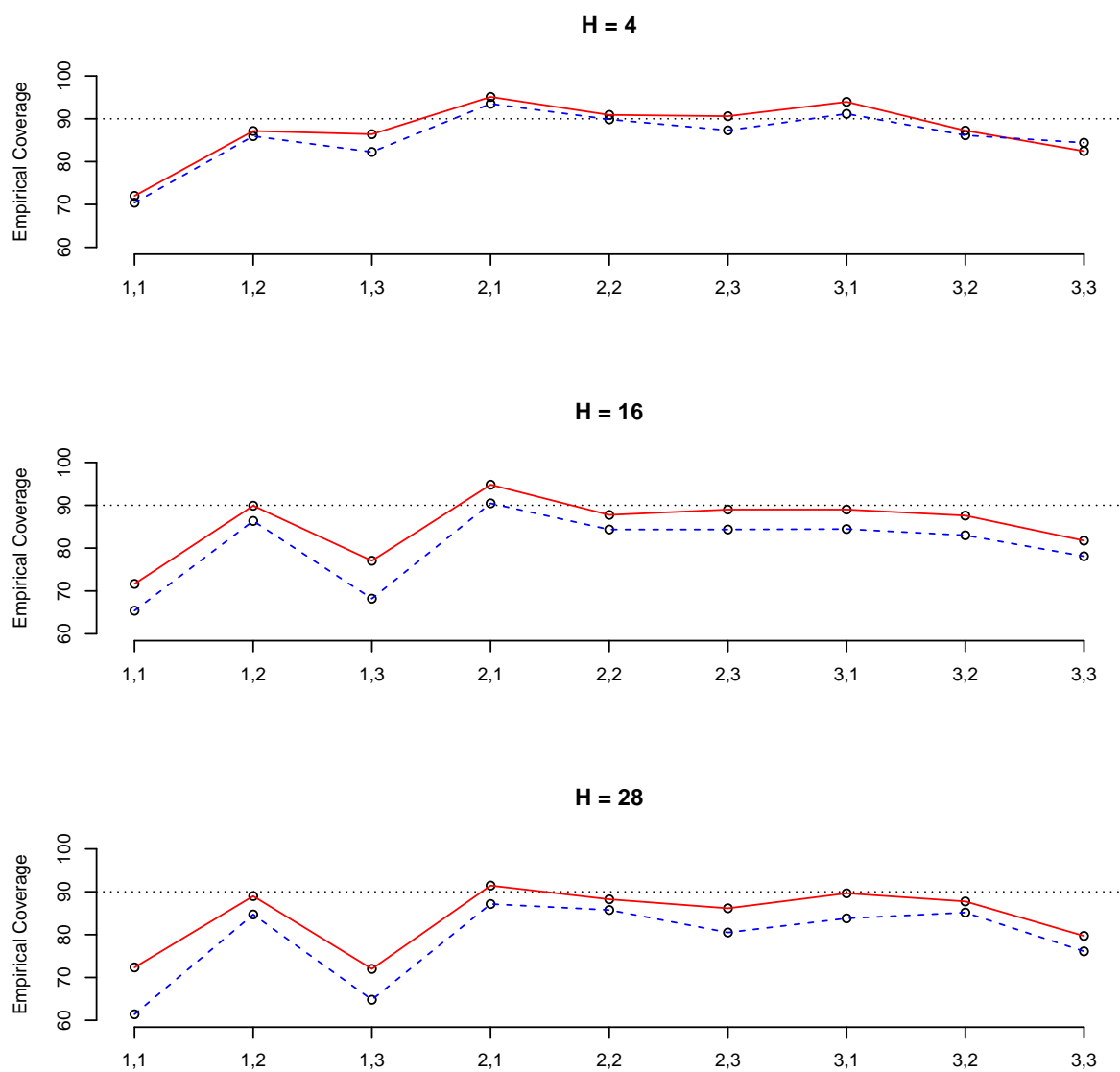


Figure 3A.12: DGP-2: Empirical coverages of the BB bands with the exogenous bootstrap (solid line) and the endogenous bootstrap (dashed line) with $T = 100$.

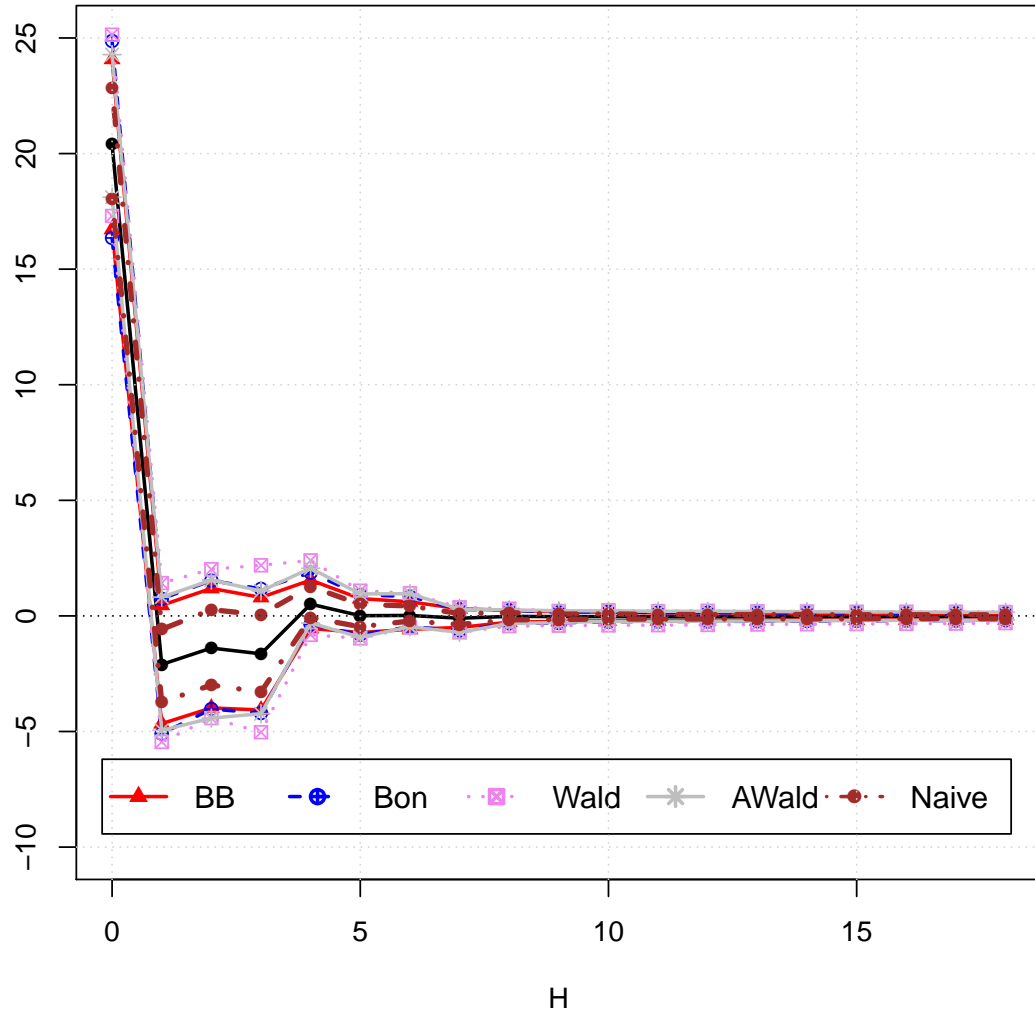


Figure 3A.13: Estimated impulse response of $\Delta prod_t$ to a one-standard-deviation shock in $\varepsilon_{t,1}$ over a maximum propagation horizon of $H = 18$ (solid line with circles) and the corresponding nominal 90% joint confidence bands.

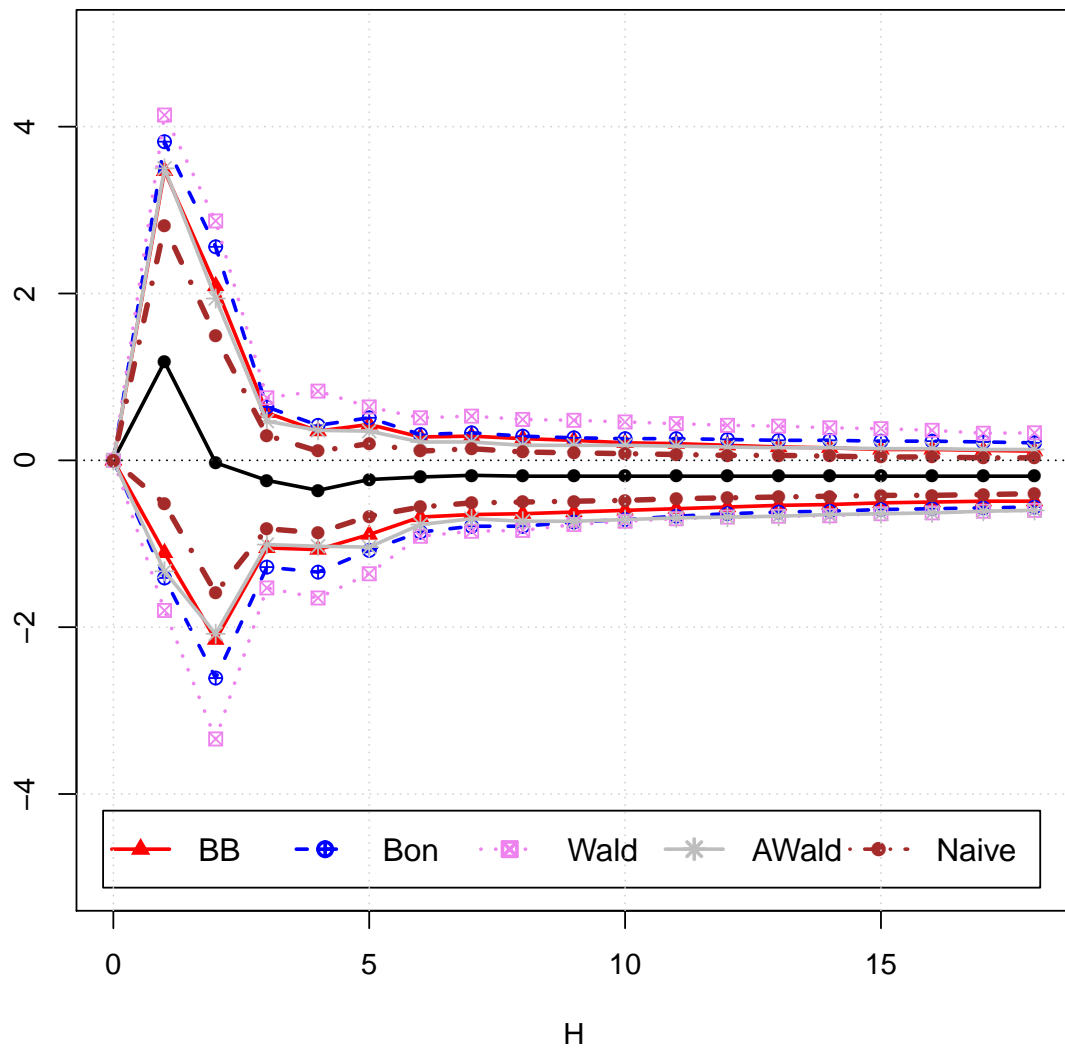


Figure 3A.14: Estimated impulse response of $real_t$ to a one-standard-deviation shock in $\varepsilon_{t,1}$ over a maximum propagation horizon of $H = 18$ (solid line with circles) and the corresponding nominal 90% joint confidence bands.

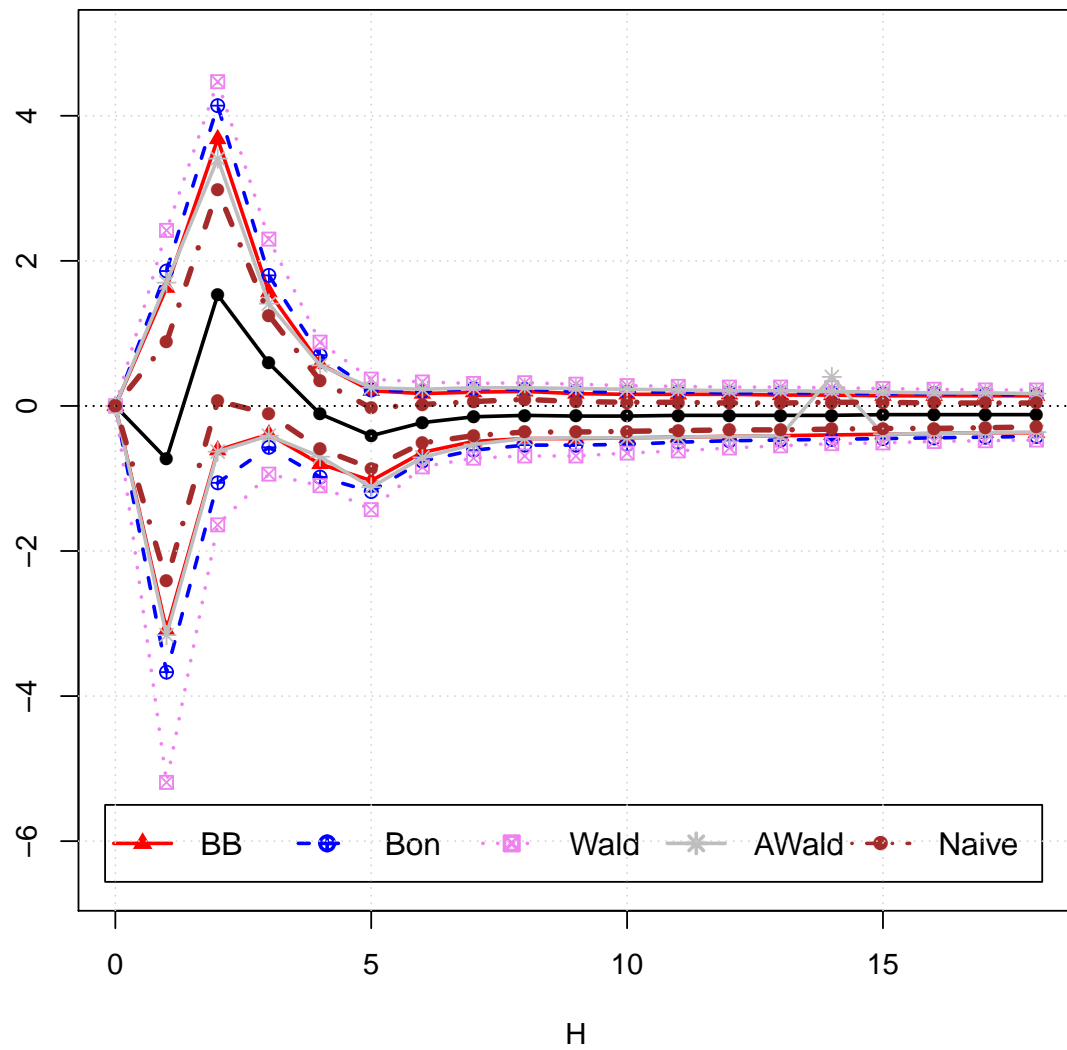


Figure 3A.15: Estimated impulse response of rpo_t to a one-standard-deviation shock in $\varepsilon_{t,1}$ over a maximum propagation horizon of $H = 18$ (solid line with circles) and the corresponding nominal 90% joint confidence bands.

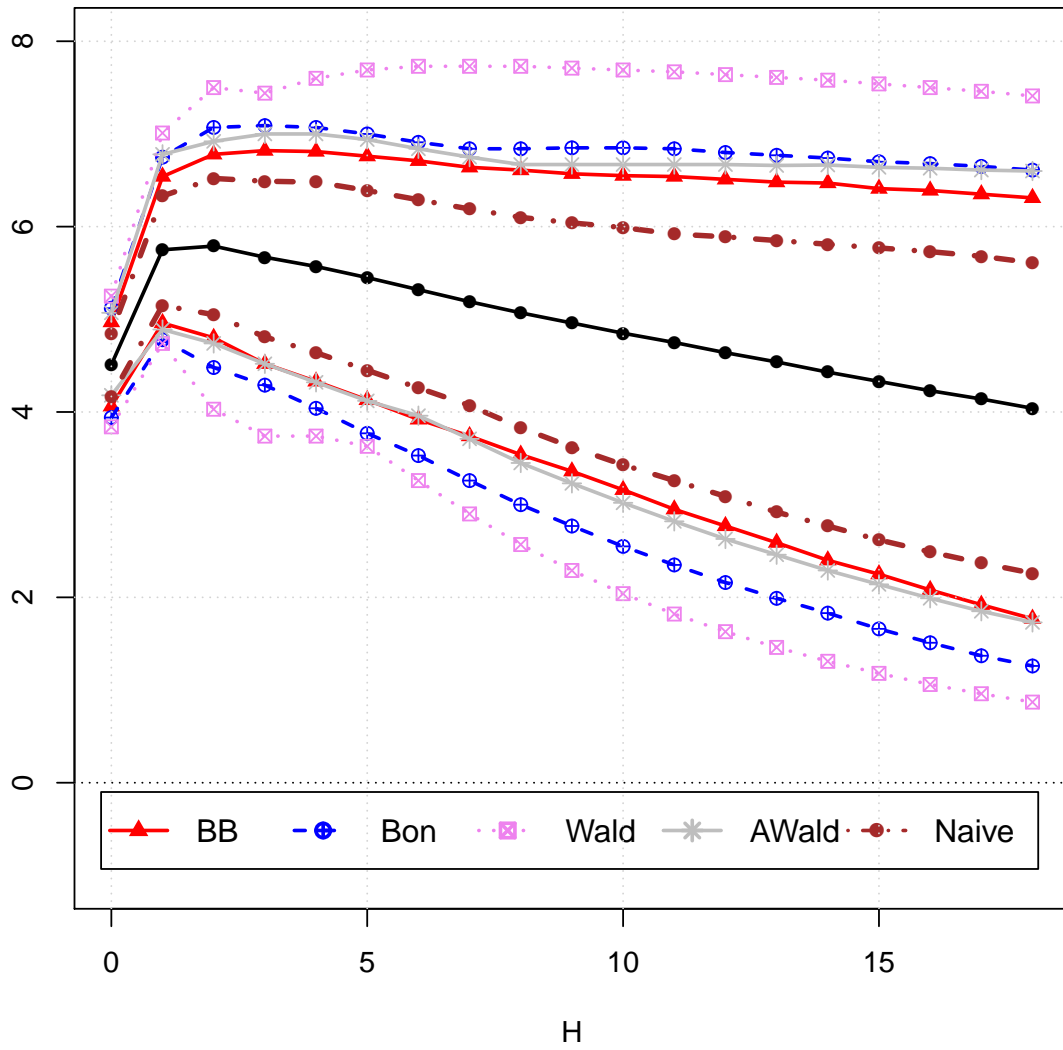


Figure 3A.16: Estimated impulse response of $real_t$ to a one-standard-deviation shock in $\varepsilon_{t,2}$ over a maximum propagation horizon of $H = 18$ (solid line with circles) and the corresponding nominal 90% joint confidence bands.

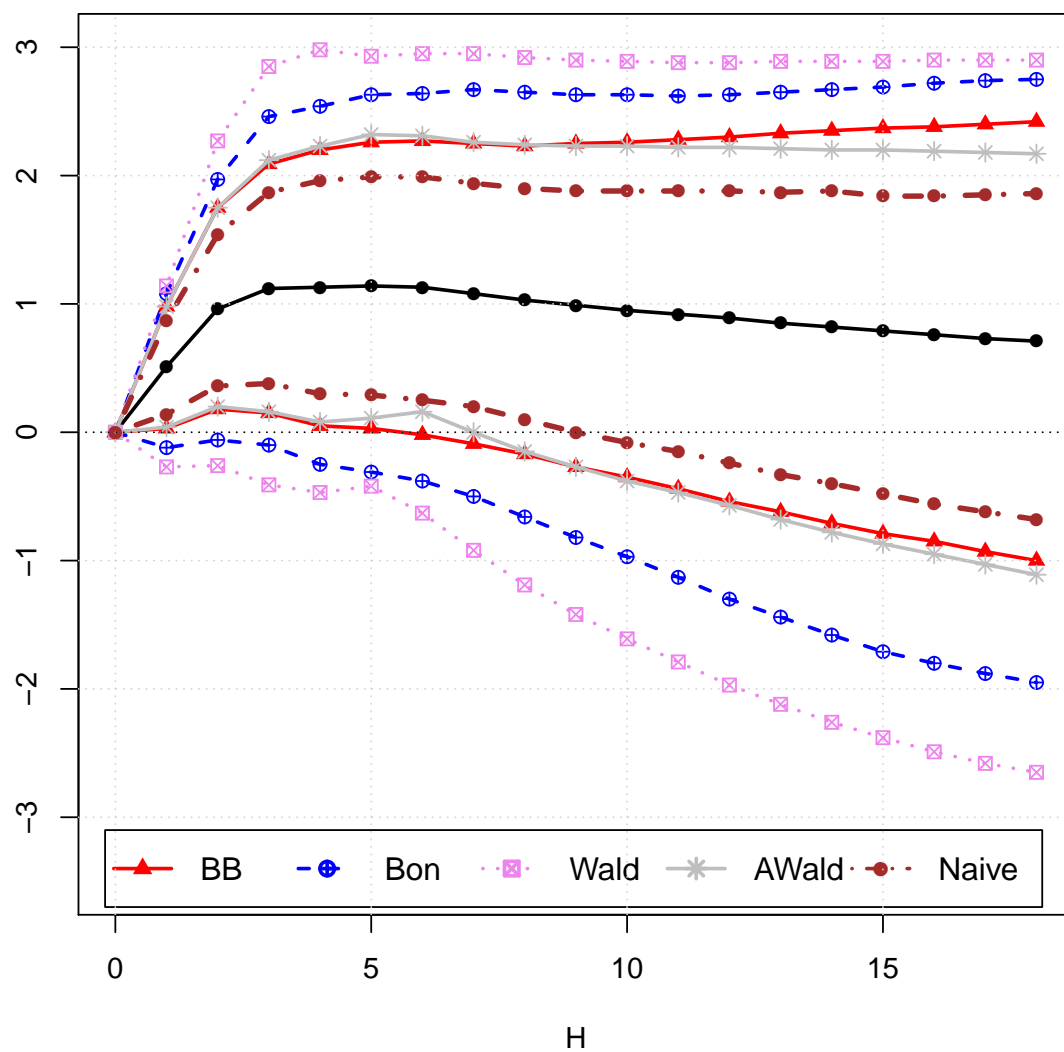


Figure 3A.17: Estimated impulse response of rpo_t to a one-standard-deviation shock in $\varepsilon_{t,2}$ over a maximum propagation horizon of $H = 18$ (solid line with circles) and the corresponding nominal 90% joint confidence bands.

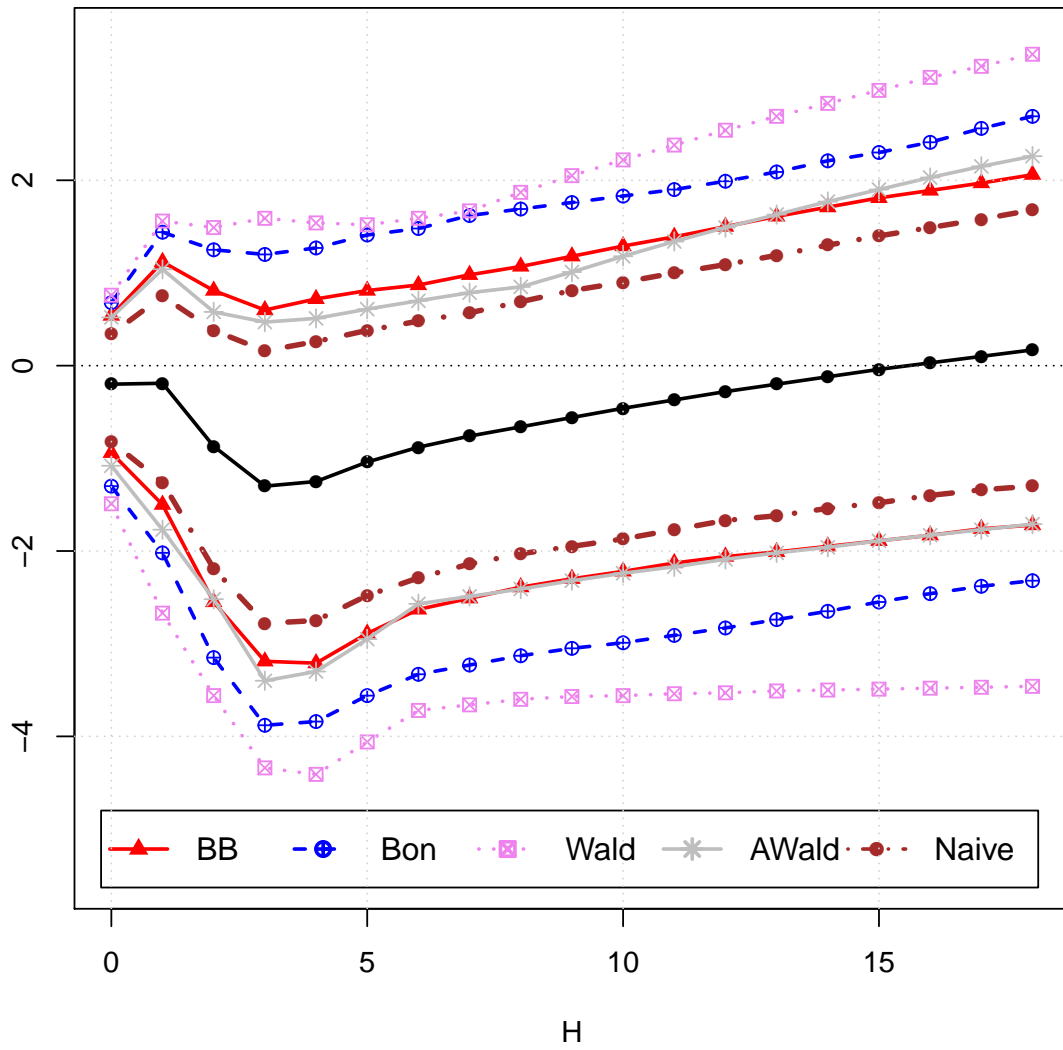


Figure 3A.18: Estimated impulse response of $\Delta prod_t$ to a one-standard-deviation shock in $\varepsilon_{t,3}$ over a maximum propagation horizon of $H = 18$ (solid line with circles) and the corresponding nominal 90% joint confidence bands.

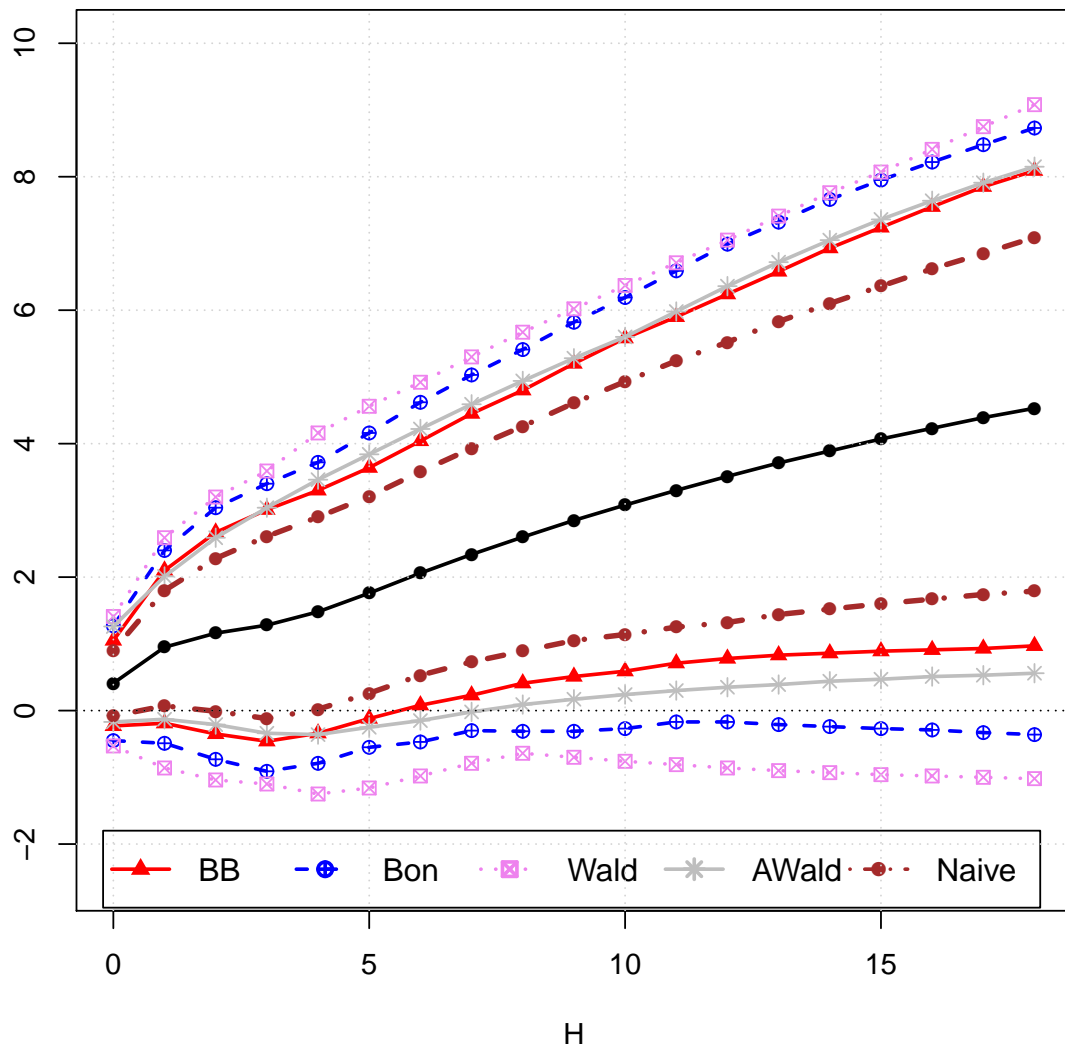


Figure 3A.19: Estimated impulse response of $real_t$ to a one-standard-deviation shock in $\varepsilon_{t,3}$ over a maximum propagation horizon of $H = 18$ (solid line with circles) and the corresponding nominal 90% joint confidence bands.

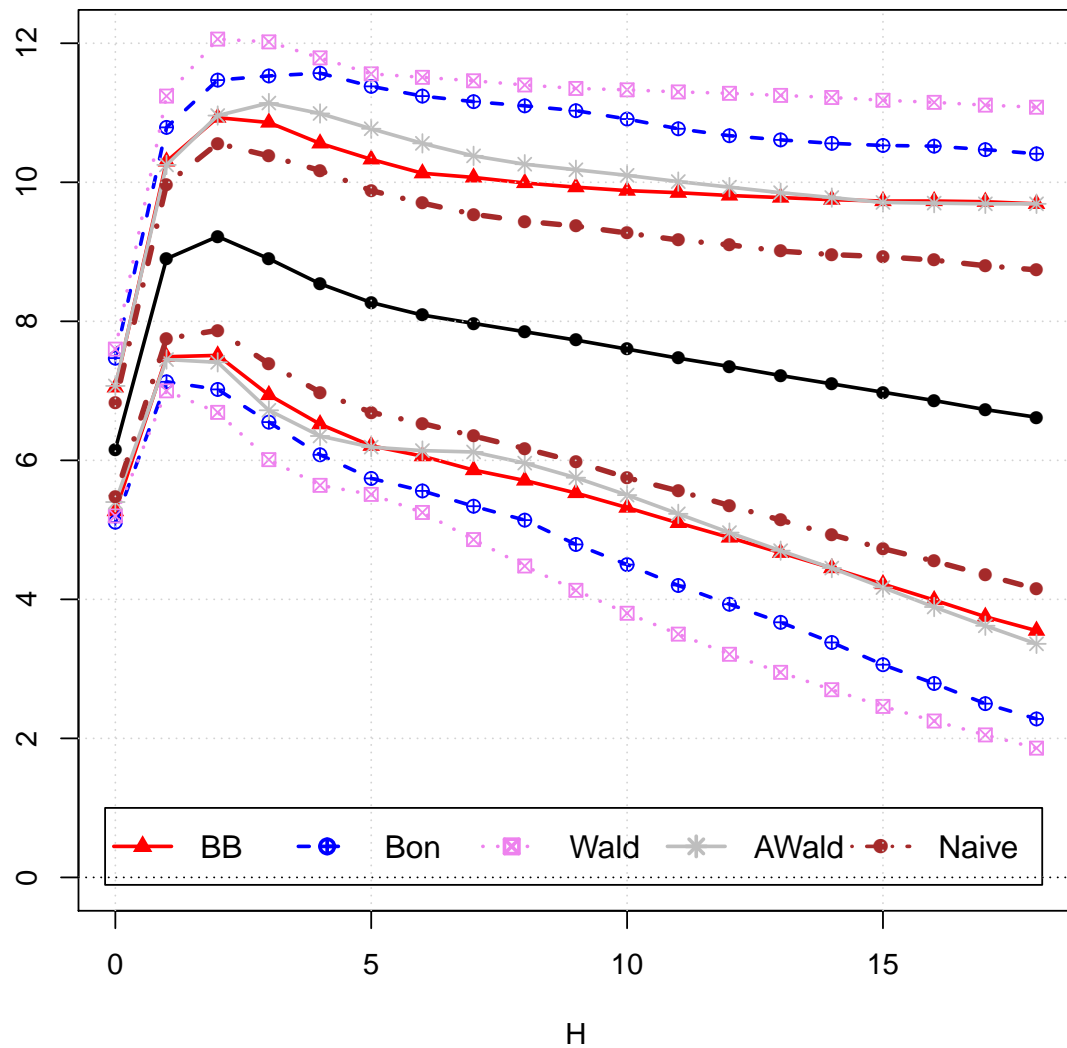


Figure 3A.20: Estimated impulse response of rpo_t to a one-standard-deviation shock in $\varepsilon_{t,3}$ over a maximum propagation horizon of $H = 18$ (solid line with circles) and the corresponding nominal 90% joint confidence bands.

3I Results for DGP-1 with Exogenous Bootstrap

DGP1	Method	$\Theta_{1,1}$		$\Theta_{1,2}$		$\Theta_{2,1}$		$\Theta_{2,2}$	
		EC	V	EC	V	EC	V	EC	V
$\rho = 0.95$	Naïve	73.45	6.52	89.50	3.55	69.05	6.20	69.50	3.78
	BB	87.95	8.56	91.05	4.16	86.40	8.44	88.05	5.17
	Bonferroni	94.20	10.12	98.70	5.88	93.05	9.76	94.50	6.19
	Wald	96.40	11.84	99.85	7.61	96.00	11.48	98.15	7.94
	Adj-Wald	88.00	8.27	90.85	4.00	85.85	8.03	90.20	5.38
$\rho = 0.90$	Naïve	75.55	5.85	87.95	3.10	69.90	5.88	68.35	3.52
	BB	87.25	7.62	92.50	3.67	86.75	7.84	89.20	4.79
	Bonferroni	93.60	8.82	98.95	5.11	92.80	8.93	94.45	5.71
	Wald	96.70	10.10	99.65	6.47	97.05	10.30	97.85	7.18
	Adj-Wald	89.60	7.43	92.35	3.56	88.10	7.59	89.85	5.01
$\rho = 0.50$	Naïve	70.25	2.04	87.20	1.15	69.45	3.19	70.70	2.13
	BB	89.40	2.98	94.45	1.48	87.80	4.63	89.80	3.02
	Bonferroni	95.35	3.35	98.25	1.96	94.60	5.08	94.30	3.50
	Wald	98.00	3.92	99.35	2.34	96.80	5.89	97.90	4.12
	Adj-Wald	89.75	2.91	92.75	1.41	88.35	4.35	91.45	3.01
$\rho = 0.00$	Naïve	67.05	1.02	87.40	0.58	68.80	1.97	72.50	1.64
	BB	93.25	1.50	95.75	0.77	88.15	2.92	87.05	2.38
	Bonferroni	96.20	1.70	98.50	1.00	94.80	3.23	94.65	2.70
	Wald	98.60	2.03	99.65	1.12	97.35	3.82	98.15	3.16
	Adj-Wald	91.70	1.52	94.45	0.73	89.00	2.79	90.95	2.29
$\rho = -0.50$	Naïve	72.30	1.65	88.80	0.49	61.75	1.70	72.10	1.55
	BB	89.00	2.40	95.55	0.68	89.70	2.50	87.60	2.23
	Bonferroni	95.20	2.65	98.00	0.86	94.85	2.76	95.10	2.51
	Wald	98.35	3.10	99.55	1.04	97.70	3.24	97.55	2.88
	Adj-Wald	91.15	2.27	94.75	0.65	87.75	2.40	90.95	2.11
$\rho = -0.90$	Naïve	73.70	5.12	87.75	1.29	60.10	2.39	62.30	1.62
	BB	85.60	6.60	94.00	1.54	85.80	3.36	88.55	2.35
	Bonferroni	94.40	7.68	98.15	2.18	90.70	3.69	90.95	2.64
	Wald	96.90	8.90	99.60	2.66	96.35	4.31	97.75	3.09
	Adj-Wald	88.40	6.60	90.90	1.50	86.25	3.33	88.75	2.32
$\rho = -0.95$	Naïve	71.85	5.15	88.65	1.53	58.15	2.37	63.90	1.65
	BB	82.20	6.55	93.30	1.76	85.70	3.34	89.35	2.36
	Bonferroni	94.05	8.07	98.30	2.56	91.80	3.73	93.60	2.67
	Wald	96.70	9.42	99.70	3.02	95.45	4.37	96.90	3.10
	Adj-Wald	85.50	6.79	91.80	1.69	84.25	3.35	89.70	2.35

Table 3.4: Empirical coverage probabilities and average volumes of nominal 90% joint confidence bands with $T = 100$, $H = 10$, normal errors, and AIC lag selection.

DGP1	Method	$\Theta_{1,1}$		$\Theta_{1,2}$		$\Theta_{2,1}$		$\Theta_{2,2}$	
		EC	V	EC	V	EC	V	EC	V
$\rho = 0.95$	Naïve	77.25	2.87	87.80	1.75	71.25	2.73	68.90	1.86
	BB	89.10	3.61	90.70	1.88	88.75	3.60	88.40	2.44
	Bonferroni	95.65	4.52	98.70	2.77	95.30	4.32	95.50	2.94
	Wald	98.10	4.97	99.35	3.20	97.80	4.79	98.05	3.38
	Adj-Wald	88.05	3.57	90.20	1.83	89.65	3.53	89.30	2.46
$\rho = 0.90$	Naïve	75.65	2.66	87.20	1.45	71.55	2.69	69.15	1.66
	BB	88.60	3.39	91.50	1.60	89.60	3.55	89.30	2.21
	Bonferroni	95.65	4.14	98.40	2.33	95.70	4.21	95.20	2.65
	Wald	97.55	4.52	99.25	2.65	97.80	4.64	97.95	3.01
	Adj-Wald	88.55	3.15	91.10	1.56	89.35	3.50	89.70	2.22
$\rho = 0.50$	Naïve	68.65	0.91	88.20	0.49	69.15	1.45	71.85	0.95
	BB	90.95	1.25	94.55	0.59	89.95	2.00	89.60	1.28
	Bonferroni	95.70	1.45	98.75	0.80	95.75	2.29	95.95	1.51
	Wald	97.70	1.63	99.05	0.91	97.65	2.55	97.40	1.70
	Adj-Wald	89.40	1.63	92.00	0.91	88.40	2.55	88.65	1.70
$\rho = 0.00$	Naïve	69.45	0.46	88.40	0.25	66.10	0.91	74.95	0.75
	BB	91.50	0.64	94.10	0.30	88.15	1.25	90.20	1.00
	Bonferroni	95.80	0.73	98.30	0.41	95.50	1.44	96.70	1.19
	Wald	98.10	0.64	99.50	0.29	87.45	1.23	98.30	0.97
	Adj-Wald	90.10	0.64	93.30	0.29	88.90	1.23	90.00	0.97
$\rho = -0.50$	Naïve	73.75	0.75	89.40	0.19	62.75	0.77	75.50	0.70
	BB	89.90	1.02	95.40	0.25	90.05	1.08	88.70	0.93
	Bonferroni	96.50	1.20	98.40	0.32	94.30	1.22	96.20	1.11
	Wald	98.35	1.33	99.25	0.36	97.50	1.37	98.50	1.23
	Adj-Wald	90.35	0.97	94.45	0.24	88.95	1.06	89.90	0.88
$\rho = -0.90$	Naïve	73.15	2.49	88.75	0.57	61.60	1.14	64.30	0.73
	BB	88.65	3.17	91.35	0.64	88.80	1.59	89.40	1.01
	Bonferroni	96.05	3.86	98.35	0.92	94.80	1.79	94.45	1.16
	Wald	97.70	4.28	99.35	1.04	96.95	1.98	97.20	1.29
	Adj-Wald	89.30	3.14	90.75	0.62	88.80	1.58	89.35	1.00
$\rho = -0.95$	Naïve	74.00	2.55	89.40	0.70	62.90	1.14	63.60	0.75
	BB	88.45	3.20	90.90	0.77	87.75	1.59	90.50	1.05
	Bonferroni	96.20	4.03	98.60	1.13	93.10	1.81	94.95	1.20
	Wald	97.85	4.53	99.10	1.26	96.80	2.02	96.80	1.33
	Adj-Wald	88.50	3.25	90.20	0.74	86.40	1.59	87.25	1.04

Table 3.5: Empirical coverage probabilities and average volumes of nominal 90% joint confidence bands with $T = 400$, $H = 10$, normal errors, and AIC lag selection.

DGP1	Method	$\Theta_{1,1}$		$\Theta_{1,2}$		$\Theta_{2,1}$		$\Theta_{2,2}$	
		EC	V	EC	V	EC	V	EC	V
$\rho = 0.95$	Naïve	71.85	14.90	88.45	6.50	66.70	14.77	68.05	6.94
	BB	86.35	20.59	92.75	8.04	86.50	20.96	88.25	9.99
	Bonferroni	94.10	22.75	99.45	12.22	93.75	22.86	96.05	12.90
	Wald	95.75	25.26	99.60	15.15	95.70	25.44	98.20	15.95
	Adj-Wald	88.50	19.09	91.85	7.84	86.60	19.27	88.85	10.53
$\rho = 0.90$	Naïve	75.00	12.31	88.10	5.14	68.60	12.84	68.45	5.85
	BB	86.75	17.42	94.20	6.65	87.20	18.58	89.45	8.71
	Bonferroni	95.20	18.84	99.35	9.92	95.60	19.82	96.10	11.11
	Wald	96.80	20.54	99.65	11.73	97.00	21.60	98.15	13.03
	Adj-Wald	88.45	15.64	93.00	6.29	88.15	16.48	89.80	8.80
$\rho = 0.50$	Naïve	69.25	2.25	84.15	1.25	64.10	3.61	68.80	2.33
	BB	89.65	3.46	95.05	1.70	88.65	5.68	90.15	3.60
	Bonferroni	96.50	4.18	99.00	2.46	96.35	6.60	96.25	4.51
	Wald	97.80	4.64	99.30	2.78	97.50	7.29	97.80	4.98
	Adj-Wald	90.60	3.37	93.25	1.64	88.80	5.26	91.00	3.55
$\rho = 0.00$	Naïve	67.90	1.05	87.35	0.61	69.15	2.09	72.90	1.76
	BB	91.85	1.58	94.85	0.83	89.00	3.18	86.85	2.62
	Bonferroni	97.10	1.93	98.85	1.17	96.90	3.79	95.65	3.24
	Wald	98.60	2.09	99.50	1.27	97.90	4.09	98.00	3.45
	Adj-Wald	91.90	1.56	94.05	0.76	89.20	2.95	91.10	2.44
$\rho = -0.50$	Naïve	70.55	1.69	87.65	0.50	60.65	1.76	73.55	1.61
	BB	87.95	2.59	95.45	0.72	92.30	2.69	87.55	2.41
	Bonferroni	96.55	3.09	98.95	1.00	96.10	3.21	95.85	2.94
	Wald	97.95	3.35	99.20	1.12	97.50	3.51	98.55	3.17
	Adj-Wald	91.15	2.44	94.75	0.69	87.75	2.56	92.15	2.30
$\rho = -0.90$	Naïve	72.25	10.88	88.15	2.03	60.05	4.23	61.70	1.89
	BB	86.05	15.20	94.15	2.59	86.05	6.30	90.70	2.90
	Bonferroni	95.65	16.55	99.00	3.96	93.95	6.67	95.70	3.46
	Wald	96.85	17.85	99.15	4.39	99.75	7.20	96.45	3.73
	Adj-Wald	87.20	13.63	91.60	2.44	85.20	5.75	89.50	2.80
$\rho = -0.95$	Naïve	70.10	12.41	88.25	2.68	54.90	4.68	61.45	2.04
	BB	82.10	16.71	93.40	3.27	85.80	6.87	89.85	3.08
	Bonferroni	95.50	19.51	99.10	5.09	93.85	7.55	95.30	3.71
	Wald	96.20	21.52	99.40	5.58	95.55	8.27	96.55	4.01
	Adj-Wald	86.55	16.44	90.60	3.11	85.10	6.65	88.60	3.03

Table 3.6: Empirical coverage probabilities and average volumes of nominal 90% joint confidence bands with $T = 100$, $H = 20$, normal errors, and AIC lag selection.

DGP1	Method	$\Theta_{1,1}$		$\Theta_{1,2}$		$\Theta_{2,1}$		$\Theta_{2,2}$	
		EC	V	EC	V	EC	V	EC	V
$\rho = 0.95$	Naïve	74.30	7.09	88.85	3.04	68.40	6.99	69.90	3.27
	BB	88.45	9.13	93.55	3.47	88.40	9.32	89.35	4.46
	Bonferroni	96.45	11.53	99.05	5.37	96.40	11.44	96.85	5.75
	Wald	97.35	11.73	99.55	4.06	96.70	11.67	98.15	6.17
	Adj-Wald	88.50	8.80	90.75	3.36	87.45	8.96	89.45	4.47
$\rho = 0.90$	Naïve	73.20	5.37	89.45	2.15	67.85	5.69	70.40	2.51
	BB	88.65	7.12	93.70	2.52	89.00	7.77	90.80	3.47
	Bonferroni	96.90	8.74	99.30	3.84	96.90	9.29	97.20	4.44
	Wald	97.85	8.89	99.35	4.06	97.35	9.46	98.00	4.68
	Adj-Wald	89.30	6.76	92.80	2.44	88.50	7.36	90.40	3.46
$\rho = 0.50$	Naïve	68.60	0.94	85.15	0.51	66.25	1.55	71.90	0.98
	BB	90.65	1.33	94.05	0.62	89.05	2.21	90.30	1.37
	Bonferroni	97.05	1.65	98.90	0.91	96.65	2.67	97.70	1.73
	Wald	97.85	1.71	99.10	0.95	97.20	2.76	97.80	1.80
	Adj-Wald	89.95	1.31	93.30	0.61	88.95	2.15	90.95	1.36
$\rho = 0.00$	Naïve	68.25	0.46	86.90	0.26	68.40	0.93	74.85	0.77
	BB	92.55	0.65	94.65	0.31	89.60	1.29	88.95	1.03
	Bonferroni	98.10	0.80	99.55	0.45	96.90	1.59	97.45	1.31
	Wald	98.00	0.84	99.20	0.47	97.45	1.64	97.60	1.36
	Adj-Wald	91.10	0.65	93.40	0.30	89.30	1.26	89.40	0.99
$\rho = -0.50$	Naïve	73.15	0.76	88.95	0.19	61.00	0.78	75.85	0.71
	BB	90.25	1.04	94.90	0.26	90.25	1.11	89.50	0.95
	Bonferroni	97.65	1.31	98.95	0.36	96.45	1.34	97.25	1.22
	Wald	98.30	1.35	99.35	0.37	97.65	1.39	98.80	1.26
	Adj-Wald	91.15	1.01	94.85	0.25	88.95	1.09	91.00	0.93
$\rho = -0.90$	Naïve	76.65	5.03	88.65	0.80	63.25	1.97	62.45	0.80
	BB	89.85	6.59	93.05	0.94	87.75	2.81	90.80	1.16
	Bonferroni	97.60	8.15	99.25	1.44	95.40	3.24	95.60	1.41
	Wald	98.15	8.40	99.45	1.51	96.90	3.34	97.60	1.46
	Adj-Wald	89.15	6.27	92.00	0.90	89.15	2.70	89.05	1.14
$\rho = -0.95$	Naïve	74.90	6.39	89.70	1.13	61.20	2.37	64.20	0.90
	BB	89.10	8.20	92.60	1.31	88.05	3.31	90.40	1.29
	Bonferroni	97.25	10.44	98.90	2.04	95.65	3.91	95.90	1.57
	Wald	97.35	10.80	99.30	2.12	95.95	4.05	96.65	1.63
	Adj-Wald	89.45	8.08	90.35	1.25	88.30	3.27	87.45	1.27

Table 3.7: Empirical coverage probabilities and average volumes of nominal 90% joint confidence bands with $T = 400$, $H = 20$, normal errors, and AIC lag selection.

3J Empirical Coverages for DGP-2 with Exogenous Bootstrap

	Method	$\Theta_{1,1}$	$\Theta_{1,2}$	$\Theta_{1,3}$	$\Theta_{2,1}$	$\Theta_{2,2}$	$\Theta_{2,3}$	$\Theta_{3,1}$	$\Theta_{3,2}$	$\Theta_{3,3}$
$H = 4$	Naïve	24.75	73.55	68.15	76.05	75.35	76.80	52.20	66.20	50.70
	BB	72.00	87.15	86.40	95.10	90.90	90.60	93.95	87.25	82.45
	Bonferroni	53.25	92.05	89.80	93.30	92.55	94.70	80.45	88.00	80.80
	Wald	88.75	99.25	98.60	99.40	98.30	99.40	97.10	97.50	97.50
	Adj-Wald	42.40	81.55	80.50	85.80	89.35	84.30	71.15	81.80	73.60
$H = 8$	Naïve	21.50	66.55	61.80	63.60	68.95	68.60	46.10	62.85	46.90
	BB	73.60	87.25	85.05	95.70	90.20	89.55	92.50	85.40	83.00
	Bonferroni	63.15	93.90	90.50	93.60	92.40	95.10	84.65	89.85	84.95
	Wald	88.40	98.45	96.90	99.00	97.70	99.30	96.45	96.30	97.00
	Adj-Wald	49.15	82.95	79.75	83.15	87.95	84.60	71.95	84.00	76.20
$H = 12$	Naïve	19.60	63.95	53.85	56.10	58.40	63.65	42.85	57.30	44.70
	BB	71.80	89.40	81.75	94.55	87.55	90.15	89.95	85.85	81.05
	Bonferroni	66.00	95.30	87.90	92.20	81.70	94.25	85.60	90.65	85.00
	Wald	84.60	98.50	93.60	98.25	97.05	98.20	94.90	96.90	95.35
	Adj-Wald	52.35	85.40	76.80	77.85	86.70	86.05	72.25	84.30	73.65
$H = 16$	Naïve	19.45	62.95	47.65	51.85	56.15	59.55	42.40	54.65	42.30
	BB	71.65	89.90	77.05	94.80	87.75	89.00	89.00	87.60	81.75
	Bonferroni	70.00	95.25	85.30	94.80	90.40	94.55	87.45	91.65	86.35
	Wald	86.15	98.05	91.40	98.35	96.25	98.15	95.45	97.00	94.45
	Adj-Wald	55.25	85.60	73.20	79.35	85.85	82.95	74.20	85.60	74.25
$H = 20$	Naïve	16.95	61.05	44.25	49.25	53.85	58.05	39.60	54.65	40.60
	BB	72.35	90.00	77.10	92.75	86.65	89.40	89.60	86.90	81.90
	Bonferroni	70.75	95.90	84.30	93.05	91.20	94.15	88.65	92.90	86.95
	Wald	85.90	98.25	91.00	97.05	96.10	96.75	95.05	96.65	94.55
	Adj-Wald	55.50	85.45	73.30	78.00	84.05	82.95	75.60	85.55	73.40
$H = 24$	Naïve	18.05	57.30	40.25	44.30	52.30	53.85	38.95	52.90	38.80
	BB	71.60	89.90	72.20	90.15	87.30	88.20	88.45	86.65	81.85
	Bonferroni	72.55	96.00	79.65	93.25	92.20	92.20	89.80	92.95	86.60
	Wald	84.25	98.30	87.55	97.20	95.95	95.60	95.15	96.20	92.60
	Adj-Wald	56.30	84.70	68.45	77.85	84.65	80.50	75.05	84.60	73.40
$H = 28$	Naïve	15.00	54.70	37.25	44.85	51.90	49.10	36.20	53.65	34.25
	BB	72.35	89.00	72.00	91.45	88.25	86.15	89.65	87.75	79.70
	Bonferroni	74.45	95.90	78.30	94.30	93.15	90.45	89.75	93.75	85.60
	Wald	85.10	98.25	85.35	97.05	96.20	94.20	94.45	96.30	91.60
	Adj-Wald	56.25	82.75	65.95	79.50	86.35	77.20	74.95	85.85	71.90

Table 3.8: Empirical coverage probabilities of nominal 90% joint confidence bands based on the exogenous bootstrap with $T = 100$, normal errors, and AIC lag selection.

	Method	$\Theta_{1,1}$	$\Theta_{1,2}$	$\Theta_{1,3}$	$\Theta_{2,1}$	$\Theta_{2,2}$	$\Theta_{2,3}$	$\Theta_{3,1}$	$\Theta_{3,2}$	$\Theta_{3,3}$
$H = 4$	Naïve	62.80	73.15	71.00	76.45	75.70	80.85	70.60	71.50	69.60
	BB	88.80	91.05	90.55	90.40	89.05	89.55	89.50	89.45	89.05
	Bonferroni	89.70	93.75	93.90	94.75	93.30	95.65	93.35	92.15	91.65
	Wald	98.20	99.55	99.60	99.50	99.60	99.45	99.75	99.45	99.20
	Adj-Wald	86.60	88.80	88.05	88.30	88.15	87.30	86.90	87.70	88.20
$H = 8$	Naïve	60.30	67.75	68.90	68.85	65.75	70.95	66.40	66.35	64.75
	BB	87.50	89.85	90.30	88.80	89.70	91.05	88.95	89.60	90.00
	Bonferroni	91.70	95.30	95.45	94.80	94.95	96.00	94.30	94.60	95.30
	Wald	98.00	99.40	99.40	99.15	99.20	99.40	99.05	99.30	99.40
	Adj-Wald	85.10	88.20	88.65	88.15	89.10	88.70	86.65	87.80	88.05
$H = 12$	Naïve	60.30	66.65	68.00	64.15	61.20	66.35	63.55	62.20	63.30
	BB	88.80	90.30	89.65	88.00	89.15	90.40	88.65	89.90	89.95
	Bonferroni	93.85	95.75	96.20	95.00	95.25	96.70	94.70	95.20	95.25
	Wald	97.55	99.20	99.30	99.35	98.80	99.45	98.70	99.15	99.05
	Adj-Wald	86.55	87.25	88.15	85.50	88.65	89.15	86.65	89.45	88.70
$H = 16$	Naïve	58.00	62.60	64.35	61.50	56.15	63.50	62.55	58.90	59.55
	BB	88.45	89.85	89.90	89.10	88.90	89.80	89.60	89.55	90.25
	Bonferroni	94.40	95.85	96.75	95.70	94.60	95.95	95.20	95.20	96.00
	Wald	97.25	99.00	99.05	99.00	98.85	98.95	98.05	98.95	99.05
	Adj-Wald	87.70	87.40	87.25	87.60	88.80	87.80	87.45	88.10	87.35
$H = 20$	Naïve	56.50	62.05	63.90	58.25	55.25	63.00	59.45	57.95	60.40
	BB	88.35	91.75	90.10	90.15	89.05	90.55	88.90	90.75	90.15
	Bonferroni	95.10	97.15	96.35	95.75	95.10	96.70	95.15	96.00	96.35
	Wald	97.20	99.35	98.50	98.50	98.55	98.60	98.15	98.75	98.50
	Adj-Wald	87.35	87.35	88.05	88.90	88.65	88.35	87.80	89.70	87.65
$H = 24$	Naïve	55.35	60.15	60.40	58.45	53.55	59.95	60.25	55.60	58.00
	BB	88.75	91.70	87.55	87.65	88.30	90.35	88.45	90.45	90.15
	Bonferroni	94.40	97.05	96.30	95.40	94.30	96.75	95.95	96.45	95.60
	Wald	96.70	99.15	98.70	98.30	98.00	98.70	98.50	98.75	98.10
	Adj-Wald	87.05	87.15	85.75	86.50	88.05	87.20	88.15	88.70	87.75
$H = 28$	Naïve	53.95	60.40	59.60	57.35	52.40	57.60	57.15	55.85	55.75
	BB	86.30	91.45	89.50	88.85	87.85	90.90	88.60	90.80	90.05
	Bonferroni	93.85	97.45	96.95	95.60	94.60	97.55	96.70	96.30	96.55
	Wald	96.40	98.95	98.90	98.40	97.90	98.80	98.50	98.75	98.70
	Adj-Wald	84.25	86.05	88.70	87.15	87.65	88.35	86.95	88.65	87.60

Table 3.9: Empirical coverage probabilities of nominal 90% joint confidence bands based on the exogenous bootstrap with $T = 400$, normal errors, and AIC lag selection.

3K Volumes for DGP-2 with Exogenous Bootstrap

	Method	$\Theta_{1,1}$	$\Theta_{1,2}$	$\Theta_{1,3}$	$\Theta_{2,1}$	$\Theta_{2,2}$	$\Theta_{2,3}$	$\Theta_{3,1}$	$\Theta_{3,2}$	$\Theta_{3,3}$
$H = 4$	Naïve	3.32	1.71	1.46	1.27	0.83	0.55	4.51	3.06	2.25
	BB	5.05	2.14	1.85	1.73	1.09	0.67	6.77	4.03	2.98
	Bonferroni	4.86	2.50	2.11	1.98	1.23	0.80	6.81	4.61	3.31
	Wald	7.41	3.89	3.23	3.28	1.93	1.22	10.88	7.56	5.27
	Adj-Wald	4.60	2.20	1.92	1.67	1.16	0.67	5.86	4.17	3.19
$H = 8$	Naïve	6.10	3.99	3.11	2.65	1.94	1.32	8.47	6.47	4.58
	BB	9.35	5.24	4.14	3.98	2.70	1.77	12.98	8.79	6.30
	Bonferroni	9.85	6.36	4.99	4.58	3.15	2.16	14.06	10.43	7.38
	Wald	13.34	8.98	6.92	6.57	4.46	2.98	19.94	14.91	10.35
	Adj-Wald	8.97	5.56	4.31	3.84	2.90	1.80	11.94	9.45	6.82
$H = 12$	Naïve	9.18	6.36	4.90	4.22	3.17	2.17	12.50	9.81	6.91
	BB	13.59	8.64	6.67	6.43	4.53	3.02	18.68	13.68	9.74
	Bonferroni	15.14	10.73	8.33	7.36	5.41	3.75	21.29	16.49	11.77
	Wald	18.98	14.38	10.93	9.73	7.32	4.91	27.76	22.08	15.52
	Adj-Wald	13.55	9.33	6.97	6.14	4.91	3.13	18.00	15.08	10.63
$H = 16$	Naïve	12.19	8.45	6.57	5.73	4.40	3.05	16.24	12.59	9.04
	BB	18.20	12.01	9.29	9.03	6.54	4.41	25.12	18.66	13.33
	Bonferroni	20.77	15.24	11.83	10.41	7.93	5.56	29.47	22.86	16.45
	Wald	25.03	19.86	15.04	13.12	10.34	7.05	36.74	29.65	20.96
	Adj-Wald	18.43	13.14	9.79	8.72	7.14	4.61	24.76	20.81	14.62
$H = 20$	Naïve	15.46	10.59	8.26	7.38	5.70	3.96	20.46	15.59	11.25
	BB	23.49	15.19	11.86	12.15	8.75	6.00	31.88	23.17	16.74
	Bonferroni	27.04	19.73	15.40	13.98	10.75	7.69	37.78	28.94	20.95
	Wald	31.59	25.25	19.20	16.97	13.70	9.50	45.59	36.87	26.19
	Adj-Wald	23.94	16.91	12.48	11.67	9.57	6.31	31.52	26.10	18.38
$H = 24$	Naïve	18.37	12.60	9.94	9.04	7.02	5.01	24.08	18.26	13.38
	BB	28.32	18.51	14.47	14.79	10.78	7.51	38.20	27.88	20.23
	Bonferroni	33.22	24.43	19.05	17.30	13.37	9.70	46.07	35.24	25.64
	Wald	38.45	30.80	23.34	20.50	16.75	11.83	54.63	44.31	31.49
	Adj-Wald	29.01	20.66	15.40	14.39	11.85	7.95	37.98	31.65	22.32
$H = 28$	Naïve	21.87	14.53	11.51	11.11	8.32	6.02	28.92	21.10	15.65
	BB	33.56	21.78	17.05	18.03	13.07	9.20	45.26	32.56	23.75
	Bonferroni	39.83	29.29	22.84	21.31	16.50	12.06	55.26	42.00	30.51
	Wald	45.63	36.42	27.61	24.79	20.35	14.46	64.53	51.93	37.03
	Adj-Wald	34.86	24.51	18.25	17.80	14.47	9.81	45.35	37.21	26.26

Table 3.10: Average volumes of nominal 90% joint confidence bands based on the exogenous bootstrap with $T = 100$, normal errors, and AIC lag selection.

	Method	$\Theta_{1,1}$	$\Theta_{1,2}$	$\Theta_{1,3}$	$\Theta_{2,1}$	$\Theta_{2,2}$	$\Theta_{2,3}$	$\Theta_{3,1}$	$\Theta_{3,2}$	$\Theta_{3,3}$
$H = 4$	Naïve	0.85	0.76	0.69	0.38	0.36	0.27	1.16	1.18	0.98
	BB	1.17	0.97	0.90	0.48	0.46	0.33	1.51	1.53	1.30
	Bonferroni	1.21	1.07	0.98	0.54	0.51	0.39	1.64	1.65	1.39
	Wald	1.76	1.57	1.43	0.79	0.75	0.56	2.41	2.42	2.02
	Adj-Wald	1.22	1.01	0.93	0.49	0.48	0.34	1.55	1.59	1.35
$H = 8$	Naïve	1.64	1.72	1.39	0.74	0.85	0.61	2.30	2.66	2.03
	BB	2.32	2.32	1.88	1.00	1.15	0.80	3.14	3.62	2.80
	Bonferroni	2.55	2.64	2.15	1.15	1.30	0.94	3.56	4.08	3.14
	Wald	3.38	3.54	2.88	1.55	1.74	1.25	4.77	5.45	4.18
	Adj-Wald	2.41	2.40	1.95	1.04	1.21	0.82	3.24	3.78	2.90
$H = 12$	Naïve	2.58	2.81	2.15	1.14	1.38	0.95	3.52	4.21	3.04
	BB	3.68	3.88	2.96	1.59	1.95	1.30	4.92	5.94	4.30
	Bonferroni	4.19	4.53	3.48	1.86	2.22	1.54	5.74	6.78	4.94
	Wald	5.23	5.81	4.42	2.39	2.83	1.96	7.29	8.63	6.26
	Adj-Wald	3.77	4.02	3.04	1.66	2.05	1.36	5.07	6.21	4.43
$H = 16$	Naïve	3.62	3.82	2.94	1.58	1.94	1.33	4.81	5.58	4.01
	BB	5.19	5.37	4.09	2.24	2.81	1.86	6.77	8.00	5.74
	Bonferroni	6.03	6.38	4.90	2.65	3.21	2.22	8.04	9.24	6.71
	Wald	7.19	7.95	6.00	3.27	3.98	2.74	9.78	11.42	8.19
	Adj-Wald	5.27	5.61	4.18	2.34	2.96	1.94	6.94	8.40	5.91
$H = 20$	Naïve	4.73	4.72	3.74	2.06	2.50	1.72	6.10	6.65	4.95
	BB	6.83	6.70	5.26	2.98	3.69	2.46	8.71	9.73	7.18
	Bonferroni	8.03	8.06	6.39	3.55	4.24	2.97	10.48	11.34	8.50
	Wald	9.23	9.87	7.60	4.24	5.13	3.56	12.31	13.75	10.14
	Adj-Wald	6.91	7.03	5.34	3.10	3.89	2.56	8.94	10.29	7.37
$H = 24$	Naïve	5.86	5.48	4.52	2.59	3.04	2.13	7.46	7.61	5.91
	BB	8.53	7.96	6.42	3.78	4.55	3.09	10.71	11.33	8.60
	Bonferroni	10.08	9.67	7.87	4.54	8.27	3.74	12.95	13.32	10.29
	Wald	11.32	11.66	9.20	5.27	6.27	4.41	14.78	15.91	12.07
	Adj-Wald	8.64	8.40	6.51	3.91	4.80	3.20	10.95	12.02	8.79
$H = 28$	Naïve	7.03	6.22	5.28	3.19	3.55	2.55	8.94	8.62	6.88
	BB	10.25	9.08	7.54	4.66	5.33	3.73	12.71	12.76	9.98
	Bonferroni	12.14	11.13	9.31	5.63	6.22	4.56	15.41	15.13	12.05
	Wald	13.39	13.24	10.69	6.38	7.32	5.28	17.17	17.84	13.93
	Adj-Wald	10.30	9.60	7.65	4.78	5.63	3.86	12.95	13.51	10.21

Table 3.11: Average volumes of nominal 90% joint confidence bands based on the exogenous bootstrap with $T = 400$, normal errors, and AIC lag selection.

3L Results for DGP-1 with Endogenous Bootstrap

DGP1	Method	$\Theta_{1,1}$		$\Theta_{1,2}$		$\Theta_{2,1}$		$\Theta_{2,2}$	
		EC	V	EC	V	EC	V	EC	V
$\rho = 0.95$	Naïve	71.50	5.20	92.05	1.66	61.75	2.43	68.80	1.73
	BB	87.40	8.59	93.35	4.35	87.65	8.51	91.45	5.37
	Bonferroni	92.60	10.10	99.55	6.14	93.35	9.81	95.90	6.48
	Wald	Na	Na	Na	Na	Na	Na	Na	Na
	Adj-Wald	Na	Na	Na	Na	Na	Na	Na	Na
$\rho = 0.90$	Naïve	75.45	5.92	91.25	3.17	69.60	5.93	70.75	3.59
	BB	87.25	7.72	94.20	3.85	87.35	7.96	91.10	5.00
	Bonferroni	94.60	8.92	99.50	5.40	94.50	9.04	95.45	6.02
	Wald	Na	Na	Na	Na	Na	Na	Na	Na
	Adj-Wald	Na	Na	Na	Na	Na	Na	Na	Na
$\rho = 0.50$	Naïve	73.30	2.08	89.65	1.18	69.40	3.22	73.15	2.17
	BB	92.40	3.06	96.70	1.58	90.40	4.71	91.70	3.17
	Bonferroni	96.30	3.50	99.45	2.18	95.70	5.23	95.75	3.77
	Wald	Na	Na	Na	Na	Na	Na	Na	Na
	Adj-Wald	Na	Na	Na	Na	Na	Na	Na	Na
$\rho = 0.00$	Naïve	69.80	1.05	90.30	0.61	71.00	2.03	75.10	1.70
	BB	92.95	1.63	96.80	0.85	90.75	3.13	92.65	2.58
	Bonferroni	96.70	2.00	99.45	1.29	96.20	3.58	96.55	3.07
	Wald	Na	Na	Na	Na	Na	Na	Na	Na
	Adj-Wald	Na	Na	Na	Na	Na	Na	Na	Na
$\rho = -0.50$	Naïve	75.30	1.67	90.80	0.51	66.50	1.73	76.90	1.58
	BB	91.40	2.51	97.10	0.76	92.75	2.67	90.75	2.41
	Bonferroni	96.25	2.89	99.20	1.34	96.85	3.06	95.40	2.87
	Wald	Na	Na	Na	Na	Na	Na	Na	Na
	Adj-Wald	Na	Na	Na	Na	Na	Na	Na	Na
$\rho = -0.90$	Naïve	75.95	5.20	89.75	1.38	63.15	2.44	67.20	1.68
	BB	87.00	6.77	95.10	1.72	89.40	3.51	91.35	2.54
	Bonferroni	95.60	7.89	99.15	3.34	95.05	3.91	95.05	3.07
	Wald	Na	Na	Na	Na	Na	Na	Na	Na
	Adj-Wald	Na	Na	Na	Na	Na	Na	Na	Na
$\rho = -0.95$	Naïve	71.70	5.23	90.75	1.64	63.00	2.43	68.90	1.71
	BB	84.55	6.77	94.65	1.95	88.10	3.49	91.85	2.56
	Bonferroni	94.90	8.33	99.50	3.96	93.90	3.98	96.20	3.15
	Wald	Na	Na	Na	Na	Na	Na	Na	Na
	Adj-Wald	Na	Na	Na	Na	Na	Na	Na	Na

Table 3.12: Empirical coverage probabilities and average volumes of nominal 90% joint confidence bands with $T = 100$, $H = 10$, normal errors, and AIC lag selection.

DGP1	Method	$\Theta_{1,1}$		$\Theta_{1,2}$		$\Theta_{2,1}$		$\Theta_{2,2}$	
		EC	V	EC	V	EC	V	EC	V
$\rho = 0.95$	Naïve	76.20	2.58	90.25	0.74	66.15	1.16	68.10	0.78
	BB	89.75	3.69	93.00	1.98	89.35	3.67	92.05	2.54
	Bonferroni	96.45	4.58	99.35	2.91	95.60	4.39	97.35	3.08
	Wald	Na	Na	Na	Na	Na	Na	Na	Na
	Adj-Wald	Na	Na	Na	Na	Na	Na	Na	Na
$\rho = 0.90$	Naïve	74.55	2.67	91.05	1.49	70.60	2.71	72.85	1.71
	BB	89.15	3.45	92.55	1.69	90.40	3.61	90.85	2.30
	Bonferroni	96.25	4.18	99.25	2.46	96.70	4.25	96.35	2.78
	Wald	Na	Na	Na	Na	Na	Na	Na	Na
	Adj-Wald	Na	Na	Na	Na	Na	Na	Na	Na
$\rho = 0.50$	Naïve	70.65	0.93	90.10	0.51	69.45	1.47	73.80	0.97
	BB	91.85	1.30	95.65	0.63	90.55	2.06	91.55	1.35
	Bonferroni	96.55	1.52	99.05	0.90	96.55	2.37	97.50	1.63
	Wald	Na	Na	Na	Na	Na	Na	Na	Na
	Adj-Wald	Na	Na	Na	Na	Na	Na	Na	Na
$\rho = 0.00$	Naïve	71.20	0.47	89.95	0.26	71.20	0.93	78.65	0.77
	BB	94.00	0.69	95.80	0.33	91.55	1.33	91.80	1.07
	Bonferroni	98.05	0.85	9.10	0.51	97.30	1.55	97.55	1.31
	Wald	Na	Na	Na	Na	Na	Na	Na	Na
	Adj-Wald	Na	Na	Na	Na	Na	Na	Na	Na
$\rho = -0.50$	Naïve	77.15	0.77	91.00	0.20	68.80	0.78	79.10	0.72
	BB	91.50	1.07	96.60	0.27	92.00	1.14	90.95	0.99
	Bonferroni	96.95	1.29	99.30	0.54	96.15	1.33	97.35	1.22
	Wald	Na	Na	Na	Na	Na	Na	Na	Na
	Adj-Wald	Na	Na	Na	Na	Na	Na	Na	Na
$\rho = -0.90$	Naïve	76.60	2.51	90.85	0.60	66.55	1.16	69.85	0.75
	BB	91.05	3.21	95.30	0.69	90.15	1.64	91.85	1.07
	Bonferroni	97.25	3.90	99.40	1.42	95.45	1.85	96.95	1.33
	Wald	Na	Na	Na	Na	Na	Na	Na	Na
	Adj-Wald	Na	Na	Na	Na	Na	Na	Na	Na
$\rho = -0.95$	Naïve	78.05	2.58	89.90	0.74	65.40	1.16	69.85	0.77
	BB	88.55	3.28	92.90	0.83	90.75	1.64	91.90	1.11
	Bonferroni	95.50	4.12	99.25	1.73	94.70	1.89	97.15	1.40
	Wald	Na	Na	Na	Na	Na	Na	Na	Na
	Adj-Wald	Na	Na	Na	Na	Na	Na	Na	Na

Table 3.13: Empirical coverage probabilities and average volumes of 90% confidence bands with $T = 400$, $H = 10$, normal errors, and AIC lag selection.

DGP1	Method	$\Theta_{1,1}$		$\Theta_{1,2}$		$\Theta_{2,1}$		$\Theta_{2,2}$	
		EC	V	EC	V	EC	V	EC	V
$\rho = 0.95$	Naïve	70.65	12.60	91.35	2.93	60.25	4.78	68.65	2.15
	BB	89.05	21.01	95.05	8.45	87.10	21.38	91.10	10.42
	Bonferroni	95.25	23.20	99.50	13.02	93.90	23.33	97.05	13.74
	Wald	Na	Na	Na	Na	Na	Na	Na	Na
	Adj-Wald	Na	Na	Na	Na	Na	Na	Na	Na
$\rho = 0.90$	Naïve	76.70	12.45	90.50	5.30	70.60	12.98	69.90	6.02
	BB	87.70	17.66	95.65	6.98	87.75	18.73	91.75	9.03
	Bonferroni	95.20	19.15	99.30	10.59	95.50	20.04	96.75	11.78
	Wald	Na	Na	Na	Na	Na	Na	Na	Na
	Adj-Wald	Na	Na	Na	Na	Na	Na	Na	Na
$\rho = 0.50$	Naïve	73.05	2.28	88.40	1.28	70.30	3.69	73.90	2.41
	BB	91.45	3.68	96.40	1.86	90.20	5.98	91.60	3.86
	Bonferroni	96.70	4.61	99.80	2.93	97.55	7.19	96.60	5.12
	Wald	Na	Na	Na	Na	Na	Na	Na	Na
	Adj-Wald	Na	Na	Na	Na	Na	Na	Na	Na
$\rho = 0.00$	Naïve	71.05	1.08	89.40	0.64	71.95	2.14	77.60	1.81
	BB	93.60	1.71	96.50	0.91	92.20	3.34	90.85	2.79
	Bonferroni	98.45	2.44	99.80	1.65	97.95	4.34	97.30	3.82
	Wald	Na	Na	Na	Na	Na	Na	Na	Na
	Adj-Wald	Na	Na	Na	Na	Na	Na	Na	Na
$\rho = -0.50$	Naïve	73.20	1.75	89.45	0.53	62.85	1.79	75.45	1.64
	BB	90.75	2.75	97.40	0.81	93.10	2.88	91.45	2.59
	Bonferroni	96.90	3.59	99.70	1.77	97.90	3.73	96.95	3.54
	Wald	Na	Na	Na	Na	Na	Na	Na	Na
	Adj-Wald	Na	Na	Na	Na	Na	Na	Na	Na
$\rho = -0.90$	Naïve	75.45	10.97	90.35	2.15	62.95	4.28	68.70	1.95
	BB	88.85	15.63	96.30	2.89	89.95	6.56	92.90	3.17
	Bonferroni	96.75	16.97	99.70	6.50	96.95	7.08	97.85	4.41
	Wald	Na	Na	Na	Na	Na	Na	Na	Na
	Adj-Wald	Na	Na	Na	Na	Na	Na	Na	Na
$\rho = -0.95$	Naïve	71.05	12.66	90.20	2.93	58.90	4.82	67.90	2.17
	BB	85.75	17.14	96.05	3.61	88.90	7.11	91.60	3.42
	Bonferroni	96.15	20.11	99.90	8.67	96.20	8.01	96.85	4.98
	Wald	Na	Na	Na	Na	Na	Na	Na	Na
	Adj-Wald	Na	Na	Na	Na	Na	Na	Na	Na

Table 3.14: Empirical coverage probabilities and average volumes of nominal 90% joint confidence bands with $T = 100$, $H = 20$, normal errors, and AIC lag selection.

DGP1	Method	$\Theta_{1,1}$		$\Theta_{1,2}$		$\Theta_{2,1}$		$\Theta_{2,2}$	
		EC	V	EC	V	EC	V	EC	V
$\rho = 0.95$	Naïve	74.85	6.40	90.65	1.21	63.10	2.39	67.85	0.94
	BB	89.05	9.33	94.40	3.62	89.10	9.42	92.20	4.62
	Bonferroni	96.55	11.60	99.65	5.67	96.35	11.51	98.25	6.05
	Wald	Na	Na	Na	Na	Na	Na	Na	Na
	Adj-Wald	Na	Na	Na	Na	Na	Na	Na	Na
$\rho = 0.90$	Naïve	75.00	5.40	89.35	2.21	70.75	5.73	71.55	2.58
	BB	90.30	7.27	95.20	2.67	91.20	7.91	92.65	3.63
	Bonferroni	97.65	8.88	99.55	4.11	97.85	9.43	97.80	4.74
	Wald	Na	Na	Na	Na	Na	Na	Na	Na
	Adj-Wald	Na	Na	Na	Na	Na	Na	Na	Na
$\rho = 0.50$	Naïve	69.45	0.97	86.05	0.53	67.75	1.58	72.90	1.02
	BB	93.95	1.39	96.05	0.67	91.65	2.29	93.05	2.44
	Bonferroni	98.65	1.77	99.85	1.06	98.05	2.82	98.70	1.93
	Wald	Na	Na	Na	Na	Na	Na	Na	Na
	Adj-Wald	Na	Na	Na	Na	Na	Na	Na	Na
$\rho = 0.00$	Naïve	72.20	0.47	89.95	0.26	69.05	0.94	76.95	0.78
	BB	93.70	0.70	96.10	0.34	92.50	1.37	91.35	1.10
	Bonferroni	98.20	1.00	99.85	0.62	98.60	1.77	98.75	1.51
	Wald	Na	Na	Na	Na	Na	Na	Na	Na
	Adj-Wald	Na	Na	Na	Na	Na	Na	Na	Na
$\rho = -0.50$	Naïve	77.45	0.78	90.60	0.20	65.00	0.80	76.20	0.73
	BB	91.60	1.08	97.30	0.28	92.75	1.16	91.85	1.01
	Bonferroni	97.85	1.46	99.85	0.66	98.35	1.51	98.65	1.40
	Wald	Na	Na	Na	Na	Na	Na	Na	Na
	Adj-Wald	Na	Na	Na	Na	Na	Na	Na	Na
$\rho = -0.90$	Naïve	75.40	5.03	92.10	0.83	65.30	1.98	69.80	0.83
	BB	91.05	6.74	95.90	1.02	91.45	2.88	94.45	1.23
	Bonferroni	98.15	8.28	99.75	2.49	97.60	3.34	98.55	1.77
	Wald	Na	Na	Na	Na	Na	Na	Na	Na
	Adj-Wald	Na	Na	Na	Na	Na	Na	Na	Na
$\rho = -0.95$	Naïve	75.30	6.41	90.65	1.21	63.95	2.39	67.95	0.94
	BB	89.15	8.31	94.70	1.42	90.50	3.37	93.00	1.37
	Bonferroni	97.15	10.54	99.85	3.52	96.90	4.03	98.55	2.07
	Wald	Na	Na	Na	Na	Na	Na	Na	Na
	Adj-Wald	Na	Na	Na	Na	Na	Na	Na	Na

Table 3.15: Empirical coverage probabilities and average volumes of nominal 90% joint confidence bands with $T = 400$, $H = 20$, normal errors, and AIC lag selection.

3M Empirical Coverages for DGP-2 with Endogenous Bootstrap

	Method	$\Theta_{1,1}$	$\Theta_{1,2}$	$\Theta_{1,3}$	$\Theta_{2,1}$	$\Theta_{2,2}$	$\Theta_{2,3}$	$\Theta_{3,1}$	$\Theta_{3,2}$	$\Theta_{3,3}$
$H = 4$	Naïve	32.40	71.25	66.40	75.50	62.00	77.45	54.45	62.85	55.85
	BB	70.40	85.95	82.25	93.50	89.85	87.30	91.15	86.15	84.40
	Bonferroni	67.50	92.15	88.80	94.15	92.20	95.00	78.50	84.85	83.45
	Wald	Na	Na	Na	Na	Na	Na	Na	Na	Na
	Adj-Wald	Na	Na	Na	Na	Na	Na	Na	Na	Na
$H = 8$	Naïve	29.50	64.80	56.15	63.10	59.20	69.50	47.05	58.05	49.40
	BB	68.65	84.30	78.95	93.45	89.00	85.90	88.70	83.35	81.30
	Bonferroni	73.85	93.15	85.45	92.55	84.95	93.45	83.55	85.10	84.85
	Wald	Na	Na	Na	Na	Na	Na	Na	Na	Na
	Adj-Wald	Na	Na	Na	Na	Na	Na	Na	Na	Na
$H = 12$	Naïve	26.50	61.00	48.00	53.10	48.90	61.75	45.65	54.30	40.25
	BB	66.65	85.45	75.80	91.40	85.65	84.75	86.50	83.00	79.30
	Bonferroni	77.40	93.70	81.00	90.75	82.05	93.85	85.25	86.30	83.80
	Wald	Na	Na	Na	Na	Na	Na	Na	Na	Na
	Adj-Wald	Na	Na	Na	Na	Na	Na	Na	Na	Na
$H = 16$	Naïve	25.65	58.55	40.15	49.70	46.95	55.30	41.55	50.05	37.25
	BB	65.40	86.35	68.20	90.45	84.35	84.35	84.45	83.00	78.10
	Bonferroni	79.45	94.90	74.20	91.60	82.20	93.00	85.30	87.25	81.50
	Wald	Na	Na	Na	Na	Na	Na	Na	Na	Na
	Adj-Wald	Na	Na	Na	Na	Na	Na	Na	Na	Na
$H = 20$	Naïve	24.85	56.30	38.10	49.00	44.80	50.80	40.25	51.75	35.65
	BB	67.25	86.65	68.90	91.30	84.85	83.90	86.80	84.05	78.95
	Bonferroni	80.85	95.35	73.45	92.85	84.85	91.30	87.55	89.10	82.15
	Wald	Na	Na	Na	Na	Na	Na	Na	Na	Na
	Adj-Wald	Na	Na	Na	Na	Na	Na	Na	Na	Na
$H = 24$	Naïve	20.15	50.60	35.90	44.05	41.85	44.65	36.15	46.85	34.00
	BB	64.75	87.5	67.00	88.00	83.80	80.65	84.45	83.35	78.30
	Bonferroni	81.30	94.65	71.75	90.60	83.50	85.80	87.45	87.00	81.50
	Wald	Na	Na	Na	Na	Na	Na	Na	Na	Na
	Adj-Wald	Na	Na	Na	Na	Na	Na	Na	Na	Na
$H = 28$	Naïve	17.70	46.95	31.90	43.65	42.30	38.75	36.65	48.60	29.85
	BB	61.40	84.70	64.80	87.15	85.75	80.50	83.80	85.15	76.10
	Bonferroni	76.95	94.50	69.25	92.40	86.40	83.80	88.60	89.95	78.80
	Wald	Na	Na	Na	Na	Na	Na	Na	Na	Na
	Adj-Wald	Na	Na	Na	Na	Na	Na	Na	Na	Na

Table 3.16: Empirical coverage probabilities of nominal 90% joint confidence bands based on the endogenous bootstrap with $T = 100$, normal errors, and AIC lag selection.

	Method	$\Theta_{1,1}$	$\Theta_{1,2}$	$\Theta_{1,3}$	$\Theta_{2,1}$	$\Theta_{2,2}$	$\Theta_{2,3}$	$\Theta_{3,1}$	$\Theta_{3,2}$	$\Theta_{3,3}$
$H = 4$	Naïve	64.35	74.20	70.50	78.15	76.10	79.45	74.60	72.85	68.90
	BB	88.75	88.30	89.30	88.95	90.05	89.75	88.55	89.05	90.90
	Bonferroni	86.45	92.35	93.05	93.40	85.10	95.35	92.60	89.75	88.75
	Wald	Na	Na	Na	Na	Na	Na	Na	Na	Na
	Adj-Wald	Na	Na	Na	Na	Na	Na	Na	Na	Na
$H = 8$	Naïve	58.95	66.75	68.25	66.80	68.20	72.65	67.00	64.45	63.05
	BB	90.35	88.90	90.40	90.35	90.10	88.70	89.40	89.45	89.90
	Bonferroni	90.65	95.40	95.40	95.70	88.95	94.85	94.20	92.95	89.90
	Wald	Na	Na	Na	Na	Na	Na	Na	Na	Na
	Adj-Wald	Na	Na	Na	Na	Na	Na	Na	Na	Na
$H = 12$	Naïve	59.00	67.45	67.45	66.00	62.05	66.20	65.05	64.15	62.00
	BB	89.25	89.35	89.55	89.70	89.35	88.80	87.85	88.90	90.60
	Bonferroni	91.20	95.45	95.80	94.80	89.85	95.90	94.40	92.60	92.05
	Wald	Na	Na	Na	Na	Na	Na	Na	Na	Na
	Adj-Wald	Na	Na	Na	Na	Na	Na	Na	Na	Na
$H = 16$	Naïve	57.25	62.65	64.30	61.10	57.85	65.80	62.70	58.95	61.10
	BB	88.55	90.05	89.70	88.50	89.30	89.25	89.70	89.25	90.35
	Bonferroni	92.20	96.15	96.50	95.45	90.95	95.75	96.10	93.20	92.15
	Wald	Na	Na	Na	Na	Na	Na	Na	Na	Na
	Adj-Wald	Na	Na	Na	Na	Na	Na	Na	Na	Na
$H = 20$	Naïve	58.35	61.55	63.15	61.25	56.50	60.70	60.60	56.80	57.90
	BB	88.30	90.20	89.50	88.95	88.25	89.40	88.05	89.75	91.95
	Bonferroni	92.60	97.10	95.95	95.60	91.60	96.05	95.00	95.05	94.25
	Wald	Na	Na	Na	Na	Na	Na	Na	Na	Na
	Adj-Wald	Na	Na	Na	Na	Na	Na	Na	Na	Na
$H = 24$	Naïve	55.80	58.10	60.65	57.50	54.50	58.15	58.85	55.05	57.85
	BB	89.50	90.05	89.10	88.40	89.25	89.35	87.40	89.15	89.85
	Bonferroni	93.55	97.05	96.60	94.70	92.35	96.65	95.25	94.35	93.95
	Wald	Na	Na	Na	Na	Na	Na	Na	Na	Na
	Adj-Wald	Na	Na	Na	Na	Na	Na	Na	Na	Na
$H = 28$	Naïve	51.60	58.55	61.00	56.20	52.35	59.60	59.00	55.35	56.75
	BB	89.10	90.55	87.70	88.60	89.50	90.10	89.35	90.75	91.10
	Bonferroni	94.25	96.65	95.90	96.05	92.35	96.90	95.90	95.65	94.50
	Wald	Na	Na	Na	Na	Na	Na	Na	Na	Na
	Adj-Wald	Na	Na	Na	Na	Na	Na	Na	Na	Na

Table 3.17: Empirical coverage probabilities of nominal 90% joint confidence bands based on the endogenous bootstrap with $T = 400$, normal errors, and AIC lag selection.

3N Volumes for DGP-2 with Endogenous Bootstrap

	Method	$\Theta_{1,1}$	$\Theta_{1,2}$	$\Theta_{1,3}$	$\Theta_{2,1}$	$\Theta_{2,2}$	$\Theta_{2,3}$	$\Theta_{3,1}$	$\Theta_{3,2}$	$\Theta_{3,3}$
$H = 4$	Naïve	2.55	1.55	1.33	1.04	0.75	0.50	3.41	2.68	2.04
	BB	3.79	1.98	1.75	1.37	1.08	0.61	4.97	3.65	2.85
	Bonferroni	3.70	2.21	1.92	1.54	1.07	0.72	5.00	3.87	2.96
	Wald	Na	Na	Na	Na	Na	Na	Na	Na	Na
	Adj-Wald	Na	Na	Na	Na	Na	Na	Na	Na	Na
$H = 8$	Naïve	4.74	3.53	2.75	2.13	1.73	1.17	6.45	5.69	4.08
	BB	7.26	4.78	3.80	3.08	2.55	1.57	9.72	8.12	5.92
	Bonferroni	7.46	5.52	4.39	3.48	2.70	1.87	10.38	8.88	6.52
	Wald	Na	Na	Na	Na	Na	Na	Na	Na	Na
	Adj-Wald	Na	Na	Na	Na	Na	Na	Na	Na	Na
$H = 12$	Naïve	7.15	5.55	4.20	3.27	2.79	1.86	9.53	8.53	5.98
	BB	11.02	7.73	5.98	4.95	4.19	2.63	14.55	12.45	8.89
	Bonferroni	11.69	9.20	7.14	5.58	4.61	3.17	16.10	13.99	10.13
	Wald	Na	Na	Na	Na	Na	Na	Na	Na	Na
	Adj-Wald	Na	Na	Na	Na	Na	Na	Na	Na	Na
$H = 16$	Naïve	9.51	7.42	5.63	4.43	3.93	2.64	12.61	11.15	7.85
	BB	14.75	10.60	8.22	6.86	5.99	3.86	19.41	16.63	11.93
	Bonferroni	16.00	12.93	9.98	7.78	6.74	4.69	21.96	19.16	13.85
	Wald	Na	Na	Na	Na	Na	Na	Na	Na	Na
	Adj-Wald	Na	Na	Na	Na	Na	Na	Na	Na	Na
$H = 20$	Naïve	11.82	9.05	6.99	5.72	5.09	3.47	15.72	13.59	9.72
	BB	18.51	13.29	10.41	8.99	7.87	5.19	24.52	20.75	15.05
	Bonferroni	20.32	16.53	12.84	10.24	9.04	6.38	28.04	24.38	17.74
	Wald	Na	Na	Na	Na	Na	Na	Na	Na	Na
	Adj-Wald	Na	Na	Na	Na	Na	Na	Na	Na	Na
$H = 24$	Naïve	14.22	10.68	8.44	6.98	6.10	4.29	18.57	15.68	11.52
	BB	22.55	15.98	12.70	11.09	9.56	6.55	29.29	24.38	18.09
	Bonferroni	24.93	20.28	15.96	12.64	11.17	8.11	33.70	29.15	21.57
	Wald	Na	Na	Na	Na	Na	Na	Na	Na	Na
	Adj-Wald	Na	Na	Na	Na	Na	Na	Na	Na	Na
$H = 28$	Naïve	16.52	12.26	9.71	8.39	7.19	5.13	21.60	17.95	13.27
	BB	26.50	18.69	14.86	13.50	11.46	7.99	34.46	28.40	21.18
	Bonferroni	29.66	24.13	18.92	15.41	13.62	9.94	40.01	34.54	25.53
	Wald	Na	Na	Na	Na	Na	Na	Na	Na	Na
	Adj-Wald	Na	Na	Na	Na	Na	Na	Na	Na	Na

Table 3.18: Average volumes of nominal 90% joint confidence bands based on the endogenous bootstrap with $T = 100$, normal errors, and AIC lag selection.

	Method	$\Theta_{1,1}$	$\Theta_{1,2}$	$\Theta_{1,3}$	$\Theta_{2,1}$	$\Theta_{2,2}$	$\Theta_{2,3}$	$\Theta_{3,1}$	$\Theta_{3,2}$	$\Theta_{3,3}$
$H = 4$	Naïve	0.87	0.76	0.70	0.38	0.36	0.27	1.17	1.18	0.99
	BB	1.21	0.96	0.89	0.47	0.47	0.33	1.49	1.54	1.32
	Bonferroni	1.21	1.04	0.96	0.52	0.49	0.38	1.60	1.62	1.35
	Wald	Na	Na	Na	Na	Na	Na	Na	Na	Na
	Adj-Wald	Na	Na	Na	Na	Na	Na	Na	Na	Na
$H = 8$	Naïve	1.66	1.72	1.40	0.74	0.85	0.61	2.31	2.67	2.04
	BB	2.40	2.28	1.87	0.99	1.16	0.79	3.10	3.61	2.80
	Bonferroni	2.54	2.58	2.10	1.12	1.26	0.91	3.47	3.97	3.05
	Wald	Na	Na	Na	Na	Na	Na	Na	Na	Na
	Adj-Wald	Na	Na	Na	Na	Na	Na	Na	Na	Na
$H = 12$	Naïve	2.61	2.81	2.16	1.15	1.39	0.95	3.54	4.24	3.05
	BB	3.78	3.78	2.91	1.57	1.94	1.28	4.88	5.84	4.26
	Bonferroni	4.16	4.38	3.39	1.82	2.15	1.50	5.61	6.56	4.80
	Wald	Na	Na	Na	Na	Na	Na	Na	Na	Na
	Adj-Wald	Na	Na	Na	Na	Na	Na	Na	Na	Na
$H = 16$	Naïve	3.65	3.83	2.95	1.58	1.94	1.33	4.82	5.59	4.02
	BB	5.33	5.26	4.05	2.23	2.78	1.83	6.76	7.88	5.70
	Bonferroni	6.03	6.20	4.80	2.60	3.11	2.17	7.92	8.97	6.54
	Wald	Na	Na	Na	Na	Na	Na	Na	Na	Na
	Adj-Wald	Na	Na	Na	Na	Na	Na	Na	Na	Na
$H = 20$	Naïve	4.76	4.72	3.74	2.07	2.51	1.72	6.13	6.67	4.96
	BB	6.93	6.55	5.19	2.96	3.65	2.43	8.70	9.62	7.13
	Bonferroni	7.96	7.84	6.25	3.50	4.13	2.90	10.33	11.08	8.32
	Wald	Na	Na	Na	Na	Na	Na	Na	Na	Na
	Adj-Wald	Na	Na	Na	Na	Na	Na	Na	Na	Na
$H = 24$	Naïve	5.90	5.50	4.54	2.62	3.06	2.14	7.53	7.68	5.95
	BB	8.62	7.74	6.33	3.77	4.47	3.03	10.69	11.13	8.49
	Bonferroni	9.98	9.37	7.69	4.47	5.10	3.63	12.77	12.94	10.02
	Wald	Na	Na	Na	Na	Na	Na	Na	Na	Na
	Adj-Wald	Na	Na	Na	Na	Na	Na	Na	Na	Na
$H = 28$	Naïve	7.03	6.24	5.31	3.19	3.56	2.56	8.90	8.63	6.89
	BB	10.33	8.88	7.45	4.66	5.27	3.68	12.75	12.66	9.94
	Bonferroni	12.04	10.84	9.14	5.56	6.08	4.46	15.29	14.87	11.87
	Wald	Na	Na	Na	Na	Na	Na	Na	Na	Na
	Adj-Wald	Na	Na	Na	Na	Na	Na	Na	Na	Na

Table 3.19: Average volumes of nominal 90% joint confidence bands based on the endogenous bootstrap with $T = 400$, normal errors, and AIC lag selection.

Chapter 4

Inference for Structural Impulse Responses in SVAR-GARCH Models

Abstract

Conditional heteroskedasticity can be exploited to identify the structural vector autoregressions (SVAR) but the implications for inference on structural impulse responses have not been investigated in detail yet. We consider the conditionally heteroskedastic SVAR-GARCH model and propose a bootstrap-based inference procedure on structural impulse responses. We compare the finite-sample properties of our bootstrap method with those of two competing bootstrap methods via extensive Monte Carlo simulations. We also present a three-step estimation procedure of the parameters of the SVAR-GARCH model that promises numerical stability even in scenarios with small sample sizes and/or large dimensions.

JEL classification: C12, C13, C32

Keywords: Bootstrap; conditional heteroskedasticity; multivariate GARCH; structural impulse responses; structural vector autoregression.

4.1 Introduction

Identifying the structural vector autoregressive (SVAR) model is typically one of the crucial issues in structural impulse response analysis. The existing literature offers a plethora of different identification strategies; see [Kilian and Lütkepohl \(2017\)](#) for an excellent overview. A recent strand of this literature exploits the presence of conditional heteroskedasticity for the identification of the SVAR model; see e.g., [Normandin and Phaneuf \(2004\)](#), [Lanne et al. \(2010\)](#), [Bouakez and Normandin \(2010\)](#) and [Herwartz and Lütkepohl \(2014\)](#).

The presence of conditional heteroskedasticity entails that the standard assumption of an independent and identically distributed (i.i.d.) error process is no longer valid and needs to be replaced by weaker assumptions on the error process, such as weak stationarity and serial uncorrelatedness; see e.g., [Lütkepohl and Milunovich \(2016, p.242\)](#). Unfortunately, the deviation from the common i.i.d. assumption invalidates inference on structural impulse responses which is based on standard residual-based bootstrap methods; see e.g., the methods of [Runkle \(1987\)](#), [Kilian \(1998a\)](#) and [Kilian \(1998b\)](#). Thus, confidence intervals that are based on these bootstrap methods may lead to wrong conclusions.

[Brüggemann et al. \(2016\)](#) consider a conditionally heteroskedastic VAR model. However, the asymptotic validity of their proposed moving-block bootstrap method is only proven for structural impulse responses that are identified via an recursive ordering approach; see [Brüggemann et al. \(2016, p.75\)](#). As of yet, it is unknown whether the validity of this moving-block bootstrap also holds when the SVAR is identified by conditional heteroskedasticity. Moreover, it turns out that there is no study that analyzes in detail the implications of identifying the SVAR by conditional heteroskedasticity for inference on structural impulse responses.

This paper takes up the just mentioned issue, that is, the construction of confidence intervals for the structural impulse responses in a conditionally heteroskedastic framework. We consider a conditionally heteroskedastic SVAR model where the conditional heteroskedasticity is driven by a multivariate generalized autoregressive conditional heteroskedastic (GARCH) process, that is, the SVAR-GARCH model.

The contribution of this paper is twofold. First, we propose a new three-step estimation

procedure of the parameters of the SVAR-GARCH model. The proposed estimation procedure exhibits numerical stability even in scenarios with small sample sizes and/or large dimensional parameter spaces. In contrast, the existing estimation procedures, see e.g., [Bouakez et al. \(2013, 2014\)](#) and [Lütkepohl and Milunovich \(2016\)](#), are prone to suffer from convergence problems in these delicate scenarios because an integral part of these estimation procedures is the Newton-type optimization of a likelihood function.

Second, we propose a bootstrap-based inference procedure for the structural impulse responses in the SVAR-GARCH model. The proposed bootstrap procedure is based on resampling (with replacement) of the devolatilized residuals and incorporates the specific GARCH structure of the conditional heteroskedasticity. In addition, we conduct a Monte Carlo experiment to compare the finite-sample properties of our proposed method with the finite-sample properties of the bootstrap methods of [Runkle \(1987\)](#) and [Brüggemann et al. \(2016\)](#).

The remainder of the paper is organized as follows. Section [4.2](#) reviews the SVAR-GARCH model and presents details about the estimation procedure. Section [4.3](#) proposes a new bootstrap method to obtain the bootstrap sampling distribution of the estimator of the structural impulse response. Section [4.4](#) describes the competing bootstrap methods. Section [4.5](#) describes the Monte Carlo experiment and presents the empirical results. Section [4.6](#) concludes. The Appendix provides additional details about the estimation procedure, boxplots describing the finite-sample properties of the various bootstrap methods and figures.

4.2 The Model

4.2.1 Some Preliminaries

Let $\{y_t : t \in \mathbb{Z}\}$ be an m -dimensional stochastic process following a reduced-form VAR(p) model

$$A(L)y_t = \nu + u_t, \quad (4.1)$$

where $y_t := (y_{1,t}, \dots, y_{m,t})$, $A(L) := I_m - \sum_{i=1}^p A_i L^i$ is a matrix polynomial in the backshift operator L , the A_i are $m \times m$ coefficient matrices, I_m is the $m \times m$ identity matrix and

$\nu \in \mathbb{R}^m$ is a deterministic intercept. The reduced-form error process $\{u_t : t \in \mathbb{Z}\}$ is *weak* white noise, that is,

$$\mathbb{E}[u_t] = 0, \quad \mathbb{E}[u_t u_t'] = \Sigma_u \quad \text{and} \quad \mathbb{E}[u_t u_{t+h}'] = 0, \quad (4.2)$$

for $h \neq 0$ and $\Sigma_u \in \mathbb{R}^{m \times m}$ is positive definite¹. Note that the common independence assumption for the reduced-form process $\{u_t : t \in \mathbb{Z}\}$ is replaced by the weaker assumption of zero serial correlation. Moreover, it is assumed that the VAR coefficient matrices A_1, \dots, A_p satisfy the following stability condition

$$\det(A(z)) \neq 0 \quad \text{for all } z \in \mathbb{C} \text{ with } |z| \leq 1.$$

The stable reduced-form VAR(p) process in (4.1) exhibits an equivalent Wold vector moving average (VMA) representation

$$y_t = \mu + \Psi(L)u_t,$$

where $\mu := A(1)^{-1}\nu$ denotes the unconditional expectation of y_t , $\Psi(L) := \sum_{i=0}^{\infty} \Psi_i L^i$ is an (infinite) matrix polynomial in L and the Ψ_i matrices are determined via $\Psi(z) = A(z)^{-1}$. In particular, $\Psi_0 = I_m$ and $\Psi_s = \sum_{j=1}^p \Psi_{s-j} A_j$ for $s \in \mathbb{N}_{>0}$.

The structural VAR (SVAR) corresponding to (4.1) is given by

$$B(L)y_t = B_0\nu + B_0u_t, \quad (4.3)$$

where $B(L) := B_0A(L)$ and $B_0 \in \mathbb{R}^{m \times m}$ is a nonsingular linear mapping that transforms the reduced-form error u_t into the (instantaneously uncorrelated) structural error ε_t , that is, $\varepsilon_t := B_0u_t$; see e.g., Kilian (2013). Thus, the structural error process $\{\varepsilon_t : t \in \mathbb{Z}\}$ satisfies

$$\mathbb{E}[\varepsilon_t] = 0, \quad \mathbb{E}[\varepsilon_t \varepsilon_t'] = \Sigma_\varepsilon \quad \text{and} \quad \mathbb{E}[\varepsilon_t \varepsilon_{t+h}'] = 0, \quad (4.4)$$

for $h \neq 0$ and $\Sigma_\varepsilon \in \mathbb{R}^{m \times m}$ is diagonal and positive definite.

¹Following Francq and Raïssi (2007), a VAR process (4.1) with (strictly stationary and ergodic) weak white noise is called a weak VAR(p) model.

When the process $\{u_t : t \in \mathbb{Z}\}$, and hence also the process $\{\varepsilon_t : t \in \mathbb{Z}\}$, is conditionally heteroskedastic, it may be possible to identify B_0 (or equivalently B_0^{-1}) without imposing additional identifying assumptions; see e.g., [Lütkepohl and Netšunajev \(2017\)](#) and the references therein. In the present paper, we assume that the reduced-form process $\{u_t : t \in \mathbb{Z}\}$ is given by a conditionally heteroskedastic multivariate GARCH process. More specifically, it is assumed that $\{u_t : t \in \mathbb{Z}\}$ follows a Generalized Orthogonal GARCH (GO-GARCH) model à la [van der Weide \(2002\)](#); the details are provided in the next section.

4.2.2 GO-GARCH Model

The assumption of a GO-GARCH model à la [van der Weide \(2002\)](#) implies that $\{u_t : t \in \mathbb{Z}\}$ can be represented as a nonsingular linear transformation of a process $\{\varepsilon_t : t \in \mathbb{Z}\}$ consisting of m conditionally uncorrelated univariate GARCH(1,1) processes, that is,

$$u_t = B_0^{-1} \varepsilon_t \quad (4.5)$$

$$= B_0^{-1} H_t^{1/2} e_t, \quad (4.6)$$

where $H_t := \text{diag}(\sigma_{t,1}^2, \dots, \sigma_{t,m}^2)$, the diagonal elements of H_t evolve according to the following univariate GARCH(1,1) specification²

$$\sigma_{t,i}^2 = (1 - \alpha_i - \beta_i) + \alpha_i \varepsilon_{t-1,i}^2 + \beta_i \sigma_{t-1,i}^2, \quad \alpha_i, \beta_i \geq 0, \quad \alpha_i + \beta_i < 1, \quad (4.7)$$

and $\{e_t : t \in \mathbb{Z}\}$ is a sequence of i.i.d. random vectors with mutually independent components $e_{t,i}$, $i = 1, \dots, m$, having mean zero and unit variance, that is, $\mathbb{E}[e_t] = 0$ and $\mathbb{E}[e_t e_t'] = I_m$.

The structural error process $\{\varepsilon_t : t \in \mathbb{Z}\}$, consisting of conditionally uncorrelated GARCH(1,1) processes, is a martingale difference sequence and conditionally heteroskedastic with diagonal conditional variance matrix H_t . Moreover, the process satisfies

$$\mathbb{E}[\varepsilon_t] = 0, \quad \mathbb{E}[\varepsilon_t \varepsilon_t'] = I_m \quad \text{and} \quad \mathbb{E}[\varepsilon_t \varepsilon_{t+h}'] = 0, \quad (4.8)$$

²See [Bollerslev \(1986\)](#) for more details about the univariate GARCH(p, q) process.

for all $h \neq 0$. The unconditional variance of ε_t is restricted to the identity matrix because of the normalization of the intercept in (4.7). This corresponds to the so-called B -normalization of SVAR models; see e.g. Lütkepohl (2005, Section 9.1). As is evident from (4.8), $\{\varepsilon_t : t \in \mathbb{Z}\}$ is weakly stationary.

The reduced-form error process $\{u_t : t \in \mathbb{Z}\}$ is a nonsingular nonlinear transformation of the structural error process (which consists of separate GARCH(1,1) processes). Hence, the reduced-form error process is also a martingale difference sequence and conditionally heteroskedastic with non-diagonal conditional variance matrix $B_0^{-1}H_tB_0^{-1'}$. The unconditional first and second moments are given by

$$\mathbb{E}[u_t] = 0, \quad \mathbb{E}[u_t u_t'] = B_0^{-1}B_0^{-1'} \quad \text{and} \quad \mathbb{E}[u_t u_{t+h}'] = 0, \quad (4.9)$$

for all $h \neq 0$. Hence, $\{u_t : t \in \mathbb{Z}\}$ is weakly stationary³. Moreover, (4.9) confirms that the assumption of a GO-GARCH model for $\{u_t : t \in \mathbb{Z}\}$ agrees with the assumption of weak white noise in Section 4.2.1.

As noted by van der Weide (2002), the GO-GARCH model is nested in the more general BEKK model of Engle and Kroner (1995). Therefore, Theorem 2.4 of Boussama et al. (2011, p.2336), which concerns the properties of BEKK models, establishes strict stationarity and ergodicity of $\{u_t : t \in \mathbb{Z}\}$ under the parameter restrictions in (4.7) and the following two additional assumptions: (i) the joint distribution of e_1 is absolutely continuous with respect to the Lebesgue measure on \mathbb{R}^m and (ii) the point zero is in the interior of the support of the joint distribution of e_1 .

4.2.3 Identification

Structural impulse responses are as such partial derivatives $\partial y_{t,i} / \partial \varepsilon_{t-h,j}$, $i, j \in \{1, \dots, m\}$, $h \in \mathbb{N}$, and hence elements of the coefficient matrices $\Psi_h B_0^{-1}$ in the structural vector moving average (VMA) representation of $\{y_t : t \in \mathbb{Z}\}$, that is,

$$y_t = \mu + \sum_{i=1}^{+\infty} \Psi_i B_0^{-1} \varepsilon_{t-i}, \quad (4.10)$$

³Alternatively, the weak stationarity of $\{u_t : t \in \mathbb{Z}\}$ follows from the weak stationarity of $\{\varepsilon_t : t \in \mathbb{Z}\}$ and the fact that $u_t = B_0^{-1} \varepsilon_t$, $t \in \mathbb{Z}$.

where $\mu = A(1)^{-1}\nu$ and $\varepsilon_t = H_t^{1/2}e_t$. A meaningful structural impulse response analysis requires an identification result that makes the two factors in $B_0^{-1}\varepsilon_t$, and hence the partial derivative $\partial y_{t,i}/\partial \varepsilon_{t-h,j}$, (at least) locally unique.

Proposition 3 of [Milunovich \(2014, p.7\)](#) implies that, if there are at least $r \geq m - 1$ nontrivial GARCH processes⁴ in the m -dimensional structural error process, the structural VMA representation is unique apart from column permutations and sign changes of B_0^{-1} and the components of ε_t . Thus, every structural VMA representation of $\{y_t : t \in \mathbb{Z}\}$ that can be written as

$$y_t = \mu + \sum_{i=1}^{+\infty} \Psi_i \check{B}_0^{-1} \varepsilon_{t-i}^*, \quad (4.11)$$

where $\check{B}_0^{-1} := B_0^{-1}DP$ and $\varepsilon_t^* := P'D^{-1}\varepsilon_t$ for some diagonal matrix $D := \text{diag}(d_1, \dots, d_m)$ with $d_i \in \{-1, 1\}$ and some permutation matrix $P \in \mathbb{R}^{m \times m}$ is observationally equivalent to the representation in (4.10). The set of observationally equivalent structural VMA representations can be characterized by

$$\mathcal{E}(B_0^{-1}) := \left\{ \check{B}_0^{-1} \in \mathbb{R}^{m \times m} \mid \check{B}_0^{-1} = B_0^{-1}DP \right\}, \quad (4.12)$$

for all matrices D and P (as defined above). In other words, the set $\mathcal{E}(B_0^{-1})$ consists of all matrices \check{B}_0^{-1} that are obtained by permutations and sign changes of the columns of B_0^{-1} . Moreover, note that $\varepsilon_t^* = P'D^{-1}\varepsilon_t = P'D^{-1}H_t^{1/2}e_t$ (for some D and P) implies that the vectors of GARCH parameters $\alpha := (\alpha_1, \dots, \alpha_m)'$ and $\beta := (\beta_1, \dots, \beta_m)'$ are also locally identified because the pre-multiplication with $P'D^{-1}$ only affects the ordering of the GARCH processes. The reordered GARCH parameter vectors that correspond to \check{B}_0^{-1} are denoted by $\check{\alpha} := P'D^{-1}\alpha$ and $\check{\beta} := P'D^{-1}\beta$, respectively.

Remark 4.2.1 As outlined above, the number of nontrivial GARCH components r in ε_t is critical for the local identification of B_0^{-1} , yet unknown in any practical application. Fortunately, [Lanne and Saikkonen \(2007\)](#) and [Lütkepohl and Milunovich \(2016\)](#) provide statistical tests to test the null hypothesis of $r = r_0$ nontrivial GARCH components in ε_t versus the two-sided alternative, that is, $\mathbb{H}_0 : r = r_0$ versus $\mathbb{H}_1 : r \neq r_0$. ■

⁴A nontrivial GARCH process exhibits a time-varying conditional variance, that is, the conditional variance equation satisfies $\tilde{\alpha} > 0 \vee \tilde{\beta} > 0$, where $\tilde{\alpha}$ and $\tilde{\beta}$ denote the parameters of the ARCH and the GARCH part, respectively.

4.2.4 Estimation

Motivation

The model parameters are the reduced-form VAR parameters ν, A_1, \dots, A_p , the transformation matrix B_0^{-1} and the GARCH parameters α and β . The literature proposes different estimation procedures. [Bouakez et al. \(2013, 2014\)](#) use a two-step procedure, that is, in the first step, the VAR parameters ν, A_1, \dots, A_p are estimated by multivariate least squares (LS) and in the second step, the parameters associated with the GO-GARCH model, that is, B_0^{-1}, α, β , are estimated by quasi-maximum likelihood (QML). [Lütkepohl and Milunovich \(2016\)](#) estimate the model parameters by a QML procedure that is to a large extent based on the procedure outlined in [Lanne and Saikkonen \(2007, p.64–65\)](#).

An integral part of both estimation procedures is the numerical optimization of a likelihood function. Hence, in scenarios with small sample sizes and/or large dimensions, both methods can be prone to numerical convergence problems⁵. Numerical instability is particularly problematic in applications where the estimation procedure has to be repeatedly applied, such as bootstrap-based inference. As a result, we propose a (partially) novel estimation procedure which is numerically stable even in the delicate scenarios mentioned above.

We propose a three-step estimation procedure. The first step consists of the estimation of the reduced-form VAR parameters ν, A_1, \dots, A_p by standard LS. The second step consists of the estimation of the parameter matrix B_0^{-1} using the method of moment (MM) estimation procedure of GO-GARCH models proposed in [Boswijk and van der Weide \(2011\)](#). The computation of the MM estimator of [Boswijk and van der Weide](#) does not involve any Newton-type optimization of an objective function but involves only iterated matrix rotations, and hence the procedure does not suffer from numerical convergence problems regardless of the available sample size and the dimension. The third step consists of the estimation of the vectors of GARCH parameters α and β using the least-squares estimator of [Preminger and Storti \(2017\)](#) component-wise. The estimator of [Preminger and Storti](#) does involve Newton-type optimization but simulation results

⁵[Hwang and Pereira \(2006\)](#) report serious convergence problems of the QML estimator of a GARCH(1,1) process in small sample sizes, and hence recommend to use at least 500 observations to estimate the model parameters (by QML). The GO-GARCH model is a multivariate GARCH model and is expected to also suffer from convergence problems in small sample sizes.

(not reported here) suggest that, in small sample scenarios, the least-squares estimator exhibits superior convergence properties compared to the standard QML estimator of GARCH models. Moreover, the simulation results of [Preminger and Storti \(2017\)](#) show that their least-squares estimator is competitive in terms of the root-mean-squared error.

Remark 4.2.2 [Kristensen and Linton \(2006\)](#) proposes a closed-form estimator of the GARCH(1,1) model which is based on the corresponding ARMA(1,1) representation. The proposed closed-form estimator is attractive from a computational point of view, but the finite-sample properties are by far inferior to the properties of the QML estimator; see [Kristensen and Linton \(2006, p.334\)](#). ■

Remark 4.2.3 For simplicity, it is assumed that the true lag order $p \in \mathbb{N}$ of the VAR is known. In a practical application the true lag order is usually unknown and has to be determined from the data; see e.g. [Lütkepohl \(2005, Chapter 4\)](#). In that case, the first estimation step consists of the estimation of $\nu, A_1, \dots, A_{\hat{p}}$, where \hat{p} denotes the estimated lag order. ■

Estimation

Estimation of the model parameters $\nu, A_1, \dots, A_p, B_0^{-1}, \alpha$ and β in three steps.

(i) *Estimation of ν, A_1, \dots, A_p :*

Using the original series $\{y_{-p+1}, \dots, y_0, y_1, \dots, y_T\}$, estimate the VAR coefficients ν, A_1, \dots, A_p by standard multivariate LS; see e.g. [Lütkepohl \(2005, Section 3\)](#) for details. Denote the LS estimators by $\hat{\nu}, \hat{A}_1, \dots, \hat{A}_p$. Next, obtain the corresponding residuals $\{\hat{u}_1, \dots, \hat{u}_T\}$ according to

$$\hat{u}_t := y_t - \hat{\nu} - \hat{A}_1 y_{t-1} - \dots - \hat{A}_p y_{t-p}, \quad t = 1, \dots, T.$$

(ii) *Estimation of B_0^{-1} :*

Using the residuals $\{\hat{u}_1, \dots, \hat{u}_T\}$ from the first step, estimate B_0^{-1} by the method of moment procedure proposed in [Boswijk and van der Weide \(2011\)](#); see [Appendix 4A](#) for details. Denote the resulting MM estimator by \hat{B}_0^{-1} . Next, obtain the structural

residuals $\{\hat{\varepsilon}_1, \dots, \hat{\varepsilon}_T\}$ according to

$$\hat{\varepsilon}_t := (\hat{B}_0^{-1})^{-1} \hat{u}_t, \quad t = 1, \dots, T.$$

(iii) *Estimation of α, β :*

Using the structural residuals $\{\hat{\varepsilon}_1, \dots, \hat{\varepsilon}_T\}$ from the second step, estimate the GARCH parameters α and β by the component-wise application of the least squares estimator of [Preminger and Storti \(2017\)](#); see Appendix [4B](#) for details. Denote the corresponding estimators by $\hat{\alpha} := (\hat{\alpha}_1, \dots, \hat{\alpha}_m)'$ and $\hat{\beta} := (\hat{\beta}_1, \dots, \hat{\beta}_m)'$, respectively.

The outlined three-step estimation procedure produces estimators of all parameters of the model, that is, $\hat{\nu}, \hat{A}_1, \dots, \hat{A}_p, \hat{B}_0^{-1}, \hat{\alpha}, \hat{\beta}$. However, the estimation of the model parameters per se is only an intermediate step, as the objects of interest are the structural impulse responses.

It is well-known that the standard plug-in estimator of the (i, j) -th structural impulse response at propagation horizon $h \in \mathbb{N}$ is a non-linear function of the VAR slope estimators $\hat{A}_1, \dots, \hat{A}_p$ and the matrix \hat{B}_0^{-1} . However, the matrix \hat{B}_0^{-1} may be replaced with an equivalent matrix $\hat{\hat{B}}_0^{-1} \in \mathcal{E}(\hat{B}_0^{-1})$ by the researcher; see e.g. [Lütkepohl and Milunovich \(2016, p.243\)](#) for a discussion of this issue. Thus, the estimator of the (i, j) -th structural impulse response at propagation horizon h is given by

$$\hat{\Theta}_{ij,h} := f_{ij,h} \left(\hat{A}_1, \dots, \hat{A}_p, \hat{\hat{B}}_0^{-1} \right). \quad (4.13)$$

Consistency of the Structural Impulse Response Estimator

The estimator $\hat{\Theta}_{ij,h}$ is a continuous function of $\hat{A}_1, \dots, \hat{A}_p$ and $\hat{\hat{B}}_0^{-1}$ for every $i, j \in \{1, \dots, m\}$ and $h \in \mathbb{N}$. Thus, by the continuous mapping theorem, the consistency of the estimators $\hat{A}_1, \dots, \hat{A}_p$ and $\hat{\hat{B}}_0^{-1}$ is sufficient for the consistency of $\hat{\Theta}_{ij,h}$.

Proposition 1 of [Francq and Raïssi \(2007, p.458\)](#) establishes the strong consistency of the LS estimators $\hat{\nu}, \hat{A}_1, \dots, \hat{A}_p$ of the parameters of a stable VAR(p) model under the assumption of a strictly stationary and ergodic reduced-form error process $\{u_t : t \in \mathbb{Z}\}$. The GO-GARCH model is strictly stationary and ergodic under mild regularity conditions

(see Section 4.2.2) and hence, under these regularity conditions, it holds that

$$\text{vec}(\hat{\nu}, \hat{A}_1, \dots, \hat{A}_p) \xrightarrow{a.s.} \text{vec}(\nu, A_1, \dots, A_p) \quad \text{as } T \rightarrow \infty, \quad (4.14)$$

where $\xrightarrow{a.s.}$ denotes almost sure convergence.

The MM estimator \hat{B}_0^{-1} is based on the reduced-form residuals from the first estimation step, that is, $\{\hat{u}_1, \dots, \hat{u}_T\}$, and not based on the unknown true errors $\{u_1, \dots, u_T\}$. However, the convergence (4.14) implies that $\hat{u}_t \xrightarrow{a.s.} u_t$ and Proposition 1 of Francq and Raïssi (2007, p.458) yields that $\hat{\Sigma}_u := T^{-1} \sum_{t=1}^T \hat{u}_t \hat{u}_t' \xrightarrow{a.s.} \Sigma_u$. As a consequence, the sample moments underlying the estimator \hat{B}_0^{-1} converge in probability to the identical population values as the estimator that is based on $\{u_1, \dots, u_T\}$. Thus, based on Theorem 1 in Boswijk and van der Weide (2011, p.122), the consistency of \hat{B}_0^{-1} is established under the following additional assumptions on the process $\{\varepsilon_t : t \in \mathbb{Z}\}$:

- $\mathbb{E}[\varepsilon_{t,i}^4] < +\infty$, $i = 1, \dots, m$.
- For some $s \in \mathbb{N}$, the autocorrelations $\rho_{ik} := \text{Corr}(\varepsilon_{t,i}^2, \varepsilon_{t-k,i}^2)$ satisfy

$$\max_{1 \leq k \leq s} \min_{1 \leq i \leq j \leq m} |\rho_{ik} - \rho_{jk}| > 0.$$

Remark 4.2.4 Boswijk and van der Weide (2011) consider a setup that allows for other more general specifications of the conditional heteroskedasticity than the GO-GARCH model. For that reason, their proof of consistency is based on a more extensive set of assumptions than the one above. However, it is straightforward to see that the assumption of a GO-GARCH model allows to narrow the set of required assumptions to establish consistency of the estimator. ■

Remark 4.2.5 A necessary and sufficient condition for a finite fourth moment of a GARCH(1,1) process is found in He and Teräsvirta (1999, p.827). Alternatively, for the special case of $e_{t,i} \stackrel{i.i.d.}{\sim} \mathcal{N}(0,1)$, a simpler (necessary and sufficient) condition for $\mathbb{E}[\varepsilon_{t,i}^4] < +\infty$ is found in Bollerslev (1986, p.311). ■

The importance of the finite fourth moment assumption for the consistency of the structural impulse response estimator (4.13) is analyzed by means of a simulation-based

root mean squared error (RMSE) analysis. More specifically, three different data generating processes (DGPs) are considered from which two DGPs satisfy all assumptions required for consistency (DGP-1a and DGP-1b) and one DGP that violates the finite fourth moment assumption (DGP-1c); see Section 4.5.1 for more details. The results for $\hat{\Theta}_{11,h}, h \in \{0, \dots, 12\}$, are found in Appendix 4D.

The analysis highlights the importance of the assumption of $\mathbb{E}[\varepsilon_{t,i}^4] < +\infty$. For the two DGPs with $\mathbb{E}[\varepsilon_{t,i}^4] < +\infty$, the RMSE of the structural impulse response estimator is strictly decreasing in the sample size and, for very large sample sizes, close to zero at all propagation horizons h . In contrast, for the DGP that violates the assumption $\mathbb{E}[\varepsilon_{t,i}^4] < +\infty$, the RMSE of the estimator is only weakly decreasing. Moreover, for small propagation horizons $h \in \{0, 1, 2, 3\}$, the RMSE is substantially away from zero even for a very large sample size of $T = 5,000$.

4.3 Inference for Structural Impulse Responses

4.3.1 Motivation

We are interested in constructing a marginal bootstrap percentile confidence interval à la Hall (1992) for the structural impulse response $\Theta_{ij,h}$ at propagation horizon $h \in \{0, \dots, H\}$. Such a percentile confidence interval for $\Theta_{ij,h}$ with a nominal coverage probability of $(1 - \alpha) \in (0, 1)$ is given by

$$\text{CI}_{h,(1-\alpha)} := \left[\hat{\Theta}_{ij,h} - q_{h,(1-\alpha/2)}^*; \hat{\Theta}_{ij,h} - q_{h,\alpha/2}^* \right], \quad (4.15)$$

where $q_{h,(1-\alpha/2)}^*$ and $q_{h,\alpha/2}^*$ are the $(1 - \alpha/2)$ - and $(\alpha/2)$ -quantiles, respectively, of the bootstrap sampling distribution (at propagation horizon h). Evidently, the confidence interval $\text{CI}_{h,(1-\alpha)}$ is derived under the usual bootstrap analogy, that is, the bootstrap sampling distribution approximates the unknown true sampling distribution

$$\mathcal{L} \left(\hat{\Theta}_{ij,h}^* - \hat{\Theta}_{ij,h} \mid y_{-p+1}, \dots, y_0, y_1, \dots, y_T \right) \approx \mathcal{L} \left(\hat{\Theta}_{ij,h} - \Theta_{ij,h} \right), \quad (4.16)$$

where $\mathcal{L}(X)$ denotes the distribution of a random variable X and $\hat{\Theta}_{ij,h}^*$ denotes the estimator computed based on artificial bootstrap data $\{y_{-p+1}^*, \dots, y_0^*, y_1^*, \dots, y_T^*\}$. Hence, a bootstrap procedure that satisfies (4.16) is expected to produce a confidence interval

$CI_{h,(1-\alpha)}$ that exhibits an actual coverage probability that is close to the nominal coverage probability $(1 - \alpha)$, and therefore provides valid inference.

The deviation from i.i.d. reduced-form errors by specifying the reduced-form error process as a conditionally heteroskedastic GO-GARCH model (see Section 4.2.2) entails that standard bootstrap procedures, such as the procedures of Runkle (1987), Kilian (1998a) and Kilian (1998b), may not result in a valid percentile confidence interval for $\Theta_{ij,h}$, even for very large sample sizes. The reason being that these bootstrap procedures are based on resampling with replacement from the empirical distribution of the reduced-form residuals, and hence the validity of these procedures essentially relies on the underlying assumption of i.i.d. reduced-form errors.

Brüggemann et al. (2016) investigate, among other things, inference for structural impulse responses in VAR models with conditional heteroskedasticity of unknown form and propose a residual-based moving block bootstrap procedure in the spirit of Künsch (1989). However, the authors prove the validity of their proposed moving block bootstrap only for structural impulse responses which are identified via a standard recursive ordering approach⁶; see Corollary 5.2 of Brüggemann et al. (2016, p.75). Thus, their theoretical result does not directly apply to structural impulse responses that are identified via the conditional heteroskedasticity of the GO-GARCH model. The same concern applies to the results of the extensive Monte Carlo study of Brüggemann et al. (2016). Moreover, we are not aware of a study that provides theoretical or simulation-based results that are applicable in the present framework where the structural impulse responses are identified via the conditional heteroskedasticity in the error process.

We propose a nonparametric bootstrap procedure that explicitly incorporates the GO-GARCH structure of the reduced-form error process. In this way, the corresponding artificial bootstrap data resembles the data generated from the true model, and hence the resulting bootstrap sampling distribution is supposed to approximate the true sampling distribution, at least for large sample sizes. Moreover, the proposed bootstrap procedure can be viewed as a multivariate generalization of the bootstrap procedure for the univariate ARMA-GARCH model outlined in Shimizu (2010, p.68–70).

The proposed bootstrap procedure is straightforward to implement, as it only requires the availability of the following quantities: (i) the estimators of the model parameters,

⁶This means that B_0^{-1} is given as the lower-triangular Cholesky decomposition of Σ_u .

that is, $\hat{\nu}, \hat{A}_1, \dots, \hat{A}_p, \hat{B}_0^{-1}, \hat{\alpha}$ and $\hat{\beta}$; (ii) the corresponding series of residuals $\{\hat{u}_1, \dots, \hat{u}_T\}$; and (iii) the pre-sample of the original data $\{y_{-p+1}, \dots, y_0\}$.

4.3.2 Residual Bootstrap

The following bootstrap algorithm, subsequently referred to as the *residual bootstrap*, produces the marginal percentile interval at each propagation horizon $h \in \{0, \dots, H\}$.

- a) For each component $i = 1, \dots, m$, compute the estimated conditional variances according to

$$\hat{\sigma}_{t,i}^2 := (1 - \hat{\alpha}_i - \hat{\beta}_i) + \hat{\alpha}_i \hat{\varepsilon}_{t-1,i}^2 + \hat{\beta}_i \hat{\sigma}_{t-1,i}^2, \quad t = 1, \dots, T,$$

where the starting values are $\hat{\varepsilon}_{0,i}^2 := \hat{\sigma}_{0,i}^2 = (1 - \hat{\alpha}_i - \hat{\beta}_i)$. Next, obtain the estimated conditional variance matrices $\hat{H}_t := \text{diag}(\hat{\sigma}_{t,1}^2, \dots, \hat{\sigma}_{t,m}^2)$, $t = 1, \dots, T$.

- b) Compute the devolatized residuals $\hat{e}_t := \hat{H}_t^{-1/2} \hat{B}_0 \hat{u}_t$, $t = 1, \dots, T$. Next, center and rescale the devolatized residuals according to

$$\check{e}_t := \hat{\Sigma}_e^{-1/2} (\hat{e}_t - \bar{e}), \quad t = 1, \dots, T,$$

where $\bar{e} := T^{-1} \sum_{t=1}^T \hat{e}_t$ and $\hat{\Sigma}_e := T^{-1} \sum_{t=1}^T (\hat{e}_t - \bar{e})(\hat{e}_t - \bar{e})'$.

- c) For each component $i = 1, \dots, m$, generate the univariate bootstrap sample $\{\hat{\varepsilon}_{1,i}^*, \dots, \hat{\varepsilon}_{T,i}^*\}$ according to

$$\begin{aligned} \hat{\varepsilon}_{t,i}^* &:= \hat{\sigma}_{t,i}^* \hat{e}_{t,i}^* \\ \hat{\sigma}_{t,i}^{*2} &:= (1 - \hat{\alpha}_i - \hat{\beta}_i) + \hat{\alpha}_i \hat{\varepsilon}_{t-1,i}^{*2} + \hat{\beta}_i \hat{\sigma}_{t-1,i}^{*2}, \end{aligned}$$

where $\hat{e}_{t,i}^*$ is a random draw with replacement from the (univariate) empirical distribution of $\{\check{e}_{t,i}\}_{t=1}^T$. The starting values are $\hat{\varepsilon}_{0,i}^{*2} := \hat{\sigma}_{0,i}^{*2} = (1 - \hat{\alpha}_i - \hat{\beta}_i)$. Next, obtain the series of bootstrap residuals $\{\hat{u}_1^*, \dots, \hat{u}_T^*\}$ via $u_t^* := \hat{B}_0^{-1} \hat{\varepsilon}_t^*$, $t = 1, \dots, T$.

- d) Generate the bootstrap sample $\{y_1^*, \dots, y_T^*\}$ according to

$$y_t^* := \hat{\nu} + \hat{A}_1 y_{t-1}^* + \dots + \hat{A}_p y_{t-p}^* + u_t^*, \quad t = 1, \dots, T,$$

where the starting values are equal to the pre-sample of the original series $\{y_{-p+1}, \dots, y_0\}$.

- e) Compute the estimators $\hat{\nu}^*, \hat{A}_1^*, \dots, \hat{A}_p^*$ and \hat{B}_0^{-1*} based on $\{y_{-p+1}^*, \dots, y_0^*, y_1^*, \dots, y_T^*\}$. Replace \hat{B}_0^{-1*} with an equivalent matrix $\hat{\hat{B}}_0^{-1*}$ which satisfies

$$\hat{\hat{B}}_0^{-1*} \in \arg \min_{B \in \mathcal{E}(\hat{B}_0^{-1*})} \left\| B - \hat{B}_0^{-1} \right\|_F ,$$

where $\|\cdot\|_F$ denotes the Frobenius norm; see Remark 4.3.1 for a comment. Next, compute the bootstrap impulse response $\hat{\Theta}_{ij,h}^* := f_{ij,h} \left(\hat{A}_1^*, \dots, \hat{A}_p^*, \hat{\hat{B}}_0^{-1*} \right)$.

- f) Repeat steps b) to d) B times and obtain the empirical bootstrap sampling distribution $\left\{ \hat{\Theta}_{ij,h,b}^* - \hat{\Theta}_{ij,h} \right\}_{b=1}^B$ for each propagation horizon $h \in \{0, \dots, H\}$. Determine the marginal percentile intervals by

$$\left[\hat{\Theta}_{ij,h} - \tilde{q}_{h,(1-\alpha/2)}^*; \hat{\Theta}_{ij,h} - \tilde{q}_{h,\alpha/2}^* \right] ,$$

where $\tilde{q}_{h,(1-\alpha/2)}^*$ and $\tilde{q}_{h,\alpha/2}^*$ are the empirical $(1 - \alpha/2)$ - and $(\alpha/2)$ -quantiles, respectively, of $\left\{ \hat{\Theta}_{ij,h,b}^* - \hat{\Theta}_{ij,h} \right\}_{b=1}^B$.

Remark 4.3.1 The replacement of \hat{B}_0^{-1*} with $\hat{\hat{B}}_0^{-1*}$ in step e) of the residual bootstrap ensures that the bootstrap structural impulse response estimator $\hat{\Theta}_{ij,h}^*$ is computed based on the particular matrix $\hat{\hat{B}}_0^{-1*} \in \mathcal{E}(\hat{B}_0^{-1*})$ that is closest to the matrix $\hat{\hat{B}}_0^{-1}$ which is at the basis of the structural impulse response estimator $\hat{\Theta}_{ij,h}$. In this way, the particular bootstrap VMA representation (characterized by $\hat{\hat{B}}_0^{-1*}$) is selected that is most similar to the VMA representation characterized by $\hat{\hat{B}}_0^{-1}$. ■

We also consider a modified version of the residual bootstrap procedure. The modified version, subsequently referred to as the *symmetrized residual bootstrap*, is obtained by the following modification in step c): $\hat{e}_{t,i}^*$ is a random draw with replacement from the empirical distribution of the *symmetrized series* $\{\tilde{e}_{1,i}, \dots, \tilde{e}_{2T,i}\} := \{\pm \check{e}_{1,i}, \dots, \pm \check{e}_{T,i}\}$ of length $2T$ instead of the empirical distribution of $\{\check{e}_{1,i}, \dots, \check{e}_{T,i}\}$ as in the residual bootstrap; see Appendix 4C for details.

The modification serves the purpose to ensure that the empirical skewness of the series $\{\tilde{e}_{1,i}, \dots, \tilde{e}_{2T,i}\}$ is zero. Furthermore, note that the first and the second empirical moment

of $\{\tilde{e}_{1,i}, \dots, \tilde{e}_{2T,i}\}$ is equal to zero and one, respectively, due to the preceding centering and rescaling in step b). Thus, in scenarios where the true distribution of $e_{t,i}$ is symmetric around zero (e.g. $e_{t,i} \sim \mathcal{N}(0, 1)$), and hence exhibits a skewness of zero⁷, the empirical distribution of $\{\tilde{e}_{1,i}, \dots, \tilde{e}_{2T,i}\}$ matches not only the first and the second moment but also the skewness of the true distribution of $e_{t,i}$. Eventually, this modification results in improved finite-sample properties of the corresponding confidence intervals in these scenarios.

4.4 Competing Methods

In order to assess the finite-sample performance of the residual bootstrap and the symmetrized residual bootstrap, we compare their finite-sample properties with two competing procedures: (i) the standard i.i.d. bootstrap originally proposed by [Runkle \(1987\)](#) and (ii) the moving-block bootstrap proposed in [Brüggemann et al. \(2016\)](#). In the following, the two competing procedures are briefly outlined.

4.4.1 I.i.d. Bootstrap

- a) Generate the bootstrap sample $\{y_1^*, \dots, y_T^*\}$ according to

$$y_t^* := \hat{\nu} + \hat{A}_1 y_{t-1}^* + \dots + \hat{A}_p y_{t-p}^* + \tilde{u}_t^*, \quad t = 1, \dots, T,$$

where \tilde{u}_t^* is a random draw with replacement from the empirical distribution of the centered and rescaled (reduced-form) residuals⁸. The starting values are equal to the pre-sample of the original series $\{y_{-p+1}, \dots, y_0\}$.

- b) identical to step e) of the residual bootstrap.
c) identical to step f) of the residual bootstrap.

4.4.2 Moving Block Bootstrap

- a) Choose a block length $l < T$ and let $N := \lceil T/l \rceil$ denote the number of blocks. Define

$B_{i,l} := (\hat{u}_{i+1}, \dots, \hat{u}_{i+l}), i = 0, \dots, T-l$ and let i_1, \dots, i_N be i.i.d. random variables

⁷Here, we tacitly assume that $\mathbb{E}[e_{t,i}^3] < +\infty$.

⁸The centering and rescaling is carried out as suggested in [Stine \(1987\)](#).

uniformly distributed on the set $\{0, 1, \dots, T - l\}$. Obtain $\{\hat{u}_1^*, \dots, \hat{u}_T^*\}$ by laying blocks $B_{i_1, l}, \dots, B_{i_N, l}$ end-to-end together and discard the last $Nl - T$ observations.

b) Center $\{\hat{u}_1^*, \dots, \hat{u}_T^*\}$ according to

$$\check{u}_{jl+s}^* := \hat{u}_{jl+s}^* - \frac{1}{T - l + 1} \sum_{r=0}^{T-l} \hat{u}_{s+r}^*, t = 1, \dots, T, \quad (4.17)$$

for $s = 1, 2, \dots, l$ and $j = 0, 1, 2, \dots, N - 1$.

c) Generate the bootstrap sample $\{y_1^*, \dots, y_T^*\}$ according to

$$y_t^* := \hat{\nu} + \hat{A}_1 y_{t-1}^* + \dots + \hat{A}_p y_{t-p}^* + \check{u}_t^*, t = 1, \dots, T,$$

where the starting values are equal to the pre-sample of the original series $\{y_{-p+1}, \dots, y_0\}$.

d) identical to step e) of the residual bootstrap.

e) identical to step f) of the residual bootstrap.

In the Monte Carlo simulations, the block lengths are given by $l \in \{10, 20, 50, 75, 200\}$ for sample sizes $T \in \{100, 250, 500, 1000, 5000\}$. For $T \in \{500, 5000\}$, the block lengths are as in [Brüggemann et al. \(2016\)](#). The sample sizes $T \in \{100, 250, 1000\}$ are not considered in their study, and hence the block lengths are found via interpolation.

4.5 Monte Carlo Simulation

4.5.1 Data Generating Processes

We consider the following bivariate model from [Brüggemann et al. \(2016\)](#), that is,

$$\text{DGP-1} \quad y_t = A_1 y_{t-1} + A_2 y_{t-2} + B_0^{-1} \varepsilon_t, \quad (4.18)$$

where

$$A_1 := \begin{pmatrix} 0.40 & 0.60 \\ -0.10 & 1.20 \end{pmatrix}, \quad A_2 := \begin{pmatrix} -0.20 & 0.00 \\ -0.20 & -0.10 \end{pmatrix} \quad \text{and} \quad B_0^{-1} := \begin{pmatrix} 1.00 & 0.00 \\ 0.50 & \sqrt{0.75} \end{pmatrix}.$$

The moduli of the roots of the characteristic polynomial of the VAR are given by 1.08, 2.78, and 5.98, which implies moderate persistence of the process $\{y_t : t \in \mathbb{Z}\}$. The following set of different GARCH(1, 1) specifications for the two components of $\{\varepsilon_t : t \in \mathbb{Z}\}$ are considered

$$\text{a) } (\alpha_1, \beta_1)' = (0.10, 0.80)'; \quad (\alpha_2, \beta_2)' = (0.20, 0.65)',$$

$$\text{b) } (\alpha_1, \beta_1)' = (0.10, 0.80)'; \quad (\alpha_2, \beta_2)' = (0.085, 0.90)',$$

$$\text{c) } (\alpha_1, \beta_1)' = (0.095, 0.90)'; \quad (\alpha_2, \beta_2)' = (0.25, 0.65)',$$

where the specific variants of DGP-1 will be denoted by DGP-1*i*, $i \in \{a, b, c\}$, depending on the specific choice of the GARCH specification.

The following two univariate distributions for the (mutually independent) components of the i.i.d. process $\{e_t : t \in \mathbb{Z}\}$ are considered:

- $e_{t,i} \sim \mathcal{N}(0, 1)$, standard normal distribution.
- $e_{t,i} \sim \frac{3}{5}t_5$, t -distribution with 5 degrees of freedom, scaled to have variance 1.

Under DGP-1*a*, the persistence of the GARCH processes, measured by $\alpha_i + \beta_i$, is given by 0.90 and 0.85, respectively which implies only moderate persistence. For both considered distributions of $e_{t,i}$, DGP1*a* implies a consistent estimator $\hat{\Theta}_{ij,h}$ of the structural impulse responses. Under DGP-1*b*, the persistence is given by 0.90 and 0.985, respectively. Similarly to DGP-1*a*, DGP-1*b* implies a consistent estimator $\hat{\Theta}_{ij,h}$ for both distributions of $e_{t,i}$. Under DGP-1*c*, the persistence of the GARCH processes is given by 0.995 and 0.90, respectively. The first component of ε_t does *not* have a finite fourth moment (for both distributions of $e_{t,i}$) and hence the assumptions underlying the consistency of $\hat{\Theta}_{ij,h}$ are violated. Hence, this DGP is included to investigate the sensitivity of the bootstrap procedure from deviations of the finite fourth moment assumption.

4.5.2 Simulation Parameters and Performance Evaluation

Data samples of length $T \in \{100, 250, 500, 1000, 5000\}$ are generated and the maximum propagation horizon is $H = 12$. The nominal confidence level of the marginal confidence bands is 90%. The number of bootstrap replications is $B = 1000$ throughout and the

number of Monte Carlo replications is 1000. The finite-sample performance of the confidence intervals is evaluated by the empirical coverage rate and the empirical length. In particular, the empirical coverage rate is computed in the usual way as

$$EC_{ij,h} := \frac{1}{1000} \sum_{m=1}^{1000} \mathbb{1}_{\{\Theta_{ij,h} \in CI_{ij,h,m}\}} ,$$

where $CI_{ij,h}$ denotes the marginal confidence interval for $\Theta_{ij,h}$ and $\mathbb{1}_{\{A\}}$ denotes the indicator function of an event A . The empirical length is computed as

$$L_{ij,h} := \frac{1}{1000} \sum_{m=1}^{1000} (u_{ij,h,m} - l_{ij,h,m}) ,$$

where $u_{ij,h,m}$ denotes the upper bound of the marginal confidence interval for $\Theta_{ij,h}$ and $l_{ij,h,m}$ denotes the corresponding lower bound.

4.5.3 Results

The boxplots summarizing the performance of the four different bootstrap methods across different scenarios are found in Appendices 4E, 4F and 4G. The tables with the simulation results (empirical coverage rates and empirical lengths) are available from the authors upon request. The main conclusions are as follows:

- Under DGP-1a with $e_{t,i} \sim \mathcal{N}(0,1)$ and $T = 100$, the empirical coverage rates of the confidence intervals based on the residual bootstrap exhibit a large dispersion among propagation horizons h and impulse responses ranging from 63.60% to 96.90%. Yet, increasing the sample size T results in a substantial reduction in the coverage bias and its dispersion. For $T = 5000$, the range of the coverage rates of the confidence intervals is given by 86.90% to 96.00%. Heavy-tailed GARCH errors, that is, $e_{t,i} \sim \frac{3}{5}t_5$, increase the coverage bias of the residual bootstrap especially for $T \in \{1000, 5000\}$.

The higher persistence in the GARCH process of $\varepsilon_{t,2}$ in DGP-1b has an overall negative effect on the coverages rates of the intervals based on the residual bootstrap, but the negative effect is more pronounced for impulse responses where the shock occurs in the second variable, that is, $\Theta_{12,h}$ and $\Theta_{22,h}$. For $T = 100$ and $e_{t,i} \sim \mathcal{N}(0,1)$, the

coverage rates range from 36.90% to 93.50%. The negative coverage bias of the residual bootstrap is decreasing in the sample size T but even with $T = 5000$ the range of the coverage rates is 77.10% to 96.40%. The heavy-tailed GARCH errors ($e_{t,i} \sim \frac{3}{5}t_5$) result in larger coverage biases for all sample sizes, where the negative effect is more pronounced than under the less persistent DGP-1a.

The non-finite fourth moment of $\varepsilon_{t,1}$ in DGP-1c has also an overall negative effect on the coverage rates of the residual bootstrap. The strongest effect is on the intervals for $\Theta_{11,0}$ and $\Theta_{11,1}$. For $T = 100$ and $e_{t,i} \sim \mathcal{N}(0, 1)$, the coverage rates for $\Theta_{11,0}$ and $\Theta_{11,1}$ are 4.40% and 27.80%, respectively, whereas the remaining coverage rates range from 61.00% to 95.30%. The effect of an increase in the sample size T is ambiguous; increasing the sample size to $T \in \{250, 500\}$ results in an overall reduction of the coverage bias of the confidence intervals, but after that, a further increase to $T \in \{1000, 5000\}$ results either in nearly no improvement or even in a deterioration of the performance (compared to the $T = 500$ scenario). Similarly to DGP-1a and DGP-1b, heavy-tailed GARCH errors result in an increase in the coverage bias.

- Overall, the symmetrized residual bootstrap exhibits a very similar performance as the residual bootstrap. Hence, the symmetrized residual bootstrap is not capable of systematically outperforming the residual bootstrap, although both considered distributions of $e_{t,i}$ are symmetric around zero.
- Under DGP-1a with $e_{t,i} \sim \mathcal{N}(0, 1)$ and $T = 100$, similar to the residual bootstrap, the empirical coverage rates of the confidence intervals based on the i.i.d. bootstrap exhibit a large dispersion among propagation horizons h and impulse responses ranging from 63.40% to 96.70%. Increasing the sample size T results in higher empirical coverage rates of the intervals based on the i.i.d. bootstrap. For $T = 5000$, the coverage rates range between 79.80% and 99.30%, however, the majority of confidence intervals exhibit coverage rates above the nominal level of 90%. The effect of heavy-tailed GARCH errors is drastic; the confidence intervals for 42 (out of 52) impulse responses exhibit a lower coverage rate with $T = 5000$ than with $T = 100$.

Under DGP-1*b*, the performance of the i.i.d. bootstrap is basically similar to DGP-1*a* except that the dispersion of the coverage rates among the propagation horizons and the structural impulse responses is more pronounced. For $T = 100$ and $e_{t,i} \sim \mathcal{N}(0, 1)$, the coverage rates range between 36.30% and 92.40% and with $T = 5000$, the range is still given by 62.90% to 100.00%. The effect of heavy-tailed GARCH errors is again disastrous. Even for the very large sample size $T = 5000$, the coverage rates of the intervals based on the i.i.d bootstrap vary between 32.00% and 79.20%.

The violation of the finite fourth moment assumption (DGP-1*c*) exhibits an overall negative effect on the confidence intervals based on the i.i.d. bootstrap. Similar to the residual bootstrap, the intervals for $\Theta_{11,0}$ and $\Theta_{11,1}$ are the most affected with coverage rates of 3.3% and 30.50% for $T = 100$ and $e_{t,i} \sim \mathcal{N}(0, 1)$. Moreover, the behavior of the coverage rates depending on the sample size is erratic; for some impulse responses the coverage rate of the corresponding interval is increasing in the sample size and for others the coverage rate is indeed decreasing in the sample size. Heavy-tailed GARCH errors result in an overall performance that is decreasing with the sample size T .

- Under DGP-1*a* with $e_{t,i} \sim \mathcal{N}(0, 1)$ and $T = 100$, the empirical coverage rates of the confidence intervals based on the moving block bootstrap also exhibit a large dispersion among propagation horizons h and impulse responses ranging from 61.00% to 92.00%. The overall coverage bias is decreasing for sample sizes $T \in \{250, 500, 1000\}$ but a further increase to $T = 5000$ exhibits an ambiguous effect on the coverage rates of the moving block bootstrap. For $T = 5000$, the range of the coverage rates is given by 76.70% to 89.90%. Heavy-tailed GARCH errors result in a downward shift of the coverage rates of the confidence intervals based on the moving block bootstrap; for $T = 5000$, the coverage rates vary between 70.00% and 87.00%.

The higher persistence of DGP-1*b* results in higher coverage biases and more dispersion. For $T = 100$ and $e_{t,i} \sim \mathcal{N}(0, 1)$, the coverage rates of the intervals based on the moving-block bootstrap are between 38.40% and 89.30%. Similar to DGP-1*a*, the overall performance continuously improves only for $T \in \{250, 500, 1000\}$. For $T = 5000$, the coverage rates range between 75.50% and 89.10%. Heavy-tailed GARCH errors increase the bias and the dispersion of the intervals based on the

moving block bootstrap.

Under DGP-1c, the violation of the finite fourth moment assumption exhibits an overall negative effect on the intervals based on the moving block bootstrap. Similar to the residual and the i.i.d. bootstrap, the intervals for $\Theta_{11,0}$ and $\Theta_{11,1}$ are the most affected with coverage rates of 2.70% and 26.20%, respectively for $T = 100$ and $e_{t,i} \sim \mathcal{N}(0, 1)$. The effect of an increasing sample size is ambiguous and depends on the particular impulse response under consideration. For $T = 5000$, the range of the coverage rates is 51.10% to 87.90%. Again, the heavy-tailed GARCH errors result in a deterioration of the performance of the confidence intervals based on the moving block bootstrap.

- The confidence intervals based on the residual bootstrap exhibits the smallest absolute deviation from the nominal level in 1188 out of the 1560 scenarios. The intervals based on the i.i.d. bootstrap and the moving block bootstrap exhibit the smallest absolute deviation in only 199/1560 and 173/1560 scenarios, respectively⁹. Hence, the residual bootstrap exhibits the best overall performance in terms of the coverage bias.
- For the small sample size $T = 100$, neither of the bootstrap methods is capable of reliably producing a bootstrap sampling distribution that constitutes a good approximation of the true sampling distribution. Hence, the resulting confidence intervals eventually understate the actual estimation uncertainty; see Appendix 4H for an analysis of the bootstrap sampling distributions as a function of the sample size.
- The results of the Monte Carlo simulations confirm the result from Brüggemann et al. (2016) that the presence of heteroskedasticity substantially increases the estimation uncertainty.

⁹The symmetrized residual bootstrap is omitted in this comparison because it is a modification of the residual bootstrap.

4.6 Conclusion

A recent strand of the literature exploits conditional heteroskedasticity to identify the structural vector autoregressions. However, the implications for inference on structural impulse responses have not been investigated in the literature yet.

In this paper, we have considered the conditionally heteroskedastic SVAR-GARCH model. We have proposed (i) an estimation procedure of the model parameters that offers numerical stability even in small sample and/or high dimension scenarios and (ii) a bootstrap procedure to construct marginal percentile confidence intervals for structural impulse responses.

By means of a Monte Carlo simulation, we have compared the finite-sample properties of our proposed bootstrap method to those of two benchmarking methods: the i.i.d. bootstrap of [Runkle \(1987\)](#) and the moving block bootstrap of [Brüggemann et al. \(2016\)](#). The confidence intervals based on our proposed bootstrap method exhibits the best overall performance. Nevertheless, the intervals may understate the estimation uncertainty by a substantial amount especially in small samples.

References

- Bollerslev, T. (1986). Generalized autoregressive conditional heteroskedasticity. *Journal of Econometrics*, 31(3):307–327.
- Boswijk, H. P. and van der Weide, R. (2011). Method of moments estimation of GO-GARCH models. *Journal of Econometrics*, 163(1):118–126.
- Bouakez, H., Chihi, F., and Normandin, M. (2014). Measuring the effects of fiscal policy. *Journal of Economic Dynamics and Control*, 47:123–151.
- Bouakez, H., Essid, B., and Normandin, M. (2013). Stock returns and monetary policy: Are there any ties? *Journal of Macroeconomics*, 36:33–50.
- Bouakez, H. and Normandin, M. (2010). Fluctuations in the foreign exchange market: How important are monetary policy shocks? *Journal of International Economics*, 81(1):139–153.
- Boussama, F., Fuchs, F., and Stelzer, R. (2011). Stationarity and geometric ergodicity of BEKK multivariate GARCH models. *Stochastic Processes and their Applications*, 121(10):2331 – 2360.
- Brüggemann, R., Jentsch, C., and Trenkler, C. (2016). Inference in VARs with conditional heteroskedasticity of unknown form. *Journal of Econometrics*, 191(1):69–85.
- Engle, R. F. and Kroner, K. F. (1995). Multivariate simultaneous generalized ARCH. *Econometric Theory*, 11(1):122–150.
- Flury, B. N. and Gautschi, W. (1986). An algorithm for simultaneous orthogonal transformation of several positive definite symmetric matrices to nearly diagonal form. *SIAM Journal on Scientific and Statistical Computing*, 7(1):169–184.
- Francq, C. and Raïssi, H. (2007). Multivariate Portmanteau test for autoregressive models with uncorrelated but nonindependent errors. *Journal of Time Series Analysis*, 28(3):454–470.
- Hall, P. (1992). *The Bootstrap and Edgeworth Expansion*. Springer, New York.

- He, C. and Teräsvirta, T. (1999). Fourth moment structure of the GARCH(p, q) process. *Econometric Theory*, 15(6):824–846.
- Herwartz, H. and Lütkepohl, H. (2014). Structural vector autoregressions with markov switching: Combining conventional with statistical identification of shocks. *Journal of Econometrics*, 183(1):104–116.
- Hill, J. B. (2015). Robust estimation and inference for heavy tailed GARCH. *Bernoulli*, 21(3):1629–1669.
- Hwang, S. and Pereira, P. L. V. (2006). Small sample properties of GARCH estimates and persistence. *European Journal of Finance*, 12(6-7):473–494.
- Kilian, L. (1998a). Accounting for lag order uncertainty in autoregressions: the endogenous lag order bootstrap algorithm. *Journal of Time Series Analysis*, 19(5):531–548.
- Kilian, L. (1998b). Small-sample confidence intervals for impulse response functions. *Review of Economics and Statistics*, 80(2):218–230.
- Kilian, L. (2013). Structural vector autoregressions. In *Handbook of Research Methods and Applications in Empirical Macroeconomics*, chapter 22, pages 515–554. Edward Elgar Publishing.
- Kilian, L. and Lütkepohl, H. (2017). *Structural Vector Autoregressive Analysis*. Themes in Modern Econometrics. Cambridge University Press.
- Kristensen, D. and Linton, O. (2006). A closed-form estimator for the GARCH(1,1) model. *Econometric Theory*, 22(2):323–337.
- Künsch, H. R. (1989). The jackknife and the bootstrap for general stationary observations. *Annals of Statistics*, 17(3):1217–1241.
- Lanne, M., Lütkepohl, H., and Maciejowska, K. (2010). Structural vector autoregressions with markov switching. *Journal of Economic Dynamics and Control*, 34(2):121–131.
- Lanne, M. and Saikkonen, P. (2007). A multivariate generalized orthogonal factor GARCH model. *Journal of Business & Economic Statistics*, 25(1):61–75.

- Lütkepohl, H. (2005). *New Introduction to Multiple Time Series Analysis*. Springer, Berlin.
- Lütkepohl, H. and Milunovich, G. (2016). Testing for identification in SVAR-GARCH models. *Journal of Economic Dynamics and Control*, 73:241 – 258.
- Lütkepohl, H. and Netsunajev, A. (2017). Structural vector autoregressions with heteroskedasticity: A review of different volatility models. *Econometrics and Statistics*, 1:2 – 18.
- Milunovich, G. (2014). Complete and partial identification of the A-and B-models in the context of heteroskedastic SVARs. Available at SSRN: <http://ssrn.com/abstract=2484300>.
- Normandin, M. and Phaneuf, L. (2004). Monetary policy shocks: Testing identification conditions under time-varying conditional volatility. *Journal of Monetary Economics*, 51(6):1217–1243.
- Preminger, A. and Storti, G. (2017). Least-squares estimation of GARCH(1,1) models with heavy-tailed errors. *Econometrics Journal*, 20(2):221–258.
- Runkle, D. E. (1987). Vector autoregressions and reality. *Journal of Business & Economic Statistics*, 5(4):437–442.
- Shimizu, K. (2010). *Bootstrapping stationary ARMA-GARCH models*. Springer, Berlin.
- Stine, R. A. (1987). Estimating properties of autoregressive forecasts. *Journal of the American Statistical Association*, 82(400):1072–1078.
- van der Weide, R. (2002). GO-GARCH: A multivariate generalized orthogonal GARCH model. *Journal of Applied Econometrics*, 17(5):549–564.

Appendix

4A Method-of-Moment Estimator of GO-GARCH Models

The following algorithm describes the computation of the method of moment estimator \hat{B}_0^{-1} outlined in [Boswijk and van der Weide \(2011\)](#) based on the series of reduced-form residuals $\{\hat{u}_1, \dots, \hat{u}_T\}$.

1. Based on $\{\hat{u}_1, \dots, \hat{u}_T\}$, estimate the unconditional variance matrix $\hat{\Sigma}_u := T^{-1} \sum_{t=1}^T \hat{u}_t \hat{u}_t'$ and obtain its symmetric square root \hat{S} . Next, compute the standardized series $s_t := \hat{S}^{-1} \hat{u}_t$, $t = 1, \dots, T$.
2. Obtain the matrix-valued series $S_t := s_t s_t' - I_m$, $t = 1, \dots, T$, and the sample auto-covariance matrices $\hat{\Gamma}(k) := T^{-1} \sum_{t=1}^T S_t S_{t-k}'$, $k = 1, \dots, \tilde{k}$. Next, obtain the sample auto-correlation matrices

$$\hat{\Phi}(k) := \hat{\Gamma}(0)^{-1/2} \hat{\Gamma}(k) \hat{\Gamma}(0)^{-1/2}, k = 1, \dots, \tilde{k},$$

where $\hat{\Gamma}(0)^{-1/2}$ denotes the symmetric square root of $\hat{\Gamma}(0)^{-1}$. Next, obtain the symmetrized sample auto-correlation matrices $\tilde{\Phi}(k) := \frac{1}{2}(\hat{\Phi}(k) + \hat{\Phi}(k)')$, $k = 1, \dots, \tilde{k}$.

3. The estimator \hat{U} is then obtained by minimizing the following objective function

$$S(U) := \sum_{k=1}^{\tilde{k}} \text{tr} \left(U' \tilde{\Phi}(k) U - \text{diag}(U' \tilde{\Phi}(k) U) \right)' \times \text{tr} \left(U' \tilde{\Phi}(k) U - \text{diag}(U' \tilde{\Phi}(k) U) \right),$$

over all orthogonal matrices U , where $\text{tr}(\cdot)$ denotes the trace operator. The solution to the minimization problem is obtained via the F-G algorithm of [Flury and Gautschi \(1986\)](#).

4. Compute the estimator $\hat{B}_0^{-1} := \hat{S} \hat{U}$.

4B Least-Squares Estimator of Univariate GARCH(1,1) Models

The following algorithm describes the computation of the least-squares estimator $(\hat{\alpha}_i, \hat{\beta}_i)'$ outlined in [Preminger and Storti \(2017\)](#) of the i -th GARCH process based on the series of structural errors $\{\hat{\varepsilon}_{1,i}, \dots, \hat{\varepsilon}_{T,i}\}$.

1. Using the univariate series $\{\hat{\varepsilon}_{1,i}, \dots, \hat{\varepsilon}_{T,i}\}$, estimate the GARCH parameters $(\alpha_i, \beta_i)'$ via the quasi-maximum tail-trimmed likelihood (QMTTL) estimator of Hill (2015, p.7); see Remark 4.6.1. Obtain the corresponding devolatilized residuals $\hat{e}_{t,i} := \hat{\varepsilon}_{1,i}/\hat{\sigma}_{t,i}, t = 1, \dots, T$, where $\hat{\sigma}_{t,i}$ denotes the estimate based on the QMTTL estimator. Next, compute

$$\hat{c}_T := \frac{1}{T} \sum_{t=1}^T \log(\hat{e}_{t,i}^2) .$$

2. The least-squares estimator $(\hat{\alpha}_i, \hat{\beta}_i)$ of Preminger and Storti (2017) is then obtained by minimizing the following objective function

$$Q_T(\tilde{\alpha}, \tilde{\beta}; \hat{c}_T) := \frac{1}{T} \sum_{t=1}^T \left(\log(\hat{\varepsilon}_{t,i}^2) - \hat{c}_T - \log(\hat{\sigma}_{t,i}^2(\tilde{\alpha}, \tilde{\beta})) \right)^2 ,$$

that is, $(\hat{\alpha}_i, \hat{\beta}_i) := \arg \min_{(\tilde{\alpha}, \tilde{\beta})' \in \Theta} Q_T(\tilde{\alpha}, \tilde{\beta}; \hat{c}_T)$.

Remark 4.6.1 Preminger and Storti (2017) use the standard quasi-maximum likelihood estimator $(\hat{\alpha}_i^{\text{QML}}, \hat{\beta}_i^{\text{QML}})'$ in the first step instead of the QMTTL estimator of Hill (2015). We replaced the standard QML estimator with the QMTTL estimator of Hill (2015) because the aforementioned estimator enjoys improved convergence properties in small samples compared to the standard QML estimator. ■

4C Symmetrized Residual Bootstrap

- a) identical to the residual bootstrap.
- b) identical to the residual bootstrap.
- c) For each component $i = 1, \dots, m$, generate the univariate bootstrap sample $\{\hat{\varepsilon}_{1,i}^*, \dots, \hat{\varepsilon}_{T,i}^*\}$ according to

$$\begin{aligned} \hat{\varepsilon}_{t,i}^* &= \hat{\sigma}_{t,i}^* \hat{e}_{t,i}^* \\ \hat{\sigma}_{t,i}^{*2} &= (1 - \hat{\alpha}_i - \hat{\beta}_i) + \hat{\alpha}_i \hat{\varepsilon}_{t-1,i}^{*2} + \hat{\beta}_i \hat{\sigma}_{t-1,i}^{*2} , \end{aligned}$$

where $\hat{e}_{t,i}^*$ is a random draw with replacement from the univariate empirical distribution of the symmetrized series $\{\tilde{e}_{1,i}, \dots, \tilde{e}_{2T,i}\} := \{\pm\check{e}_{1,i}, \dots, \pm\check{e}_{T,i}\}$ of length $2T$. The starting values are $\hat{\varepsilon}_{0,i}^{*2} = \hat{\sigma}_{0,i}^{*2} = (1 - \hat{\alpha}_i - \hat{\beta}_i)$. Next, obtain the series of bootstrap residuals $\{\hat{u}_1^*, \dots, \hat{u}_T^*\}$ via $u_t^* = \hat{B}_0^{-1} \hat{\varepsilon}_t^*$, $t = 1, \dots, T$.

- d) identical to the residual bootstrap.
- e) identical to the residual bootstrap.
- f) identical to the residual bootstrap.

4D RMSE

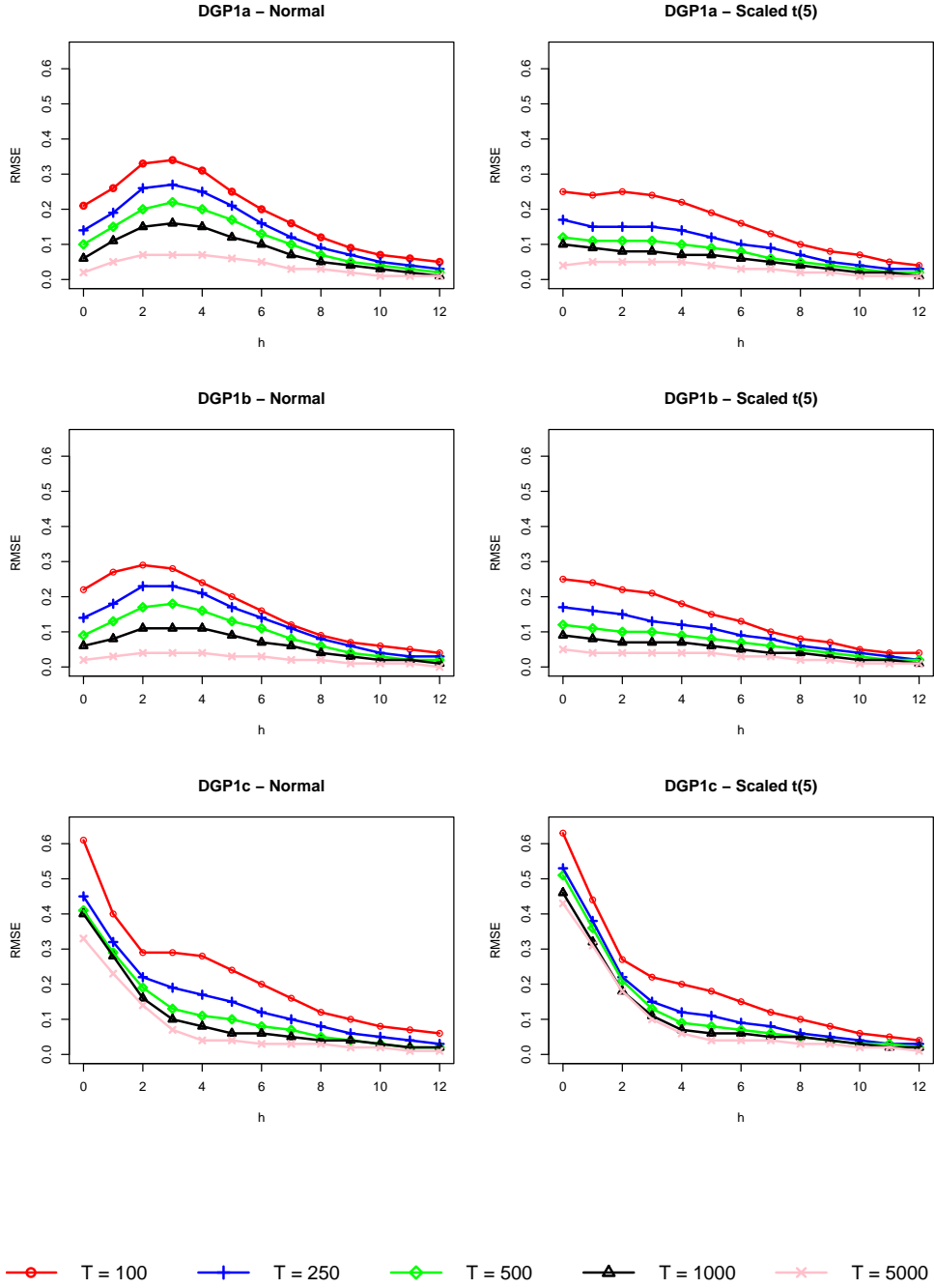


Figure 4A.1: Root mean squared error (RMSE) of $\hat{\Theta}_{11,h}$ for propagation horizons $h \in \{0, \dots, 12\}$ with $T \in \{100, 250, 500, 1000, 5000\}$ based on 10,000 Monte Carlo repetitions.

4E DGP-1a

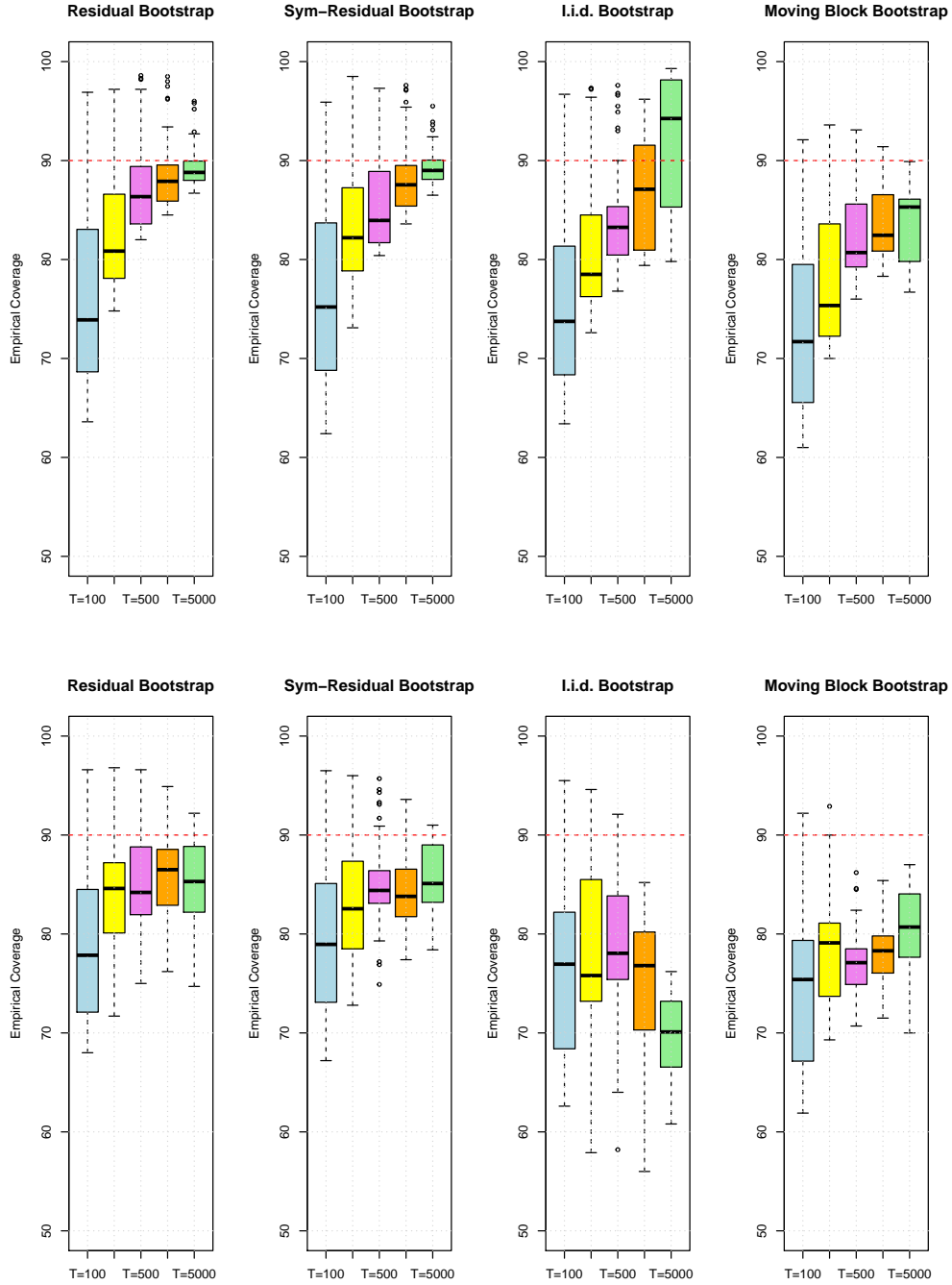


Figure 4A.2: Boxplots of the empirical coverages across all impulse responses and all propagation horizons (52 parameter constellations in total) of nominal 90% marginal confidence intervals for $T \in \{100, 250, 500, 1000, 5000\}$. The first row corresponds to $e_{t,i} \stackrel{\text{i.i.d.}}{\sim} \mathcal{N}(0, 1)$ and the second row corresponds to $e_{t,i} \stackrel{\text{i.i.d.}}{\sim} \frac{3}{5}t_5$.

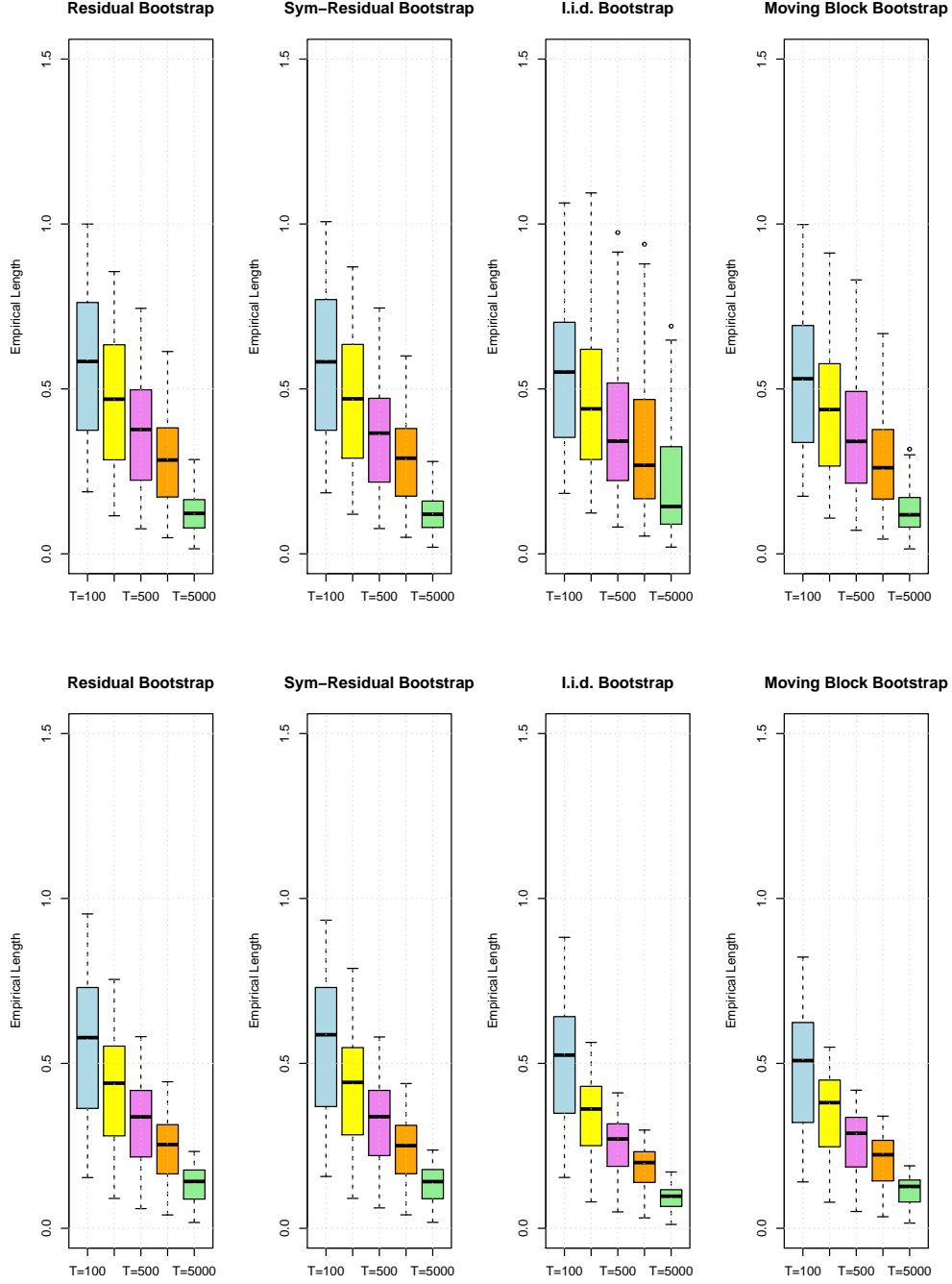


Figure 4A.3: Boxplots of the empirical lengths across all impulse responses and all propagation horizons (52 parameter constellations in total) of nominal 90% marginal confidence intervals for $T \in \{100, 250, 500, 1000, 5000\}$. The first row corresponds to $e_{t,i} \stackrel{\text{i.i.d.}}{\sim} \mathcal{N}(0, 1)$ and the second row corresponds to $e_{t,i} \stackrel{\text{i.i.d.}}{\sim} \frac{3}{5}t_5$.

4F DGP-1b

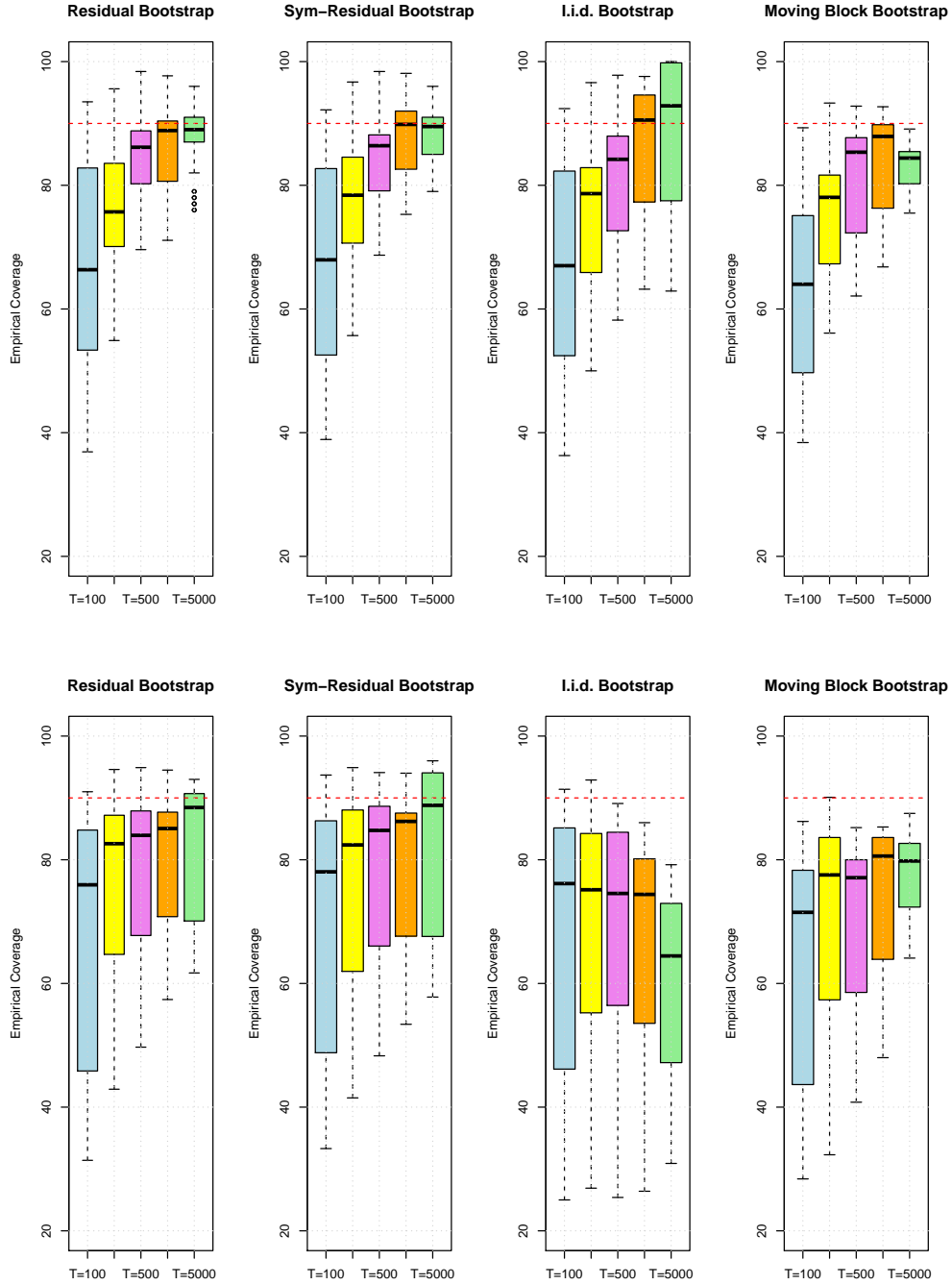


Figure 4A.4: Boxplots of the empirical coverages across all impulse responses and all propagation horizons (52 parameter constellations in total) of nominal 90% marginal confidence intervals for $T \in \{100, 250, 500, 1000, 5000\}$. The first row corresponds to $e_{t,i} \stackrel{\text{i.i.d.}}{\sim} \mathcal{N}(0, 1)$ and the second row corresponds to $e_{t,i} \stackrel{\text{i.i.d.}}{\sim} \frac{3}{5}t_5$.

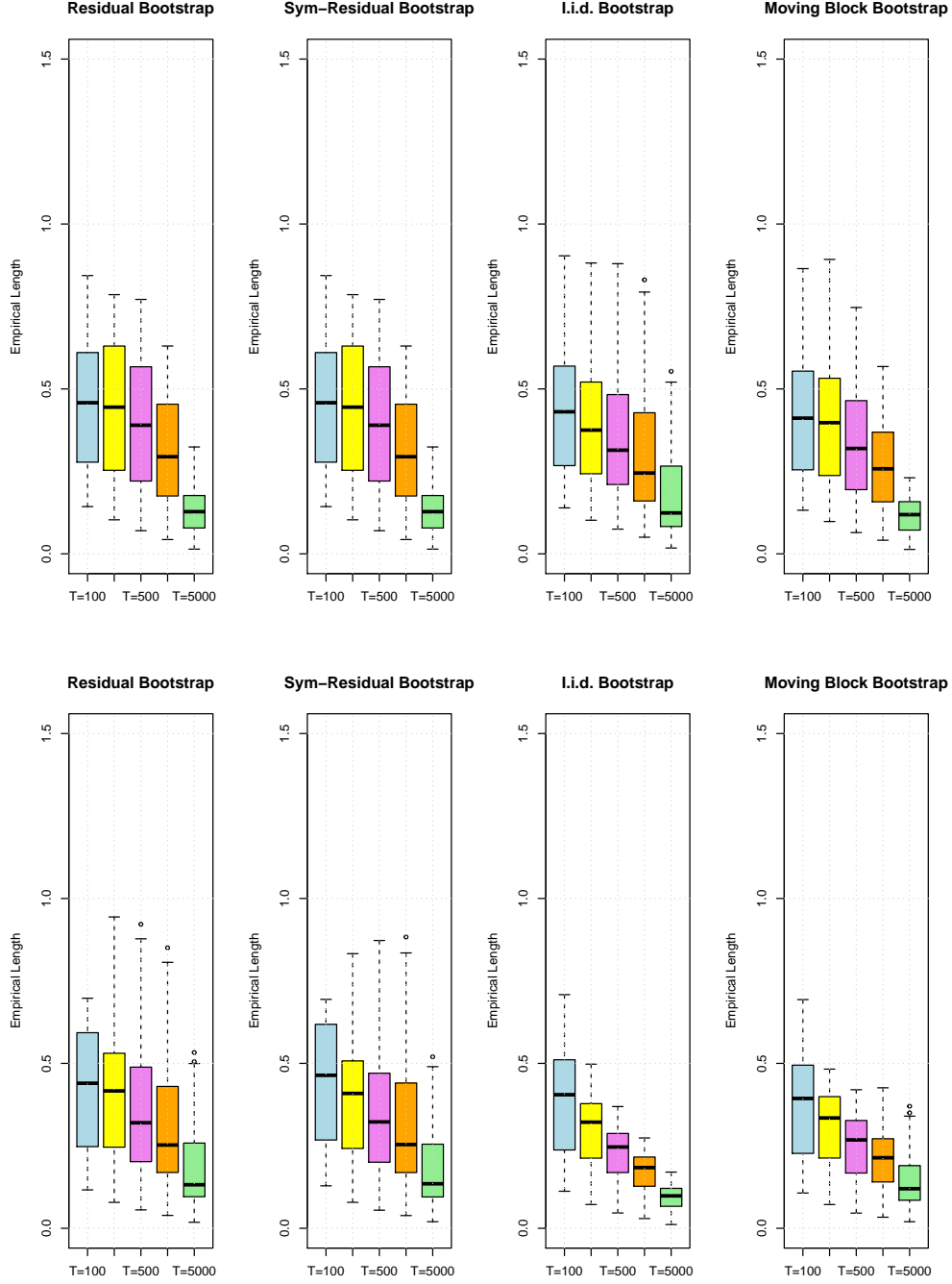


Figure 4A.5: Boxplots of the empirical lengths across all impulse responses and all propagation horizons (52 parameter constellations in total) of nominal 90% marginal confidence intervals for $T \in \{100, 250, 500, 1000, 5000\}$. The first row corresponds to $e_{t,i} \stackrel{\text{i.i.d.}}{\sim} \mathcal{N}(0, 1)$ and the second row corresponds to $e_{t,i} \stackrel{\text{i.i.d.}}{\sim} \frac{3}{5}t_5$.

4G DGP-1c

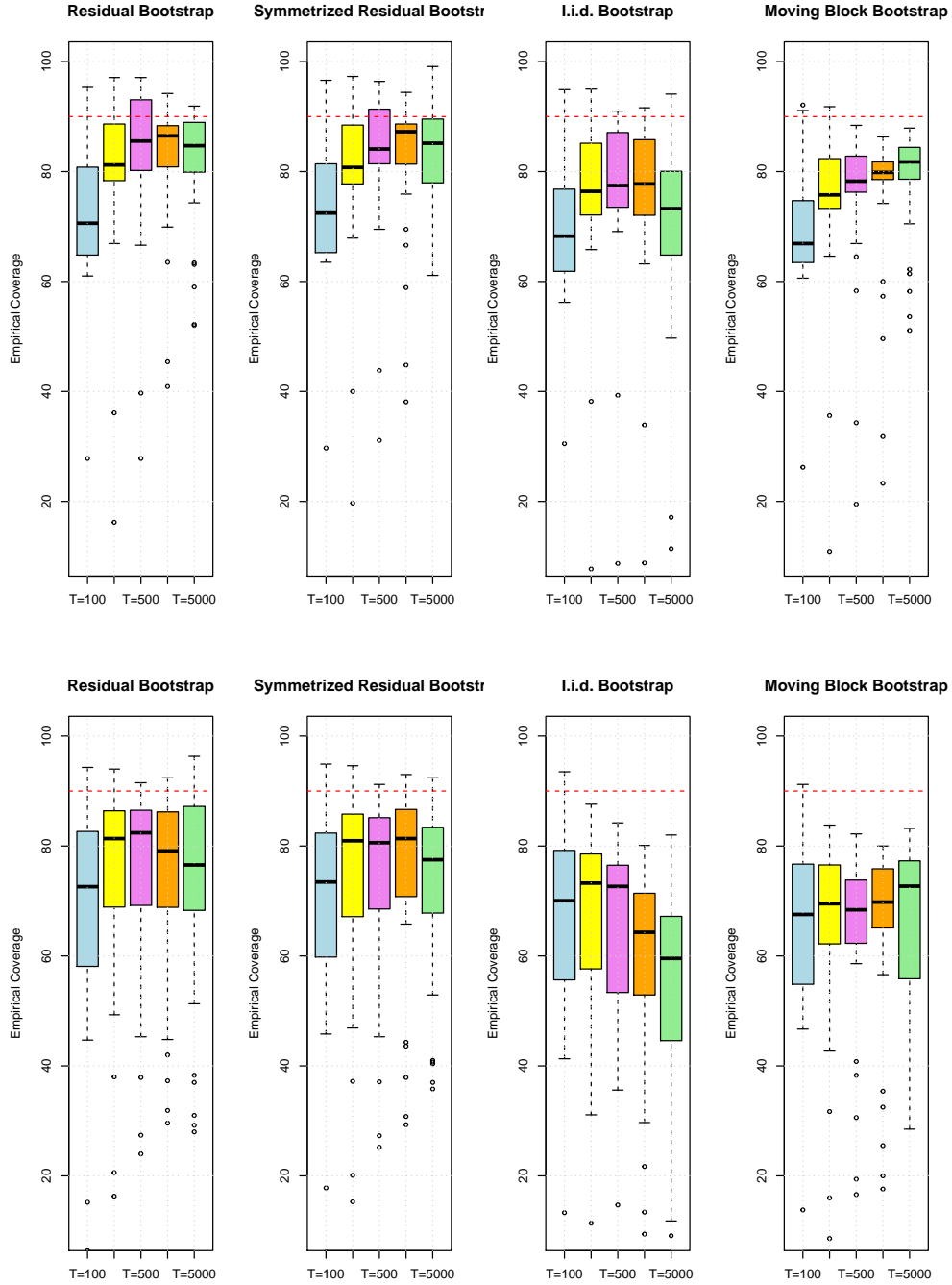


Figure 4A.6: Boxplots of the empirical coverages across all impulse responses and all propagation horizons (52 parameter constellations in total) of nominal 90% marginal confidence intervals for $T \in \{100, 250, 500, 1000, 5000\}$. The first row corresponds to $e_{t,i} \stackrel{\text{i.i.d.}}{\sim} \mathcal{N}(0,1)$ and the second row corresponds to $e_{t,i} \stackrel{\text{i.i.d.}}{\sim} \frac{3}{5}t_5$.

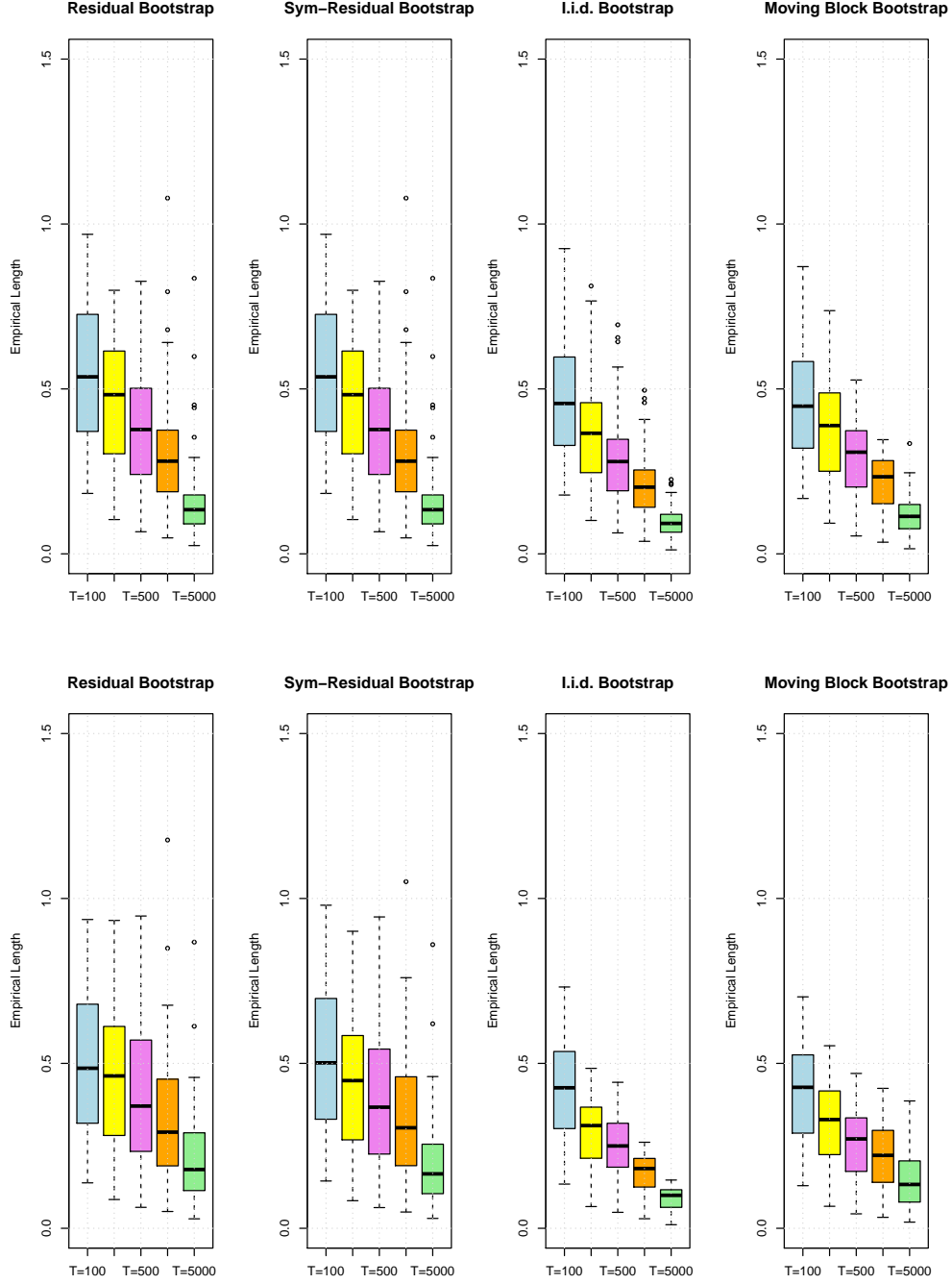


Figure 4A.7: Boxplots of the empirical lengths across all impulse responses and all propagation horizons (52 parameter constellations in total) of nominal 90% marginal confidence intervals for $T \in \{100, 250, 500, 1000, 5000\}$. The first row corresponds to $e_{t,i} \stackrel{\text{i.i.d.}}{\sim} \mathcal{N}(0, 1)$ and the second row corresponds to $e_{t,i} \stackrel{\text{i.i.d.}}{\sim} \frac{3}{5}t_5$.

4H Bootstrap

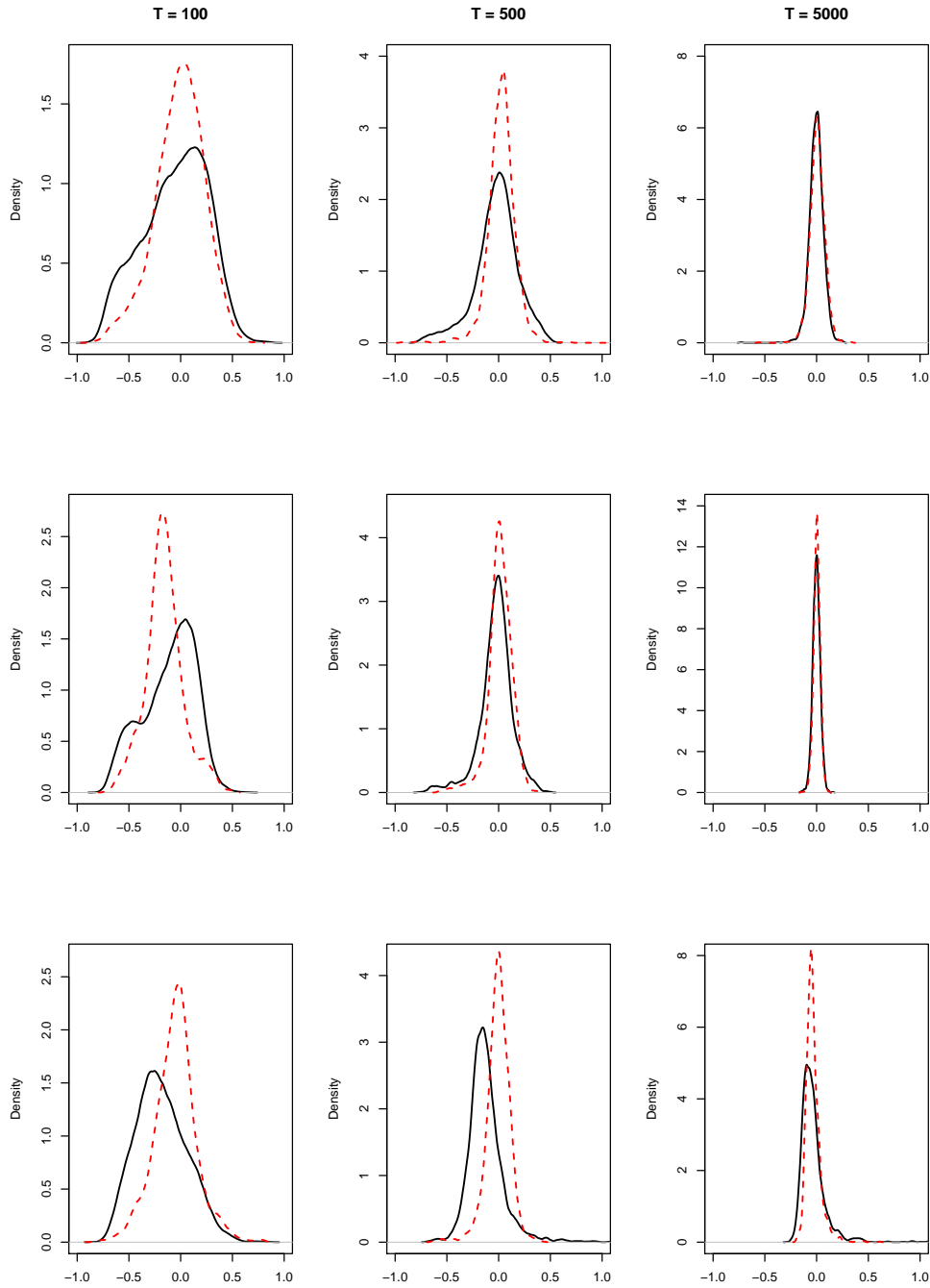


Figure 4A.8: The simulated density of the sampling distribution $\hat{\Theta}_{11,3} - \Theta_{11,3}$ (solid line) versus the simulated density of the bootstrap sampling distribution $\hat{\Theta}_{11,3}^* - \hat{\Theta}_{11,3}$ (dashed line) using the residual bootstrap. Both densities are estimated with the Epanechnikov kernel and based on 2'000 simulated observations. The first column corresponds to DGP-1a, the second column to DGP-1b and the third column to DGP-1c.

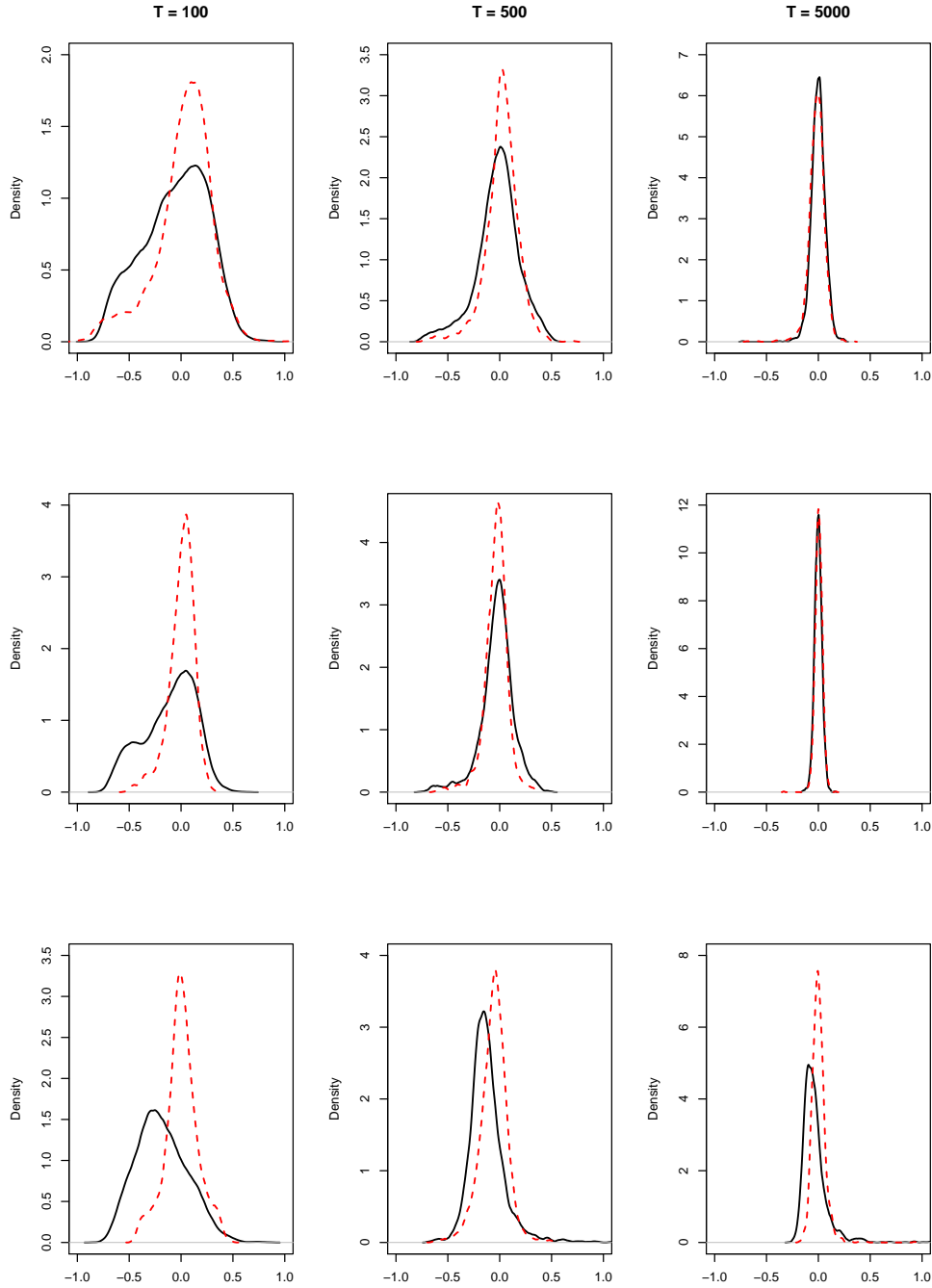


Figure 4A.9: The simulated density of the sampling distribution $\hat{\Theta}_{11,3} - \Theta_{11,3}$ (solid line) versus the simulated density of the bootstrap sampling distribution $\hat{\Theta}_{11,3}^* - \hat{\Theta}_{11,3}$ (dashed line) using the symmetrized residual bootstrap. Both densities are estimated with the Epanechnikov kernel and based on 2'000 simulated observations. The first column corresponds to DGP-1a, the second column to DGP-1b and the third column to DGP-1c.

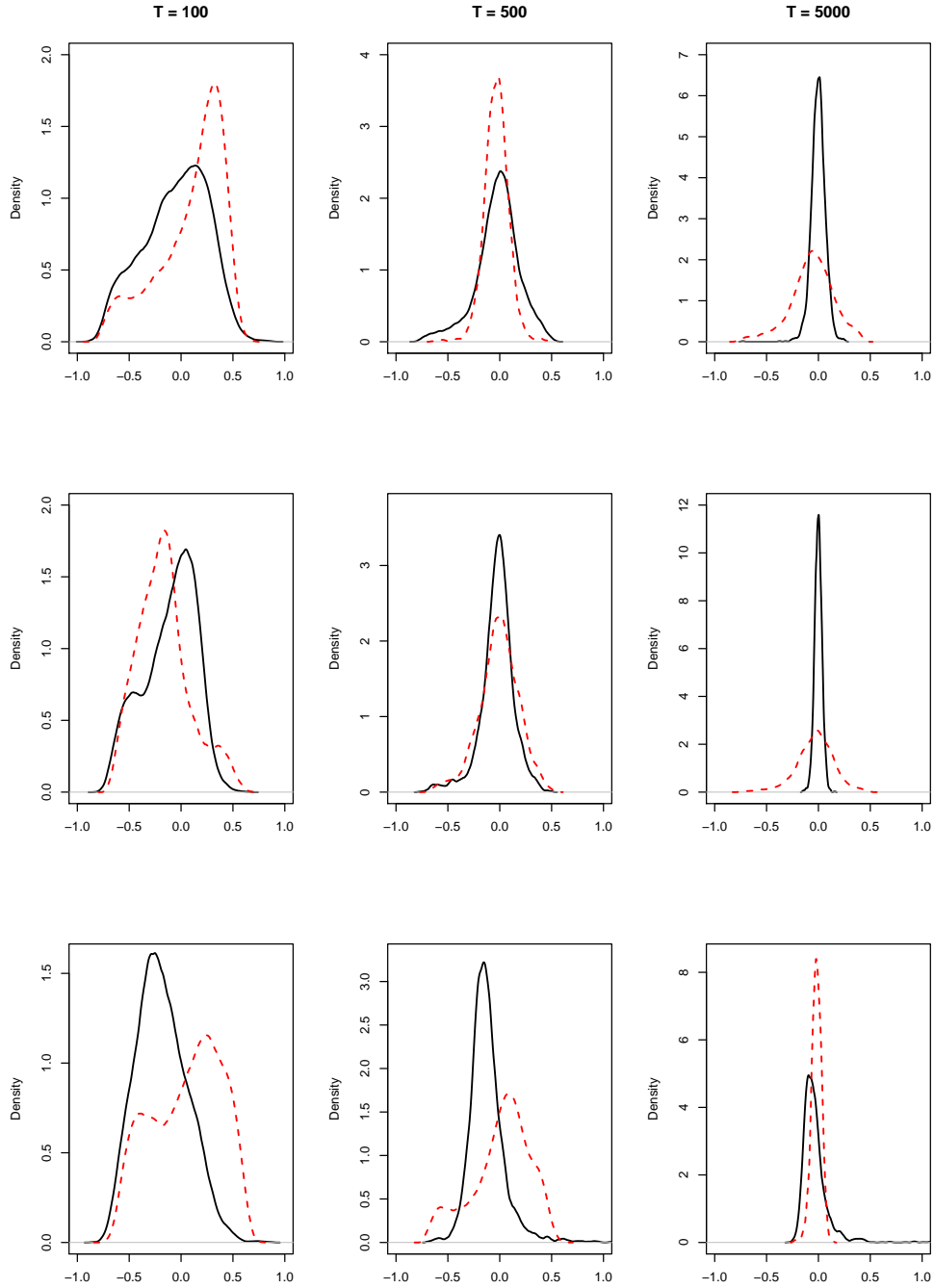


Figure 4A.10: The simulated density of the sampling distribution $\hat{\Theta}_{11,3} - \Theta_{11,3}$ (solid line) versus the simulated density of the bootstrap sampling distribution $\hat{\Theta}_{11,3}^* - \hat{\Theta}_{11,3}$ (dashed red line) using the i.i.d. bootstrap. Both densities are estimated with the Epanechnikov kernel and based on 2'000 simulated observations. The first column corresponds to DGP-1a, the second column to DGP-1b and the third column to DGP-1c.

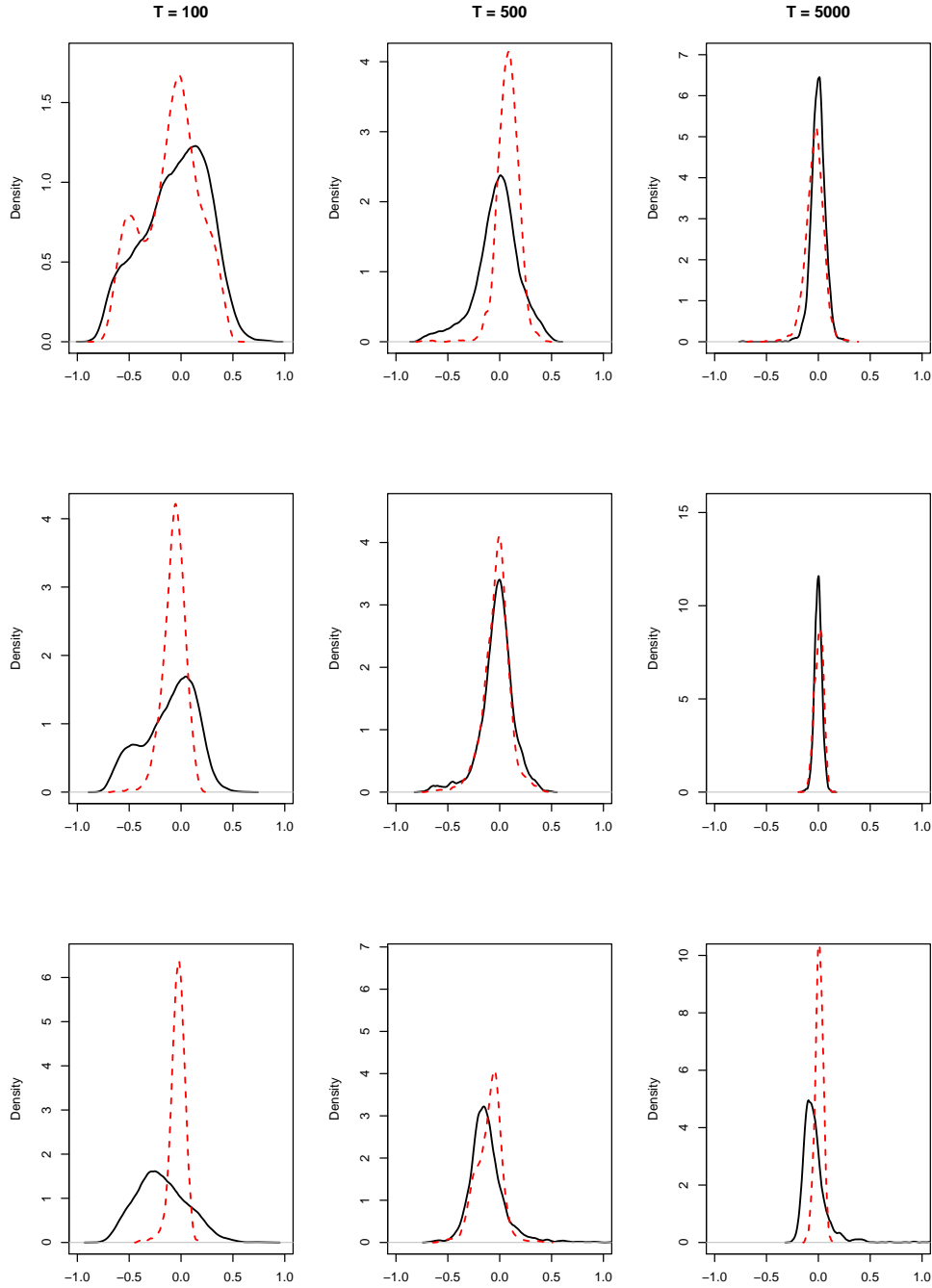


Figure 4A.11: The simulated density of the sampling distribution $\hat{\Theta}_{11,3} - \Theta_{11,3}$ (solid line) versus the simulated density of the bootstrap sampling distribution $\hat{\Theta}_{11,3}^* - \hat{\Theta}_{11,3}$ (dashed red line) using the moving block bootstrap. Both densities are estimated with the Epanechnikov kernel and based on 2'000 simulated observations. The first column corresponds to DGP-1a, the second column to DGP-1b and the third column to DGP-1c.

Curriculum Vitae

STEFAN BRUDER

Born December 9th 1986
in Zurich, Switzerland
Swiss national

EDUCATION

2013 – 2018	Doctoral program at the <i>Zurich Graduate School of Economics</i> , University of Zurich, Switzerland
2010 – 2013	Master of Arts in <i>Economics</i> , University of Zurich, Switzerland
2006 – 2010	Bachelor of Arts in <i>Economics</i> , University of Zurich, Switzerland

PROFESSIONAL EXPERIENCE

2012 – 2018	Research associate at the Department of Economics, University of Zurich, Switzerland
2010 – 2012	Research assistant at Hinder Asset Management AG, Zurich, Switzer- land

April, 2018